

Distribution Agreement

In presenting this thesis or dissertation as a partial fulfillment of the requirements for an advanced degree from Emory University, I hereby grant to Emory University and its agents the non-exclusive license to archive, make accessible, and display my thesis or dissertation in whole or in part in all forms of media, now or hereafter known, including display on the world wide web. I understand that I may select some access restrictions as part of the online submission of this thesis or dissertation. I retain all ownership rights to the copyright of the thesis or dissertation. I also retain the right to use in future works (such as articles or books) all or part of this thesis or dissertation.

Signature:

Lauren C. Fleischer

Date

Engineering novel chimeric antigen receptors (CARs) for T-cell malignancies using innate immune cells

By

Lauren C. Fleischer
Doctor of Philosophy

Graduate Division of Biological and Biomedical Science
Molecular & Systems Pharmacology

H.Trent Spencer, PhD
Advisor

Christopher B. Doering, PhD
Committee Member

Brian G. Petrich, PhD
Committee Member

Cassandra L. Quave, PhD
Committee Member

Accepted:

Lisa A. Tedesco, Ph.D.
Dean of the James T. Laney School of Graduate Studies

Date

Engineering novel chimeric antigen receptors (CARs) for T-cell malignancies using innate immune cells

By

Lauren Cari Fleischer
B.S. Cornell University, 2014

Advisor: H. Trent Spencer, PhD

An abstract of
A dissertation submitted to the Faculty of the
James T. Laney School of Graduate Studies of Emory University
in partial fulfillment of the requirements for the degree of
Doctor of Philosophy in the
Graduate Division of Biological and Biomedical Science
Molecular & Systems Pharmacology

2019

Abstract

Engineering novel chimeric antigen receptors (CARs) for T-cell malignancies using innate immune cells

By Lauren C. Fleischer

CAR T-cell therapy has successfully treated B-cell malignancies, however, there are many challenges translating these therapies for treatment of T-cell malignancies, including fratricide, T-cell aplasia, and product contamination. Approaches to address these challenges include targeting an antigen specific to a subset of T cells, disrupting target antigen expression on CAR-modified cells, non-viral delivery methods, safety mechanisms, and utilizing third party donor non-alloreactive cells or genome editing to prevent alloreactivity. This dissertation explores some of these approaches for the specific treatment of T-cell acute lymphoblastic leukemia (T-ALL) using CD5-CAR therapy. We evaluate the potential for i) CRISPR-Cas9 genome editing of CD5 to reduce fratricide and increase CAR expression, ii) NK-92 cells and $\gamma\delta$ T cells as alternative effector cells within allogeneic settings to avoid product contamination, iii) AAV CAR-delivery to limit long-term expression to reduce concern of T-cell aplasia, as well as iv) a novel class of CARs, non-signaling CARs (NSCARs), to avoid fratricidal constraints.

Our studies show that disruption of CD5 expression in T cells increased CD5-CAR surface expression, however, this did not translate into enhanced CD5-specific cytotoxicity. Using a CD5-negative NK-derived lymphoma cell line, NK-92 cells, we demonstrated in an NSG xenograft model of T-ALL that mice treated with CD5-CAR-modified NK-92 cells, exhibited a survival advantage over control mice. However, due to rapid CD5 down-regulation, fratricide is not a primary concern for CD5-targeted therapy. Therefore, we used $\gamma\delta$ T cells because NK-92 cells require irradiation to prevent expansion of the lymphoma cell line *in vivo*. AAV6 resulted in efficient modification of $\gamma\delta$ T cells and as these cells exhibit limited persistence *in vivo* and because AAV is primarily non-integrating, the combination of these approaches can regulate CAR expression. While fratricide is of minimal concern for CD5-targeted CAR T-cell therapies, other T-cell antigens do not down-regulate rapidly and completely. Therefore, we generated NSCARs, which lack signaling domains and are only advantageous in cells with endogenous cytotoxicity mechanisms, such as $\gamma\delta$ T cells. We demonstrate NSCAR-modified $\gamma\delta$ T cells exhibited enhanced anti-tumor cytotoxicity *in vitro*. Herein, we assess novel approaches for CAR-modified T-cell generation for the treatment of T-cell malignancies.

Engineering novel chimeric antigen receptors (CARs) for T-cell malignancies using innate immune cells

By

Lauren Cari Fleischer
B.S. Cornell University, 2014

Advisor: H. Trent Spencer, PhD

A dissertation submitted to the Faculty of the
James T. Laney School of Graduate Studies of Emory University
in partial fulfillment of the requirements for the degree of
Doctor of Philosophy in the
Graduate Division of Biological and Biomedical Science
Molecular & Systems Pharmacology

2019

Table of Contents

Abstract

Table of Contents

List of Figures and Tables

List of Abbreviations

Chapter 1 – Introduction 1

 1.1 Chimeric Antigen Receptor (CAR) T-cell Therapy 3

 1.2 Translating CAR T-cell Therapy for Treatment of T-cell Malignancies 6

 1.3 “Off-the-shelf” CAR T-cell Therapy 17

 Alternative Effector Cell Types 19

 NK cells and NK-92 cells 19

 Gamma Delta T cells 23

 1.4 Prevention of T-cell Memory Formation and T-cell Aplasia 26

 Non-viral Delivery Methods 27

 Adeno-Associated Viral Vector 29

 Suicide Genes and Safety Switches 30

 1.5 Summary and Conclusions 34

Chapter 2 – Development of chimeric antigen receptors targeting T-cell malignancies using two structurally different anti-CD5 antigen binding domains in NK and CRISPR-edited T cell lines . . 38

 2.1 Abstract 39

 2.2 Introduction 39

 2.3 Materials and Methods 41

 2.4 Results 47

 2.5 Discussion 67

 2.6 Supplemental Figures 71

Chapter 3 – CRISPR-Cas9 gene delivery and CD5-CAR modification of $\alpha\beta$ T cells	80
3.1 Abstract	81
3.2 Introduction	81
3.3 Materials and Methods	83
3.4 Results	85
3.5 Discussion	93
Chapter 4 – $\gamma\delta$ T cells as an alternative effector cell type for CAR T-cell therapy	100
4.1 Abstract	101
4.2 Introduction	101
4.3 Materials and Methods	104
4.4 Results	108
4.5 Discussion	130
Chapter 5 – Non-signaling chimeric antigen receptors (NSCARs) enhance antigen-directed killing by $\gamma\delta$ T cells in contrast to $\alpha\beta$ T cells	136
5.1 Abstract	137
5.2 Introduction	137
5.3 Materials and Methods	140
5.4 Results	145
5.5 Discussion	160
5.6 Supplemental Figures	164
Chapter 6 – Discussion	170
References	181

Figures and Tables

Figure I - 1: Outcomes of CAR T-cell therapy in patients with T-cell disease 7

Figure I - Table 1: Clinical trials targeting T-cell antigens 8

Figure I - Table 2: Off-the-shelf approaches targeting T-cell antigens 20

Figure I - 2: Strategies to overcome challenges in translating CAR therapy to treat T-cell malignancies 37

Figure II - 1: Schematic of CAR structures containing the CD5-directed variable lymphocyte receptor (VLR) or single-chain variable fragment (scFv) 48

Figure II - 2: NK-92 cell-mediated cytotoxicity against a CD5-positive T-ALL cell line using CD5-CARs 50

Figure II - 3: Initial comparison of VLR- and scFv-based CD5-CARs 53

Figure II - 4: CD5 knockout in Jurkat T cells using CRISPR-Cas9 genome editing 56

Figure II - 5: CD5-edited CD5-CAR-modified Jurkat T cells have reduced self-activation and increased CD5-CAR expression 58

Figure II - 6: CD5-edited CD5-CAR-modified effector cells in culture with naïve target T cells stimulates effector-cell activation and target cell down-regulation of CD5 63

Figure II - 7: CD5-scFv-CAR NK-92 cells are superior to CD5-VLR-CAR NK-92 cells in delaying disease progression and improving survival in a T-ALL xenograft mouse model 66

Supplemental Figure II - S1: Activation of Jurkat T cells expressing a CD5-CAR 71

Supplemental Figure II - S2: Western blot analysis of CD5-CAR expression in Jurkat T cells 72

Supplemental Figure II – S3: Viral vector copy number (VCN) in CD5-CAR-modified Jurkat T cells 73

Supplemental Figure II – S4: Transduction efficiency of non-edited and CD5-edited Jurkat T cells... 74

Supplemental Figure II – S5: Western blot analysis of CD5 expression in CD5-CAR-modified Jurkat and CD5-edited Jurkat T cells 75

Supplemental Figure II - S6: CD5-CAR expression measured by flow cytometry and Western blot analysis in Jurkat and CD5-edited Jurkat T cells 76

Supplemental Figure II – S7: Primary T cell CD5 and CD5-CAR expression measured by flow cytometry	77
Supplemental Figure II – S8: CD5 expression in CD5-scFv-CAR-modified Jurkat T cells when cultured with non-modified Jurkat T cells	78
Supplemental Figure II – S9: Persistence of CD5-scFv-CAR-modified NK-92 cells in the absence of IL-2 in NSG mice	79
Figure III - 1: Nucleoporation to edit CD5 in T cells using CRISPR-Cas9 DNA	87
Figure III - Table 1: T-cell electroporation protocols illustrating different parameters tested	88
Figure III – 2: pMax GFP and CRISPR-Cas9 transfection of T cells.	89
Figure III - 3: CD5-editing of T cells using electroporation delivery of CRISPR-Cas9 DNA	90
Figure III - 4: CD5-edited CD5-CAR-modified T-cell cytotoxicity against CD5-positive Jurkat cells	92
Figure III - 5: CD5-edited, FACS sorted, CD5-CAR-modified $\alpha\beta$ T-cell cytotoxicity against CD5-positive Jurkat cells	94
Figure III – 6: Lentiviral vector delivery of CRISPR-Cas9 DNA to Jurkat T cells	98
Figure IV-1: Expansion of $\gamma\delta$ T cells from PBMCs	109
Figure IV-2: Nucleoporation of $\gamma\delta$ T cells	111
Figure IV- Table 1: Electroporation parameters for introducing CRISPR-Cas9 plasmid DNA into $\gamma\delta$ T cells	113
Figure IV - 3: CD5 expression and viability in $\gamma\delta$ T cells following CD5-editing by electroporation ..	114
Figure IV - 4: $\gamma\delta$ T cells transduced with CD5-CAR lentiviral vector	116
Figure IV - 5: Cytotoxicity of CD5-CAR-modified $\gamma\delta$ T cells against a T-ALL cell line	121
Figure IV - 6: Transduction of $\gamma\delta$ T cells with AAV encoding GFP	123
Figure IV - 7: Transduction of $\gamma\delta$ T cells using an AAV6-CD5-CAR vector.	127
Figure IV - 8: Persistence of naïve $\gamma\delta$ T cells in NSG mice	129

Figure IV - 9: GFP intensity correlates with CD5 expression in $\gamma\delta$ T cells transduced with CD5-CAR vectors	134
Figure V - 1: Schematic of CD5-based and CD19-based NSCAR constructs.	139
Figure V - 2: CD5 expression and activation of NSCAR-modified Jurkat T cells.	146
Figure V - 3: CD5-NSCAR-modified Jurkat T cells cultured with non-modified Jurkat T cells.	148
Figure V - 4: NSCAR-modified $\gamma\delta$ T-cell expansion and CD5-downregulation	151
Figure V - 5: NSCAR-modified $\gamma\delta$ T-cell cytotoxicity against T-ALL and B-ALL cell lines	154
Figure V - 6: CD5-NSCAR-modified $\alpha\beta$ T-cell cytotoxicity.	158
Figure V - 7: CD5 expression on Jurkat T cells when cultured in $\gamma\delta$ T-cell supernatant.	159
Supplemental Figure V - S1: Variable expression of CD5-NSCAR and CD5 antigen expression in Jurkat T cells.	164
Supplemental Figure V - S2: CD5-NSCAR-modified CD5-edited Jurkat T cells cultured with non-modified Jurkat T cells	166
Supplemental Figure V – S3: CD19-NSCAR- and CD19-CAR-modified $\gamma\delta$ T-cell cytotoxicity against 697 cells	167
Supplemental Figure V – S4: CD5-NSCAR- and CD5-CAR-modified $\alpha\beta$ T cells.	168
Supplemental Figure V – S5: CD19 expression on 697 cells when cultured in $\gamma\delta$ T-cell supernatant. ..	169

List of Abbreviations

AAV: Adeno-associated viral vector
ADCC: Antibody-dependent cellular cytotoxicity
AITL: Angioimmunoblastic T-cell lymphoma
ALCL: Anaplastic large cell lymphoma
AML: Acute myeloid lymphoma
APC: Antigen presenting cell
ATLL: Adult T-cell leukemia/lymphoma
B-ALL: B-cell acute lymphoblastic leukemia
BCMA: B-cell maturation antigen
BMT: Bone marrow transplantation
Cap: Capsid
CAR: Chimeric antigen receptor
cGMP: Current good manufacturing process
CLL: Chronic lymphocytic leukemia
CMV: Cytomegalovirus
COSMID: CRISPR off-target sites with mismatches, insertions, and deletions
CR2: Complete second remission
CRISPR: Clustered regularly interspaced short palindromic repeats
CRS: Cytokine release syndrome
CTCL: Cutaneous T-cell lymphoma
DLBCL: Diffuse large B-cell lymphoma
EATL: Enteropathy-associated T-cell lymphoma
eGFP: Enhanced green fluorescent protein
EGFR: Epidermal growth factor receptor
ELISA: Enzyme-linked immunosorbent assay
ANOVA: Analysis of variance
ENKTL: Extranodal NK-T-cell lymphoma
epCAM: Epithelial cell adhesion molecule
ETP-ALL: Early T-cell precursor acute lymphoblastic leukemia
FACS: Fluorescence-activated cell sorting
FBS: Fetal bovine serum
FDA: Food and drug administration
FPPS: Farnesyl pyrophosphate synthase
gag: Group-specific antigens
gRNA: Guide RNA
GvHD: Graft versus host disease
HER2: Human epidermal growth factor receptor 2
HIV: Human immunodeficiency virus
HL: Hodgkin's lymphoma
HLA: Human leukocyte antigen
HRP: Horseradish peroxidase
HSCT: Hematopoietic stem cell transplantation
HSTCL: Hepatosplenic T-cell lymphoma
HTLV1: Human T-cell lymphocytic virus type I
hUBC: Human ubiquitin C promoter
huEGFRt: Truncated human EGFR
ICAM1: Intracellular adhesion molecule 1

iCas9: Inducible Cas9
IgG: Immunoglobulin G
IL-2 SP: Interleukin-2 signal peptide
iMC: Inducible MyD88/CD40
Indels: insertions and deletions
IPP: Isopentenyl pyrophosphate
iRC9: Rapamycin-inducible iCas9
ITR: Inverted terminal repeat
IVIG: Intravenous immunoglobulin
KIR: Killer-cell immunoglobulin-like receptor
LDL-R: Low-density lipoprotein receptor
LRR: Leucine rich repeat
LTR: Long terminal repeat
MCSP: Melanoma-associated chondroitin sulfate proteoglycan
MF: Mycosis fungoides
MHC: Major histocompatibility complex
MOI: Multiplicity of infection
MRD: Minimal residual disease
NK: Natural killer
NKG2D: NK group 2 member D
NSCAR: Non-signaling chimeric antigen receptor
NSG: NOD *scid* IL2R γ -chain knockout
PBMCS: Peripheral blood mononuclear cells
PBS: Phosphate buffered saline
PBS-MK: PBS supplemented with MgCl₂ and KCl
PD-1: Programmed cell death receptor-1
PEBL: Protein expression blocker
PEG: Polyethylene glycol
pol: Polymerase
PTCL: Peripheral T-cell lymphoma
PTCL-NOS: PTCL-not-otherwise-specified
PVDF: Polyvinylidene difluoride
qPCR: Quantitative polymerase chain reaction
Rep: Replication
RIPA: Radioimmunoprecipitation assay
ROI: Regions of interest
RRE: Rev-response element
SAN: Salt active nuclease
scFv: Single-chain variable fragment
SDS-PAGE: Sodium dodecyl sulfate polyacrylamide gel electrophoresis
SIN: Self-inactivating
SS: Sezary syndrome
TALEN: Transcription activator-like effector nuclease
T-ALL: T-cell acute lymphoblastic leukemia
TCR: T-cell receptor
TIDE: Tracking of indels by decomposition
TILs: Tumor-infiltrating lymphocytes
TIRs: Terminal inverted repeats

T-LGL: T-cell large granular lymphocytic leukemia
T-LLY: T-cell lymphoblastic lymphoma
TNFR: Tumor necrosis factor receptor
T-PLL: T-prolymphocytic leukemia
TRAC: T-cell receptor alpha constant
TRAF: TNF receptor-associated factor
TRAIL: TNF-related apoptosis-inducing ligand
TRBC: T-cell receptor beta constant
VCN: Vector copy number
V_H: Variable heavy chain
VIP: Vasoactive intestinal peptide
V_L: Variable light chain
VLR: Variable lymphocyte receptor
VPD450: Violet proliferation dye 450
VSVG: Vesicular stomatitis virus G-protein

Chapter I

Introduction

Targeting T-cell malignancies using CAR-based immunotherapy

Lauren C. Fleischer^{1,2}, H. Trent Spencer^{1,2} and Sunil S. Raikar²

¹Program in Molecular and Systems Pharmacology, Graduate Division of Biological and Biomedical Sciences, Laney Graduate School, Emory University School of Medicine, Atlanta, Georgia.

²Cell and Gene Therapy Program, Department of Pediatrics, Aflac Cancer and Blood Disorders Center, Children's Healthcare of Atlanta and Emory University, Atlanta, GA, USA

This is an Accepted Manuscript of an article published in *Journal of Hematology and Oncology*

Introduction

T-cell malignancies encompass a heterogeneous group of diseases, each reflecting a clonal evolution of dysfunctional T cells at various stages of development. T-cell acute lymphoblastic leukemia (T-ALL) accounts for 15% and 25% of childhood and adult ALL cases respectively, and is the most common form of T-cell cancer seen in children (1; 2). Adult T-cell leukemia/lymphoma (ATLL) is an extremely aggressive form of blood cancer driven by the human T-cell lymphocytic virus type 1 (HTLV1) (3-5). Other rare forms of T-cell leukemia include T-cell large granular lymphocytic leukemia (T-LGL) and T-prolymphocytic leukemia (T-PLL) (6). T-cell lymphomas are broadly divided into two categories, cutaneous T-cell lymphoma (CTCL) and peripheral T-cell lymphoma (PTCL) (7). Mycosis fungoides (MF) and Sezary syndrome (SS) represent the two most common subtypes of CTCL, accounting for the majority of cases (8). PTCL can be classified into several different subtypes, among which include anaplastic large cell lymphoma (ALCL), angioimmunoblastic T-cell lymphoma (AITL), extranodal natural killer (NK)-T-cell lymphoma (ENKTL), enteropathy-associated T-cell lymphoma (EATL), hepatosplenic T-cell lymphoma (HSTCL) and PTCL-not-otherwise specified (PTCL-NOS) which is the most common of the group (9; 10).

The overall prognosis for T-cell malignancies varies depending on the type of disease, but in general is much poorer when compared to B-cell malignancies. While the survival in T-ALL has significantly improved with the intensification of chemotherapy, there still remain very limited options for patients with relapsed/refractory disease (11-13). ATLL remains a very challenging disease to treat, with a median survival of less than twelve months for the acute form of this disease (3-5). Advanced stage CTCL has a median overall survival of 5 years (14; 15), whereas outcomes of PTCL vary depending upon the subtype, with ENKTL, EATL and HSTCL having the poorest prognosis (9; 10). While immunotherapy has revolutionized the treatment landscape of various cancers with the use of monoclonal antibodies, checkpoint inhibitors, bispecific T-cell engagers, and chimeric antigen receptor (CAR) T-cell therapy, only limited responses have been seen in T-cell disease (15). Some promising results have been seen with use of brentuximab vedotin, a CD30-directed immunotoxin, in CD30-positive PTCL and CTCL (16; 17) and

the use of pembroluzimab, a programmed cell death receptor 1 (PD-1) inhibitor, in the treatment of ENKTL (18); however, these positive results have been limited to very specific subsets of T-cell disease. One form of immunotherapy that has not yet been successfully translated to T-cell malignancies is that of chimeric antigen receptor (CAR)-based immunotherapy. CAR T-cell therapy has been extremely successful in relapsed/refractory B-cell malignancies as evidenced by the recent Food and Drug Administration (FDA) approval of two CAR T-cell therapeutics for this disease (19-23). However, implementing this technology to treat T-cell malignancies has been difficult, primarily due to the lack of a tumor specific surface antigen in cancerous T cells. In this review, we will discuss the challenges involved in translating this novel technology to T-cell disease, review all the pre-clinical and clinical progress made in adapting this therapy for this challenging disease and examine potential solutions for the future development of this innovative therapy.

Chimeric Antigen Receptor (CAR) T-cell Therapy

Genetic engineering of primary T cells was first presented in the late 1980s (24). Since then, CAR T cells have emerged as a promising technique for the treatment of relapsed/refractory malignancies. CAR therapy brings together numerous fields including immunology, tumor biology, genetic engineering, synthetic biology and pharmacology. CARs are comprised of the intracellular signaling domain from the natural T-cell receptor (TCR), CD3 ζ , linked to a single-chain variable fragment (scFv) which serves as the antigen recognition domain. The scFv sequence is derived from a monoclonal antibody by combining the variable heavy (V_H) and light (V_L) domains using a small peptide linker. In the late 1990s, second-generation CARs were engineered with a CD28 costimulatory domain to improve persistence, cytokine production and proliferative capacity (25). Inclusion of alternative costimulatory domains were described soon after involving 4-1BB, ICOS and OX-40 (26). Third-generation CARs were first presented in the late 2000s, comprised of two costimulatory domains, in order to improve the response (27). However, the most appropriate CAR, regarding identity and number of co-stimulatory domains may vary for different indications.

Although the kinetics have yet to be fully elucidated, it is essential that CAR T cells have mechanisms of trafficking to the tumor site where they can recognize their cognate antigen, resulting in CAR T-cell activation and expansion, and ultimately cytolytic activity against cells expressing the target antigen. CAR-based ligand recognition is advantageous compared to TCR-based ligand recognition because CAR-targeting is not restricted by major histocompatibility complex (MHC) interactions. Therefore, CARs can recognize cell surface proteins that have not been processed and presented by antigen presenting cells (APCs). Importantly, the interactions between scFvs and ligands have much higher affinity and avidity compared to that of TCR-ligand interactions (28). Furthermore, the immune synapse formed from the interaction between a CAR and its ligand likely results in a much greater functional avidity than is observed using a targeted antibody approach with the same antibody (28).

CARs targeting the B-cell antigen CD19 have been studied extensively for the treatment of B-cell malignancies. In 2017, the FDA approved the first CAR T-cell therapy, Kymriah, a CD19-directed CAR therapy for the treatment of relapsed/refractory B-cell acute lymphoblastic leukemia (B-ALL) and in 2018, Yescarta was approved to treat relapsed diffuse large B-cell lymphoma (DLBCL). These therapies, including others in clinical trials, have been widely successful in eliminating malignant cells and re-inducing remission in patients who were otherwise treatment-refractory (19; 20; 29-31). Patients receiving CAR therapy undergo leukapheresis resulting in the collection of T cells, which are subsequently modified using a lentiviral or retroviral vector to express the CAR. These cells are expanded *ex vivo* while the patient undergoes lymphodepletion, a process involving chemotherapeutic agents. Finally, the CAR T cells are re-infused into the patient (32). Lymphodepletion prior to re-infusion of the autologous T cells has been shown to augment both CAR T-cell proliferation as well as persistence (33-35). The administered dose of CAR T cells and the pre-existing tumor burden do not appear to be the sole determinants of the degree of T-cell expansion, engraftment, and overall response. Other factors may be involved, such as the density of cognate antigen expression on the cancer cells (36). However, the optimal degree of persistence of CAR T cells required to prevent leukemic relapse has not been determined (28; 37).

One of the mechanisms of relapse post-CD19 CAR-T therapy is due to surface antigen escape with relapsed leukemia cells being CD19-negative. The mechanism may be due to the expansion of a small subset of CD19-negative cancer cells or alternatively, the cells may down-regulate CD19 from the cell surface in order to evade detection by CAR T cells, rendering them resistant (19; 31; 38-41). Additionally, it was recently shown that a phenomenon referred to as trogocytosis is a mechanism of antigen escape whereby the antigen is transferred to the CAR T cell (42). It was also shown that the transduction of a single leukemic blast with an anti-CD19 CAR that was re-infused into a B-ALL patient ultimately resulted in relapse and death of the patient (43). Transduction of a leukemic cell resulted in masking of the target antigen through interactions between the CAR and the cognate antigen on the same cell. Clonal expansion of this population resulted in resistance to CAR therapy. This report emphasized the importance of strict and perfect isolation of normal, healthy T cells for modification with the CAR construct. As we discuss below, this is particularly challenging in T-cell leukemia patients who are more likely to have circulating cancerous T cells, and therefore a higher probability of these cells being isolated, transduced, and reinfused.

Of note, there are severe toxicities that have been associated with CAR therapy. Cytokine release syndrome (CRS) is a systemic inflammatory response directly resulting from robust T-cell activation following infusion. IL-6 is one pro-inflammatory cytokine that is secreted at high levels during CRS. During a particularly severe CRS condition, tocilizumab, an IL-6R antagonist monoclonal antibody, was used to rapidly and effectively reverse the symptoms of a pediatric patient (30). Tocilizumab has since been FDA approved for treatment of CAR T cell-induced life-threatening CRS (44). Neurological toxicities have been reported following CAR T-cell infusion as well and preventative approaches remain elusive (40; 45-48). Compared to CRS and neurotoxicity, a much more manageable consequence of CAR T-cell therapy targeting B-cell malignancies is the resulting B-cell aplasia. This is a potentially lifelong outcome due to memory-cell formation against a B-cell antigen. However, B-cell aplasia is managed by frequent intravenous administration of immunoglobulin. This would be an extremely problematic outcome for T-cell cancers, as T-cell aplasia would be life threatening. There are currently >200 clinical trials using CAR T cells registered at clinicaltrials.gov being carried out in the United States. However, the majority of these

trials are enrolling patients with B-cell malignancies. Advances are being made to expand CAR T-cell therapy to the treatment of other cancers and to minimize toxicities associated with treatment while reducing difficulty and cost of production.

Translating CAR T-cell Therapy for Treatment of T-cell Malignancies

Harnessing and redirecting the cytotoxicity of T cells to malignant B cells has been established, but reprogramming T cells to kill malignant T cells, while sparing normal T cells, is much more complex and challenging. This requires aberrant expression of an antigen on malignant T cells that is absent or expressed at very low levels on normal T cells. CAR therapy requires isolation of healthy T cells from malignant T cells, a complicated procedure that can result in product contamination and subsequent CAR-modification of tumor cells. Additionally, expression of the targeted antigen on CAR T cells results in fratricide and limited expansion of the CAR T cells. Furthermore, targeting of an antigen regularly expressed on normal T cells would result in T-cell aplasia, leading to profound immunosuppression, associated with high rates of morbidity and mortality (**Figure 1**).

Various approaches have been used to overcome these challenges, including CRISPR-Cas9 genome editing to remove the antigen from the CAR T cells (49-51), Tet-OFF expression system to limit fratricide during *ex vivo* expansion (52), protein expression blocker (PEBL) to retain the antigen in the ER/Golgi to prevent cell surface expression (53; 54), or using CAR-modified NK cells or NK-92 cell line instead of T cells (49; 55-58). Additionally, to date, two targets have been investigated as targets for CAR T-cell therapy for the treatment of T-cell malignancies with limited to no expression in the normal population of T cells, CD30 and CD37 (59-61). Below, we review the preclinical and clinical CAR studies targeting different antigens expressed in T-cell malignancies. A summary of CAR-based clinical trials targeting T-cell disease is presented in Table 1.

CD5

Figure I-1: Outcomes of CAR T-cell therapy in a patient with T-cell disease.

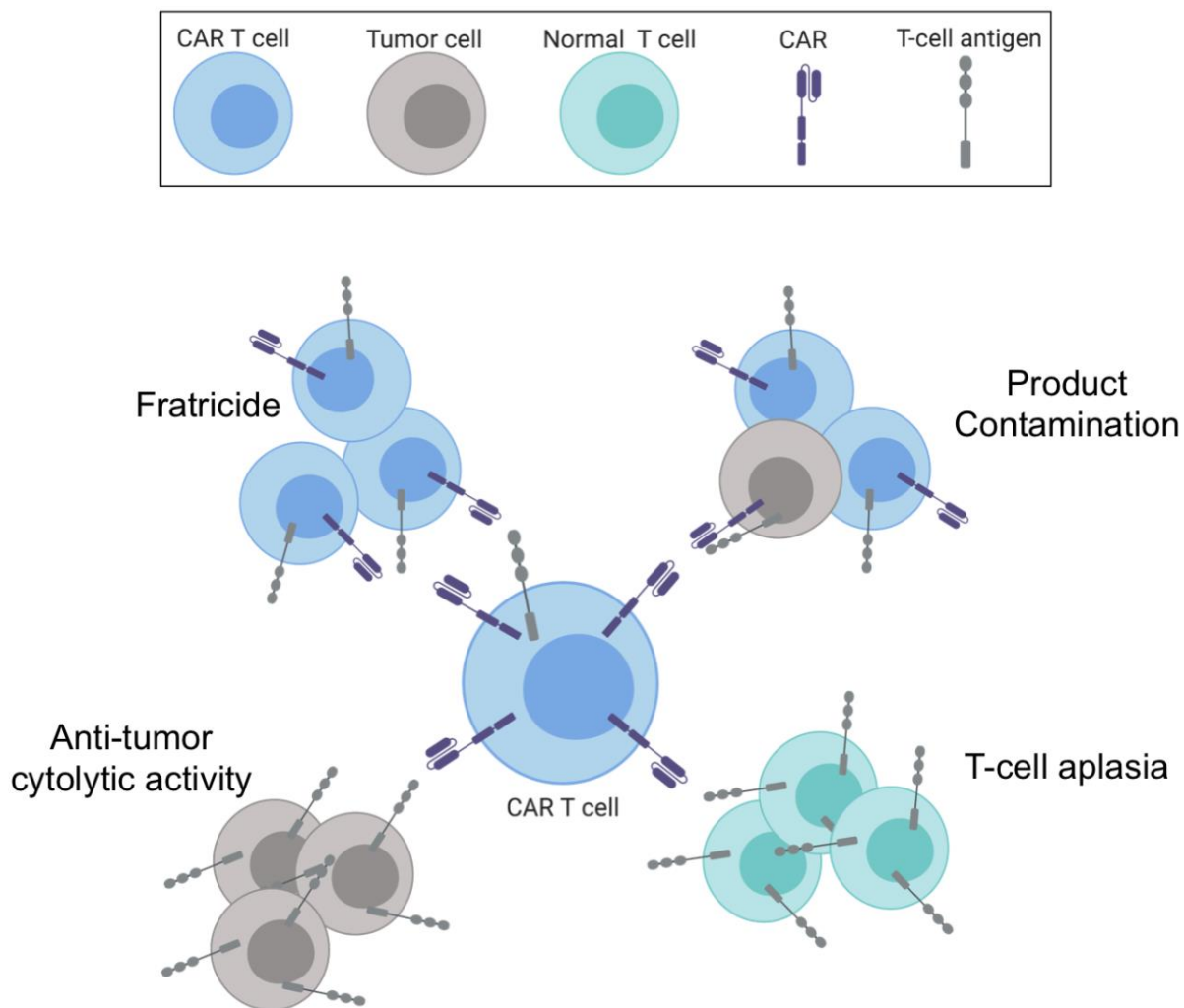


Figure 1: Upon re-infusion into a patient, CAR T cells recognize their cognate antigen, expand upon this recognition, and initiate an attack. However, due to shared antigen expression on CAR T cells, normal healthy T cells, and tumor cells, numerous outcomes are observed. The CAR T cells target tumor cells as intended, reducing tumor burden. However, without further engineering, the CAR-modified T cells are likely to express the targeted antigen as well, resulting in fratricide. CAR T cells also target healthy T cells, resulting in T-cell aplasia through CAR expression on memory T cells. Lastly, CAR T-cell therapy involves isolating healthy T cells from malignant T cells for CAR-modification. A single malignant cell contaminating this population can result in masking of the antigen, leading to antigen-positive relapse.

*Figure was created using BioRender

Figure I-Table 1: Clinical trials targeting T-cell antigens.

T-cell antigen	Clinical Trials	Sponsor	CAR co-stimulatory domain	Additional intervention	Phase	Status	Ref	
CD5	NCT03081910 (MAGENTA)	Baylor College of Medicine	CD28	None	Phase I	Recruiting		
CD7	NCT04004637	PersonGen BioTherapeutics			Phase I	Recruiting		
	NCT04033302	Shenzhen Geno-Immune Medical Institute			Phase I/II	Recruiting		
	NCT03690011	Baylor College of Medicine	CD28	CRISPR/Cas9 CD7-editing	Phase I	Not yet recruiting		
	NCT02742727	PersonGen BioTherapeutics	CD28 and 4-1BB	NK-92 cells	Phase I/II	Unknown		
CD4	NCT03829540	Stony Brook University	CD28 and 4-1BB		Phase I	Recruiting		
CD30	NCT01192464	Baylor College of Medicine		EBV-specific CTL	Phase I	Active, not recruiting		
	NCT03383965	Immune Cell Inc	2 nd generation		Phase I	Recruiting		
	NCT02690545	UNC Lineberger Comprehensive Cancer Center			Phase I/II	Recruiting	[104]	
	NCT02259556	Chinese PLA General Hospital	4-1BB		Phase I/II	Recruiting	[106]	
	NCT02958410	Southwest Hospital, China			Phase I/II	Recruiting		
	NCT03049449	NCI			Phase I	Recruiting		
	NCT01316146	UNC Lineberger Comprehensive Cancer Center	CD28		Phase I	Active, not recruiting	[60]	
	NCT02917083 (RELY-30)	Baylor College of Medicine	CD28		Phase I	Recruiting	[105]	
	NCT04008394	Wuhan Union Hospital, China	3 rd generation		Phase I	Recruiting		
	NCT03602157	UNC Lineberger Comprehensive Cancer Center			CCR4 overexpression	Phase I	Recruiting	
	NCT02663297	UNC Lineberger Comprehensive Cancer Center	CD28			Phase I	Recruiting	
TRBC1	NCT03590574	Autolus Limited		RQR8 safety mechanism	Phase I/II	Recruiting		

Table 1: Clinical trials targeting T-cell antigens. Organized by antigen. Available details regarding the specificities of the CAR construct are included. References are included where applicable.

CD5 expression is limited to normal T cells and a small subpopulation of B cells, called B-1a cells (62-66). CD5 acts as a negative regulator of TCR signaling and has a role in protecting against autoimmunity (67; 68). CD5 is highly expressed on many T-cell malignancies, particularly T-ALL and PTCLs, rendering it a good target for CAR T-cell therapy (69-71). Since CD5 expression on T cells is approximately ten times that on B cells (72), a low-affinity, high-avidity CAR targeting CD5 may steer clear of CD5-positive B cells while selectively killing T cells (73; 74). Furthermore, CD8⁺ tumor-infiltrating lymphocytes (TILs) express lower levels of CD5 compared to that of peripheral blood T cells, and one study showed down-regulation of CD5 improves the ability of T cells to lyse malignant cells (75). CD5 was previously targeted as a tumor antigen in clinical trials using immunotoxin-conjugated CD5 monoclonal antibodies, with responses seen in patients with cutaneous T-cell lymphoma and T-ALL (76; 77).

Mamonkin et al showed that expression of a CD5-CAR with a CD28 co-stimulatory domain resulted in surface downregulation of CD5 in CAR T cells. As a result, fratricide was observed only transiently, allowing the CD5-CAR T cells to expand. These cells had significant *in vitro* cytotoxicity against two T-ALL cell lines and primary T-ALL cells and delayed leukemia progression in two different CD5-positive T-ALL models (78). Based on these results, CD5-CAR T cells with a CD28 costimulatory domain are being tested in T-ALL patients with refractory or relapsed disease (MAGENTA trial, NCT03081910). Our group used CRISPR-Cas9 to knockout CD5 expression in primary T cells prior to transduction with the CD5-CAR. We showed that gene editing of CD5 in effector CAR T cells increased CAR surface expression and decreased self-activation (49). The increased CAR surface expression is predicted to enhance CAR T-cell anti-tumor efficacy. We also showed antagonism of vasoactive intestinal peptide (VIP) signaling in conjunction with inhibition of the PI3K δ pathway increased expansion of CD5-CAR-modified T cells as well as their cytotoxicity against CD5-specific tumor cell lines. This combination of compounds was also demonstrated to prolong *in vivo* persistence of treated T cells in NOD *scid* IL2R γ -chain knockout (NSG) mice (79).

Interestingly, use of 4-1BB as the costimulatory domain in a CD5-CAR resulted in a significant fratricidal effect (52). It was shown that TNF receptor-associated factor (TRAF) signaling from the 4-1BB endodomain upregulated the intercellular adhesion molecule 1 (ICAM1), which subsequently stabilized the fratricidal immunological synapse between CD5-CAR T cells containing the 4-1BB costimulatory domain. To limit and control the effects of fratricide, a Tet-OFF expression system was used, which allowed for controlled transgene expression under a small molecule, doxycycline, inducible promoter. In the presence of doxycycline, CD5-41BB-CAR T cells expanded *ex vivo* without evidence of fratricide, while maintaining a more naïve genotype. Doxycycline was removed from the culture prior to injecting the CD5-41BB-CAR T cells into mice, resulting in CD5-CAR expression and improved survival outcomes in a T-ALL mouse model. Furthermore, there was a survival advantage in mice treated with Tet-OFF CD5-41BB-CAR T cells compared to survival of mice treated with CD5-CD28-CAR T cells without the Tet-OFF expression system (52).

Alternatively, we expressed the CD5-CAR in NK-92 cells, which are inherently CD5-negative. Our data demonstrates CD5-CAR-modified NK-92 cells have increased cytotoxicity against T-cell leukemia cell lines compared to the cytotoxicity of naïve NK-92 cells (49; 55), and there is a significant improvement in survival of T-ALL xenograft mouse models compared to survival of mice treated with naïve NK-92 cells (49). This data confirms previously published data illustrating significantly improved survival and enhanced tumor reduction in irradiated T-ALL mouse models treated with CD5-CAR-modified NK-92 cells compared to that of mice treated with control NK-92 cells (45). Recently, another group considered CD5-CAR-modified NK-92 cells; however, the 2B4 costimulatory domain, an NK-specific domain, was used in the CAR constructs (80). A previous study demonstrated CAR-modified NK-92 cells containing the 2B4 domain enhanced activity against ovarian cancer *in vivo* (81). Similarly, the CD5-2B4-CAR-modified NK-92 cells displayed superiority to CD5-41BB-CAR-modified NK-92 cells, *in vitro* and *ex vivo*. Additionally, both CARs significantly prolonged survival in a mouse model, with the 2B4-CAR-NK-92-treated mice surviving ~13 days longer than those treated with the conventional CAR-modified NK-92 cells (80).

CD7

CD7 is a transmembrane glycoprotein with expression on T cells and NK cells (82). The majority of T-ALLs are CD7-positive, despite some populations lacking expression of other common markers, such as the TCR (83; 84). Additionally, early T-cell precursor acute lymphoblastic leukemia (ETP-ALL), a high-risk subset of T-ALL due to poor responses to standard of care therapy, including hematopoietic stem cell transplantation (HSCT), highly express CD7 (83; 85; 86). Two clinical trials have been initiated in China studying CD7-CAR-modified T cells for the treatment of CD7-positive malignancies (NCT04033302 and NCT04004637). However, preclinical studies demonstrate use of anti-CD7-CAR T cells resulted in significantly reduced expansion compared to control T cells, as a result of fratricide (50; 53). Fratricide appears to be observed to a greater extent in CD7-CAR T cells compared to CD5-CAR T cells (50). It is hypothesized that this is due to a more incomplete internalization mechanism of CD7 from the cell surface following ligation of the antigen with an anti-CD7 scFv. CRISPR-Cas9 editing of CD7 from the cell surface of T cells prior to CAR expression demonstrated a superior method of developing CD7-CAR T cells. These cells exhibited limited fratricide, expanded *in vitro*, and showed no evidence of impaired cytotoxicity *in vitro* nor *in vivo*. Investigations in a T-ALL mouse xenograft model revealed a statistically significant prolonged survival of CD7-edited CD7-CAR-treated mice compared to survival of control mice (50). Previous murine studies indicate that while CD7 has a costimulatory role in T-cell activation, CD7 knockout mice exhibited limited deficiencies in T-cell function (87; 88). Based on these results, a phase I clinical trial has been initiated testing CD7-CD28-CAR T cells in T-ALL patients (NCT03690011). Additionally, a UCART7 was generated using CRISPR-Cas9 genome editing to disrupt the CD7 and TCR α constant (TRAC) loci. This study demonstrated NSG mice engrafted with primary T-ALL blasts and treated with UCART7 donor cells exhibited tumor clearance from the peripheral blood, and, did not develop graft versus host disease (GvHD) or other severe side effects (51).

A new technique using protein expression blockers (PEBLs) has been established as an alternative to genome editing. This strategy couples an scFv with a retention peptide to maintain the protein of interest in the ER/Golgi preventing cell surface expression of the antigen. PEBL-CD7-CAR T cells exhibited

superior cytotoxicity against primary T-ALL cells *in vitro* compared to non-PEBL CD7-CAR T cells. Using a PDX model of ETP-ALL, upon detection of leukemic cell expansion in peripheral blood, PEBL-CD7-CAR T cells were injected. PEBL-CD7-CAR T-cell treated mice had a significant survival advantage over control mice. However, CD7-positive relapse did occur in all PEBL-CD7-CAR T-cell treated mice (53).

Despite CD7 expression on NK-92MI cells, they have been used for CD7-CAR therapy demonstrating only a small percentage of cells are CD7-positive, and upon CD7-CAR expression, fewer than 1% CD7-positive NK-92MI cells remain (89). A humanized CD7 nanobody was generated that specifically bound CD7 with high affinity. Nanobody technology is based on single-domain antibodies found in camelids, which consist only of heavy chains. Linkage of two single-variable domain nanobodies using glycine and serine residues results in a bivalent nanobody (90; 91). A CD7-CAR constructed using the CD7 nanobody was expressed on NK-92MI cells and demonstrated enhanced CD7-specific cytotoxicity against T-ALL cell lines and primary patient cells *ex vivo*. The bivalent CD7-CAR-modified-NK-92MI cells exhibited slightly greater cytotoxicity compared to that of the monovalent CAR-modified cells, however the granzyme B production was significantly more robust from the former. The anti-tumor activity of the bivalent CD7-CAR-modified-NK-92MI cells was tested in a PDX mouse model. Three NSG mice were injected with primary T-ALL cells, and splenic T cells subsequently harvested and transplanted into 30 mice, half of which received a higher dose of cells, while the other half received a lower dose of cells. The mice were treated three days later with naïve NK-92MI or bivalent CD7-CAR-modified-NK-92MI cells with multiple infusions. Mice that received the low dose of T-ALL cells and treated with the CAR-modified cells had a significant survival advantage over mice treated with naïve cells, however this advantage was only ~8 days. A significant survival advantage was also seen in the mice that received high dose of T-ALL cells and treated with the CAR-modified NK-92MI cells compared to those treated with the naïve cells. However, survival was only extended ~5 days (89).

CD4

Most cancers derived from lineage differentiated T cells are likely to be of CD4-positive origin, making CD4 a good target for CAR therapy. A preclinical study was performed to consider the cytotoxicity of CD4-CAR-modified T cells against T-ALL tumors in NSG mice. This study also included the use of alemtuzumab to clear the CAR T cells as a safety mechanism. NSG mice were injected with luciferase-expressing Jurkat T cells and subsequently treated with naïve T cells or CD4-CAR-modified T cells. CAR-treated mice displayed a survival advantage and an ~80% reduction in tumor burden compared to mice treated with naïve T cells. CD4-CAR-modified T cells were also injected into mice to evaluate the ability of alemtuzumab to effectively eliminate CAR-modified T cells. Alemtuzumab was administered 24 hours post-CAR T-cell injection. A >95% depletion of CD4-CAR-modified T cells was observed within six hours following injection signifying the use of alemtuzumab as a safety mechanism for CAR T-cell therapy (92). Additionally, a phase I clinical trial to assess the safety and feasibility of CD4-CAR T-cell infusions in patients with relapsed/refractory T-cell lymphoma and T-cell leukemia has been initiated (NCT03829540).

However, expression of CD4 on T cells can complicate CD4-CAR T-cell therapy as previously described. NK-92 cells are inherently CD4-negative, and therefore the use of NK-92 cells as opposed to T cells reduces risk of fratricide and avoids the need for further modifications. Additionally, it abrogates the risk of aplasia of CD4-positive cells that can occur with long-term engraftment of CAR T cells. Anti-CD4-CAR NK-92 cells have shown *in vitro* success eliminating PTCL cell lines and both adult and pediatric primary cells. Using a xenograft model in NSG mice, CD4-CAR NK-92 cell-treated mice demonstrate significantly prolonged survival compared to control-modified NK-92 cell-treated mice (58).

CD37

CD37 is a member of the tetraspanin superfamily with expression limited to lymphoid tissues, particularly B cells (93; 94). CD37 expression in cancer cells is typically characteristic of B-cell malignancies, however its expression can be found in some cases CTCL and PTCL (95; 96). Since CD37 is not expressed in T cells, there is no evidence of fratricide occurring in anti-CD37-CAR T cells. However, in the presence of CD37-positive PTCL cell lines, CD37-CAR T cells exhibit increased activation and

degranulation as well as specific cytolytic activity *in vitro* (61). The restricted expression of CD37 makes it a safer target for CAR T-cell therapy, given there would be no concern of T-cell aplasia. Additionally, CD37 is not expressed in NK cells, providing an opportunity to utilize NK cells as effector cells in place of T cells. The versatility of CD37-CARs to treat B-cell and T-cell lymphomas suggest this may be an important target for further investigations. While CD37 is predominantly being examined for dual targeting for B-cell malignancies, the target has potential for CAR therapy against T-cell malignancies.

CD30

CD30, a member of the tumor necrosis factor receptor (TNFR) superfamily, promotes T-cell proliferation and cytokine production following TCR stimulation, while also having an opposing role in promoting apoptosis (97). Expression is limited to a subset of activated lymphocytes found around the follicular regions of lymphoid tissues (98-100). While CD30 is well known for its strong expression in virtually all classical Hodgkin's lymphoma (HL), expression of CD30 can also be found on a subset of PTCLs, including ALCL (97-99; 101). One study demonstrated CD30 expression is upregulated during chemotherapy regimens in T-ALL patients. Of 34 T-ALL patients, approximately 38% had CD30-positive T-ALL (101). Therefore, some T-ALL patients who relapse following chemotherapy may still respond to CAR therapy.

Preclinical studies have previously demonstrated CD30-CAR T-cell capacity for lysing tumor cells (102; 103) and numerous clinical investigations into CD30-CAR T-cell therapy have been launched with encouraging results. Eleven phase I/II trials treating patients with CD30-positive malignancies are currently active. To date, no toxicities related to CAR T-cell infusion nor impaired immunity against common viruses has been reported from these trials (NCT01316146 (60), NCT01192464, NCT03049449, NCT02690545 (104), NCT02958410, NCT02663297, NCT03383965, NCT02917083 (105), NCT04008394, NCT02259556 (106) and NCT03602157). However, one trial reported the *in vivo* CAR T-cell expansion and persistence was reduced following subsequent infusions compared to those following initial doses (60). The decreased persistence of the CAR T cells may have prevented the development of severe adverse events

such as CRS and neurotoxicities that are commonly observed following CAR T-cell infusion. Of the two ALCL patients in this trial, one patient was non-responsive to the therapy, while the other entered complete remission lasting nine months (60). One phase I/II trial is currently ongoing in China for patients with relapsed/refractory Hodgkin's lymphoma (NCT02259556). Although only one patient in this study has ALCL, the results of this trial corroborate the limited toxicity and anti-tumor activity of CD30-CAR T cells (106).

TRBC1

T cells express the $\alpha\beta$ TCR; the β -chain can either be encoded by the T-cell receptor beta constant 1 (TRBC1) gene or TRBC2 gene (107; 108). Therefore, expression of TRBC1 and TRBC2 is mutually exclusive. Additionally, CD4- and CD8-positive T-cell populations express both subsets and CD8-positive T-cell populations specific for common viruses also contain both TRBC1 and TRBC2 cells (109). However, as malignant T cells develop from a single cell, the entire population of cancerous cells will be either TRBC1- or TRBC2-positive. Numerous T-cell malignancy cell lines and primary samples have been analyzed by flow cytometry to validate the homogeneity of β -chain expression in a malignant cell population (109). Many cancer cells down-regulate the $\alpha\beta$ TCR, however it is expressed on >95% of PTCLs (110) and >30% of T-ALLs (111).

Anti-TRBC1 CAR T cells exhibited specific and efficient cytotoxicity against the JKO T-cell line transduced with TRBC1, but not against non-transduced cells or cells transduced with TRBC2, even in a mixed population. Furthermore, in primary samples from patients with T-cell malignancies, the anti-TRBC1 CAR T cells preserved a significant fraction of healthy T cells (TRBC2 cells), thereby circumventing a limitation of CAR T-cell therapy for the treatment of T-cell malignancies (109). In an NSG mouse model using TRBC1-positive Jurkat T cells to establish cancer, mice treated with the anti-TRBC1 CAR T cells exhibited reduced tumor burden and elongated survival. In additional pre-clinical studies, NSG mice were injected with both TRBC1 and TRBC2 cancer cells, and then treated with either naïve T cells or

anti-TRBC1 CAR T cells. TRBC1-positive Jurkat T cells could not be detected in mice treated with anti-TRBC1 CAR T cells, however TRBC2-positive cells were identified. This is in contrast to mice treated with naïve T cells, whose bone marrow confirmed the presence of both TRBC1-positive and TRBC2-positive cells (109). Targeting TRBC1-positive malignant cells offers a unique approach to avoiding T-cell aplasia, a consequence of many proposed CAR T-cell therapies for the treatment of T-cell malignancies.

CD3

CD3 is a pan T-cell marker comprised of four distinct polypeptide chains, epsilon, gamma, delta and zeta, which form pairs of dimers, transmitting T-cell activation signals. As CD3 is exclusively expressed on T cells, it has been a popular target in pre-clinical CAR T-cell therapies for the treatment of T-cell malignancies. As expected, due to fratricidal issues, manufacturing of anti-CD3 CAR T cells does not yield a viable cellular product (112). Various approaches using an anti-CD3 CAR have been investigated including the use of transcription activator-like effector nuclease (TALEN) mRNA to disrupt the TRAC locus and using NK-92 cells in place of T cells as the effector cell type. Disruption of the TRAC locus prevents assembly of the TCR $\alpha\beta$ /CD3 complex, allowing for anti-CD3-CAR expression without compromising cellular proliferation and viability. Enrichment of the CAR-positive, CD3-negative population was observed. In patient T-ALL samples, anti-CD3 CAR T cells demonstrated specific cytotoxicity against CD3-positive cells. In a T-ALL NSG model, anti-CD3 CAR T cells were shown to clear luciferase-expressing CD3-positive Jurkat cells, but showed no effect in NSG mice engrafted with CD3-negative Jurkat cells (112).

To circumvent the need for additional modifications, NK-92 cells can also be used to express the anti-CD3-CAR, since they are CD3-negative cells. CD3-CAR NK-92 cells demonstrated efficient *ex vivo* lysis of PTCL primary samples, resulting in less than 0.5% lymphoma cells remaining at 5:1 effector to target ratios suggesting a potential use for this therapy in achieving minimal residual disease (MRD) for eligibility for HSCT. Furthermore CD3-CAR NK-92 treated T-ALL NSG mice exhibited prolonged survival with ~87% reduced tumor burden through day 23 (56).

“Off-the-shelf” CAR T-cell Therapy

One of the greatest challenges in utilizing autologous CAR T-cell therapy for the treatment of T-cell malignancies is the separation of healthy T cells from malignant T cells in order to modify only healthy T cells with the CAR. To date, there has been one reported case from the University of Pennsylvania of CD19-CAR modification of a single, leukemic B cell, resulting in CD19-positive relapse and ultimately death of the patient (43). This task of isolating only the healthy T cells is even more difficult when a proportion of the patient's T cells are malignant, especially in cases of T-cell leukemia wherein there is a high likelihood of circulating leukemia T cells in the peripheral blood. Thus, manufacturing of autologous CAR T cells for the treatment of T-cell malignancies has a very high likelihood of resulting in CAR-modified leukemic cells. Additionally, there remain numerous challenges to using a patient's own cells to manufacture CAR T cells. Patients with advanced disease undergoing CAR T-cell therapy typically are heavily pre-treated, having previously undergone numerous rounds of chemotherapy, which can result in low T-cell counts and/or T cells that may not be healthy enough to expand well making it very difficult to manufacture an efficacious CAR T-cell product (113). This issue is much more prevalent in adult patients due to the decreasing proportion of naïve T cells associated with aging (113-116). Moreover, due to intensive pre-treatment, the cells may exhibit reduced cytotoxic potential. Additionally, given many of these patients have advanced disease, a patient may experience disease progression, co-morbidities or even death in the time it takes to manufacture autologous CAR T cells once the patient has become eligible. This is especially true in most relapsed T-cell malignancies, which tend to be aggressive and chemo-resistant in nature. Lastly, each starting autologous T-cell product is different – variable function, maturation, CD4/CD8 ratios and phenotypic ratios – and the heterogeneity of each individual product has led to unpredictable results and variable potency of the therapy.

An alternative to autologous CAR T-cell manufacturing is the use of allogeneic T cells as the cell source. Expression of the endogenous $\alpha\beta$ TCR in allogeneic CAR T cells must be blocked as it would likely result in GvHD, unless the donor is a human leukocyte antigen (HLA) match. This process involves

leukapheresis from a healthy donor, followed by isolation and activation of the donor's T cells. Transduction using a lenti- or gamma-retroviral vector is performed to express the CAR and subsequent genome editing prevents expression of the endogenous TCR. Cells that remain TCR-positive are depleted from the expanded CAR T-cell product prior to cryopreservation. This creates an off-the-shelf cellular product that can be banked until it is needed for any patient requiring the therapy. This approach resulted in successful remission in two infant B-ALL cases treated with allogeneic CD19-CAR T cells that had been modified at the TRAC and CD52 loci. The allogeneic CAR T cells persisted until conditioning for stem cell transplant (117). Another group utilized shRNA to knock down β 2-microglobulin in conjunction with a knock-in strategy to insert a CD19-CAR into the TRAC locus. Knock down of β 2-microglobulin reduces the ability of class I HLA molecules to form heterodimers on the cell surface. Reducing expression of both β 2-microglobulin and TRAC resulted in decreased allogeneic attack by CD8 T cells and NK cells (118). This strategy may be useful to reduce allo-recognition in patients receiving CAR T-cell therapy. Other groups have exploited similar approaches in preclinical CAR T-cell investigations targeting CD7 and CD3, as previously described (51; 112).

CRISPR-Cas9 genome editing has become a popular technique to prevent gene expression or to correct gene expression. One study targeting CD7 generated "fratricide resistant, allo-tolerant" CAR T cells using CRISPR-Cas9 to disrupt both CD7 and the TRAC loci (UCART7). NSG mice engrafted with primary T-ALL blasts developed GvHD when treated with wildtype donor T cells, however, mice treated with UCART7 donor cells were able to clear the tumor cells from the peripheral blood, and, furthermore, did not develop GvHD or other severe side effects (51).

TALENs, an alternative genome editing technique, have also been used to prevent expression of the TRAC locus in order to limit fratricide of anti-CD3-CAR T cells and prevent MHC-recognition of foreign host cells. Genome editing the TRAC locus prevents stable assembly of the TCR $\alpha\beta$ /CD3 complex. Disruption of the TRAC locus using TALEN mRNA prior to transduction with an anti-CD3-CAR lentiviral vector yielded CAR T cells that proliferated well and greatly reduced tumor burden in an NSG mouse model

of human leukemia. This manufacturing process can be applied to healthy non-HLA-matched donor T cells for use in an allogeneic transplant (112).

As described above, PEBLs have been recently developed to selectively prevent expression of individual proteins. PEBLs have been shown to effectively retain CD3 ϵ in the ER/Golgi to prevent MHC recognition of host cells during allogeneic transplant of anti-CD19 CAR T cells. Disruption of TCR $\alpha\beta$ signaling had no effect on T-cell proliferation. There was no evidence of GvHD in an NSG mouse model of leukemia treated with the PEBL-CD19-CAR T cells, whereas 60% of the mice treated with CAR T cells that were not expressing the CD3 ϵ PEBL developed GvHD. Furthermore, both PEBL and CAR can be expressed from the same vector using a 2A sequence, resulting in only one transduction of the cells (54). While this study utilized PEBL in conjunction with an anti-CD19-CAR, this system can be applied with other CAR constructs to target T-cell antigens. Preclinical studies utilizing off-the-shelf approaches for the treatment of T-cell malignancies are outlined in **Table 2**.

Alternative Effector Cell Types

While CAR-modified $\alpha\beta$ T cells can have a memory phenotype resulting in T-cell aplasia, NK cells and V γ 9V δ 2 expanded $\gamma\delta$ T cells will not. Utilizing these innate cells for CAR therapy is a viable alternative that groups are exploring. One disadvantage to preventing memory-cell formation and using effector cells with limited persistence is reduced tumor control. These therapies require numerous infusions of CAR-modified cells, which can increase the cost of therapy. However, as these cells can be used in an allogeneic setting, they can be cryopreserved, ready for use. Short-lived CAR-expressing cells can be effectively used to induce remission these patients, thus providing a bridge to an allogeneic HSCT.

NK cells and NK-92 cells

Ex vivo-expanded NK cells are short-lived, and do not persist for extended periods of time *in vivo* compared to that of $\alpha\beta$ T cells (119). CAR-modified NK cells have a turnover time of 1-2 weeks, therefore

Figure I-Table 2: Off-the-shelf approaches targeting T-cell antigens.

T-cell antigen	Off-the-shelf Approach	Preclinical Study References
CD5	NK-92 cells	[45, 49, 55, 80]
CD7	UCART7: CRISPR-Cas9 at CD7 and TRAC loci	[51]
	NK-92MI	[89]
CD4	NK-92 cells	[58]
CD3	NK-92 cells	[56]
	TALENs targeting TRAC locus	[112]

Table 2: Off-the-shelf approaches targeting T-cell antigens. Organized by antigen.

there is reduced concern of aplasia of antigen-expressing cells (120). Currently there are two active clinical trials using anti-CD19-CAR-modified NK cells (NCT00995137 and NCT01974479). Additionally, some studies use NK-92 cells, an IL-2-dependent NK-derived cell line. NK-92 cells are often used as an alternative to primary NK cells due to their ease of expansion under current good manufacturing process (cGMP) conditions (121) and transfection with CAR mRNA (122). CAR-modified HLA, killer-cell immunoglobulin-like receptor (KIR) mismatched NK donor cell infusion or CAR-modified NK-92 cell infusion can result in tumor cell clearance without the risk of GvHD. Therefore, these cells only require one genetic modification. Additionally, with the exception of CD7, NK cells typically do not express antigens targeted in T-cell malignancies, and they have limited persistence *in vivo*. Therefore, neither fratricide nor T-cell aplasia are of primary concern.

NK-92 cells modified with a CAR construct to obtain antigen-specific cytotoxicity have been extensively assessed in preclinical studies for the treatment of various diseases including B-cell malignancies (123-125), multiple myeloma (126), acute myeloid lymphoma (AML) (127), breast carcinoma (128; 129), neuroblastoma (130), and glioblastoma (131). As previously discussed, multiple groups have initiated preclinical studies using CAR-modified NK-92 cells for the treatment of T-cell malignancies, targeting antigens such as CD5, CD7, CD4 and CD3, demonstrating reduced tumor burden and an overall survival benefit in NSG mouse models of T-cell leukemia compared to mice treated with naïve NK-92 cells (45; 49; 56; 58). The safety and efficacy of NK-92 cells has been evaluated in clinical trials displaying a good safety profile with few mild to moderate adverse events (132-134) (NCT00900809, NCT00990717). To date, five clinical trials have been initiated involving infusion of CAR-modified NK-92 cells targeting a variety of antigens, including CD33, human epidermal growth factor receptor 2 (HER2), B-cell maturation antigen (BCMA), CD19, and the T-cell antigen, CD7 (NCT02944162, NCT03383978, NCT03940833, NCT02892695 and NCT02742727).

Inherent NK-cell cytotoxicity is dependent on the balance of activating and inhibitory killer-cell immunoglobulin-like receptor (KIR) signals. Inhibitory and activating KIRs on NK cells form a balance, as there are often signals from both inhibitory and activating receptors. The inhibitory signals predominate,

typically through higher affinity for their ligands, however strong activating signals can override the inhibitory signals, licensing NK cells to kill. If donor inhibitory KIRs do not recognize patient HLA, there is reduced inhibitory signaling to counteract the activating signaling (135; 136). While NK-92 cells lack many of the inhibitory KIRs expressed on primary NK cells, they have a wide range of activating receptors. NK-92 cells are highly cytotoxic against cancer cells (137). Similar to NK cells, NK-92 cells have the capability to produce perforin and granzyme upon activation, as well as display cytotoxic activity through up-regulation of TNF-related apoptosis-inducing ligand (TRAIL), FasL and TNF α (138). Additionally, NK-92 cells have demonstrated evidence of serial killing, with each cell killing numerous target cells (139). However, as NK-92 cells are an NK lymphoma cell line, they require irradiation prior to infusion into a patient to prevent expansion, resulting in persistence for about one week *in vivo* and potentially exhibiting reduced cytotoxicity as a result. Alternatively, suicide mechanisms can be engineered into the cells to eliminate the risk of NK-92-cell persistence *in vivo* and eliminate the need for irradiation, thereby resulting in greater cytotoxicity of the infused cells.

A major limitation to the use of CAR T cells is antigen escape, however, as NK cells can kill through other mechanisms, down-regulation of the cognate antigen on tumor cells may not halt anti-tumor activity. Differences in the cytokine secretion profile, namely reduced release of proinflammatory cytokines, and extensive inhibitory signals involved in NK-cell therapy are assumed to play a role in the reduced risk of CRS compared to that seen with T-cell CAR therapy (139). NK cells can exhibit their cytotoxic activity through numerous means including expression of FasL or TRAIL, secretion of perforin and granzyme, as well as through antibody-dependent cellular cytotoxicity (ADCC) mechanisms (136; 140; 141). High expression of Fc γ RIII (CD16) facilitates ADCC through administration of a monoclonal antibody and can be augmented by the addition of cytokines (142-147). Combination therapy using both CAR NK cells and a monoclonal antibody has demonstrated improved efficacy, however few antibodies have been developed for this purpose in T-cell malignancies (148). Natural Killer Group 2D (NKG2D) receptor recognizes stress ligands including MICA and MICB (149; 150), resulting in cytotoxicity against exceedingly stressed cells. As NK cells do not recognize targets on healthy cells, they have limited off-

target toxicity (136). Additionally, their serial killing capability allows each individual NK cell to kill, on average, four tumor cells (151). However, NK cells are notoriously difficult to expand *ex vivo*, transduce with viral vectors, cryopreserve and they have limited life span *in vivo* (134; 152). While autologous NK cells can be obtained by leukapheresis followed by selection of CD56-positive cells, allogeneic NK cells derived from a 3rd party donor requires an additional step for depletion of alloreactive T cells from the donor product (153).

Purification and expansion of NK cells from peripheral blood mononuclear cells have been optimized in cGMP protocols to clinically relevant numbers (154-156). This is a time-consuming process as only 10% of peripheral blood mononuclear cells (PBMCs) are NK cells (157). However, recently developed methods are being used to enhance NK-cell expansion, such as through K562-feeder cell expression of OX40 ligand (158). As mentioned above, a limitation to NK CAR therapy is the extreme sensitivity of NK cells to cryopreservation. They have demonstrated poor viability and diminished cytotoxicity after cryopreservation. While cytotoxicity can be restored to normal levels after a few days in culture with exogenous IL-2, the low viability post-cryopreservation remains a concern (153).

$\gamma\delta$ T cells

While $\alpha\beta$ T cells function as a part of the adaptive immune system, $\gamma\delta$ T cells play roles for both the innate and the adaptive immune system. $\gamma\delta$ T cells and $\alpha\beta$ T cells originate from two distinct T-cell lineages (159). $\gamma\delta$ T cells are the only innate immune cells expressing a TCR (160), however, their target recognition is independent of MHC-recognition (161; 162). Lack of MHCI- and MHCII-restriction renders $\gamma\delta$ T cells optimal candidates for allogeneic cell therapy. $\gamma\delta$ T cells are excellent effector cells for CAR T-cell therapy and V γ 9V δ 2 T cells represent the most commonly studied subset of $\gamma\delta$ T cells in this context. Studies by our group have demonstrated similar transduction efficiencies can be achieved in V γ 9V δ 2 T cells grown under cGMP serum-free conditions as are achieved in $\alpha\beta$ T cells using lentiviral vectors. Additional studies were performed revealing peak low-density lipoprotein receptor (LDL-R) expression on

days 6-8 of $\gamma\delta$ T-cell expansion (163). As LDL-R is the major receptor for VSV-G-pseudotyped lentiviral vectors, this data suggests greater transduction efficiency can be achieved on these days using lentiviral vectors compared to earlier or later in the expansion (164).

To date, numerous preclinical studies have evaluated CAR-modified $\gamma\delta$ T cells. These studies have focused on the treatment of neuroblastoma (165; 166), melanoma (167), B-cell malignancies (166; 168) and epithelial cell adhesion molecule (epCAM)-positive adenocarcinomas (169). While none of these studies focus on targeting T-cell malignancies, they all demonstrate CAR expression on $\gamma\delta$ T cells improves anti-tumor cytotoxicity in an antigen-specific manner. GD2-CAR-modified $\gamma\delta$ T cells expressing the RQR8 suicide gene were shown to expand 2.5-fold upon antigen exposure and, as $\gamma\delta$ T cells exhibit innate trafficking to tumor microenvironments, no changes in migration towards neuroblastoma cells using a transwell migration assay were detected (165). Furthermore, both GD2-CAR- and CD19-CAR-modified $\gamma\delta$ T cells were demonstrated to secrete proinflammatory cytokines in the presence of GD2- or CD19-expressing tumor cells, respectively (166). While these studies utilized viral vectors to express the CAR, electroporation of a Sleeping Beauty transposon has also been shown to result in CD19-CAR expression in $\gamma\delta$ T cells, resulting in anti-tumor cytotoxicity both *in vitro* and *in vivo* against CD19-positive tumor cells (168). Additionally, expression of a CAR targeting melanoma-associated chondroitin sulfate proteoglycan (MCSP) was established in $\gamma\delta$ T cells using RNA transfection. Despite comparable anti-tumor cytotoxicity, lower cytokine secretion was observed in MCSP-CAR-modified $\gamma\delta$ T cells compared to that from conventional CAR-modified $\alpha\beta$ T cells (167). Reduced proinflammatory cytokine secretion is favorable due to anticipated reduced occurrence or severity of CRS. Lastly, epCAM-CAR-modified $\gamma\delta$ T cells were either studied fresh, or cryopreserved for one month, and cultured for 24 hours upon thawing. epCAM-CAR-modified $\gamma\delta$ T cells demonstrated high levels of *in vitro* cytotoxicity of tumor cell lines when $\gamma\delta$ T cells were both fresh and cryopreserved. Additionally, $\alpha\beta$ -depletion on day 7 of expansion eliminated $\alpha\beta$ T cells from the culture; however, the cells maintained overall cytotoxicity against tumor cell lines *in vitro* (169). These studies pave the way for additional trials using CAR-modified $\gamma\delta$ T cells targeting T-cell

malignancies. They demonstrate engineering of $\gamma\delta$ T cells and enhanced *in vitro* and *in vivo* cytotoxicity upon CAR expression.

Clinical trials using CAR-modified $\alpha\beta$ T cells have reported numerous cases of antigen escape – a major mechanism of treatment resistance and relapse despite strong presence of CAR T cells. CAR-modified $\gamma\delta$ T cells may be able to overcome this antigen escape obstacle by relying on their innate ability to recognize the tumor cells through other means and impart their cytotoxic effects on the proportion of cells that down-regulate the targeted antigen, avoiding resistance to the treatment. Naïve $\gamma\delta$ T cells have been shown to have anti-tumorigenicity activity against leukemia, neuroblastoma and colon cancer cell lines as well as primary cancer cells *in vitro* (170-173). They are found in peripheral blood, spleen and lymph nodes in addition to almost all mucosal tissues, functioning as immune-surveillance of epithelial tissues by scanning for inflammatory threats (174; 175). They also have an intrinsic capability to kill cells expressing danger signals, with no priming required, including tumor cells. The $\gamma\delta$ TCR recognizes self-antigens that serve as endogenous danger signals such as heat shock proteins, which are upregulated in cells with increased metabolism, like cancer cells. Expression of scavenger receptors like the NK group 2 member D receptor, NKG2D, enables $\gamma\delta$ T-cell activation through the interactions between NKG2D and self-antigens that are indicative of cellular stress such as MIC-A, MIC-B and ULBPs (160; 176-179). These interactions result in cellular cytotoxicity facilitated by the secretion of $\text{TNF}\alpha$ and IL-2R up-regulation (175; 178; 180). Additionally, $\gamma\delta$ T cells express chemokine receptors that can detect chemokines secreted by cancer cells, likely facilitating their migration towards the tumor site (181). $\gamma\delta$ T cells also express FasL (CD95L) as a means of recognizing Fas expression on tumor cells and initiating apoptosis (182). One mechanism by which tumor cells can evade immune recognition is through down-regulation of the MHC. The ability of $\gamma\delta$ T cells to recognize stress antigens, heat shock proteins and chemokines secreted by tumor cells presents an advantage to $\gamma\delta$ T-cell therapy instead of using $\alpha\beta$ T cells, which cannot recognize tumor cells following a reduction in antigen expression.

Another mechanism by which $\gamma\delta$ T cells can recognize tumor cells is through stimulation by phosphoantigens. Phosphoantigens such as isopentenyl pyrophosphate (IPP) are recognized by the $\gamma\delta$ TCR. While there are many subsets of $\gamma\delta$ T cells, phosphoantigens specifically expand the V γ 9V δ 2 subset. IPP is used as a substrate in the mevalonate pathway by farnesyl pyrophosphate synthase (FPPS) enzyme. Bisphosphonates overproduced in cancer cells block the FPPS enzyme, resulting in a buildup of IPP, which is subsequently recognized by V γ 9V δ 2 cells resulting in the secretion of IFN γ and TNF α and potent $\gamma\delta$ T-cell cytotoxicity (183-186). Bisphosphonate stimulation of $\gamma\delta$ T cells has been applied to *in vitro* expansion of $\gamma\delta$ T cells in conjunction with IL-2 in serum-free conditions (163). A preclinical study involving nude mice receiving repeated dosing of $\gamma\delta$ T cells resulted in decreased tumor growth, however, tumor growth resumed upon completion of the $\gamma\delta$ T-cell infusions (187). In phase I clinical trials, adoptive transfer of $\gamma\delta$ T cells to patients receiving *ex vivo* expanded $\gamma\delta$ T cells with a combination of IL-2 and bisphosphonate stimulation or *in vivo* IL-2 infusions with or without bisphosphonates demonstrated the safety of the infused product and suggested the therapy could be efficacious in slowing the progression of the disease, however, no complete remissions were observed and only one case of a partial remission. Combinatorial therapies involving $\gamma\delta$ T cells are likely to be more beneficial compared to $\gamma\delta$ T-cell therapy alone (183; 188-191).

While autologous transfer of CAR-modified $\alpha\beta$ T cells targeting a T-cell malignancy can be used as a bridge to transplant (although the risk remains that a single CAR T cell will be left behind ultimately resulting in the development of T-cell aplasia), it cannot be a curative option unless a near perfect design of a suicide gene, switch mechanism, or another system has been implemented to reliably eliminate all CAR T cells upon completion of the treatment. Therefore, $\gamma\delta$ T cells, NK-92 cells or NK cells may be advantageous effector cells for CAR T-cell therapy. Other techniques such as mRNA electroporation or AAV can also be useful in preventing long-term CAR T-cell persistence, as described below.

Prevention of T-cell Memory Formation and T-cell Aplasia

While current CAR T-cell therapies for the treatment of B-cell malignancies have been hugely successful in initiating and maintaining remission, these therapies have prevented the re-emergence of endogenous B cells in patients in whom the CAR T cells have persisted. The CAR T cells can have a memory phenotype that allows them to remain dormant until re-stimulation with the cognate antigen, CD19, expressed on all endogenous B cells. While B-cell aplasia is an undesirable side effect of these therapies, it has been managed by continued periodic intravenous immunoglobulin injections (40). The long-term implications of persistent B-cell aplasia remain unknown. In contrast, treatment of T-cell malignancies using CAR T cells targeting antigens expressed on the majority of normal T cells is predicted to result in T-cell aplasia. While B-cell aplasia is tolerable, there is no such treatment for T-cell aplasia. Patients who develop T-cell aplasia will have profound immunosuppression and thus will succumb to deadly infections (40). Therefore, prevention of memory cell formation of CAR T cells and T-cell aplasia remains an essential challenge to translating CAR T-cell therapy for the treatment of T-cell malignancies.

Non-viral Delivery Methods

There are numerous disadvantages to using retroviral vectors for CAR T-cell therapy, including risk of clonal dominance (192; 193), high cost of production (194), maximum cargo size (195; 196), the inability to “turn off” transgene expression and unpredictable integration sites potentially resulting in insertional oncogenesis (197; 198). The indefinite period of CAR expression can result in severe on-target off-tumor toxicities, which is particularly challenging to manage in T-cell disease. To overcome these unintended side effects, groups are alternatively exploring delivery of CAR-RNA through electroporation as a safer method (199-201). As with the use of effector cells with limited persistence *in vivo*, therapies with transient CAR-expression require multiple infusions into the patients. Use of mRNA electroporation of T cells for CD19-CAR expression has been reported in a pre-clinical model demonstrating reduced tumor burden one day post-treatment. This study illustrates prolonged survival of a xenograft mouse model after a single injection of CAR-mRNA, however, as predicted, as mRNA levels decrease, the tumor burden

increases. Median survival did not differ between the mRNA-treated mice and the lentiviral vector-treated mice (199).

Published results from the first non-viral CD19-CAR clinical trial using RNA electroporation to deliver the CAR into T cells demonstrate the safety and efficacy of this treatment in four relapsed/refractory classical HL patients. While CAR-RNA was detected 48 hours post-infusion, no RNA could be detected by day 21. At 1-month post-treatment, one patient had complete response, another had a partial response, a third had stable disease and the fourth patient had progressive disease. The patient with a complete response exhibited the longest persistence of RNA, while the patient with progressive disease had the least RNA persistence. However, the results were transient and the patient who had complete response had progressive disease 3 months later (202).

Transposons such as Sleeping Beauty, piggyBac or Tol2 have also been explored as alternatives to viral vectors for gene delivery (168; 203-208). Transposons encode the gene of interest flanked by terminal inverted repeats (TIRs). For gene therapy applications, DNA transposase can be co-transfected with the transposon. The transposase recognizes the TIRs flanking the target sequence and can insert the therapeutic DNA into the genome resulting in integration of the DNA and stable expression. Additionally, transposons can be used for gene disruption by inserting the transposon into an endogenous gene. (209). Preclinical data illustrate CD19-CAR T cells generated by transposons demonstrate engraftment of the CAR T cells resulting in tumor cell clearance in an *in vivo* xenograft murine model (208; 210-212). Other transposon-generated CAR T cells are being evaluated in preclinical studies for the treatment of ALL (204), juvenile myelomonocytic leukemia (213), breast cancer (214), cholangiocarcinoma (215) and sarcomas (203; 216; 217). To our best knowledge, transposons have yet to be utilized for expression of CARs targeting T-cell antigens. However, there is potential in this modality for the treatment of T-cell malignancies as its safety and efficient delivery has been demonstrated in clinical trials for the treatment of B-cell malignancies. CD19-CAR T cells against B-cell malignancies have been infused into patients following HSCT to reduce risk of post-transplant relapse (autologous: NCT00968760; allogeneic: NCT01497184; long-term follow-up: NCT01492036). Autologous transplant of transposon-generated CD19-CAR T cells resulted in 83% of

progression-free survival after 30 months and long-term persistence of CAR T cells was detected (218). Additional clinical trials have evaluated transposon-generated CD19-CAR T cells in patients with chronic lymphocytic leukemia (CLL) (NCT01653717).

This system is advantageous over viral vector delivery methods for numerous reasons including the ability to transfer large therapeutic genes as well as the lower processing cost due to cell-independent production. However, both transposons and viral vector gene delivery typically result in integration of the transgene into the host-cell genome. Furthermore, use of transposons incorporates advantages of plasmid DNA delivery, such as avoiding activation of natural cellular defense mechanisms against viral infection.

Adeno-Associated Viral Vector

AAV is an alternative viral delivery method that overcomes some of the disadvantages of using integrating viral vectors previously discussed. Efficient transduction of innate immune cells by AAV encoding a CAR against a T-cell antigen would address the threat of T-cell aplasia. Innate immune cells, such as NK cells and $\gamma\delta$ T cells, as previously discussed, are potential effector cells for CAR-mediated therapy. A common challenge reported in using these cell types is the low transduction efficiency using integrating viral vectors, delaying progress in the development of these therapies. AAV gene transfer of a CAR into innate immune cells would offer the opportunity to develop an allogeneic off-the-shelf CAR therapy that can control CAR expression, mitigating CRS and other adverse events, and that does not form memory against T-cell antigens and therefore will not result in T-cell aplasia.

AAV is a single-stranded, non-enveloped DNA virus with a cargo capacity of approximately 4.7 kilobases (219). Upon deletion of the Rep protein, the viral transgene forms circular concatamers that exist episomally in the nucleus of the cell. AAV expression is therefore diluted upon each mitotic division (220; 221). Episomal expression of the transgene is one unique quality of AAV that makes it suitable for gene therapy applications, particularly CAR therapy. AAV delivery of a CAR transgene can control the duration of CAR expression, which is a desired quality of CAR therapy to regulate cytokine production and mediate toxicities, however AAV-delivered transgenes integrate at a low frequency into the host cell genome (222-

224). In particular, transient CAR expression may prove advantageous in situations targeting T-cell malignancies by preventing T-cell aplasia. As a result, the use of AAV for gene transfer can mitigate some of the concerns of CAR technology by regulating CAR expression.

The AAV capsid directs the infectivity of different tissues, and therefore the appropriate capsid must be used to maximize transduction of the desired cell type. The capsid sequence, which determines the AAV serotype, influences the infectivity profiles of different cell types (225; 226). Previous studies have reported the tropism for each AAV serotype. AAV6 has been shown to result in higher transduction of hematopoietic stem and progenitor cells than have other serotypes (227-229).

Suicide Genes and Safety Switches

While the motivation behind the incorporation of suicide genes and safety switches into CAR constructs was to mediate the severe adverse events commonly reported following extensive expansion of CAR T cells, they can also serve an alternative purpose. Using pharmacologic agents, the apoptotic pathway in CAR T cells can be activated, triggering selective cell death of the effector cells, without destroying bystander cells. Therefore, they can be valuable in the setting of T-cell malignancies as they can prevent T-cell aplasia. There are three main classes of suicide gene technologies, classified by the mechanism of action of the incorporated gene. They i) convert non-toxic compounds to toxic drugs via metabolic pathways (230-233), ii) induce dimerization of inducible Cas9 (iCas9) (234; 235), or iii) mediate ADCC using monoclonal antibodies (236-238). Co-expression of the suicide gene with the CAR in a bicistronic vector would result in two populations of cells – those that express both the CAR and the suicide gene, and those that express neither. This strategy eliminates the risk of a CAR-positive cellular population that does not include the safety transgene. For simply controlling CAR expression in cases of severe adverse events, a less than pure population would suffice. However, all the CAR-positive cells must also express the safety transgene in order to confidently eliminate the entire CAR population and, in the context of targeting T-cell antigens, control T-cell aplasia.

The first reported suicide gene utilized expression of the herpes simplex virus thymidine kinase (HSV-TK) in donor lymphocytes prior to HSCT. Metabolism of ganciclovir by HSV-TK in patients that developed GvHD resulted in a toxic substance killing the cells (239). As discussed above, administration of alemtuzumab, an anti-CD52 antibody commonly used in lymphodepleting regimens, has recently been evaluated as a mechanism for clearing CAR T cells to prevent T-cell aplasia. Specifically, alemtuzumab has been assessed for CD4-CAR T-cell elimination following tumor cell eradication in NSG mice. Within six hours following alemtuzumab infusion, >95% of the CAR T cells had been depleted (92). Another study demonstrated CD123-CAR T-cell mediated tumor ablation in a human AML PDX mouse model, followed by CAR T-cell depletion upon alemtuzumab administration (240). A third study evaluated the use of alemtuzumab as a safety mechanism for dual CD123-CD33 CAR T cells. Dual targeting resulted in tumor clearance in an *in vivo* model. Upon alemtuzumab infusion, rapid depletion of CAR T cells was observed. Within six hours, ~90% of CAR T cells had been depleted. By five days post-alemtuzumab administration, CAR T cells were undetected in the peripheral blood, bone marrow, spleen and liver of the mice (241).

In London, an epitope-based marker/suicide gene system (RQR8) was developed to both track the transduced cells and selectively deplete them by combining epitopes from CD34 and CD20. Use of Miltenyi's clinically approved CliniMACS CD34 system allows for selection of the CAR-modified T cells while the binding of rituximab results in ADCC and selective elimination of the adoptively transferred T cells. Co-expression of RQR8 with an anti-GD2 CAR demonstrated selection of CAR T cells with >95% purity and clearance of >97% of the CAR-positive population. C57BL/6 splenocytes were transduced with RQR8 retroviral vector and sorted using Miltenyi CD34 beads and then injected into C57BL/6 x BALB/c cross mice. The transgenic T cells were detected at day 7, however, following rituximab administration, they were no longer detected in peripheral blood. Control mice demonstrated increased levels of transgenic T cells in peripheral blood (242). This RQR8 system has been tested in clinical trials for the treatment of T-cell non-Hodgkin lymphoma targeting TRBC1 (NCT03590574).

Recently, the safety mechanism gaining the most attention has been the inclusion of an iCas9 suicide gene into the CAR construct. Pharmacologic activation of the iCas9 results in effective and rapid

elimination of CAR T cells. iCas9 inclusion in a CD19-CAR construct regulates CAR T cells in a dose-dependent manner, allowing for either control over the CAR T cells to reduce toxicities, or complete elimination of all CAR T cells to facilitate B-cell reconstitution (243; 244). This is especially significant in cases with severe adverse events, such as GvHD or CRS. iCas9 has recently been included in CAR constructs containing an IL-15 gene to introduce control over CAR T-cell function. The IL-15 gene arms the T cells to produce IL-15, which, while increasing T-cell survival and enhancing specific cytotoxicity, can also result in unrestricted proliferation and increased toxicity. Inclusion of an iCas9 gene in these CAR constructs can provide control to this therapy and increase the safety profile (245).

Bellicum Pharmaceuticals demonstrated an activation switch on CAR T cells comprised of rimiducid-inducible MyD88 and CD40 (iMC) signaling elements provided increased proliferation and survival and enhanced specific cytotoxicity both *in vitro* and *in vivo* upon rimiducid administration (246). The heightened costimulation can also act negatively, dramatically increasing toxicity through CRS or autoreactivity. Therefore, this construct was modified to include an iCas9 gene to confer control over CAR T-cell function. Similar to iMC, clinically validated iCas9 relies on activation by rimiducid. In order to incorporate both iMC and iCas9 into a CAR construct, a novel mechanism for iCas9 activation is required. Therefore, a rapamycin-inducible iCas9 (iRC9) was generated to be used in conjunction with iMC in CAR T cells to enhance anti-tumor cytotoxicity while exhibiting control over CAR T-cell function (247). In addition to CD19-CARs, iCas9 has been included in other CAR constructs including an anti-CD20-CAR, demonstrating enhanced tumor clearance *in vivo* and a 90% reduction in CAR T cells in the peripheral blood of mice following activation of the iCas9 suicide gene, compared to CAR T cells detected in peripheral blood of control mice (248). Additionally, a GD2-CAR including the iCas9 gene is being assessed for the treatment of neuroblastoma (NCT01822652), sarcoma (NCT01953900), osteosarcoma and melanoma (NCT02107963) in phase I clinical trials.

A few groups have evaluated the use of CD20 adoptive transfer into T lymphocytes using a retroviral vector as a novel suicide mechanism. Their data supports infusion of the anti-CD20 antibody, rituximab, an approved antibody for *in vivo* therapeutic applications, results in efficient, specific elimination

of CD20-positive T lymphocytes *in vitro* through complement activation as well as ADCC (236; 237; 249). CD20 co-expression with a CD123-CAR demonstrated strong and rapid anti-leukemia activity in a human AML mouse model. Upon the infusion of rituximab, CAR T cells were cleared and mice were successfully engrafted with human bone marrow cells, mimicking allogeneic stem cell transplantation (240). CD20 can additionally be used as a selection marker. Studies have demonstrated rituximab can eliminate CD20-positive cells *in vivo* through inducing complement-dependent cytotoxicity, a rapid and efficient mode of cell death (250). Both iCas9- and CD20-based safety systems allow for rapid and efficient elimination of the CAR T cells (251).

Dual constructs for tracking and elimination have been designed to facilitate the selection of CAR-positive T cells, tracking of the cells *in vivo* and selective elimination as a safety mechanism. Truncated human EGFR (huEGFRt) is one such polypeptide that has been evaluated for this purpose. The ligand binding domains and intracellular signaling domains were removed from the protein, however the epitope for binding cetuximab, an anti-EGFR monoclonal antibody, remains. Modification of T cells with the CAR and huEGFRt allows for selection using cGMP biotin immunomagnetic beads and biotinylated cetuximab and tracking using flow cytometry or immunohistochemistry. Upon administration of cetuximab, CAR T cells become the targets for ADCC, resulting in *in vivo* depletion of CAR T cells. T-cell engraftment and ADCC-mediated CAR T-cell elimination were exemplified in NSG and NOD/*scid* mice, respectively (252). Additionally, the huEGFRt suicide mechanism has been assessed in a phase I clinical trial in an anti-MUC-16^{ecto} CAR construct to treat patients with platinum-resistant ovarian cancer (253).

An alternative approach to suicide genes is the generation of a split receptor consisting of two distinct polypeptides: the antigen recognition domain and the intracellular signaling domains. Upon activation from a dimerization-inducing small molecule, the two peptides dimerize, resulting in a functional receptor. However, antigen stimulation is still required to facilitate a response. The small molecule can be titrated for optimal response, controlling the timing and dosage of active CAR T cells. Removal of the small molecule can reversibly regulate CAR T-cell activity. These ON-switch CAR T cells demonstrate specific cytotoxicity *in vitro* and *in vivo* only when exposed to the small molecule. In a mouse xenograft model,

mice treated with ON-switch CAR T cells displayed a reduction in the K562 cells engineered to express CD19, only in the presence of the small molecule, similarly to mice treated with conventional CD19-CAR T cells. However, in the absence of the small molecule, there was no difference in mice treated with ON-switch CAR T cells compared to mice treated with vehicle (254).

Summary and Conclusions

CAR therapies targeting CD19 have resulted in unparalleled success. However, there are many challenges in translating these therapies beyond the treatment of B-cell malignancies. We have highlighted some of these challenges in this review. While numerous antigens have been identified for the treatment of T-cell malignancies, targeting of many of these antigens results in fratricide and T-cell aplasia. Multiple gene editing approaches are being evaluated to prevent fratricide by reducing expression of the targeted antigen on CAR-modified cells. For example, it has been shown that CD5 is down-regulated rapidly from the cell surface upon interaction with the CD5-CAR. Therefore, only transient and limited fratricide is observed (78), in contrast to the targeting of antigens with incomplete down-regulation (50). Furthermore, a clinical trial has been initiated using CD5-CAR modified T cells that have not undergone additional modifications (MAGENTA trial, NCT03081910). However, this trial can only be successful if overexpression of the CD5-CAR is achieved, as only levels above endogenous CD5 antigen will result in surface expression of the CAR.

The identification of tumor-specific antigens would greatly enhance CAR therapy targeting T-cell malignancies by avoiding fratricide. To date, few antigens with limited expression on normal cells have been assessed as CAR targets to treat T-cell malignancies, including CD30, CD37 and TRBC1. A focus on targets with such limited expression on T-cell malignancies is unlikely to have a wide-ranging impact on the treatment of patients with T-cell disease. However, CD30 and CD37 are commonly found on B-cell malignancies, and CARs targeting these antigens have been successful in these settings. In contrast, TRBC1 is expressed on a much larger population of T cells and therefore it is likely to be found on a higher percentage of T-cell malignancies, comparatively. To the best of our knowledge, only one study has

evaluated anti-TRBC1-CAR T-cell therapy. The data suggests TRBC1 is a very promising marker for targeting T-cell malignancies and the field would benefit from studies further developing this therapy.

While targeting CD5 or antigens with selective expression on T cells may overcome the issue of fratricide, the concern regarding T-cell aplasia has not been addressed. The potential for life-threatening T-cell aplasia emphasizes the need for a safety mechanism that is completely effective at eliminating CAR T cells following tumor eradication. Adjusting the effector cell type to NK cells, NK-92 cells or $\gamma\delta$ T cells can also limit the risk of a memory-cell response against a T-cell antigen. While NK-92 cells are an NK-derived lymphoma cell line, they have demonstrated safety in clinical trials. However, they require irradiation prior to infusion to prevent expansion of lymphoma cells in a patient (132; 133). As stated, no safety concerns have arisen from trials involving irradiated NK-92 cells, however, therapeutic effect of NK-92 CAR therapy has not been demonstrated (255). Alternatively, mRNA or AAV delivery systems, which result in transient CAR T-cell expression could be utilized. While CAR therapy most commonly uses $\alpha\beta$ T cells for CAR expression, short-lived NK cells or $\gamma\delta$ T cells could be taken advantage of, especially for use in allogeneic settings and to avoid product contamination. These solutions address the challenge of preventing and managing toxicities as well.

However, these strategies do not address the pressing issue of isolating normal healthy T cells from malignant T cells upon leukapheresis, prior to modification with a CAR construct. A perfect system needs to be in place in order to confidently prevent transduction of a leukemic blast, a phenomenon that has occurred, resulting in relapse and ultimately death of a B-ALL patient (43). In order to eliminate any risk of this event, 3rd party donor cells must be used. Disruption of TCR expression is required to limit GvHD when using $\alpha\beta$ T cells for CAR expression. However, NK cells and $\gamma\delta$ T cells can both be used in an allogeneic setting as they are unlikely to cause GvHD. Use of allogeneic CAR-modified cells addresses the challenges of high cost and difficulty of production, since healthy donor cells can be expanded more easily and cryopreserved as an off-the-shelf therapy until they are required in an allogeneic setting. Additionally, allogeneic cell delivery allows for titratable dosing as well as multiple infusions, if such is required.

Many avenues are currently being explored to enhance the safety and efficacy of CAR therapy. However, the majority of these strategies do not address all three main challenges to utilizing CAR therapy to treat T-cell malignancies. Of the approaches evaluated in this review, only those incorporating NK cells or NK-92 cells can overcome all of these primary challenges (**Figure 2**). NK cells i) are non-alloreactive and can be obtained from healthy donors, eliminating risk of product contamination, ii) do not form memory responses, preventing T-cell aplasia, and iii) do not express the same antigen repertoire as T cells, avoiding fratricidal concerns. CD7 is an exception as it is found on NK cells and therefore fratricide could occur. While NK and NK-92 CAR therapy have a potential that should continue to be investigated and optimized, particularly for the treatment of T-cell malignancies, many groups are currently exploring this avenue. Other, equally promising approaches, such as utilizing $\gamma\delta$ T cells as the cellular vehicle for CAR therapy represents an alternative, less studied approach. Similar to NK cells, $\gamma\delta$ T cells are non-alloreactive and are unlikely to form a memory response against a T-cell antigen. However, $\gamma\delta$ T cells are likely to succumb to fratricide in certain circumstances. As previously described, some T-cell antigens down-regulate rapidly and result in only transient and limited fratricide. Therefore, $\gamma\delta$ T cells can be especially advantageous in the targeting of rapidly down-regulating T-cell antigens for the treatment of T-cell malignancies. Furthermore, $\gamma\delta$ T cells exhibit trafficking to tumor microenvironments and express innate MHC-independent mechanisms of cytotoxicity by which they can recognize tumor cells. CAR therapy using $\gamma\delta$ T cells represents an understudied avenue with the potential of developing into a superior cellular product.

Many advances have been made towards translating CAR therapy for the treatment of T-cell malignancies. Both academia and industry are focused on the identification of tumor-specific antigens to enhance the safety and efficacy of CAR T-cell products as well as on the development of superior cellular products. Unfortunately, due to vast variability in the design and execution of preclinical studies, it is difficult to compare the different strategies. However, the numerous preclinical and clinical studies underway for the treatment of T-cell malignancies provide optimism for successful translation of this therapy to treat this aggressive and challenging group of diseases.

Figure I-2: Strategies to overcome challenges in translating CAR therapy to treat T-cell malignancies.

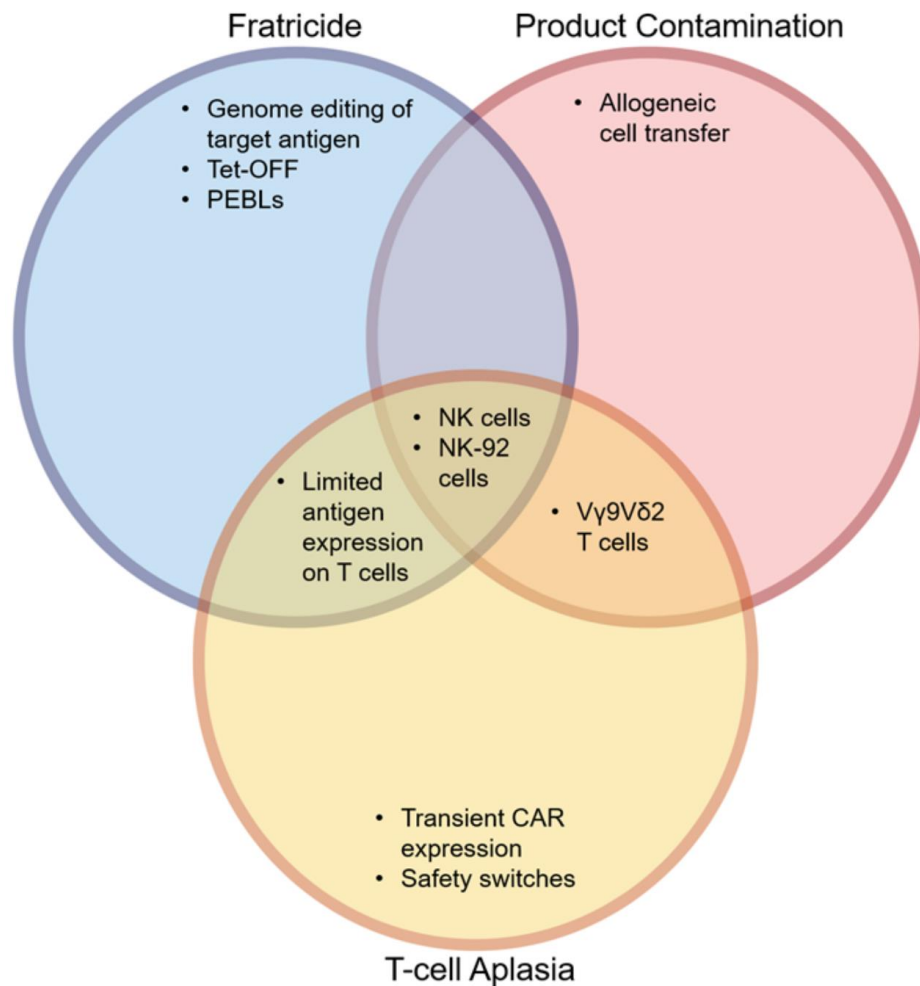


Figure 2: Many approaches have been evaluated to overcome the barriers to utilizing CAR therapy to target T-cell malignancies. However, few of these strategies address more than one challenge, and only one strategy has been assessed to overcome the three primary challenges: use of NK or NK-92 cells.

Chapter II

Development of chimeric antigen receptors targeting T-cell malignancies using two structurally different anti-CD5 antigen binding domains in NK and CRISPR-edited T cell lines

Lauren C. Fleischer^{1,2,a} & Sunil S. Raikar^{1,a}, Robert Moot^{1,2}, Andrew Fedanov¹, Na Yoon Paik¹,
Kristopher A. Knight¹, Christopher B. Doering^{1,2}, H. Trent Spencer^{1,2}

^aS.S.R. and L. F. contributed equally to this work.

¹Aflac Cancer and Blood Disorders Center, Department of Pediatrics, Emory University School of Medicine, Atlanta, Georgia; ²Department of Molecular and Systems Pharmacology, Graduate Division of Biological and Biomedical Sciences, Emory University School of Medicine, Atlanta, Georgia

This is an Accepted Manuscript of an article published by Taylor & Francis in *OncImmunology* on December 26, 2017, available online at

<https://www.tandfonline.com/doi/full/10.1080/2162402X.2017.1407898>

Abstract

Relapsed T-cell malignancies have poor outcomes when treated with chemotherapy, but survival after allogeneic bone marrow transplantation (BMT) approaches 50%. A limitation to BMT is the difficulty of achieving remission prior to transplant. Chimeric antigen receptor (CAR) T-cell therapy has shown successes in B-cell malignancies. This approach is difficult to adapt for the treatment of T-cell disease due to lack of a T-lymphoblast specific antigen and the fratricide of CAR T cells that occurs with T-cell antigen targeting. To circumvent this problem two approaches were investigated. First, a natural killer (NK) cell line, which does not express CD5, was used for CAR expression. Second, CRISPR-Cas9 genome editing technology was used to knockout CD5 expression in CD5-positive Jurkat T cells and in primary T cells, allowing for the use of CD5-negative T cells for CAR expression. Two structurally distinct anti-CD5 sequences were also tested, i) a traditional immunoglobulin-based single chain variable fragment (scFv) and ii) a lamprey-derived variable lymphocyte receptor (VLR), which we previously showed can be used for CAR-based recognition. Our results show i) both CARs yield comparable T-cell activation and NK cell-based cytotoxicity when targeting CD5-positive cells, ii) CD5-edited CAR-modified Jurkat T cells have reduced self-activation compared to that of CD5-positive CAR-modified Jurkat T cells, iii) CD5-edited CAR-modified Jurkat T cells have increased activation in the presence of CD5-positive target cells compared to that of CD5-positive CAR-modified Jurkat T cells, and iv) although modest effects were seen, a mouse model using the CAR-expressing NK cell line showed the scFv-CAR was superior to the VLR-CAR in delaying disease progression.

Introduction

Chimeric antigen receptor (CAR) T-cell therapy is among the most promising anti-cancer therapeutics, with great success achieved in relapsed/refractory B-cell malignancies (19-22). This approach for the treatment of T-cell malignancies is complicated by the lack of a T-lymphoblast specific surface antigen. As a result, CAR T cells generated to target malignant T cells are at risk of fratricide and, therefore, their activation against targeted cancer T cells is compromised (78). We explore two alternative methods

that can be used to apply this innovative therapy to T-cell disease; the first is through the use of a NK cell line as the CAR-expressing effector cell, and the second is by knocking-out surface expression of the target antigen in CAR T cells using CRISPR-Cas9 genome editing.

CD5 is a pan T-cell marker that is commonly over-expressed in most T-cell malignancies (69; 71). Expression of CD5 by normal cells is restricted to thymocytes, peripheral T cells, and a minor subpopulation of B lymphocytes, called B-1 cells (67; 256; 257). Additionally, CD5 is a negative regulator of T-cell receptor (TCR) signaling and has a role in protecting against autoimmunity (68; 72; 258). As a result, we have chosen CD5 as the target antigen for our CARs. Clinical trials have previously studied CD5 as the tumor target antigen using immunotoxin-conjugated CD5 monoclonal antibodies, with responses documented in patients with cutaneous T-cell lymphoma and T-ALL (76; 77). A pre-clinical study using anti-CD5 CAR T cells had favorable results, but did demonstrate some evidence of fratricide among the engineered CAR T cells due to inherent CD5 expression (78). CD5-negative cells, such as NK cells or CD5-CRISPR-Cas9-edited T cells, may be a more suited option for CAR-modified effector cells for the targeting of T-cell malignancies (45). The CRISPR system (259-262), has been adapted to function in eukaryotes and can be used to induce genetic modifications, such as highly specific and permanent gene knockout (263-265). We hypothesized that CD5-CRISPR-edited T cells would have decreased self-activation when expressing a CD5-CAR compared to that of CD5-positive T cells.

We have previously shown that a variable lymphocyte receptor (VLR) can be used for CAR-mediated antigen recognition instead of the more traditional immunoglobulin-based single chain variable fragment (scFv) (55). VLRs represent the functional unit of the adaptive immune system in jawless vertebrates (lamprey and hagfish), and are analogous, but not homologous to immunoglobulins (266; 267). VLRs have a fundamentally different structure and geometry than immunoglobulin-based antibodies, while still demonstrating high degrees of specificity and avidity. We hypothesize VLRs can bind antigens in a geometrically dissimilar manner compared to that of scFvs, and therefore can potentially interact with epitopes unavailable to an scFv, thereby increasing the repertoire of targetable antigens. Importantly for the production of CAR-based therapeutics, they exist naturally as single chain crescent-shaped proteins with

their variable region consisting of multiple assembled repeating sequences, termed leucine rich repeats (LRRs) (266-269). VLRs function as avidity-based antibodies with the individual monomeric VLR units exhibiting lower affinity towards their target compared to their multimeric form (270; 271). The unique single chain structure of VLRs allows for rapid insertion into a CAR scaffold, compared to the corresponding use of an immunoglobulin, in which the variable heavy and light chains need further engineering for adapting to CAR technologies. We hypothesized that a CD5-directed VLR-CAR would have equal or superior efficacy compared to a corresponding scFv-CAR.

We tested both the CD5-VLR-CAR and CD5-scFv-CAR in NK-92 cells, non-edited and CD5-edited Jurkat T cells, and non-edited and CD5-edited primary T cells. Our *in vitro* studies demonstrate that both CD5-CARs have comparable outcomes in terms of T-cell activation and NK-92 cell mediated CAR cytotoxicity, and that CD5-edited CD5-CAR T cells have increased CD5-CAR expression and exhibit decreased self-activation while maintaining their ability to activate in the presence of CD5-positive target cells. However, *in vivo* the scFv-CAR had an advantage over the VLR-CAR when tested in a T-cell leukemia mouse model using NK-92 cells.

Materials and Methods

Cell lines. The Jurkat and NK-92 cell lines were obtained from American Type Culture Collection (ATCC, Manassas, VA). The MOLT-4 and 697 cell lines were kindly provided to us by the laboratory of Dr. Douglas Graham (Emory University). The Jurkat T cell clone used is heterogeneous in CD5 expression. The primary culture media for the Jurkat cell line was RPMI (Corning, Manassas, VA) with 10% fetal bovine serum (FBS) and 1% penicillin/streptomycin. For NK-92 cells, AIMV (Thermo Fisher Scientific, Waltham, MA) was used with 20% FBS, 1% penicillin/streptomycin and 1000 U/mL recombinant interleukin-2 (IL-2, PeproTech, Rocky Hill, NJ).

Primary Cells. Primary T cells were generously donated by the Chandrakasan laboratory at Emory University. These cells were isolated from PBMCs from healthy, consented donors. Cells were expanded

in X-VIVO 15 media (Lonza, Switzerland) with 10% FBS, 1% penicillin/streptomycin/amphotericin B (Lonza, Switzerland), 50 ng/mL IL-2 (PeproTech, Rocky Hill, NJ) and 5 ng/mL IL-7 (PeproTech, Rocky Hill, NJ).

Cloning of the CD5-CAR sequences. The CD5 scFv cDNA sequence was derived from a humanized murine immunoglobulin protein sequence targeting CD5 (272). The variable heavy and variable light sequences were joined by a (G4S)₃ peptide linker. The CD5 VLR cDNA sequence was generated from a published protein sequence of a VLR targeting CD5 (270). Both cDNA sequences were then codon optimized for human cell expression and subcloned into a vector containing the remaining necessary components for CAR production, which were obtained by gene synthesis from Genewiz (South Plainfield, NJ). We used a bicistronic construct to allow for dual expression of enhanced green fluorescent protein (eGFP) and the CD5-CAR using a P2A peptide sequence. The BCL-VLR-CAR control was cloned by substituting the CD5-VLR for the BCL-VLR into the CAR cassette as previously described (55).

Generation of CAR encoding lentiviral vector. High-titer, recombinant, self-inactivating (SIN) HIV lentiviral vector was produced using a four-plasmid system. Briefly, the expression plasmid encoding the CD5-CAR constructs and BCL-VLR-CAR construct, as well as packaging plasmids containing the gag, pol, and envelope (VSV-g) genes were transiently transfected into HEK-293T cells by calcium phosphate transfection. Cells were cultured in DMEM (Thermo Fisher Scientific, Waltham, MA) supplemented with 10% FBS and 1% penicillin/streptomycin. Twenty-four hours after transfection, the cell culture medium was replaced with fresh medium. At 48 and 72 hours the vector supernatant was collected, filtered through a 0.22 μm filter and stored at -80°C . After the final collection, the vector supernatant was pooled and concentrated overnight via centrifugation at 10,000 x g at 4°C . Pelleted vector was then re-suspended in serum-free StemPro media (Thermo Fisher Scientific, Waltham, MA). Titering was performed on HEK-293T cell genomic DNA using quantitative polymerase chain reaction (qPCR). Titers of the concentrated recombinant viral vectors to be $\sim 1 \times 10^7$ TU/mL.

Lentiviral vector transduction of cell lines. Transduction of recombinant HIV-1-based lentiviral vector particles was carried out by incubating cells with vector in appropriate culture medium supplemented with 6 µg/mL polybrene (EMD Millipore, Billerica, MA), unless otherwise stated. Twenty-four hours after transduction, culture medium was replaced with fresh medium. The transduced cells were then cultured for at least 3 days before being used for downstream applications. Jurkat T cells were transduced at multiplicity of infection (MOI) ranging from 1 to 20.

Lentiviral vector spinoculation of primary T cells. Transduction of recombinant HIV-1-based lentiviral vectors was carried out by incubating cells with vector in appropriate culture medium supplemented with 5 µg/mL polybrene (EMD Millipore, Billerica, MA) and then centrifuged at 3000 RPM for 2.5 hours. Twenty-four hours after spinoculation, culture medium was replaced with fresh medium. The transduced cells were then cultured for at least 3 days before being used for downstream applications.

Flow cytometry analysis and sorting. Analysis was done using a BD FACS Canto II Flow Cytometer and BD LSRII Flow Cytometer (BD Biosciences, San Jose, CA). Data was analyzed using the BD FACSDiva software and FlowJo, LLC. Antibodies used included anti-CD69 APC-Cy7 and anti-CD5 PerCP/Cy5.5 (BD Biosciences, San Jose, CA). Additionally, a CD5-Fc fusion protein was used to detect CD5-CAR surface expression through binding of the CAR to the CD5 portion of the protein (G&P Biosciences, Santa Clara, CA). A secondary anti-IgG-Fc conjugated to PE was used to detect the CD5-Fc (Jackson Immunoresearch Laboratories, West Grove, PA). For the cytotoxicity studies, target cells were stained with the membrane dye PKH26 and cell death was assessed using 7-AAD (described below). Flow sorting for CD5 and eGFP was performed using a SH800S Cell Sorter (Sony Biotechnology Inc. U.S., San Jose, CA).

Western blotting with CD3ζ and CD5 antibodies. Cells were lysed using RIPA buffer (Sigma-Aldrich, St. Louis, MO). Cell lysates were clarified by centrifugation and protein was quantified using the Pierce™

BCA Protein Assay Kit (Thermo Fisher Scientific, Waltham, MA). Equal quantities of protein were loaded and cell lysates were separated by SDS-PAGE under reducing conditions and transferred to a nitrocellulose membrane (Bio-Rad Laboratories, Hercules, CA). The protein-loaded and blocked membrane was incubated with an anti-CD3 ζ mAb (1:500) or anti-CD5 mAb (0.5 μ g/mL) followed by a HRP-labeled goat anti-mouse IgG secondary Ab (1:2500) or HRP-labeled anti-goat IgG secondary Ab (1:1000), respectively.

Cytotoxicity assay. Target cells were labeled with membrane dye PKH26 using the manufacturer's protocol (Sigma-Aldrich, St. Louis, MO). Effector cells were left unstained. Effector (E) and target (T) cells were counted and viability assessed using trypan blue. Labeled target cells were mixed with effector cells in 12x75 mm FACS tubes at E:T ratios ranging from 0:1 to 10:1 in a total volume of 200 μ L. Target cells (50,000) were added to 12x75mm FACS tubes along with the corresponding number of effector cells. The cell mixture was incubated for 4 hours at 37°C in 5% CO₂. After incubation, cells were washed and stained with 7-AAD (BD Biosciences, San Jose, CA). Flow cytometry analysis was performed to assess 7-AAD positive cells. All experiments were performed in triplicate. To calculate specific cytotoxicity, the number of spontaneously lysed target cells in the absence of effector cells was subtracted from the number of dead target cells, which were identified as PKH26 and 7-AAD double positive in the measured sample.

Real time quantitative PCR. Genomic DNA was extracted using the Qiagen DNeasy Blood & Tissue Kit according to the manufacturer's recommended protocol (Qiagen, Germantown, MD). Oligonucleotide primers were designed for a 150bp amplicon of the Rev-response element (RRE). Real-time PCR was performed in an Applied Biosystems® StepOne™ System (Thermo Fisher Scientific, Waltham, MA) in 25 μ L reaction volumes using 50 ng of template DNA, using the default thermocycler program for all genes: 10 minutes of pre-incubation at 95°C followed by 40 cycles of 15 seconds at 95°C and one minute at 60°C.

Transfection of Jurkat T cells and primary T cells. Jurkat T cells and primary T cells were transfected using the Lonza Nucleofector 2b Device and the Amaxa Cell Line Nucleofector Kit V or the Amaxa Human

T Cell Nucleofactor kit, respectively, according to the manufacturer's protocol (Lonza, Switzerland). Cells were transfected with 6 µg of a single plasmid CRISPR-Cas9 system encoding both the guide RNA (gRNA) and Cas9. By day 5 post-transfection, the CD5 knockout was confirmed using BD LSR II Flow Cytometer (BD Biosciences, San Jose, CA).

Tracking of Indels by DEcomposition (TIDE) analysis of genome editing. Genomic DNA was isolated using the Qiagen DNeasy Blood & Tissue Kit according to the manufacturer's recommended protocol (Qiagen, Germantown, MD). Naïve Jurkat genomic DNA and CD5-edited Jurkat genomic DNA samples were sequenced by GeneWiz (South Plainfield, NJ) using primer sequences that flanked the predicted Cas9 cut site within the CD5 gene. The sequencing traces were uploaded into the TIDE software as well as the guide RNA sequence. Parameters were adjusted to fit the uploaded sequences and indels +/- 10 bp were analyzed. Sequencing and analysis of forward and reverse amplifications confirmed the results.

Co-culture assay using CAR-modified effector T cells and naïve target T cells. Naïve and CD5-edited Jurkat T cells were transduced by incubating with high titer, recombinant, SIN lentiviral vectors encoding eGFP-P2A-CD5-scFv-CAR or eGFP-P2A-CD5-VLR-CAR at MOI 5. After 24 hours, culture medium was replaced with fresh medium. On day 5 after transduction, flow cytometry using BD LSR II Flow Cytometer (BD Biosciences, San Jose, CA) confirmed eGFP expression. The same day, transduced cells were cultured with naïve Jurkat T cells labeled with Violet Proliferation Dye 450 (VPD450) at effector (E) to target (T) ratios of 2:1, 1:1 and 1:5. The final concentration of each culture was 5×10^5 cells/mL. Naïve Jurkat T cells were labeled according to the manufacturer's protocol (BD Biosciences, San Jose, CA). Flow cytometry was used to analyze changes in CD5 on the effector and target cells, as well as CD69 expression on effector cells at 24 hours after initiation of the co-culture. All experiments were performed in triplicate.

Generation of a T-cell leukemia murine xenograft model and treatment with CD5-CAR expressing NK-92 cells. NOD/SCID/IL2R γ null (NSG) mice were purchased from The Jackson Laboratory (Bar Harbor,

ME) and were maintained in a specific pathogen-free environment. Mice were cared for according to the established principles of the Institutional Animal Care and Use Committee (IACUC) and all animal protocols were approved by the IACUC. A luciferase-expressing Jurkat T-cell leukemia cell line was kindly provided to us by Dr. Douglas Graham (Atlanta, GA). All intravenous injections were performed using retro-orbital injections. To determine the treatment dosing regimen with NK-92 cells, we intravenously injected NSG mice with non-irradiated CD5-scFv-CAR NK-92 cells without supplementation of IL-2 and followed persistence of the NK-92 cells over time. Mice were evaluated for evidence of NK-92 cells by flow cytometry in peripheral blood, bone marrow and spleen 1, 3, and 18 days post injection. Based on results from this experiment, a twice-weekly dosing regimen for non-irradiated NK-92 cells without IL-2 supplementation was established.

Seven- to nine-week-old NSG mice were then intravenously injected with 2×10^6 luciferase-expressing Jurkat T cells on day 0 to establish disease. Cells were re-suspended in 100uL phosphate buffered saline (PBS) prior to injection. Treatment was started on day 7 after tumor injection. There were four treatment groups; mice either received PBS (control), unmodified naïve NK-92 cells, CD5-VLR-CAR NK-92 cells or CD5-scFv-CAR NK-92 cells. For mice receiving cells, each treatment consisted of 10^7 NK-92 cells re-suspended in 100 uL PBS administered intravenously. Each mouse received 4 treatments on days 7, 11, 14 and 18. Mice underwent *in vivo* bioluminescence imaging every seven days to monitor tumor burden. Animals were monitored frequently and were euthanized upon signs of leukemia progression (weight loss >20%, decreased activity, and/or hind limb paralysis).

In vivo bioluminescence imaging. NSG mice were anesthetized with inhaled isoflurane and maintained with 2% isoflurane during imaging procedures. Bioluminescence imaging was performed with the IVIS® Spectrum imaging system (PerkinElmer, Boston, MA). Each mouse was given an intraperitoneal injection of 150 mg/kg D-luciferin (PerkinElmer, Boston, MA) dissolved in PBS. Images were captured 10-15 minutes after the D-luciferin injection. Bioluminescence intensity was quantified using the Living

Image® advanced *in vivo* imaging software. Total flux values were determined by drawing regions of interest (ROI) of identical size over each mouse and are presented in photons/second.

Statistical analysis. Unpaired 2-tailed Student *t* test and One-way ANOVA were used to determine statistical significance. For *in vivo* survival data, Kaplan–Meier curves were plotted and compared using a log-rank test. A *p*-value of <0.05 is considered statistically significant for all studies unless otherwise stated. All statistics were calculated with SigmaPlot, version 13.0 (Systat Software, Chicago, IL).

Results

Construction of CD5-directed CARs

The CD5-VLR-CAR (previously described (55)) was generated using a VLR protein sequence shown to be specific for the CD5 antigen (270). The sequence for the CD5-scFv was generated using a published humanized murine immunoglobulin protein sequence (272), and the cDNA sequence designed to express the scFv was codon optimized for human cell expression. The C-terminus of V_H was joined with the N-terminus of V_L using a 15 bp linker encoding a glycine and serine pentapeptide repeat (G4S)₃ (273). The entire CD5-scFv sequence totaled 720 bp compared to the shorter 570 bp CD5-VLR sequence. The two CD5 sequences were cloned into the CAR cassette, which is a second-generation CAR composed of an N-terminal IL-2 signal peptide followed by the CD5-VLR or -scFv antigen binding domain, the transmembrane and intracellular domains of CD28, and the intracellular signaling domain of CD3ζ (**Fig. 1A**). A bicistronic vector co-expressing eGFP and the CD5-CAR via a self-cleaving 2A peptide sequence (P2A) was used to enable selection of positively transduced cells by flow sorting (**Fig. 1B**).

CD5-CAR NK-cell mediated cytotoxicity

To demonstrate CAR-directed cytotoxicity, the well-characterized cytotoxic human NK cell line, NK-92, was used, which is an interleukin-2 (IL-2) dependent immortalized cell line that has maintained its

Figure II-1: Schematic of CAR structures containing the CD5-directed variable lymphocyte receptor (VLR) or single-chain variable fragment (scFv).

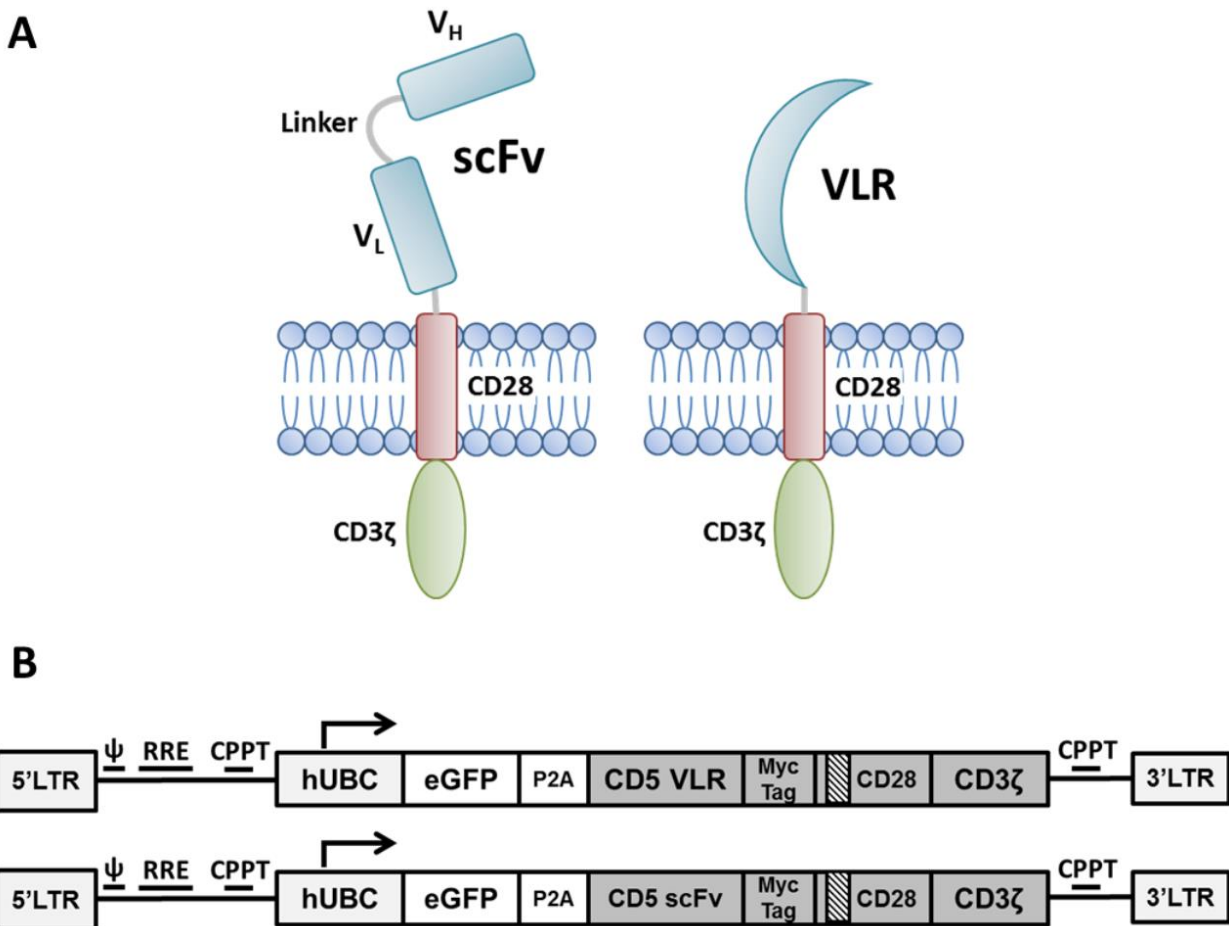


Figure 1: (A) Second generation CAR structures with CD28 containing a scFv (left) or VLR (right) as the antigen recognition domain. (B) Schematics of the bicistronic transgene sequences used for expressing enhanced green fluorescent protein (eGFP) and the CD5-CARs using a p2a sequence. It includes a 5' long terminal repeat (LTR), human ubiquitin C promoter (hUBC), eGFP sequence, p2a sequence, an interleukin-2 signal peptide (IL-2 SP), the CD5-VLR (top) or CD5-scFv (bottom), a myc epitope tag, the CD28 region, the CD3 ζ intracellular domain and a 3' LTR.

cytotoxic capabilities (121). NK-92 cells do not display CD5 on their surface, and this allows for expression of the CD5-CAR without self-activation and fratricidal killing of transduced cells. Generation of the CD5-VLR-CAR-expressing NK-92 cell line has been previously described (55). To generate CD5-scFv-CAR expressing NK-92 cells, they were transduced with the bicistronic construct expressing eGFP and the CD5-scFv-CAR. As expected, poor transduction efficiency (< 5%) was observed after the initial lentiviral vector transduction. As with the CD5-VLR-CAR-expressing NK-92 cells, flow sorting was used to generate a CD5-scFv-CAR expressing NK-92 cell line using eGFP as a selection marker for positively transduced cells. After two rounds of flow sorting for eGFP, a CD5-scFv-CAR expressing NK-92 population was generated with 99% eGFP expression (**Fig. 2A**). qPCR analysis demonstrated an average of 1.0 transduced gene copy/cell in the sorted and expanded cells. To confirm CD5-CAR expression in the flow sorted NK-92 cell lines, western blot analysis was performed using a CD3 ζ antibody. Bands of 48 and 55 kDa were visible corresponding to the CD5-VLR-CAR and CD5-scFv-CAR proteins respectively (**Fig. 2B**). To assess their cytotoxic potential, CD5-CAR expressing NK-92 effector (E) cells were cultured with CD5-positive Jurkat and MOLT-4 T-cell leukemia target (T) cells at varying E:T ratios. The CD5-negative B-cell leukemia cell line 697 was used as a negative control. The target cells were pre-labeled with the membrane dye PKH26, which allowed for easy distinction from the non-labeled effector cells using flow cytometry. Cytotoxicity was measured via uptake of 7-AAD, a marker for cell death, into target cells (274). A significant increase in cytotoxicity was observed with the CD5-CAR expressing NK-92 cells compared to naïve NK-92 cells, even at the lowest E:T ratios ($p < 0.01$ for all cell groups) (**Fig. 2C and 2D**). Greater cytotoxicity was observed in the CD5-scFv-CAR group at the higher E:T ratios, however, the difference in cytotoxicity was not significant between the VLR-CAR and scFv-CAR at the lower 1:1 E:T ratio. No increase in cytotoxicity was seen when the CD5-CAR NK-92 cells were tested against the CD5-negative 697 cell line (**Fig. 2E**).

CD5 CAR-directed T-cell activation

Figure II-2: NK-92 cell-mediated cytotoxicity against a CD5-positive T-ALL cell line using CD5-CARs.

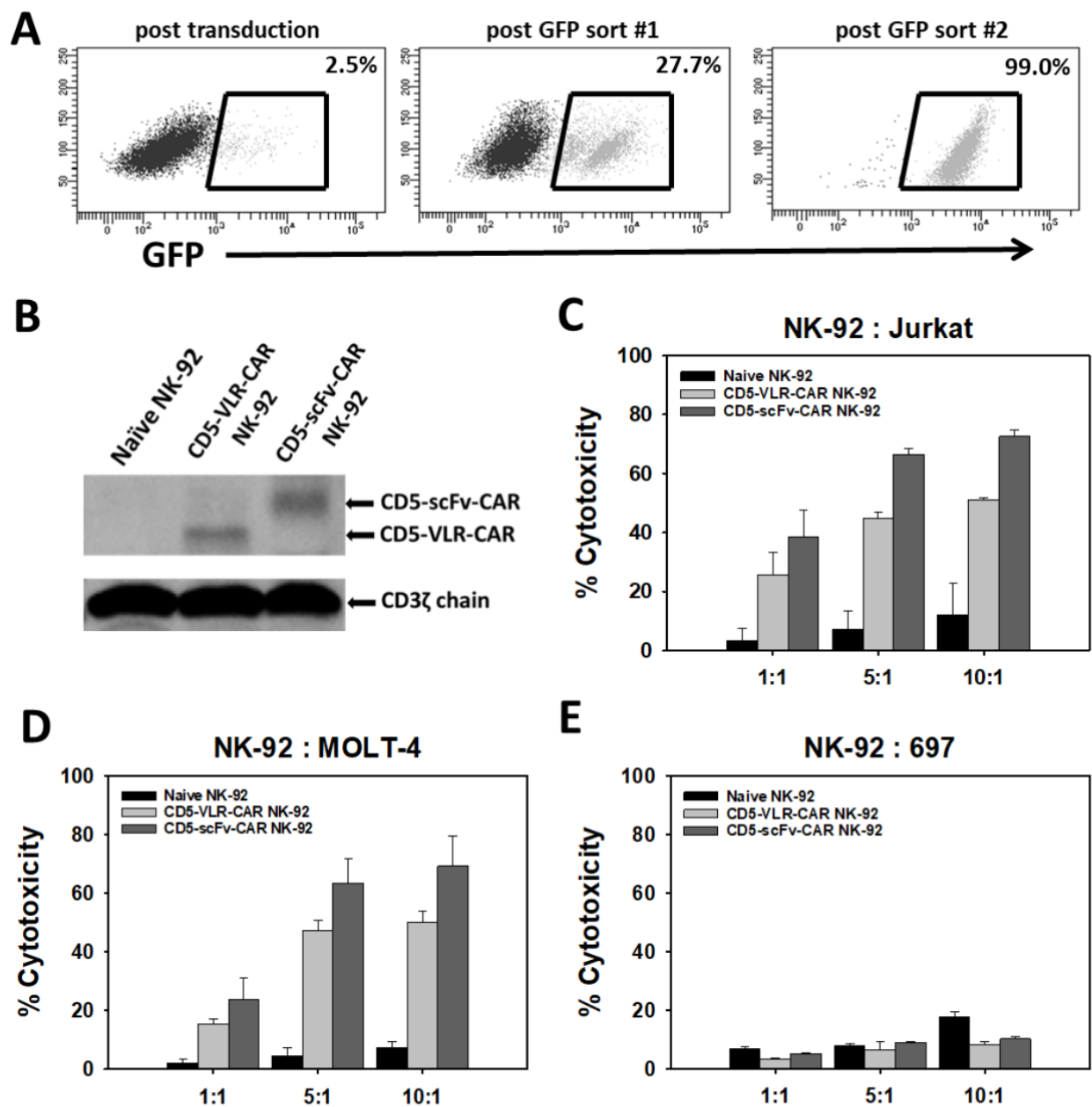


Figure 2: (A) NK-92 cells were transduced with the eGFP-P2A-CD5-scFv-CAR lentiviral vector and sorted for GFP-expressing cells. After two rounds of sorting an enriched population of CAR-expressing NK-92 cells was generated with 99% eGFP expression. (B) Western blot using anti-CD3ζ antibody on

whole cell lysates of NK-92 cells shows the presence of CD5-VLR-CAR and CD5-scFv-CAR protein in the sorted and expanded cells. (C & D) Both CD5-CAR expressing NK-92 cells were mixed with CD5-positive target cells, Jurkat and MOLT-4 cells, at various ratios and the percent cytotoxicity of the Jurkat T cells was measured by flow cytometry. CD5-CAR modified NK-92 cells showed a significantly greater cytotoxicity ($p < 0.01$) against the CD5-positive Jurkat and MOLT-4 cells when compared to unmodified NK-92 cells in a four-hour assay. (E) No increase in cytotoxicity is seen when CD5-CAR NK-92 cells are cultured with CD5-negative 697 cells. Errors bars represent standard deviations.

In order to analyze the effect of CD5-CARs on T cells, the CD5-positive Jurkat T-cell leukemia line was transduced with the lentiviral vector encoding eGFP and a CD5-CAR at MOIs ranging from 1 to 20. To measure T-cell activation induced by engagement of CD5-CARs with CD5 on neighboring cells, surface expression of the T-cell activation marker, CD69, was measured by flow cytometry 4 and 12 days after transduction (**Fig. 3A**). The degree of activation correlated with the transduction vector amount, with increasing activation in a dose-dependent manner. Higher activation was observed in the CD5-VLR-CAR expressing Jurkat T cells compared to those expressing the CD5-scFv-CAR, and no activation was observed in eGFP negative cells (**Fig. 3B and S1**). To confirm integration of the CD5-CAR transgene into the Jurkat T-cell genome, proviral vector copy number (VCN) was measured using quantitative PCR. Increases in VCN were correlated with increases in vector amount and increases in activation (**Fig. 3C**). The CD5-VLR-CAR Jurkat T cells had a higher VCN compared to the CD5-scFv-CAR cells at corresponding MOIs (data not shown), which is likely the reason for the slightly higher activation observed in the CD5-VLR-CAR cells (**Fig. 3B**). When comparing the activation between the two CD5-CAR-modified cell populations as a function of VCN, we found a linear correlation in both groups ($R^2 = 0.91$ for CD5-VLR-CAR, $R^2 = 0.82$ for CD5-scFv-CAR) and the CD5-scFv-CAR cells exhibited higher activation compared to the CD5-VLR-CAR cells (**Fig. 3C**). As a means of measuring CD5-CAR protein expression in the transduced T cells, Western blot analysis was performed on whole cell lysates 9 days after transduction. CD5-CAR proteins were detected using an anti-CD3 ζ antibody. Proteins of approximately 48 and 55 kDa were observed, which corresponded to the predicted sizes of the CD5-VLR-CAR and CD5-scFv-CAR respectively, as well as an 18 kDa band, which corresponded to the molecular weight of the endogenous CD3 ζ protein known to be expressed in Jurkat T cells (**Fig. S2**). CAR expression increased in a vector MOI-dependent manner. On day 12 post-transduction, activation and VCN were measured again in both CD5-CAR-expressing Jurkat T-cell populations. A decrease in VCN from day 4 to day 12 was observed, as was a corresponding decrease in CD69 expression (**Fig. 3D and S3**). Although this decrease in Jurkat T-cell activation and VCN can, in part, be due to pseudo transduction, it also likely results from the faster proliferation rate of non-modified cells compared to CD5-CAR expressing cells, as well as from activation-induced cell death resulting from

Figure II-3: Initial comparison of VLR- and scFv-based CD5-CARs.

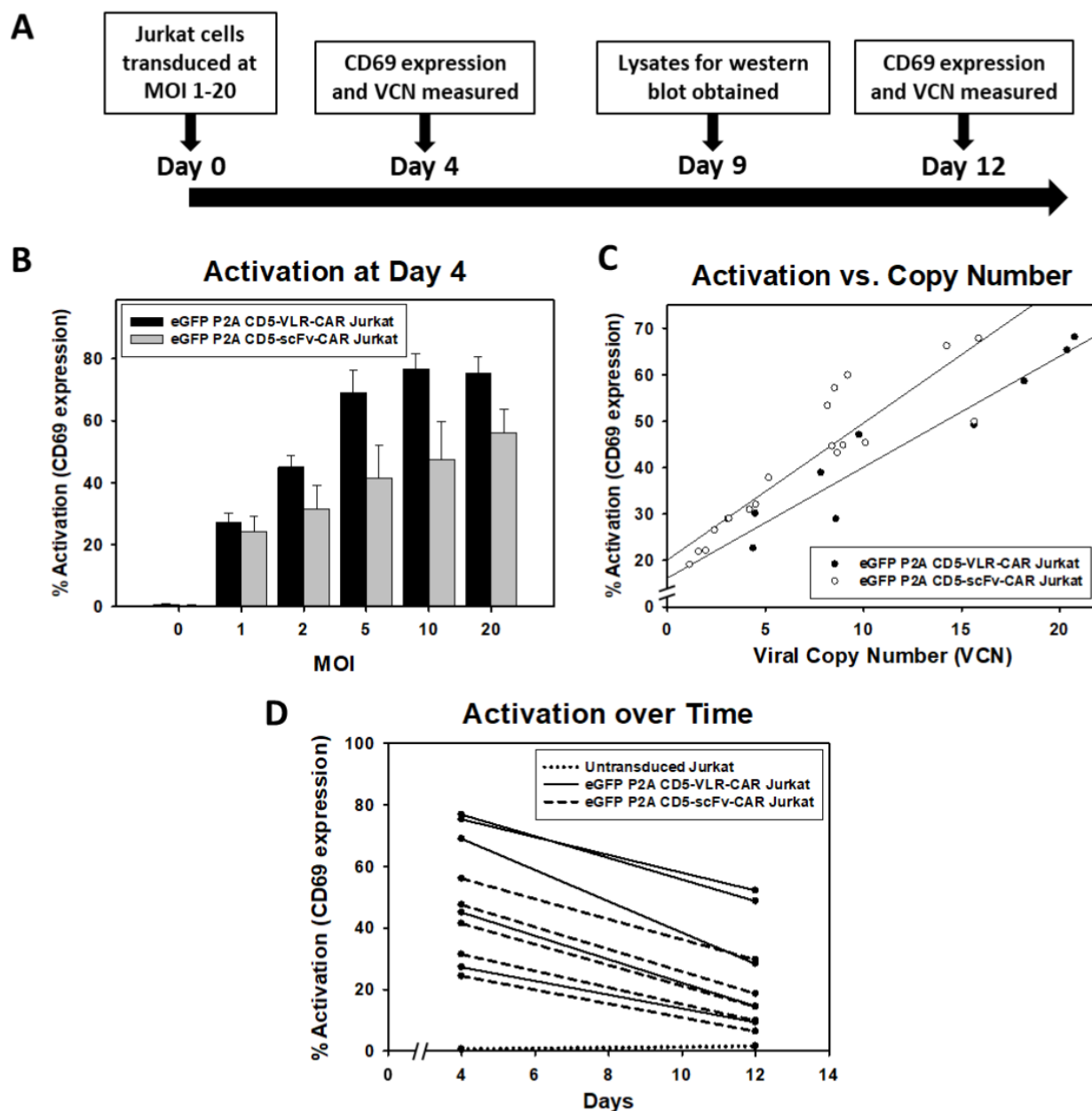


Figure 3: (A) Jurkat T cells were transduced with lentiviral vectors encoding either an scFv- or VLR-based CD5-CAR with co-expression of eGFP. Schematic of the Jurkat T-cell activation assay shows time points for measurement of T-cell activation and Western blot analysis. (B) Activation measured by surface CD69 expression four days after transduction increased as the amount of viral vector increased. Greater activation

was observed in CD5-VLR-CAR Jurkat cell group. (C) The percentage of activated cells was compared to the vector copy number (VCN) obtained for each transduced population of cells. The inset to the figure defines each group. (D) CD69 expression was measured 4 and 12 days after transduction, which showed activation decreased over time in both CD5-CAR expressing Jurkat cell groups. Errors bars represent standard deviations.

continuous activation of the transduced cell population through interactions with CD5 antigen on self and neighboring cells.

CD5 knockout in Jurkat T cells using CRISPR-Cas9 genome editing

To increase the effectiveness of anti-CD5-directed CAR T cells, we knocked out CD5 expression in Jurkat T cells using CRISPR-Cas9 genome editing. In T cells, only full-length CD5 protein is expressed. However, in CD5-positive B cells, alternative splicing of exon 1 results in an alternate exon, termed exon 1B, that encodes a truncated, cytosolic CD5 protein (275). We reasoned that targeting sequences early in the gene, upstream of the splice site, would generate a non-functional protein product and avoid the alternative splicing event. Although T cells do not express exon 1B naturally, a balance between the expression of exon 1A and exon 1B has been implicated in T cells, which may occur if exons downstream to 1A are edited (275). We generated three gRNAs with different targeting sequences within the first 100 bp of exon 1A to knockout CD5 expression. Each gRNA was expressed in conjunction with Cas9, derived from *Streptococcus pyogenes*, on a single plasmid. Using nucleoporation, we transfected naïve Jurkat T cells with each CRISPR-Cas9 construct and determined the percentage of CD5-negative cells five days after transfection. CD5-CRISPR gRNA #2 yielded the greatest increase in CD5-negative Jurkat T cells, resulting in 48% CD5-negative cells, compared to the mock transfected cells, which is a clone that is naturally 15% CD5-negative. gRNA #1 and gRNA #3 resulted in 38% and 24% CD5-negative cells, respectively (**Fig. 4A**). Using COSMID (CRISPR Off-target Sites with Mismatches, Insertions, and Deletions), a public webtool, we were able to predict sites within the human genome that had the most likelihood of being targeted by our CRISPR system (276). Using the same search parameters, we identified potential off-target sites that could result from using gRNAs #1 and #2; gRNA #1 was predicted to have likely off-target sites in three genes, with one site being within the CD5 gene (separate location from the intended target site), and gRNA #2 was predicted to have likely off-target sites only within the CD5 gene. Given the more efficient CD5 knockout and decreased potential for off-target binding, gRNA #2 was used in subsequent experiments.

Figure II-4: CD5 knockout in Jurkat T cells using CRISPR-Cas9 genome editing.

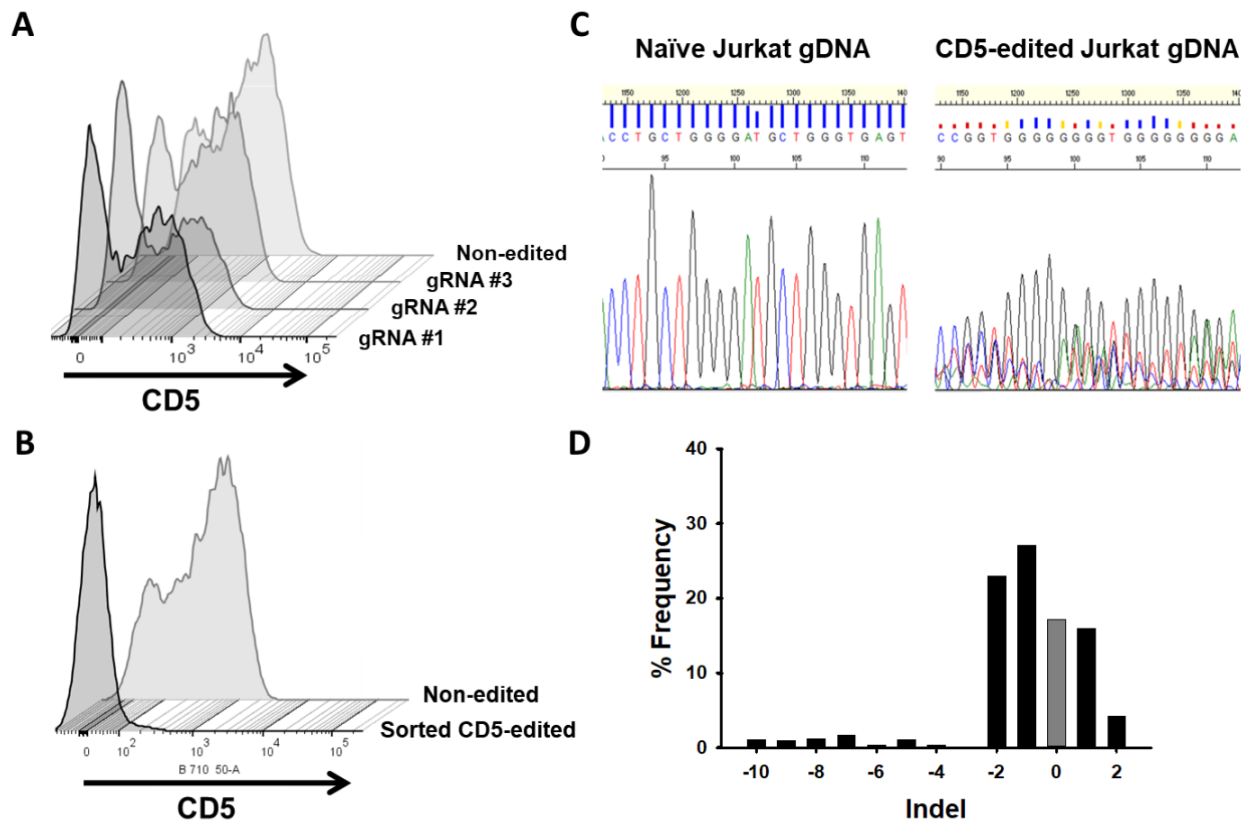


Figure 4: (A) CD5 expression, measure by flow cytometry, in Jurkat T cells five days following mock transfection or transfection with plasmid encoding Cas9 and one of three different gRNA target sequences. Histogram plots for CD5 expression in mock-transfected and transfected Jurkat T cells are shown along a single axis. (B) Overlay image of histogram plots of CD5 expression in naïve Jurkat T cells and flow-sorted CD5-negative Jurkat T cells that were transfected with the CD5-CRISPR gRNA #2. (C) Representative Sanger sequencing traces from naïve (top left) and sorted CD5-edited (top right) Jurkat T-cell genomic DNA PCR amplified for CD5. TIDE analysis of the frequency of indels within the CD5 gene after the predicted break-site generated by Cas9 (D). Results show 77% CD5-negative cells were edited with 27% having a -1 deletion.

Flow sorting allowed for the isolation and expansion of the population of CD5-negative Jurkat T cells from the mixed population of cells edited with CD5-CRISPR gRNA #2. Only 2.1% of sorted cells expressed CD5 (**Fig. 4B**). To characterize the frequency of mutations within the CD5-edited cells, we utilized TIDE (Tracking of Indels by DEcomposition) software. This analysis uses trace sequences generated by Sanger sequencing to identify the predominant insertions and deletions (indels) in CD5-edited Jurkat T-cell genomic DNA compared to naïve Jurkat T-cell genomic DNA. A representative section of the trace sequences is shown in **Fig. 4C**. Using a decomposition algorithm, the software identifies the frequency of indels around the break site (277). TIDE analysis indicated that within our sorted population of CD5-negative Jurkat T cells, 77% of the population was edited. Within the edited population, 27% have a -1 deletion, compared to naïve Jurkat T cells, and approximately 17% of the population was not edited (**Fig. 4D**). Although by flow cytometry we determined approximately 98% of the cells in this population are CD5-negative, some are not CRISPR-edited due to naturally occurring CD5-negative cells within our starting Jurkat T-cell population. Therefore, after sorting, approximately 17% of the collected cells, lack mutations in the genome but maintain their CD5-negative characteristics.

CD5-edited CAR-modified T cells have reduced self-activation and increased CD5-CAR expression

Naïve and sorted CD5-CRISPR-edited Jurkat T cells were transduced with the lentiviral vectors encoding eGFP and the CD5-CARs. Additionally, a third lentiviral vector encoding eGFP and BCL-VLR-CAR was used as a negative control. We previously showed the BCL-VLR-CAR expressed in Jurkat T cells does not stimulate T-cell activation in the absence of BCL cells (55). It was hypothesized that both CD5-CARs would activate naïve Jurkat T cells to a greater degree than CD5-edited Jurkat T cells, whereas the BCL-VLR-CAR would stimulate low and equivalent levels of T-cell activation in all Jurkat T cells. eGFP expression was used as a marker of transduced Jurkat T cells to identify the CAR-expressing cell population, and cells were transduced at MOIs of 1, 10 or 20. As expected, for all three vectors, there is an increase in eGFP-positive cells as the vector titer increases, and this increase is similar and consistent in both cell populations (**Fig. 5A and S4**). As the vector amount of CD5-CAR increased, there is a decrease

Figure II-5: CD5-edited CD5-CAR-modified Jurkat T cells have reduced self-activation and increased CD5-CAR expression.

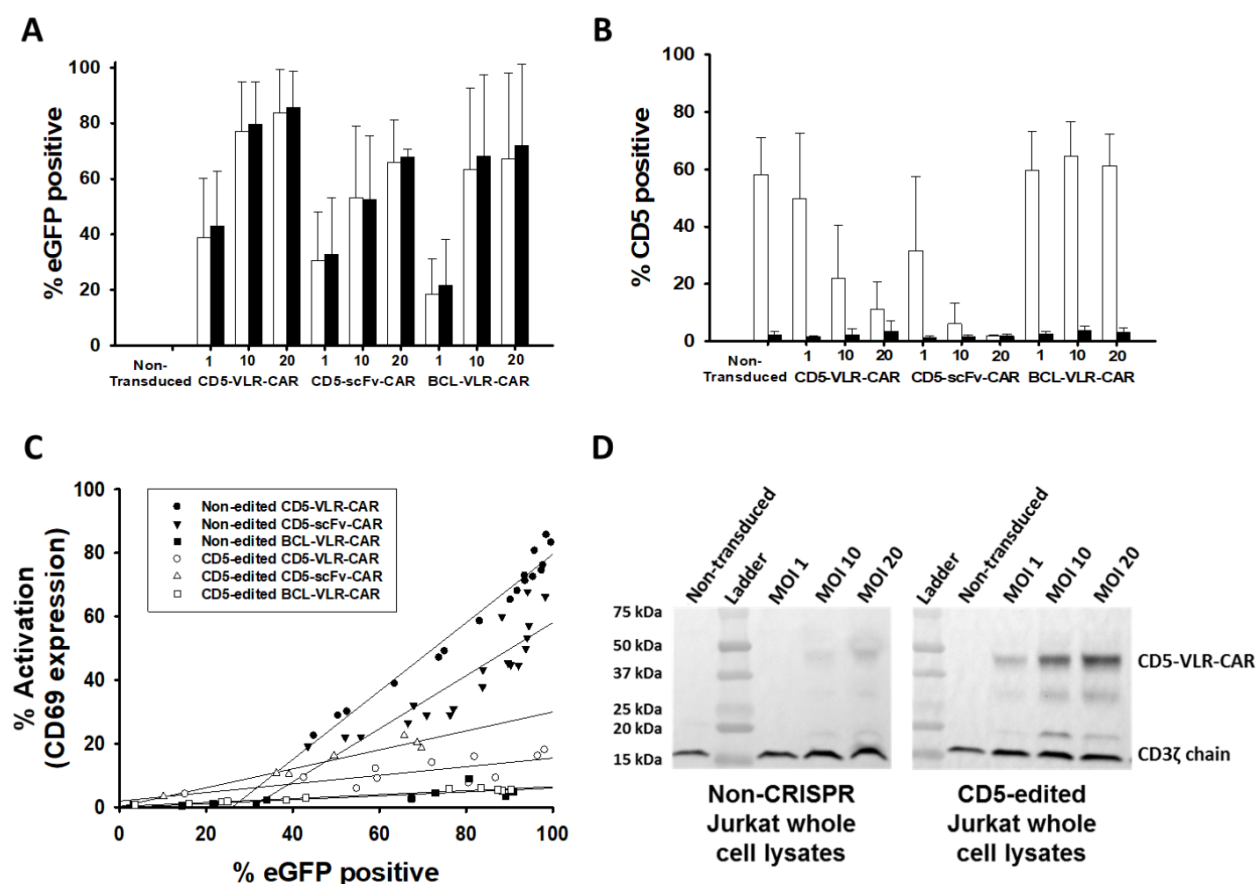


Figure 5: Naïve (white) and CD5-edited Jurkat T cells (black) were transduced with eGFP-p2a-CD5-VLR-CAR, eGFP-p2a-CD5-scFv-CAR or control eGFP-p2a-BCL-VLR-CAR lentiviral vectors at MOIs 1, 10 and 20. Polybrene was not used during transduction, which provided a greater separation in transduction efficiency between MOIs of 1 and 10. Experiments were performed with replicates of three or greater (error bars are generated using the standard deviation from the mean) except for CD5-scFv-CAR at MOI 10 and 20, which were performed in duplicate, providing the difference of the mean. **(A)** Transduction efficiency, measured by eGFP-positive cells, of each CAR vector at MOIs 1, 10 and 20 in both populations of Jurkat T cells. **(B)** CD5 expression in both populations of Jurkat T cells transduced with each CAR vector at each MOI. **(C)** Activation was measured by monitoring CD69 expression and transduction efficiency was

measured by eGFP expression. A correlation exists between activation and eGFP expression in CD5-CAR-transduced Jurkat T cells. Non-edited CD5-CAR-modified cells have increased T-cell activation compared to CD5-edited CD5-CAR-modified cells. **(D)** Western blots on whole cell lysates of non-edited Jurkat T cells (left) and CD5-edited Jurkat T cells (right) when transduced with each CAR vector, using a CD3 ζ antibody. Endogenous CD3 ζ is represented by the 18 kDa bands and CD3 ζ in the CAR construct is represented by the 48, 55, and 47 kDa bands in the CD5-VLR-CAR, CD5-scFv-CAR, and BCL-VLR-CAR constructs, respectively. eGFP, CD5 and CD69 surface expression were measured by flow cytometry.

in CD5 expression on non-edited Jurkat T cells (**Fig. 5B**). This decrease is most pronounced in CD5-scFv-CAR-modified Jurkat T cells. This effect was not observed in BCL-VLR-CAR-modified T cells, showing these results are a consequence of CD5-CAR expression, which is consistent with previously published results (5). Furthermore, we compared CD69 expression to eGFP expression in all cell groups. A positive correlation was observed between eGFP expression and activation in both the scFv- and VLR-based CARs, as well as in edited and non-edited cells (**Fig. 5C**). The increase in activation was dramatically dampened in CD5-edited cells expressing either the CD5-VLR-CAR or the CD5-scFv-CAR. The BCL-VLR-CAR only stimulated very low levels of T-cell activation.

Western blot analysis using whole cell lysates collected 9 days after transduction confirmed the decrease in CD5 expression in CD5-CAR-modified Jurkat T cells compared to naïve Jurkat T cells and BCL-CAR-modified Jurkat T cells (**Fig. S5A**). As expected, Western blot analysis showed CD5-edited Jurkat T cells have lower CD5 expression compared to non-edited cells for both transduced and non-transduced cells (**Fig. S5B**). We hypothesized that if the decrease in CD5 levels is due to interactions between the CD5-CAR and the CD5 cell surface protein, then CD5-CAR levels may also be influenced by CD5 expression. Therefore, cells with lower CD5 expression levels will have increased CD5-CAR protein expression due to reduced interactions with the CD5 antigen. To test this, we ran flow cytometry using a CD5-Fc fusion protein consisting of the CD5 antigen fused to the Fc portion of an IgG. Jurkat T cells were stained with the CD5-Fc protein and then stained a second time using an anti-IgG Fc antibody conjugated to phycoerythrin (PE). As expected, the CD5-scFv-CAR-modified CD5-edited Jurkat T cells bind CD5-Fc to a greater degree than do CD5-scFv-CAR-modified non-edited Jurkat T cells. This data also shows evidence of potential pseudo-transduction at day 4, however, CD5-Fc binding decreases by day 8 and then appears to plateau. (**Fig. S6A**). Significant differences are observed early after transduction, however they become less significant after CD5-CAR expression decreases in non-edited cells and normalizes. On day 8 post-transduction, 18.6% of non-edited Jurkat T cells were bound to CD5-Fc protein and eGFP, compared to 35.7% of CD5-edited Jurkat T cells (**Fig. S6B**).

Our experiments in Jurkat T cells serve as a basis for using primary T cells. We expanded primary T cells in media containing IL-2 and IL-7, and using the same CRISPR-Cas9 system used in Jurkat T cells, we knocked out CD5 expression in 38.6% of our primary T cells (**Fig. S7A and B**). We transduced non-edited and CD5-edited primary T cells with CD5-scFv-CAR lentiviral vector and measured eGFP and CD5-Fc binding via flow cytometry on day 9 post-transduction. Similar to our Jurkat T cell data, we show increased percentage of CD5-edited cells bound to CD5-Fc protein compared to non-edited cells, with 64.4% CD5-Fc-bound CD5-edited cells, compared to 6.1% CD5-Fc-bound non-edited cells (**Fig. S7C and D**).

The difference in CD5-Fc binding to edited compared to non-edited cells could be a result of steric hindrance from CD5 binding the CAR on non-edited cells, blocking CD5-Fc from binding the CAR, as opposed to reduced CAR expression on these cells. To test this, we performed Western blot analysis on Jurkat whole cell lysates using a CD3 ζ antibody to detect endogenous CD3 ζ (18 kDa) and CD3 ζ in the CAR constructs (48, 55, and 47 kDa in the CD5-VLR-CAR, CD5-scFv-CAR and BCL-VLR-CAR constructs, respectively). Importantly, using endogenous CD3 ζ as a reference, the CD5-edited Jurkat T cells express both CD5-CARs at greater levels compared to the non-edited Jurkat T cells (**Fig. 5D and S6C**). Furthermore, there is not an effect on BCL-CAR expression when comparing transduced cells with or without CD5 editing (**Fig. S6C**). We can conclude that non-edited Jurkat T cells have down-regulated CD5-CAR expression.

CD5-edited effector cells are efficiently stimulated by target T cells, which down-regulate CD5

We hypothesized that culturing CD5-CAR-modified effector cells with naïve Jurkat T cells would result in i) an increase in non-edited effector CD5 expression because of competition between CD5 expressed on the CAR-modified cells and CD5 expressed on the target cells, ii) target cell down-regulation of CD5 expression and iii) increased activation of CD5-edited effector cells compared to non-edited cells. Non-edited and CD5-edited Jurkat T cells were transduced with lentiviral vector encoding CD5-scFv-CAR or CD5-VLR-CAR at an MOI of 5. Flow cytometry five days after transduction confirmed eGFP

expression, as well as an expected decrease in CD5 expression on the non-edited Jurkat T cells (as previously demonstrated in **Fig. S4 and S5**). Naïve Jurkat T cells were labeled with Violet Proliferation Dye 450 (VPD450) to distinguish target cells from effector cells, and subsequently cultured with the CAR-modified effector cells at E:T ratios of 2:1, 1:1 and 1:5. After 24 hours, cells were collected and flow cytometry was used to measure CD5 expression on the effector and target cells, as well as CD69 expression on the effector cells. CD5 expression was low in effector cells in edited and non-edited transduced cells when co-cultured with target cells (**Fig. S8**), showing there is little effect on CD5 expression on the effector cells during co-culture. To compare CD5 expression in the target cells, the level of CD5 expression in VPD450-labeled naïve Jurkat T cells cultured alone was set as the baseline CD5 expression in the target cells. When in culture with CD5-scFv-CAR- (**Fig. 6A**) and CD5-VLR-CAR-modified effector cells (**Fig. 6B**), CD5 expression decreased in the target cells, with a greater decrease observed in target cells cultured with the CD5-scFv-CAR-edited cells. At E:T ratios of 2:1 and 1:1, there is a significant difference in target cell CD5 expression between the groups cultured with CD5-edited CD5-scFv-CAR-effector cells (**Fig. 6A**) and CD5-edited CD5-VLR-CAR-effector cells (**Fig. 6B** (2:1: $p = 0.001$, 1:1: $p < 0.001$)). Additionally, significant differences in target cell CD5 expression were found at all E:T ratios comparing the non-edited effector cell group and the CD5-edited effector cell group ($p < 0.05$). However, at low E:T ratios (high percentage of target cells relative to effector cells), the decrease in CD5 expression was less pronounced (**Fig. 6A and 6B**, E:T ratio of 1:5 $p = 0.028$ and $p = 0.045$ in CD5-scFv-CAR-effector cell cultures and CD5-VLR-CAR-effector cell cultures, respectively). These results show CD5-edited CAR-modified effector T cells have increased association with the target cells compared to non-edited, CAR-modified effector T cells, which results in the dramatic decrease in CD5 expression on the target cells. To determine if there are differences in effector cell activation, CD69 expression was measured. At all E:T ratios, CD5-edited, CD5-scFv-CAR- (**Fig. 6C**) and CD5-edited, CD5-VLR-CAR-modified (**Fig. 6D**) effector T cells had a significant increase in activation compared to their activation prior to culture with naïve target cells (**Fig. 6C and 6D**, $p < 0.05$ for all ratios). A control experiment measuring the same parameters using non-CAR-modified, CD5-edited effector cells demonstrated the cells alone had no effect (data not shown). This

Figure II-6: CD5-edited CD5-CAR-modified effector cells in culture with naïve target T cells stimulates effector-cell activation and target cell down-regulation of CD5.

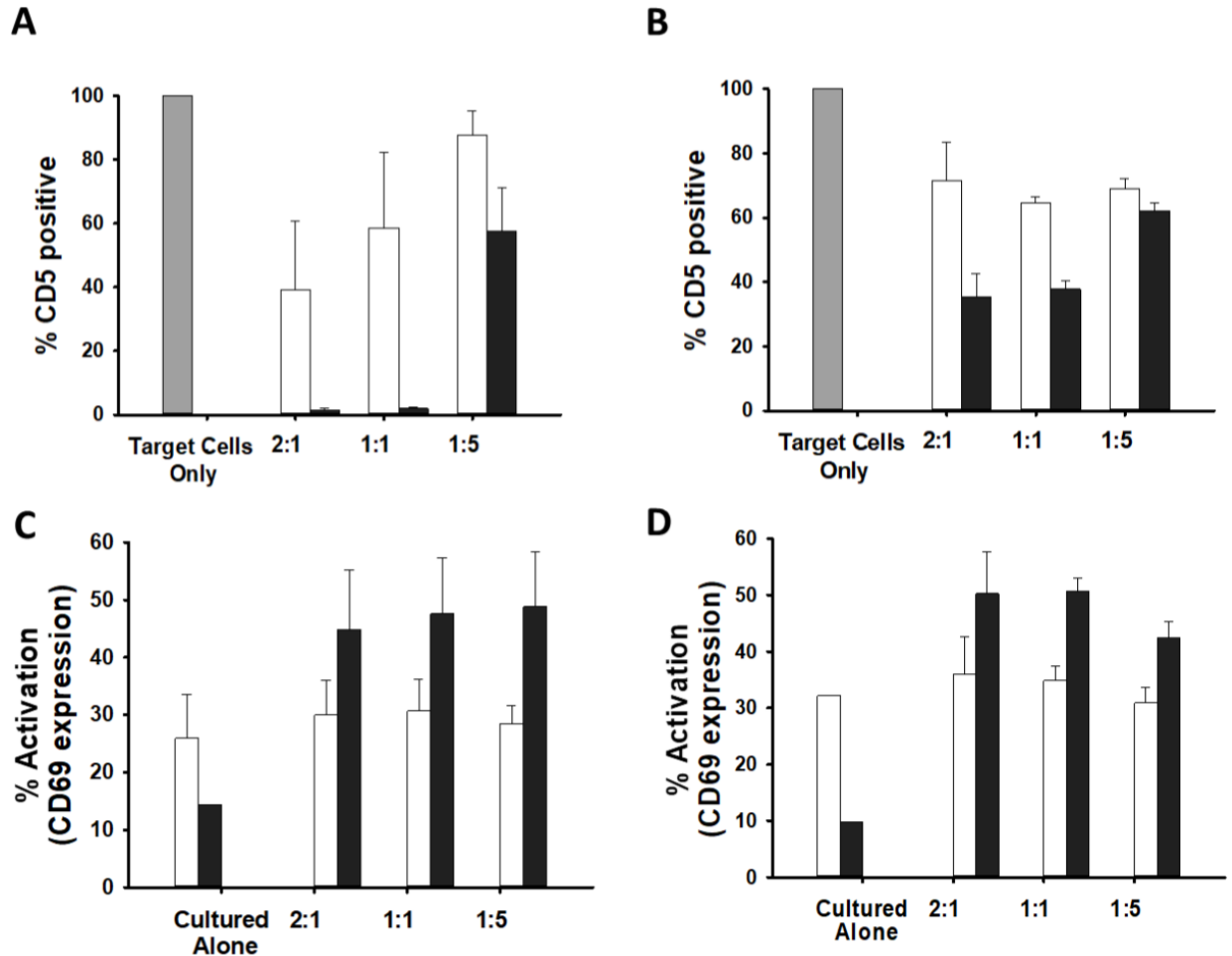


Figure 6: Naïve and CD5-edited Jurkat T cells were transduced with eGFP-p2a-CD5-scFv-CAR or eGFP-p2a-CD5-VLR-CAR lentiviral vectors at MOI 5. Polybrene was not used during transduction. Target naïve Jurkat T cells were labeled with VPD450. On day five post-transduction, effector cells were cultured with labeled target cells at E:T ratios 2:1, 1:1 and 1:5. The cells were analyzed by flow cytometry 24 hours later. White bars signify non-edited effector cells; black bars signify CD5-edited effector cells. Experiments were performed with three replicates and error bars represent standard deviation from the mean. **(A and B)** Percent of baseline CD5 expression in target Jurkat T cells cultured with non-edited and CD5-edited

effector Jurkat T cells expressing (A) the CD5-scFv-CAR or (B) the CD5-VLR-CAR. CD5 expression in target cells cultured alone (gray bar) was used as baseline and set at 100%. (C and D) T-cell activation of non-edited and CD5-edited effector Jurkat T cells expressing (C) the CD5-scFv-CAR or (D) the CD5-VLR-CAR when cultured alone and in culture with target Jurkat T cells.

data illustrates CD5-edited effector T cells have increased interactions with target cells compared to non-edited effector T cells, which results in an increase in effector cell activation.

CD5-scFv-CAR NK-92 cells are superior to CD5-VLR-CAR NK-92 cells in delaying disease progression in a xenograft T-cell leukemia mouse model

To further compare the cytotoxic potential of the two CD5-CAR structures, we tested the efficacy of the CD5-CAR expressing NK-92 cells in a T-cell leukemia xenograft mouse model. Luciferase-expressing Jurkat T cells were used to establish our leukemia model, which allowed for monitoring of tumor burden using bioluminescence imaging. Treatment was started seven days after tumor injection as described in the Materials and Methods section. NK-92 cells were injected intravenously twice weekly for a total of 4 doses without any supplementation of IL-2. The twice-weekly dosing regimen was based on our experiments showing non-irradiated NK-92 cells, in the absence of IL-2, do not persist in the peripheral blood beyond three days, and show no evidence of engraftment in the bone marrow (**Fig. S9**). A significant decrease in tumor burden was evident in the CD5-scFv-CAR NK-92 treatment group at Day 21 ($p = 0.02$ using one-way ANOVA) (**Fig. 7A and 7B**). Significance ($p < 0.05$) for multiple comparisons tests by Holm-Sidak method was shown for CD5-scFv-CAR vs saline, and CD5-scFv-CAR vs naïve NK-92 groups, but not for the CD5-scFv-CAR vs CD5-VLR-CAR group. A similar overall trend was observed at days 14 and days 28 in terms of disease burden, however the one-way ANOVA test was underpowered to compare all groups. Although only modest effects were observed, as expected due to the cell dose and persistence of the NK-92 cells, the scFv-CAR-treated group had a significant advantage in survival compared to all three other groups ($p = 0.003$ by log-rank test, $p < 0.05$ for all multiple comparisons tests between CD5-scFv-CAR and other groups by Holm-Sidak method) with a median survival of 49 days compared to 40, 41, and 42 days for the saline, naïve NK-92 and CD5-VLR-CAR NK-92 groups respectively (**Fig. 7C**). In contrast, the CD5-VLR-CAR-NK-92 mice did not exhibit a significant survival advantage over the saline- and naïve NK-92-treated groups.

Figure II-7: CD5-scFv-CAR NK-92 cells are superior to CD5-VLR-CAR NK-92 cells in delaying disease progression and improving survival in a T-ALL xenograft mouse model.

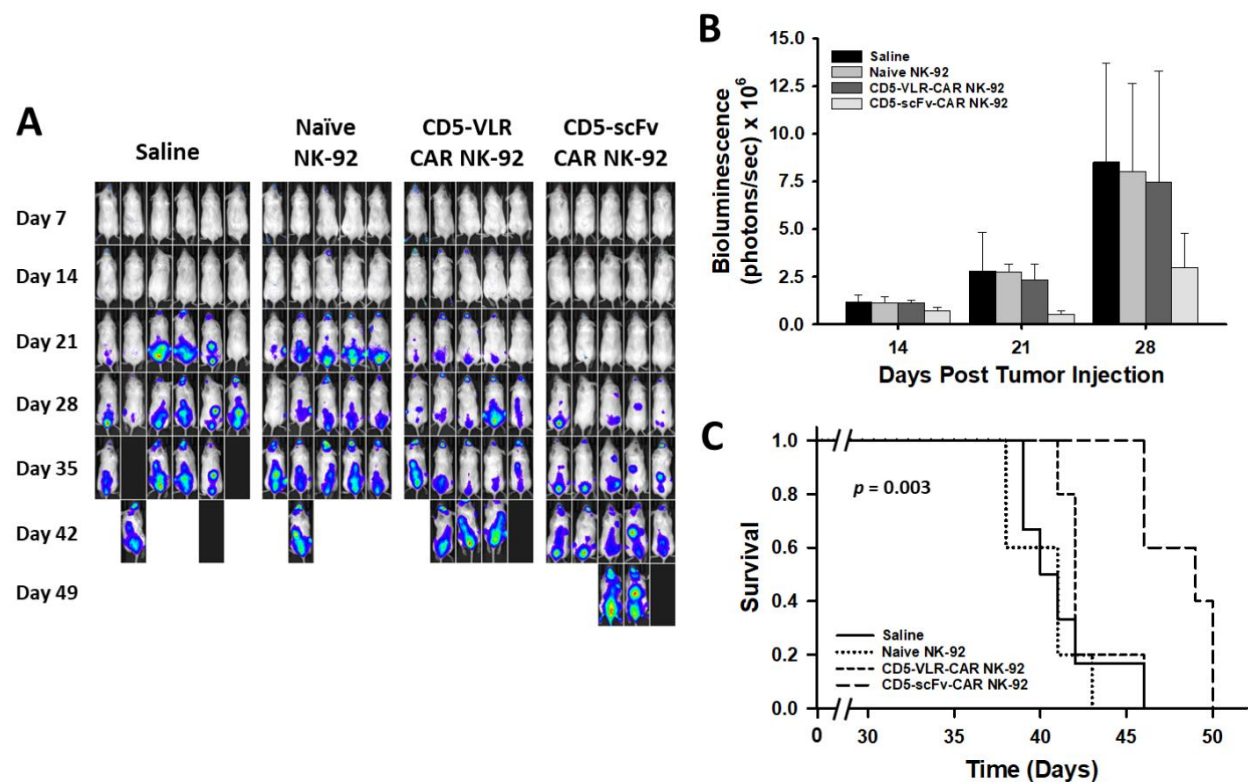


Figure 7: (A) NSG mice were injected with 2×10^6 luciferase-expressing Jurkat T cells intravenously on day 0. Treatment was started 7 days after tumor injection with each mouse receiving a total of 4 treatments on days 7, 11, 14 and 18. Mice were assigned to 4 different treatment groups – saline, naïve NK-92, CD5-VLR-CAR NK-92 or CD5-scFv-CAR NK-92. A dose of 10^7 cells per mouse were administered at each treatment time. Bioluminescence imaging was performed every seven days to monitor tumor burden. (B) Total bioluminescence from Jurkat T cells on days 14, 21, and 28 post tumor injection. A significant decrease ($p < 0.05$) in tumor burden is observed in the CD5-scFv-CAR NK-92 group. Errors bars represent standard deviations. (C) Kaplan-Meier survival curves showing overall survival. Mice treated with CD5-scFv-CAR NK-92 showed significant increased survival ($p < 0.05$) when compared to all other treatment groups. Mice treated with CD5-VLR-CAR NK-92 did not have a significant advantage over saline and naïve NK-92 treatment groups.

Discussion

Patients with relapsed T-cell acute lymphoblastic leukemia or lymphoblastic lymphoma (T-ALL/T-LLy) have dismal outcomes, with mortality rates greater than 80%, when treated with chemotherapy alone (11; 12; 278). Allogeneic hematopoietic stem cell transplantation (HSCT) offers the greatest chance of cure in these patients. A recent study by the Center for International Blood and Marrow Transplant Research showed the 3-year overall survival (OS) with HSCT is 48% for patients able to achieve complete second remission (CR2) prior to transplantation (279). For patients with first relapse of T-ALL/LLy, achieving CR2 is the most important step prior to HSCT, as disease status at the time of transplantation remains the most important factor associated with overall survival (280). However, attaining clinical remission after relapse remains the biggest therapeutic challenge in T-cell disease, and most patients are unable to receive transplantation given the aggressive nature of relapsed disease (281). Thus, in order to maximize and improve upon the benefits of an allogeneic HSCT, there remains a need to develop newer strategies to induce remission in these relapsed patients. CAR-based immunotherapy can play an important role by providing a sustained remission post-relapse, thereby acting as a bridge to stem cell transplantation. Unlike CAR therapy in B-cell malignancies, where sustained B-cell aplasia due to off-target toxicity can be managed with periodic intravenous immunoglobulin infusions, persistent T-cell aplasia caused by T-cell-directed CAR therapy would result in life threatening severe immunosuppression. Thus, HSCT to allow for immune reconstitution following CAR T cell therapy is a reasonable strategy.

CD5 was first studied as a target tumor antigen using a monoclonal CD5 antibody linked to an immunotoxin ricin A chain, and was tested in patients with T-cell leukemia and cutaneous T-cell lymphoma (76; 77; 282). A phase 1 clinical trial in patients with cutaneous T-cell lymphoma demonstrated partial responses in 4 patients with no significant side effects. Two additional studies have used the CD5-directed immunoconjugate to treat graft-versus-host disease by targeting normal T cells (283; 284). Due to the success of these studies, the restricted expression of CD5, and the role of CD5 in the suppression of TCR signaling (72; 285), we hypothesized CD5 would be a good target for CAR therapy. Two studies have previously demonstrated the effectiveness of using CD5 as a target antigen for a CAR construct. Mamonkin

et al. showed that CD5-CAR expressing T cells were effective in targeting T-cell disease in an *in vivo* model, however, they also reported evidence of fratricide among the CAR-expressing T-cells (78). A clinical trial NCT03081910 has now been initiated based on this approach. Additionally, Chen et al. showed that NK-92 cells expressing an anti-CD5 CAR had potent anti-tumor activity against T-cell leukemia (45). While we have shown similar cytotoxicity results here using the anti-CD5-scFv-CAR, we have also demonstrated cytotoxicity and T-cell activation using an anti-CD5-VLR-CAR and have tested an alternative approach to using CD5-CAR T cells by CRISPR-Cas9 genome editing in an effort to prevent fratricide.

Overall, the studies of this report, with our previous studies and reports from others (5, 23), illustrate self-activation of CD5-positive CD5-CAR-modified effector cells due to interactions with self and neighboring CD5 antigens. We show when using both scFv- and VLR-based CD5-CARs that this effect diminished over time as the average number of transgene copies per cell decreased. This is likely due to a decreased proliferation rate and activation-induced cell death of the CAR-modified, activated cells (286). One approach to prevent effector cell activation in the absence of malignant cells is to use CD5-negative NK cells modified to express the anti-CD5 CARs. The use of NK cells as the CAR-expressing effector cells has been demonstrated in several previous preclinical CAR studies, in which either primary human NK cells or the IL-2 dependent NK cell line, NK-92, have been used as the effector cells (120; 124; 126; 129; 139; 287-294). Primary human NK cells have been used in CAR-based clinical trials, with mRNA electroporation being the means of inducing CAR expression (294-296). Our *in vitro* and *in vivo* data show that NK-92 cells modified to express CD5-CARs are effective in targeting a CD5-positive T-cell leukemia cell line. While we only show a modest effect with NK-92 cells, our results are comparable to the NK-92 studies by Chen *et al* (45). The lack of persistence of NK-92 cells in the absence of IL-2, as we have demonstrated, is the likely reason for this low effectiveness. This can be overcome by repeated effector cell dosing or by transitioning to primary NK CD5-CAR cells to demonstrate enhanced anti-tumor efficacy in our T-cell leukemia mouse model.

Our second approach was to knock out the target antigen from the effector cells using genome-editing. The CRISPR-Cas9 system has been widely used since its discovery and characterization in prokaryotes and has been engineered for use in eukaryotes (260; 262; 264; 297-299). Genome editing technologies are quickly progressing toward clinical uses, and the NIH recently approved the initiation of a clinical trial using CRISPR-Cas9 to treat refractory metastatic non-small cell lung cancer (300). We demonstrated CD5-edited CD5-CAR-modified Jurkat T cells exhibit decreased self-activation, yet increased activation when cultured with target cells. CD5-edited effector cells were significantly more activated when in culture with target T cells compared to their initial levels of activation in culture alone. We and others (5) have now shown that CD5-CAR expression in T cells results in down-regulation of CD5. Interestingly, our data also shows non-edited CAR-modified T cells have decreased CD5-CAR protein expression compared to CD5-edited CAR-modified T cells. This data is shown in both Jurkat T cells and primary T cells. CAR down-regulation is likely similar to the mechanism of CD5 down-regulation in that the interaction between the CAR and CD5 results in processing of both proteins from the cell membrane. This result can be important for the expression of other CARs on effector cells that express variable levels of the target antigen. Furthermore, in cultures with CD5-edited effector cells and target cells, effector cells interact more robustly with CD5 on target cells; whereas CD5-positive, non-edited effector T cells interact with CD5 antigen on both effector and target cells, reducing their potency. Overall, the data shows CD5-negative effector cells are advantageous compared to CD5-positive effector cells due to their decreased self-activation and increased CAR expression.

Interestingly, CD5-edited effector cells have a greater effect on target cell CD5 expression. This effect is much stronger with CD5-scFv-CAR effector cells compared to CD5-VLR-CAR effector cells. This is the first study comparing a VLR-based CAR to a more traditional scFv-based CAR. The CD5-VLR used in the CAR construct is an avidity-based antibody, with the multimeric form of the VLR antibody binding to human CD5 with a higher efficiency compared to the monomeric form (270). The scFv was derived from the murine H65 anti-human CD5 IgG antibody (272). It cannot be concluded from these *in vitro* studies which CD5-CAR would be most advantageous, as both demonstrate substantial target cell association and

effector cell activation. However, our *in vivo* studies showed the VLR-CAR did not perform as well as the scFv-CAR. This result is possibly due to the avidity nature of this particular VLR. We cannot conclude that other VLRs would not provide adequate target cell killing, as our *in vitro* studies certainly show VLR sequences can efficiently activate T cells. There may be particular circumstances in which a VLR may be advantageous over an scFv. Previous CAR studies have shown that differing CAR affinities usually do not affect the maximum level of T-cell activation seen, however decreased selectivity can be seen with higher affinity CARs (301; 302). Since the target cells in our study have high CD5 antigen expression, it is unlikely that affinity alone could account for the differences in efficacy between the VLR and scFv-CAR. It is possible that the limited persistence of NK-92 cells in the *in vivo* setting had a significantly higher negative effect on the VLR-CAR compared to the scFv-CAR.

Our results show both approaches, NK-cells as effector cells and CD5 knockout in effector T cells, modified with the CD5-CARs have the potential to overcome the barriers of self-activation and fratricide, which are issues that are hampering the use of CAR therapies from being applied to the treatment of T-cell malignancies. Although our goal is to provide a bridge to allogeneic transplantation for relapsed patients, strategies using CAR-modified immunocompetent cells also are being developed as therapeutics to attain long-term remission in these patients. All approaches will require a functional anti-T-cell CAR construct, and this study advances our understanding of this possibility.

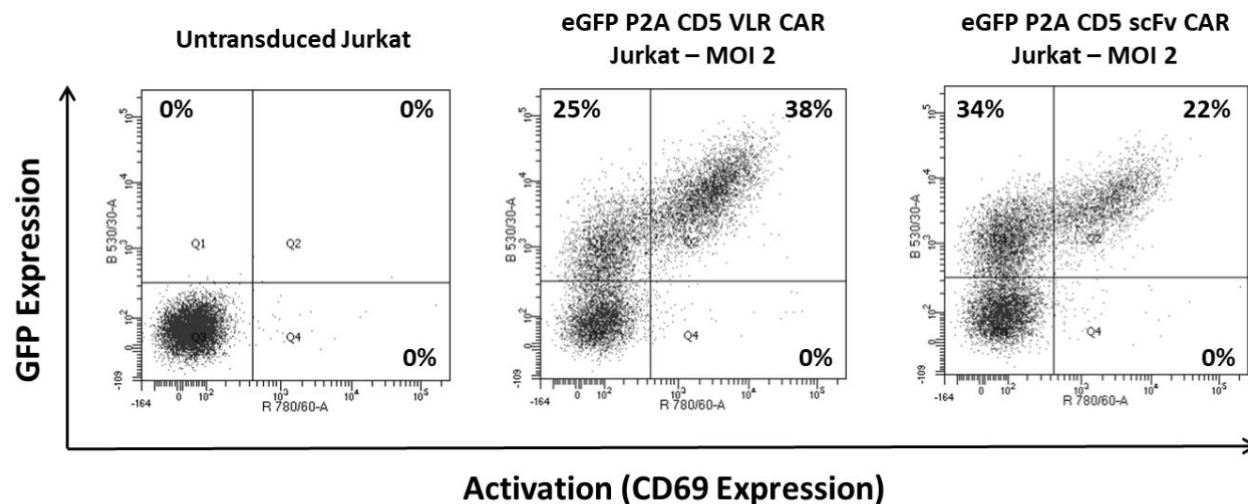
Supplemental Figure II-S1: Activation of Jurkat T cells expressing a CD5-CAR.

Figure S1: Activation (CD69 expression) in Jurkat T cells transduced with the eGFP-p2a-CD5-CAR lentivirus correlates with eGFP expression in both CD5-CAR groups. Data above shows activation in Jurkat T cells transduced at a multiplicity of infection (MOI) of 2, four days post-transduction. No activation is seen in the eGFP-negative Jurkat T cells.

Supplemental Figure II-S2: Western blot analysis of CD5-CAR expression in Jurkat T cells.

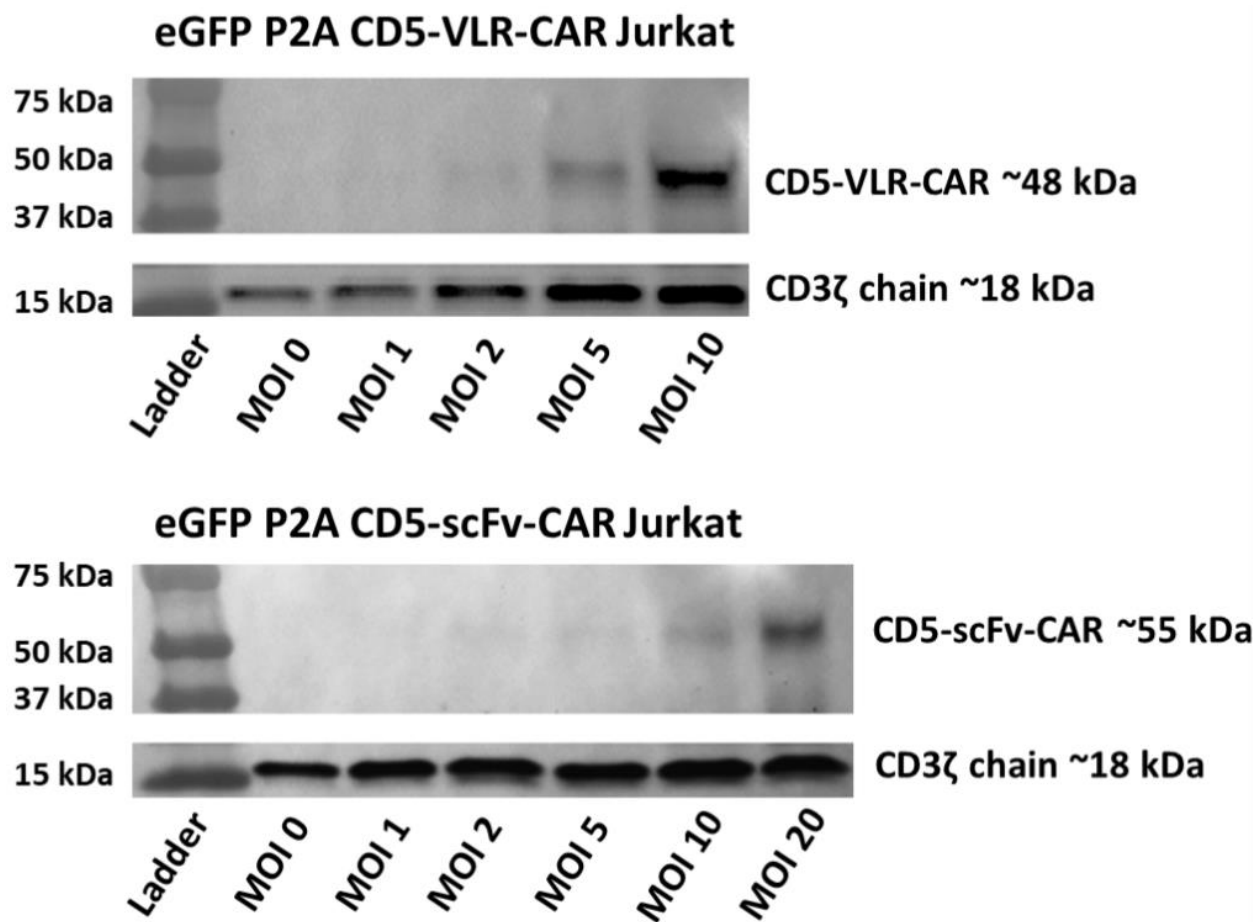


Figure S2: CD5-CAR expression is demonstrated in Jurkat T cells transduced with the eGFP-p2a-CD5-CAR lentivirus by a Western blot using a CD3ζ antibody. CD5-CAR expression increased with a corresponding increase in MOI. The Western blot was performed nine days post-transduction.

Supplemental Figure II-S3: Viral vector copy number (VCN) in CD5-CAR-modified Jurkat T cells.

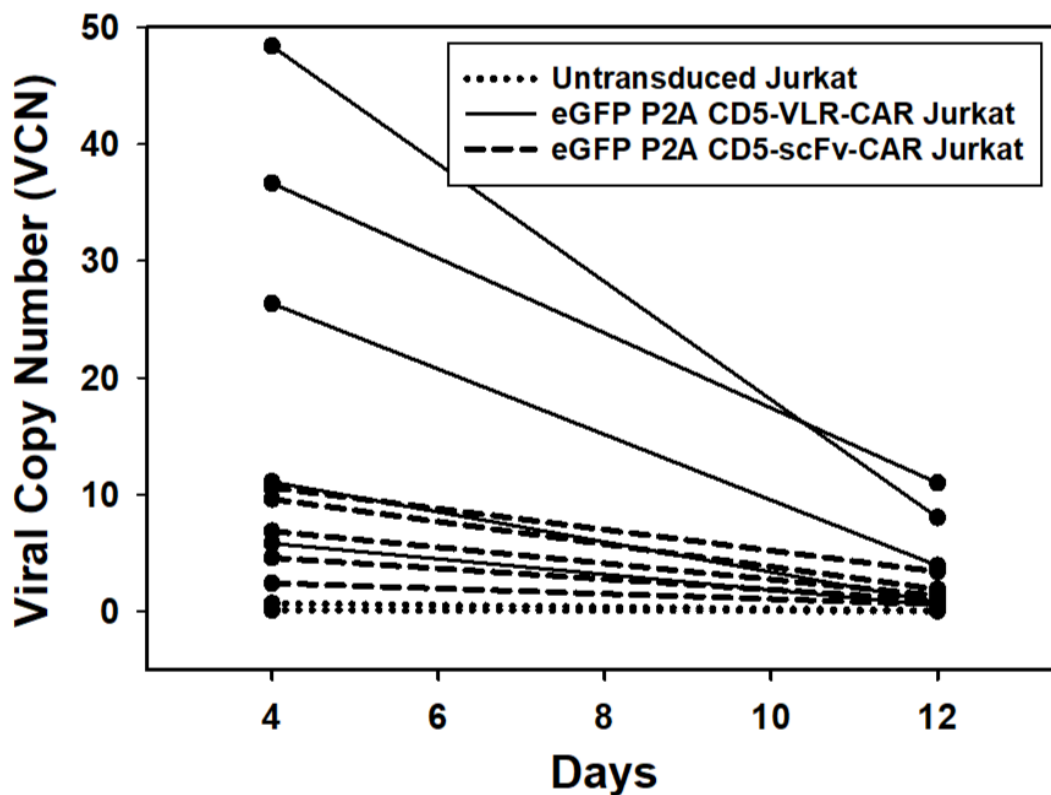


Figure S3: Transduced viral vector copy number (VCN) in Jurkat T cells transduced with the eGFP-p2a-CD5-CAR lentivirus decreased over time. The decrease in VCN corresponded with a decrease in activation as measured by surface CD69 expression.

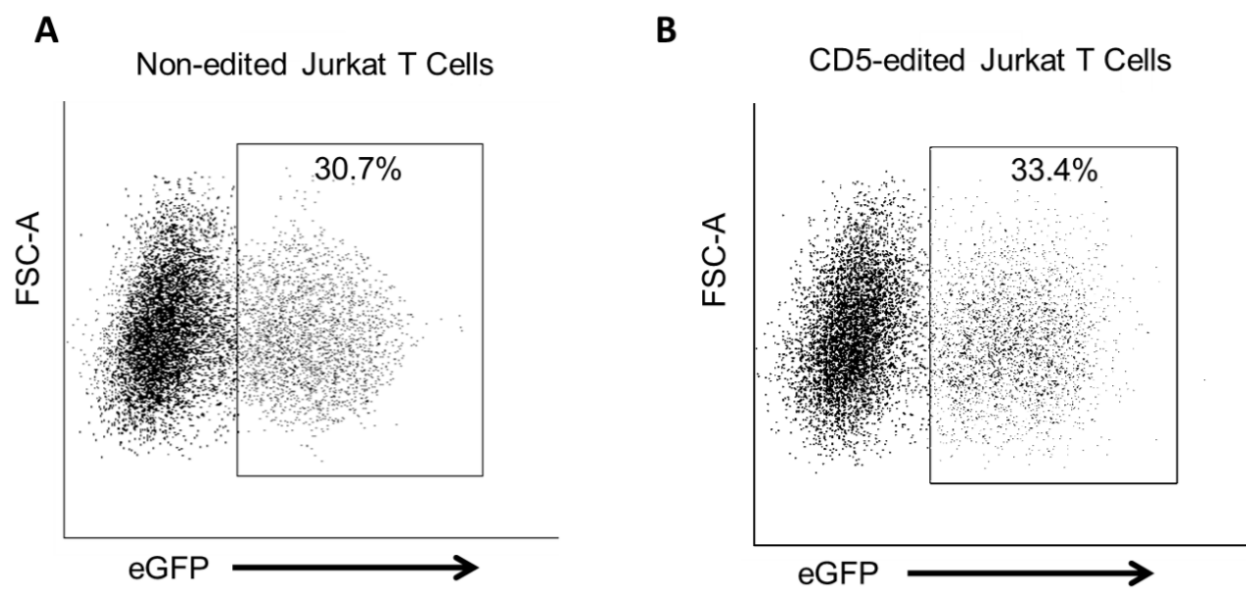
Supplemental Figure II-S4: Transduction efficiency of non-edited and CD5-edited Jurkat T cells.

Figure S4: Non-edited (**A**) and CD5-edited Jurkat T cells (**B**) were transduced with the eGFP-p2a-CD5-scFv-CAR lentivirus. eGFP expression was measured by flow cytometry.

Supplemental Figure II-S5: Western blot analysis of CD5 expression in CD5-CAR-modified Jurkat and CD5-edited Jurkat T cells.

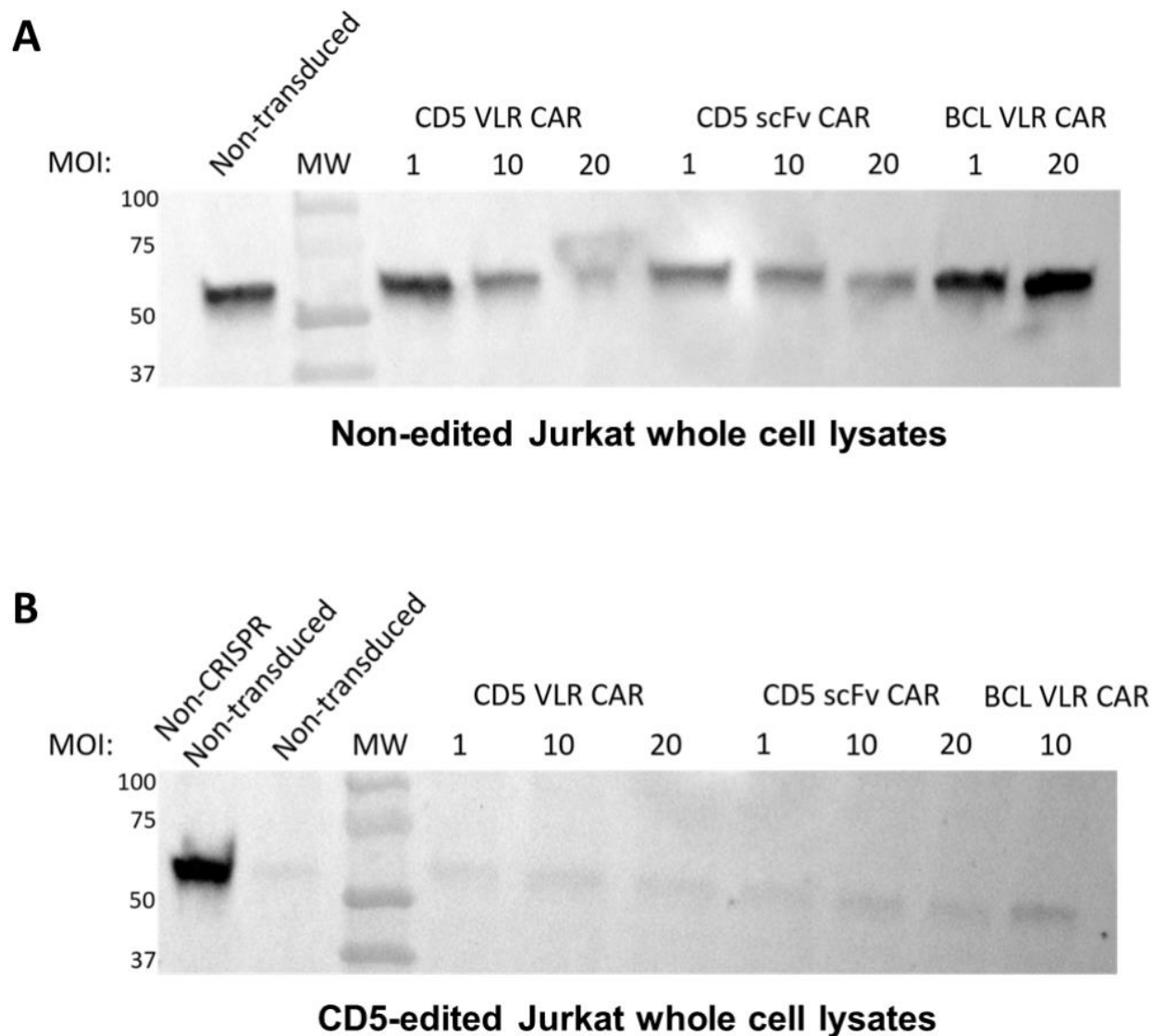


Figure S5: Western blot using anti-CD5 antibody on whole cell lysates from non-edited (A) and CD5-edited Jurkat T cells (B) transduced with CD5-VLR-CAR, CD5-scFv-CAR or BCL-VLR-CAR lentivirus at MOIs 1, 10 and 20.

Supplemental Figure II-S6: CD5-CAR expression measured by flow cytometry and Western blot analysis in Jurkat and CD5-edited Jurkat T cells.

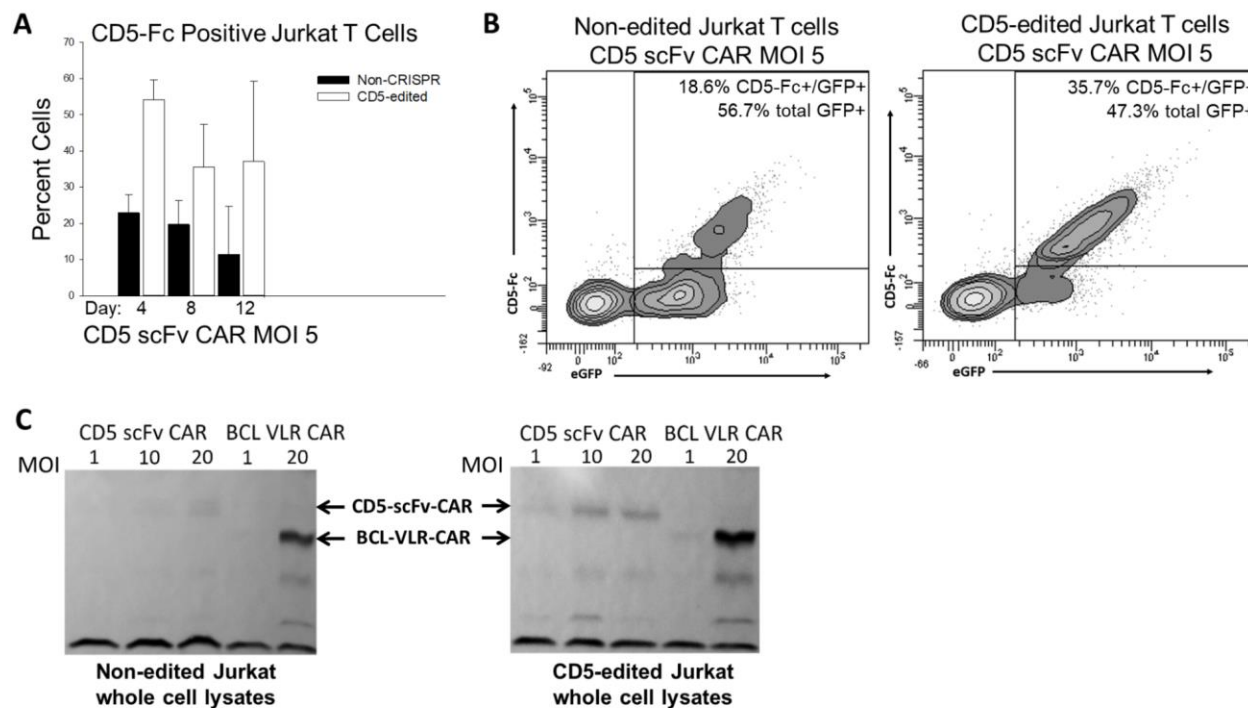


Figure S6: (A and B) CD5-scFv CAR-modified CD5-edited Jurkat T cells bind CD5-Fc to a greater degree than do CD5-scFv-CAR-modified non-edited Jurkat T cells at similar levels of eGFP expression, as measured by flow cytometry. (C) CAR protein expression measured by Western blot using anti-CD3 ζ antibody on whole cell lysates from non-edited (left) and CD5-edited Jurkat T cells (right) transduced with CD5-scFv-CAR lentivirus at MOIs 1, 10 and 20 and BCL-VLR-CAR lentivirus at MOIs 1 and 20. CD5-scFv-CAR is expressed at higher levels in CD5-edited Jurkat T cells. No change in BCL-VLR-CAR expression is seen.

Supplemental Figure II-S7: Primary T cell CD5 and CD5-CAR expression measured by flow cytometry.

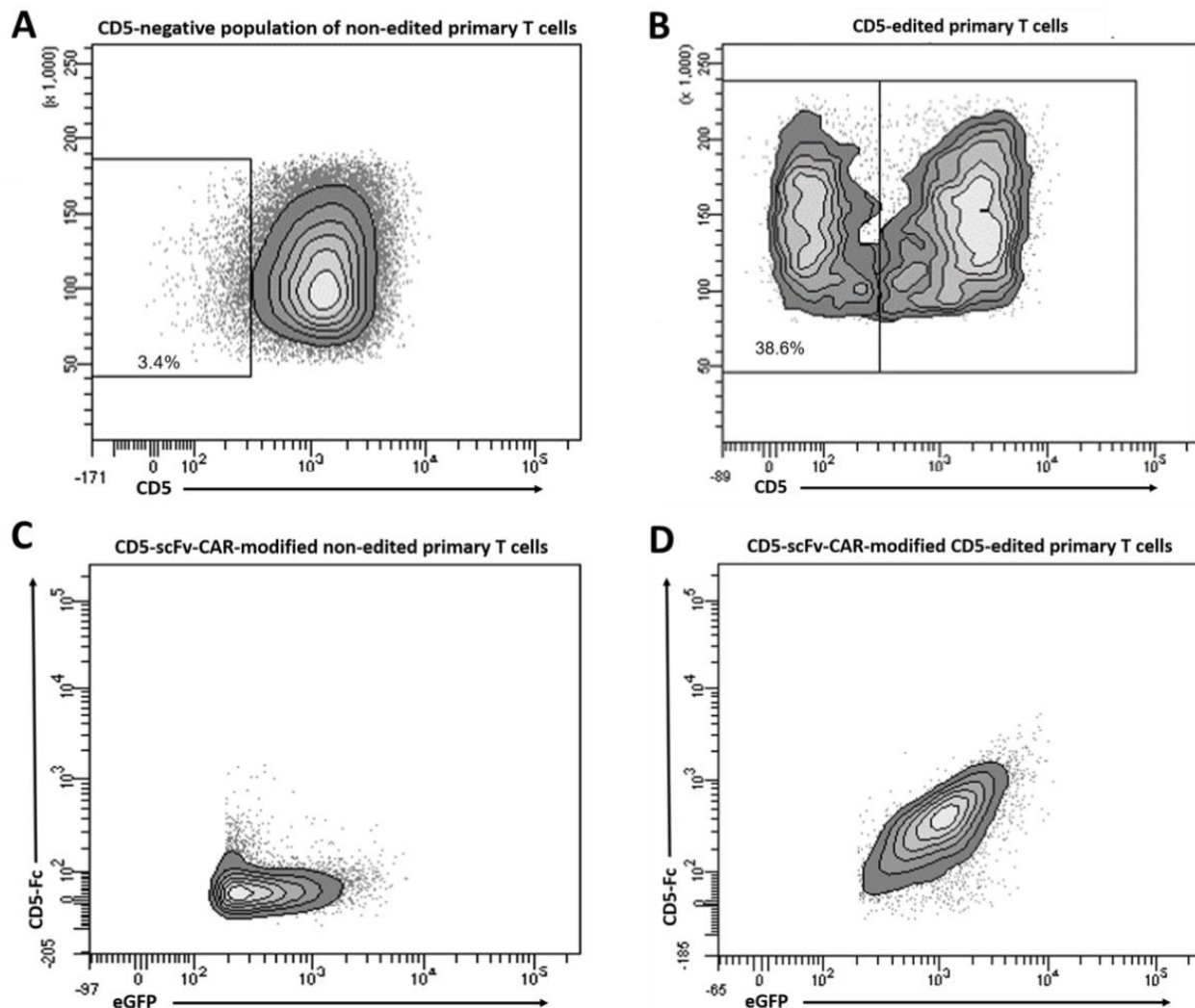


Figure S7: CD5 expression in non-edited (A) and CD5-edited primary T cells (B). CD5-CAR expression measured by CD5-Fc binding in eGFP-positive non-edited (C) and CD5-edited primary T cells (D).

Supplemental Figure II-S8: CD5 expression in CD5-scFv-CAR-modified Jurkat T cells when cultured with non-modified Jurkat T cells.

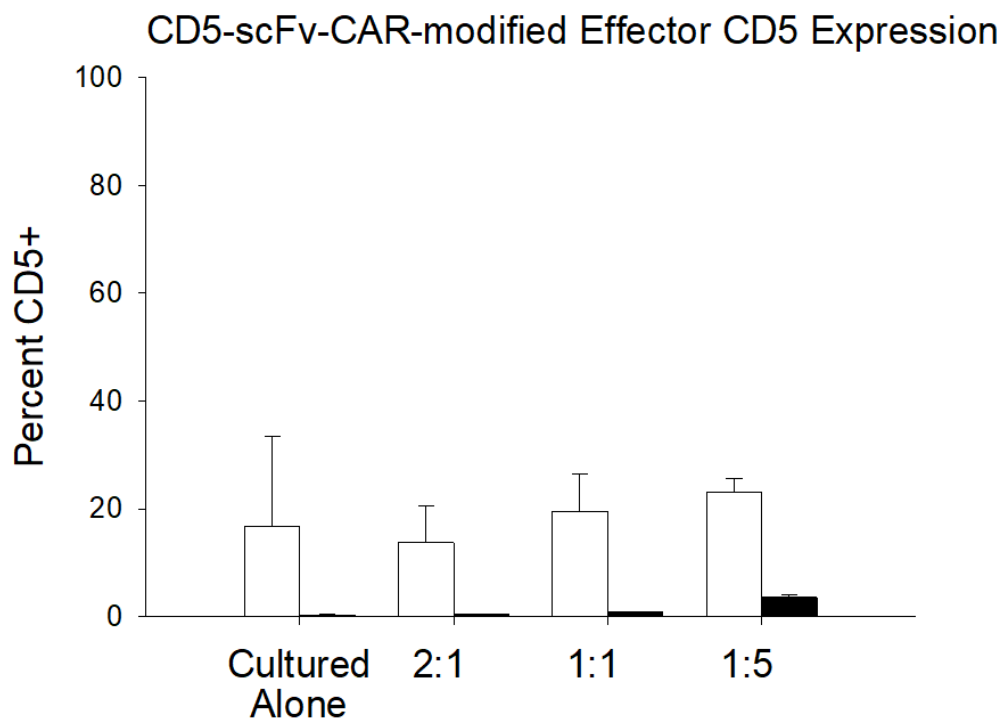


Figure S8: CD5 surface expression on CD5-scFv-CAR-modified effector Jurkat T cells in culture with naïve Jurkat target T cells. Flow cytometry was used to measure CD5 expression on effector cells cultured alone or at E:T ratios 2:1, 1:1, 1:5. White bars signify non-edited effector cells; black bars signify CD5-edited effector cells.

Supplemental Figure II-S9: Persistence of CD5-scFv-CAR-modified NK-92 cells in the absence of IL-2 in NSG mice.

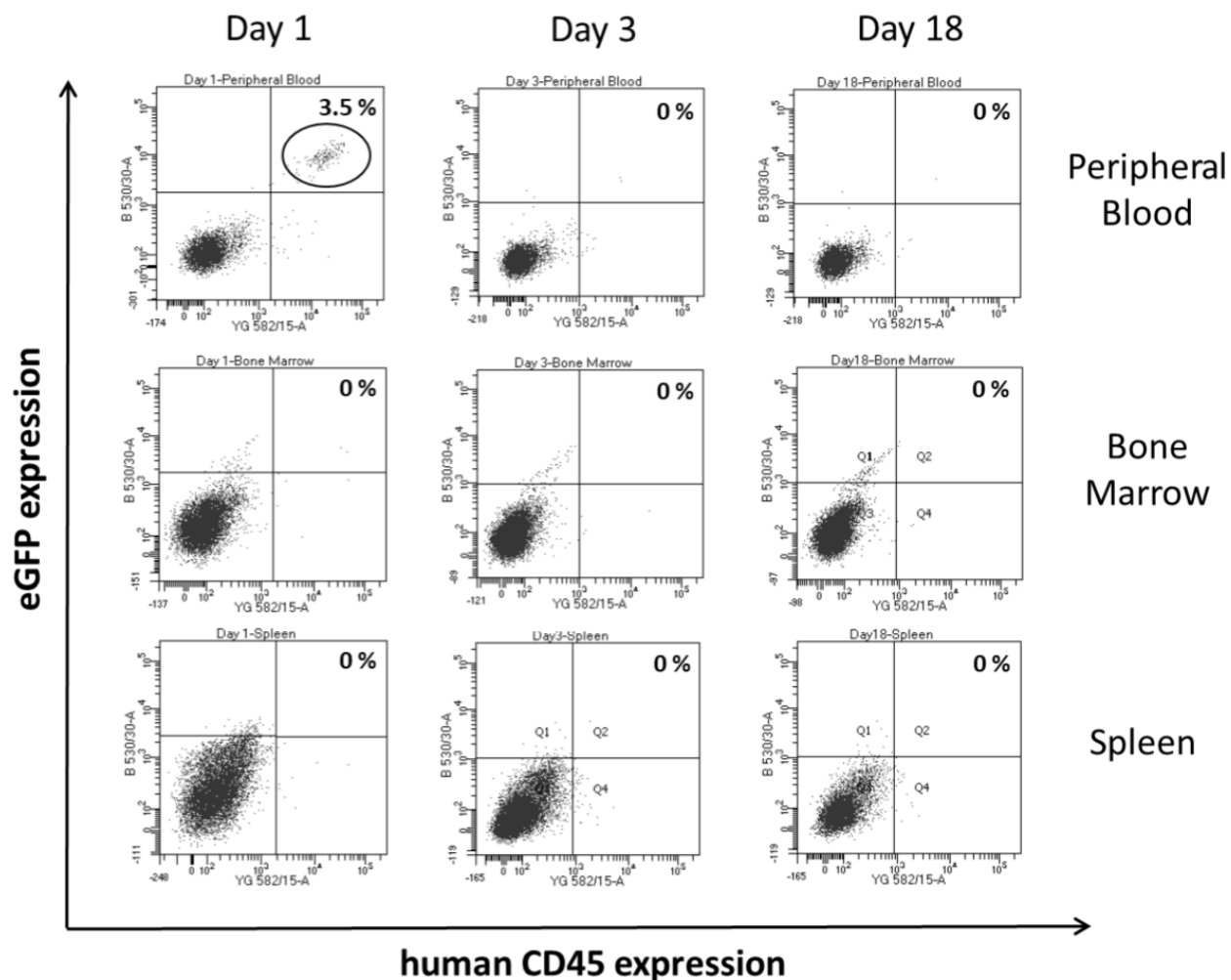


Figure S9: Persistence of CD5-CAR expressing NK-92 cells in absence of IL-2. 10^7 non-irradiated eGFP-p2a-CD5-scFv-CAR expressing NK-92 cells were injected into NSG mice. Mice were not given IL-2. Peripheral blood, bone marrow and spleen were evaluated for presence of CAR expressing NK-92 cells using eGFP and human CD45 expression. No evidence of CAR-NK-92 cells were seen by day 3. No evidence of engraftment in bone marrow was seen. No evidence of disease from NK-92 cells was seen seven weeks post injection.

Chapter III

CRISPR-Cas9 gene delivery and CD5-CAR modification of $\alpha\beta$ T cells

Abstract

CD5-editing of T cells prior to CD5-CAR-modification increases the CD5-CAR expression on the T-cell surface. We hypothesized greater CAR expression would translate into enhanced CD5-specific cytotoxicity. Here, we describe a series of protocols designed and tested to transfect T cells with CRISPR-Cas9-encoding DNA. Nucleoporation and electroporation techniques were used, and electroporation was optimized utilizing a variety of buffers, temperatures and specific parameters such as voltage and pulse length. Our data demonstrate, through optimization of these techniques, that we can achieve 20% CD5-editing. However, upon CD5-CAR-modification of CD5-edited T cells, we did not observe any change in cytotoxicity against a CD5-expressing T-ALL cell line compared to the cytotoxicity elicited by non-edited CD5-CAR-modified T cells of similar gene modification. Sorting the CD5-edited population of T cells prior to CD5-CAR transduction resulted in ~15% CD5-CAR-modified CD5-edited T cells. However, despite a pure population of CD5-negative T cells, there was no advantage to CD5-editing regarding anti-tumor cytotoxicity. Specifically, our data suggest decreased cytotoxicity by CD5-edited, sorted, CD5-CAR-modified T cells against Jurkat T cells, resulting in ~10% dead Jurkat T cells, compared to that of non-edited CD5-CAR-modified T cells, killing ~18% Jurkat T cells at a 3:1 E:T ratio. We hypothesize the T cells were not healthy following the double modification of electroporation and transduction and therefore lost cytotoxic potential. We determined that improving the health of the T cells may result in equivalent, high levels of transduction in non-edited and CD5-edited T cells. However, we hypothesize there would not be an advantage regarding cytotoxicity due to either high levels of exhaustion markers on the CD5-edited T cells or high transduction efficiency, resulting in a plateau of CD5-CAR surface expression. Therefore, we conclude editing T cells with CRISPR-Cas9 using transfection prior to lentiviral CAR transduction is not a practical approach to improving anti-tumor cytotoxicity.

Introduction

As demonstrated in chapter 2, we can edit $\alpha\beta$ T cells with CRISPR-Cas9 to disrupt the CD5 gene. Upon CD5-CAR modification of the CD5-edited T cells, the CD5-CAR is expressed to a higher degree on

the cell surface compared to CAR expressed on non-edited T cells, despite equivalent transduction efficiency (49). We hypothesize this is due to cis- and trans-interactions between the CD5 antigen and the anti-CD5-CAR, resulting in down-regulation of both antigen and CAR. A previously published case study demonstrated that modification of a single leukemic blast resulted in masking of the target antigen through interactions between the CAR and antigen on the same cell, developing a novel mechanism of resistance. Proliferation of this cell ultimately caused relapse and death of the patient (43). This study confirms the CAR can interact with an antigen that is expressed on the same T cell. Our studies suggest that the two proteins can interact in trans as well, with the CD5 antigen on one cell interacting with the CD5-CAR expressed on another cell. We have demonstrated that the entire population of cells (Jurkat cells and T cells) down-regulates the CD5 antigen, despite the CD5-CAR being expressed on only a proportion of the T cells (49).

We hypothesized that increased CD5-CAR expression on CD5-edited T cells would lead to increased interactions among CD5-positive tumor cells, ultimately resulting in enhanced CD5-specific cytotoxicity. However, we recognize the increased interactions with tumor cells may in turn increase the rate of T-cell exhaustion. T-cell exhaustion is characterized by the upregulation of inhibitory receptors and loss of effector-cell function (303). CARs with stronger affinity for an antigen exhibit greater signs of exhaustion, likely due to higher levels of activation (304). Additionally, CAR T cells with reduced expression, blockade or CRISPR-Cas9 mediated disruption of PD-1 demonstrate increased efficacy *in vitro* as well as prolonged persistence and enhanced anti-tumor activity *in vivo* (305-308). Numerous CARs have been studied extensively, each having different properties related to *in vivo* persistence, expansion, and anti-tumor efficacy. Our CD5-CAR is unique from other CD5-CARs comprising of a CD28 costimulatory domain in that it has a myc tag between the scFv and CD28 regions (49). However, we predict the myc tag has minimal effect on the function of our CAR, and therefore our CD5-CAR functions similar to that of other published CD5-CAR constructs with a CD28 costimulatory domain and a similar length hinge region.

In order to determine the potential effects of CD5-editing on the functionality of CD5-CAR-modified T cells, we required methods for both transient expression of CRISPR-Cas9 in the T-cell as well

as introduction of the CD5-CAR into the CD5-edited cells. We previously published methods for both techniques, however, our T-cell transfection protocol yielded high efficiency coupled with poor viability. Therefore, these methods necessitate optimization prior to CD5-CAR transduction in order to yield a practical cell product. Upon optimization of CRISPR-Cas9 introduction into T cells, a second modification using a CD5-CAR lentiviral vector is required. The cytotoxic capabilities of this final cell product can then be assessed by targeting T-ALL cell lines *in vitro*.

Materials and Methods

Culture of cell lines: The Jurkat cell line clone E6-1 was purchased from American Type Culture Collection (ATCC, Manassas, VA). Jurkat T cells were cultured in complete RPMI medium as previously described (49).

Culture of primary cells: Blood was obtained from consented, healthy adults. Ficoll-Paque density gradient to isolate PBMCs from 20-40 mL blood was performed using the manufacturer's protocol. Immediately following isolation, PBMCs underwent a Pan T-cell isolation using the MACS human Pan T-cell Isolation Kit according to the manufacturer's protocol (Miltenyi Biotec, Germany). Subsequently, T cells were stimulated with CD3/CD28 Dynabeads at a 1:1 ratio for 24 hours. After 24 hours, beads were removed. T cells were expanded in X-VIVO 15 medium (Lonza, Switzerland), supplemented with FBS, penicillin/streptomycin, IL-2 and IL-7 as previously described (49).

Engineering of CAR constructs: The CD5-CAR containing the myc tag was generated as previously described (49). We replaced the myc tag with a CH3 hinge. The CH3 hinge sequence was derived from IgG1. Both CD5-CAR constructs contain the scFv extracellular antigen-recognition domain as previously described as well as a p2a peptide sequence facilitating dual expression of enhanced green fluorescent protein (eGFP) and the CAR (49).

Production of lentiviral vector: High-titer rHIV SIN lentiviral vector was produced and titered for all CAR constructs as previously described (49).

Transduction of T cells: Transduction using lentiviral particles was performed as previously described with 6 ug/mL polybrene supplementation (EMD Millipore, Billerica, MA) (49). T cells were transduced immediately after 24-hour stimulation with CD3/CD28 Dynabeads. Cells were incubated with lentiviral particles for 18-24 hours, at which point the cells were centrifuged and seeded in fresh medium. The transduced T cells were cultured for 3-4 days prior to being used in cytotoxicity assays.

Flow cytometry: Analysis was performed using a BD LSRII Flow Cytometer (BD Biosciences, San Jose, CA). Data was analyzed using DIVA and FCS Express 6 software. Antibodies used included anti-CD5 PerCP/Cy5.5 and anti-CD3 BV421. To detect CD5-CAR expression, CD5-Fc fusion protein (G&P Biosciences, Santa Clara, CA) and a secondary anti-IgG Fc antibody (Jackson ImmunoResearch Laboratories, West Grove, PA) were used, as previously described (49). Violet Proliferation Dye 450 (VPD450) was used to label Jurkat cells to detect them in the cytotoxicity assays with T cells. Cell death was assessed using eFluor 780 (Thermo Fisher Scientific, Waltham, MA). Flow sorting of CD5-edited T cells was performed using a SH800S Cell Sorter (Sony Biotechnology Inc. U.S., San Jose, CA) as previously described (49).

Nucleoporation of T cells: T cells were nucleoporated using the Lonza Nucleofector 2b device and the Amaxa Human T-cell Nucleofector kit as previously described (Lonza, Switzerland) (49). Cell counts and viability were measured by using a Cellometer (Nexcelom, Lawrence, MA) and Trypan Blue staining (Thermo Fisher Scientific, Waltham, MA). On day 4 post-nucleoporation, the percentage of CD5-edited cells was determined by flow cytometry (BD LSRII, BD Biosciences, San Jose, CA).

Electroporation of T cells: T cells were electroporated using the ECM 830 Square Wave Electroporator (BTX, Holliston, MA) in 1 mm gap cuvettes. Buffers used for transfection were Opti-MEM (Thermo Fisher Scientific, Waltham, MA) and BTXpress Solution (BTX, Holliston, MA). Cell number per cuvette ranged from 2.5×10^5 cells to 1×10^6 cells. Cells were electroporated with 40 ug pMAX GFP plasmid (Lonza, Switzerland) or CD5-CRISPR-Cas9 plasmid DNA (between 33 ug - 160 ug). DNA (dissolved in molecular grade nuclease-free water) was added to the cells at ~13% final volume. Final cuvette volume was 50 uL. Cells were incubated at room temperature for 0-10 minutes following electroporation and were subsequently plated in culture medium at a final concentration of 1×10^6 cells/mL. Culture medium was replaced 18-24 hours following electroporation. Buffer, temperature, quantity of DNA, and electroporation parameters all varied with each protocol. See Table 1. Cell counts and viability were measured by using a Cellometer and Trypan Blue staining.

Cytotoxicity assays: Jurkat cells were labeled with VPD450 proliferation dye 24-36 hours prior to flow cytometry as per the manufacturer's protocol. Effector T cells and Jurkat target cells were mixed in 12x75 mm FACS tubes at effector to target (E:T) ratios of 1:1, 3:1 and/or 5:1. The appropriate number of effector cells were added to each tube, followed by 50,000 target cells and additional media up to 250 uL. The cells were co-cultured for 12 or 24 hours at 37°C in 5% CO₂. Following the co-culture, cells were washed in PBS and stained with eFluor780 viability dye for 30 minutes, followed by a second PBS wash. Flow cytometry was subsequently performed to measure the percentage of dead target cells in each culture (double positive VPD450 and eFluor780).

Results

Transfection of T cells using CRISPR-Cas9 plasmid

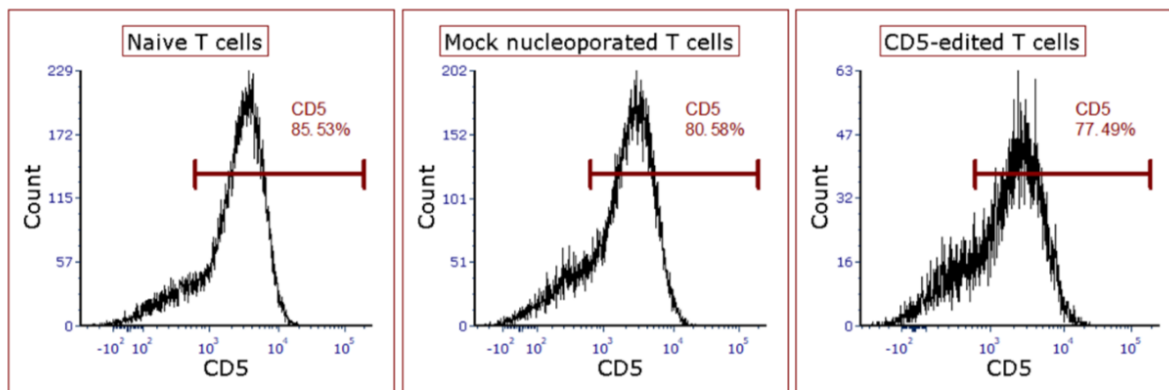
As demonstrated in chapter 2, we can introduce the CRISPR-Cas9 plasmid into T cells to disrupt expression of the CD5 antigen by nucleoporation (49). However, these methods routinely resulted in poor viability of the cell product. It is difficult to optimize nucleoporation using the Amaxa due to proprietary

buffers and the pre-defined programs preventing the adjustment of conditions. Using various pre-loaded programs on the Amaxa, we observed poor T-cell viability, poor transfection efficiency, or sometimes both (**Figure 1**). Therefore, we turned our efforts to electroporation using the BTX ECM 830 Square Wave Electroporator. In contrast to nucleoporation, electroporation allows for flexibility in user-defined protocols to modify a variety of parameters including: cuvette size, quantity of plasmid, temperature, high salt vs low salt buffers, voltage, resistance, capacitance, length and number of pulses and intervals between each pulse. We tested a number of iterations in order to optimize a protocol maximizing both viability and transfection efficiency of T cells, some of which are exemplified in **Table 1**. The CRISPR-Cas9 plasmid is a bicistronic construct expressing eGFP through a p2a sequence; therefore, GFP can be used to detect transduction of the T cells.

Initially, we optimized protocols for the transfection of pMax GFP plasmid into T cells using Trypan blue to measure viability and fluorescent microscopy to visualize GFP-positive cells. As seen in Table 1, protocols for transfecting pMax GFP maintained cell viability at >85% and resulted in high transfection efficiency (**Figure 2A**). We attempted a similar protocol with a slightly higher voltage using both pMax GFP and the CRISPR-Cas9 plasmids. The CRISPR-Cas9 plasmid was transfected with a comparatively reduced pulse length (**Table 1**). This increase in voltage had a great effect on cell viability, reducing viability of pMax transfected cells to 40% and CRISPR-Cas9 transfected cells to 30%. However, while many GFP-positive cells can be detected in pMax transfected populations, only a few GFP-positive cells can be detected among those transfected with CRISPR-Cas9 DNA (**Figure 2B**). One possible explanation is the quality of the pMax DNA is much purer compared to the DNA we isolate in our laboratory. The protocols that resulted in the greatest CD5-editing without compromising viability are bolded in Table 1. One of these protocols resulted in >20% CD5-editing as measured by flow cytometry, however viability was reduced to 65% measured by Trypan blue staining (**Figure 3A**). A similar protocol was then developed that yielded ~15% CD5-editing in T cells while maintaining 85% viability (**Figure 3B**). Despite a number of attempts, I was unable to generate a protocol resulting in greater transfection efficiency without compromising viability. However, it remained unknown the percentage of gene-editing

Figure III-1: Nucleoporation to edit CD5 in T cells using CRISPR-Cas9 DNA.

A



B

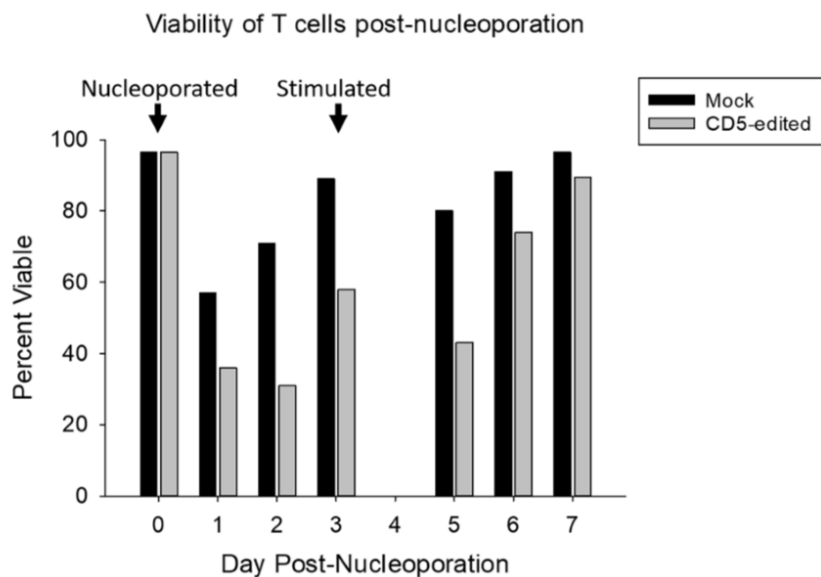


Figure 1: (A) Flow cytometry plots of CD5 surface expression in naïve (left), mock nucleoporated (middle) or CRISPR-Cas9 nucleoporated T cells (right). (B) Viability of T cells following nucleoporation with or without CRISPR-Cas9 DNA. Black bars = mock nucleoporated; Gray bars = CD5-CRISPR-Cas9 nucleoporated. One replicate is depicted.

Figure III-Table 1: T-cell electroporation protocols illustrating different parameters tested.

Buffer	Temperature (°C)	DNA (µg)	Number of cells	Voltage	Pulse Length	Number of pulses	Pulse interval	Day 1 Viability	Percent CD5-edited cells
Pre-warmed OptiMEM	Pre-chilled cuvettes Room temp reaction	pMax GFP 40 ug	2.5e5	300 V	400 µseconds	1		86%	
Pre-warmed OptiMEM	Pre-chilled cuvettes Room temp reaction	pMax GFP 40 ug	1e6	350 V	500 µseconds	1		42%	
Pre-warmed OptiMEM	Pre-chilled cuvettes Room temp reaction	CRISPR-Cas9 33 ug	1e6	350 V	400 µseconds	1		28%	Not Viable
Pre-warmed OptiMEM	Pre-chilled cuvettes Room temp reaction	CRISPR-Cas9 70 ug	1e6	350 V	400 µseconds	1		37%	Not Viable
Pre-warmed OptiMEM	Pre-chilled cuvettes Room temp reaction	CRISPR-Cas9 95 ug	1e6	350 V	400 µseconds	1		27%	Not Viable
Pre-warmed OptiMEM	Pre-chilled cuvettes Room temp reaction	CRISPR-Cas9 67 ug	1e6	200 V	5 milliseconds	1		32%	Not Viable
Pre-warmed OptiMEM	Room temp reaction	CRISPR-Cas9 95 ug	2.5e5	125 V	700 µseconds	1		26%	Not Viable
Pre-warmed OptiMEM	Room temp reaction	CRISPR-Cas9 95 ug	2.5e5	100 V	700 µseconds	1		72%	7.5%
Pre-warmed OptiMEM	Room temp reaction	CRISPR-Cas9 95 ug	2.5e5	80 V	400 µseconds	2	100 milliseconds	92%	10.5%
Pre-warmed BTXpress Solution	Pre-chilled cuvettes Room temp reaction	CRISPR-Cas9 95 ug	1e6	280 V	600 µseconds	1		52%	22%
Room temp BTXpress Solution	Room temp reaction	CRISPR-Cas9 100 ug	1e6	220 V	750 µseconds	3	100 milliseconds	56%	4.5%
Room temp BTXpress Solution	Room temp reaction	CRISPR-Cas9 100 ug	1e6	200 V	1 millisecond	3	100 milliseconds	41%	14%
Room temp BTXpress Solution	Room temp reaction	CRISPR-Cas9 100 ug	1e6	100 V	1 millisecond	5	100 milliseconds	86%	6%
Room temp BTXpress Solution	Room temp reaction	CRISPR-Cas9 100 ug	1e6	150 V	1 millisecond	8	100 milliseconds	38%	
Room temp BTXpress Solution	Room temp reaction	CRISPR-Cas9 100 ug	1e6	100 V	1 millisecond	10	100 milliseconds	80%	
Room temp BTXpress Solution	Room temp reaction	CRISPR-Cas9 160 ug	1e6	100 V	1 millisecond	10	100 milliseconds	64%	17%

Figure III-2: pMax GFP and CRISPR-Cas9 transfection of T cells.

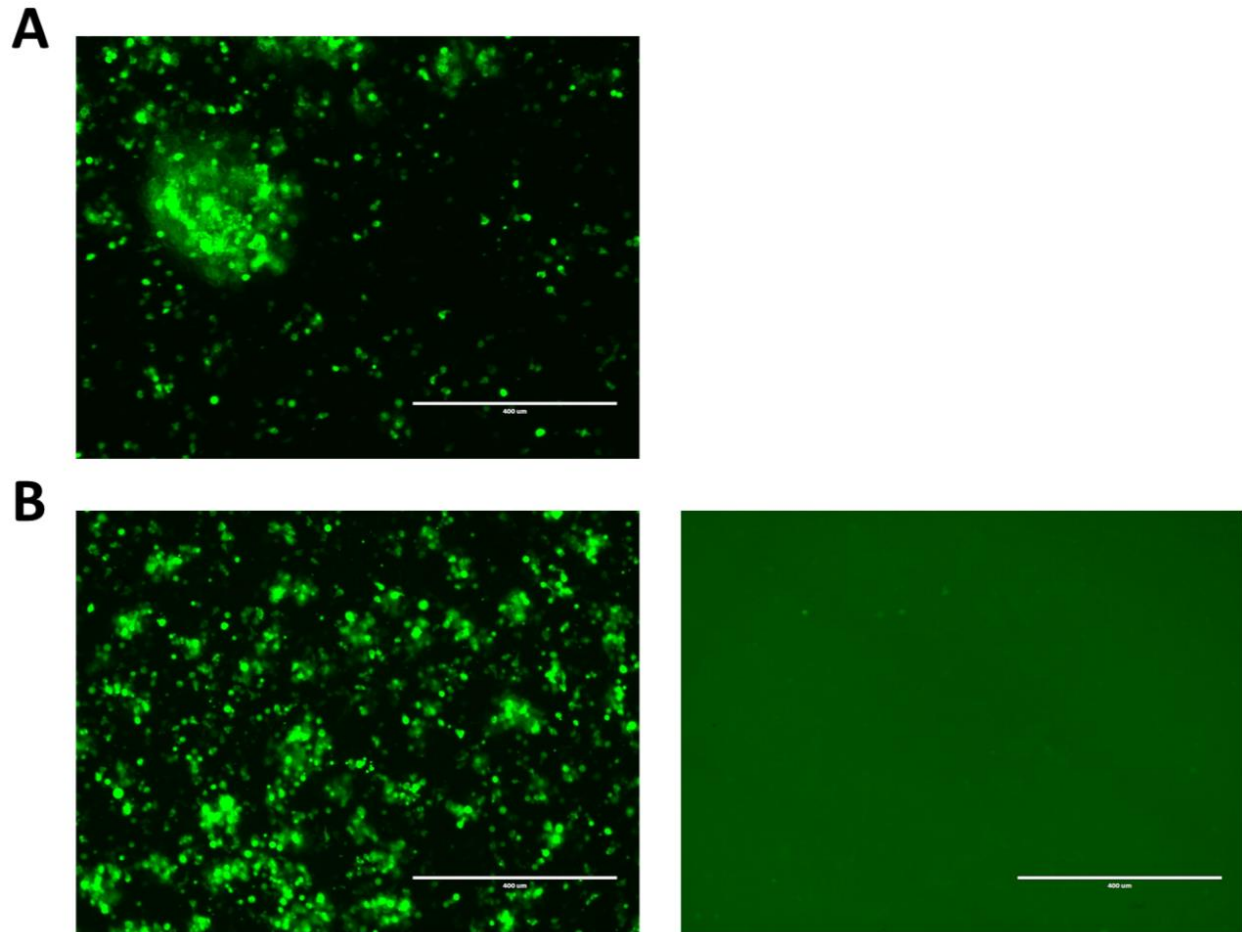


Figure 2: (A) Representative image of fluorescent microscopy of 2.5×10^5 T cells electroporated with 40 μg pMax GFP DNA using parameters of 300 V and 400 μs . (B) Representative image of fluorescent microscopy of 1×10^6 T cells electroporated with 40 μg pMax GFP DNA (left) and 33 μg CRISPR-Cas9 (right) using parameters of 350 V and 500 μs or 400 μs , respectively.

Figure III-3: CD5-editing of T cells using electroporation delivery of CRISPR-Cas9 DNA.

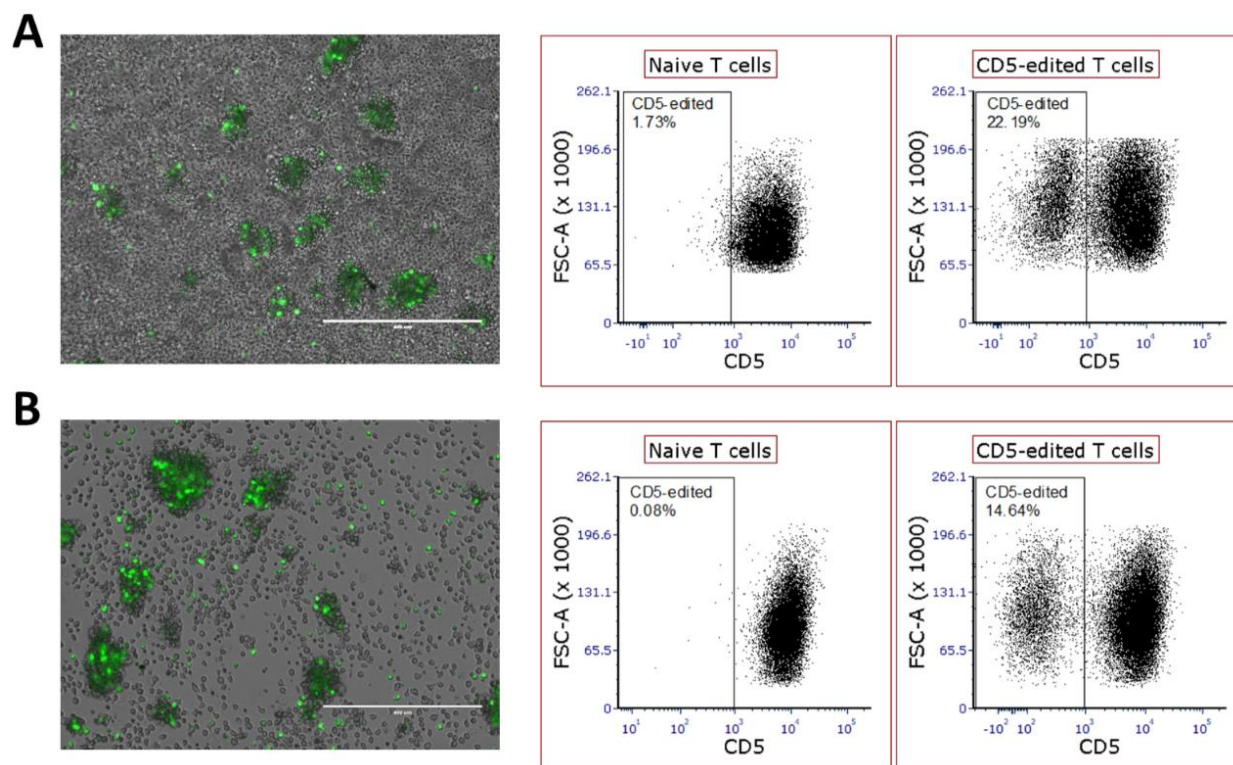


Figure 3: (A) Representative fluorescent microscopy of T cells electroporated with CRISPR-Cas9 DNA using a protocol that yielded ~65% viability (left). Flow cytometry plots indicate CD5-negative cells in a population of naïve T cells (middle) compared to that of CD5-edited T cells (right). (B) Representative fluorescent microscopy of T cells electroporated with CRISPR-Cas9 DNA using a protocol that yielded ~85% viability (left). Flow cytometry plots indicate CD5-negative cells in a population of naïve T cells (middle) compared to that of CD5-edited T cells (right).

that would be required to result in increased CAR expression and enhanced cytotoxicity.

Determining the cytotoxicity of CD5-edited CD5-CAR modified T cells against Jurkat T cells

To determine if moderate levels of CD5-editing of T cells would enhance their cytotoxicity, PBMCs were isolated from blood on day 0 from consented, healthy adult donors and underwent a Pan T-cell isolation immediately followed by stimulation using 1:1 ratio of cells to CD3/CD28 Dynabeads. Using the optimized electroporation protocol yielding 15% CD5-edited T cells, cells were electroporated on day 2 post-isolation. On day 4 post-transfection (day 6 of culture), flow cytometry was used to confirm CD5 gene-editing (**Figure 3B**). The CD5-edited T cells were stimulated the same day with CD3/CD28 Dynabeads for 24 hours as described previously. Upon removal of the beads, non-edited and CD5-edited T cells were transduced with the bicistronic eGFP-p2a-CD5-CAR at MOI 34. Flow cytometry confirmed GFP expression demonstrating transduction of the CD5-CAR-modified cells (**Figure 4A & 4B**).

We hypothesized that increased CD5-CAR on the surface of transduced cells could be achieved by inhibiting CD5 through genome editing, and the increase in CAR expression would translate to increased target cell killing. To test this, on day 4 post-transduction, we performed a 24-hour cytotoxicity assay using CD5-edited, CD5-CAR-modified T cells and Jurkat target cells. Jurkat cells were previously labeled with VPD450 proliferation dye to distinguish them from the effector cells by flow cytometry. Upon completion of the 24-hour incubation (day 5 post-transduction), cells were collected and stained with eFluor 780 viability dye and flow cytometry was performed to detect the percentage of dead target cells. There was no difference in cytotoxicity against Jurkat T cells by non-edited CD5-CAR modified T cells compared to that by CD5-edited CD5-CAR modified T cells (**Figure 4C**). We hypothesized that this finding was attributable to the low editing efficiency of the cells resulting in only 15% CD5-editing prior to CAR-modification. This degree of editing may not be sufficient to result in enhanced CD5-directed cytotoxicity. We used this data to guide additional testing to determine if greater CD5-editing would affect CD5-directed cytotoxicity.

Figure III-4: CD5-edited CD5-CAR-modified T-cell cytotoxicity against CD5-positive Jurkat cells.

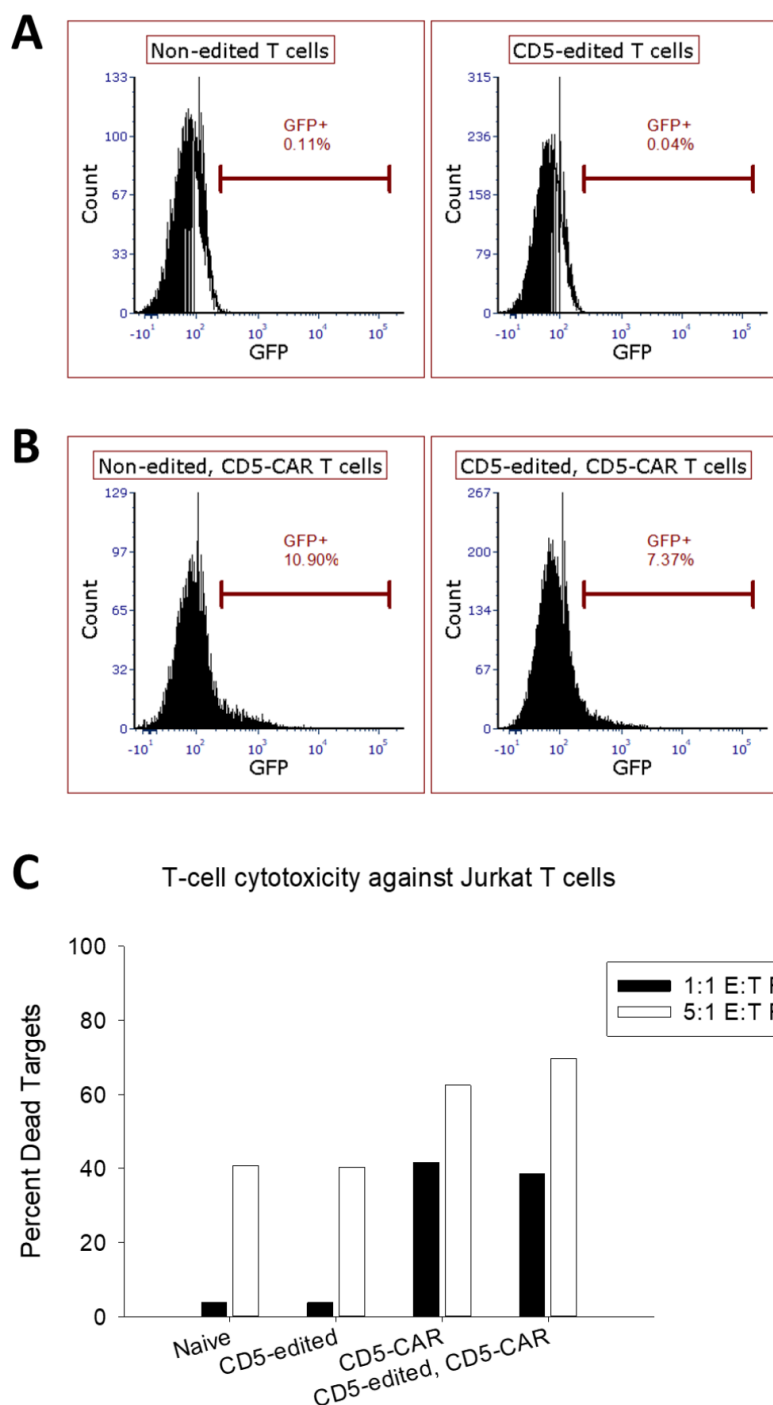


Figure 4: (A) GFP expression in non-transduced non-edited (left) and CD5-edited $\alpha\beta$ T cells (right). (B) Transduction efficiency of non-edited (left) and CD5-edited (right) T cells with the CD5-CAR as measured by flow cytometry. (C) Percent dead Jurkat T cells as measured by double positive eFluor 780 and VPD450 cells cultured at 1:1 and 5:1 E:T ratios with $\alpha\beta$ T cells. The data represents one replicate.

Assessing the effect of greater CD5-editing of T cells prior to CD5-CAR modification on T-cell cytotoxicity

To determine if 15% CD5-editing is insufficient to enhance CD5-directed cytotoxicity, we isolated, stimulated and electroporated T cells from blood as described above and on day 2 post-electroporation, performed flow cytometry to determine the efficiency of CD5-editing (**Figure 5A**). We used FACS to isolate the CD5-negative and CD5-positive populations of T cells. These cells were expanded for three days, after which they were stimulated again for 24 hours with CD3/CD28 Dynabeads and subsequently transduced with the CD5-CAR at MOI 100, which is a viral dose similar to what has been developed to transduce HSCs in a clinical trial designed by our group. Flow cytometry on day 3 post-transduction confirmed non-edited and CD5-edited T cells were transduced similarly (**Figure 5B**). That same day, a 12-hour cytotoxicity assay was established with Jurkat target cells. A 24-hour cytotoxicity assay was described previously, however we chose a shorter duration for this flow-based assay to avoid losing detection of dead cells that, over time, are broken down into debris, which is undetectable using flow cytometry. We did not observe an advantage to using sorted CD5-edited CD5-CAR-modified T cells compared to non-edited CAR-modified T cells in terms of cytotoxicity against Jurkat T cells (**Figure 5C**). Therefore, we conclude CD5-editing of T cells does not enhance cytotoxic activity against Jurkat T cells *in vitro*.

Discussion

We previously demonstrated that CD5-editing of T cells is advantageous by increasing the CAR expression on the cell surface (49), however, we hypothesize the health of these cells is impaired by the multiple modifications and cell sorting, ultimately reducing cytotoxic potential. Therefore, despite comparable transduction of CD5-edited T cells and non-edited T cells, our cytotoxicity assays demonstrate equivalent CD5-specific cytotoxicity against Jurkat T cells. While we see variability among donors regarding baseline cytotoxicity against Jurkat target cells, the CD5-edited CD5-CAR-modified T cells do not demonstrate an advantage over the non-edited CD5-CAR-modified T cells in either assay. This suggests

Figure III-5: CD5-edited, FACS sorted, CD5-CAR-modified $\alpha\beta$ T-cell cytotoxicity against CD5-positive Jurkat cells

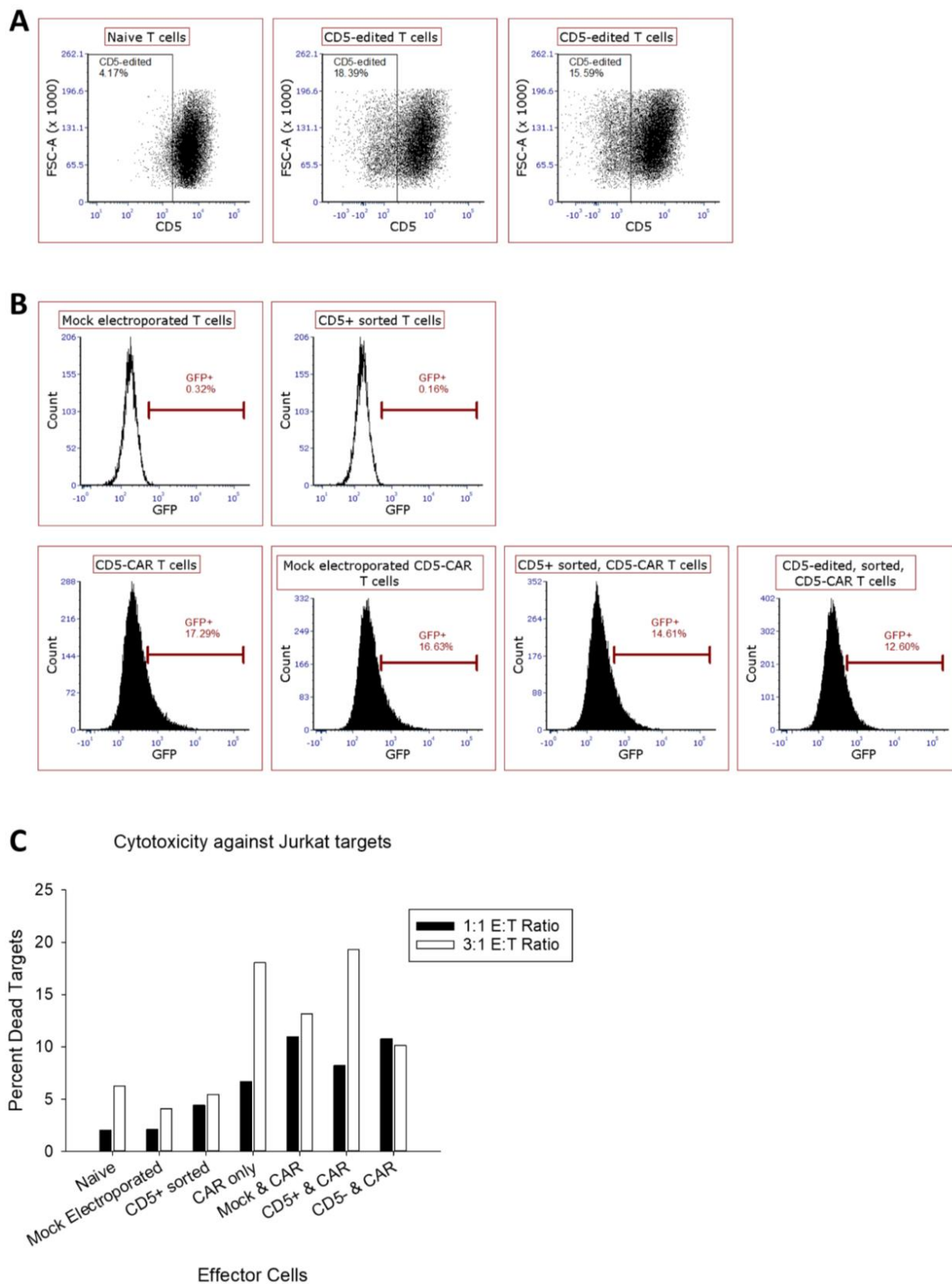


Figure 5: (A) CD5-editing efficiency as measured by CD5-negative cells detected by flow cytometry. Naïve cells are depicted on the left. Cells were electroporated in two cuvettes (middle, right) and later combined into a single population. (B) GFP expression as measured by flow cytometry to depict the percentage of transduced cells. Top row: non-transduced mock electroporated (left) and CD5-positive electroporated, sorted $\alpha\beta$ T cells (right). Bottom row: CD5-CAR modified $\alpha\beta$ T cells: naïve (far left), mock-electroporated (left center), CD5-positive, sorted (right center) and CD5-negative, sorted (far right). (C) $\alpha\beta$ T-cell cytotoxicity against CD5-positive Jurkat cells at 1:1 and 3:1 E:T ratios. Percent dead Jurkat T cells were considered double positive eFluor780 and VPD450 events. One replicate was performed.

that either CD5-editing does not enhance CD5-specific cytotoxicity, or the health of the CD5-edited T cells was impaired and needs to be remedied in order to consider this strategy for enhancing antigen-specific cytotoxicity. One approach is to improve the quality of DNA for transfection. We isolate DNA using Qiagen Plasmid DNA Purification Maxi kit (Qiagen, Germany) and resuspend the DNA in Molecular Biology Grade water (Thomas Scientific, Swedesboro, NJ). The DNA was concentrated using a high-speed centrifuge in order to increase the quantity of DNA utilized for each transfection. DNA quality was further confirmed by agarose gel electrophoresis (data not shown). The size of the plasmid is an additional factor in efficiency of gene delivery, therefore we could remove eGFP from the CRISPR-Cas9 plasmid to reduce the size. Another approach is to introduce CRISPR-Cas9 mRNA by electroporation as opposed to DNA. Studies have demonstrated the ease of mRNA transfections compared to DNA transfections, resulting in higher post-transfection viability and expression (309-311). Milder parameters can be used to transfect T cells to preserve the health of the cells while still yielding high transfection efficiency. Additionally, extending the length of time the cells are in culture could result in better evaluation of the cytotoxicity of CD5-edited T cells. It is plausible that additional time to recover following electroporation prior to transduction will be sufficient to restore their capability to kill target cells. However, we demonstrate that the sorted CD5-positive fraction of electroporated cells modified with the CD5-CAR kill to the same degree as the non-edited T cells. This suggests that electroporation itself and the length of time the cells recovered in culture did not hinder the overall cytotoxic capabilities of T cells. Therefore, although we've previously demonstrated CD5-editing of T cells prior to CD5-CAR modification increases CD5-CAR surface expression on T cells (49), this property is not sufficient to enhance CD5-directed cytotoxicity against Jurkat T cells.

It is possible the health of the cells has not been affected by the double modification, but at the high MOI used to transduce the T cells, there is no longer an advantage to using CD5-edited cells as opposed to non-edited cells. Our studies using Jurkat T cells suggest that as the MOI increases, the need for CD5-editing decreases. At lower MOIs there is a clear advantage in terms of CD5-CAR detection on the cell surface, however, this gap closes as the MOI increases (data not shown). Furthermore, as the MOI increases,

the number of integrated transgene copies per cell is likely to increase. Since lentiviral vectors integrate randomly into the genome, increased numbers of integration sites increases the potential for unfavorable integration.

Another consideration is the exhaustion of the T cells. As the amount of CAR expressed on the cell surface increases, the cells will have increased interactions with the CD5 antigen leading to increased activation of the cells. This can result in activation-induced cell death and/or T-cell exhaustion. If T-cell exhaustion is in fact hindering the cytotoxic capabilities, a different CAR construct can be used. CARs containing 4-1BB typically exhibit greater persistence, while CD28 inclusion yields rapid tumor clearance (37; 312; 313). However, the costimulatory domain(s) that make up the most superior CAR in terms of overall anti-tumor efficacy *in vivo* has yet to be determined (37). Therefore, one approach to reduce exhaustion, would be to utilize a 41BB-CAR as an alternative to the CD28-CAR used in this model.

To determine if CD5-editing of T cells prior to CAR modification is a viable strategy under more optimal conditions, we utilized a lentiviral vector for CRISPR-Cas9 delivery as a proof-of-concept study. This is an alternative approach to determine if CD5-editing prior to CAR modification should be optimized further. Using a lentiviral vector encoding Cas9 and our designed gRNA to transduce Jurkat T cells, we achieved considerable CD5-editing in Jurkat T cells. However, the efficiency of CD5-editing plateaus at ~70% edited cells and this plateau begins at MOI 3 (**Figure 6**). These promising preliminary results will facilitate future studies testing the effects of lentiviral CD5-editing in primary T cells.

An additional modality to assess the advantages of CRISPR-Cas9 genome editing in T cells is to use AAV delivery. While most viral vectors insert the transgene into the host cell genome, transgenes delivered through AAV are primarily expressed episomally. Therefore, the Cas9 would not persist in the cells, which is advantageous due to the potential for off-target cleavage upon prolonged expression (314-316). Therefore, while lentiviral vector delivery of Cas9 can only be considered as a “proof-of-concept” strategy, AAV delivery is a more practical method. Preliminary data from our laboratory suggest T cells are easily modified using an AAV vector and this modification does not considerably affect cell viability. Additionally, our preliminary data suggests high transgene expression in 60% of the T cells upon AAV

Figure III-6: Lentiviral vector delivery of CRISPR-Cas9 DNA to Jurkat T cells

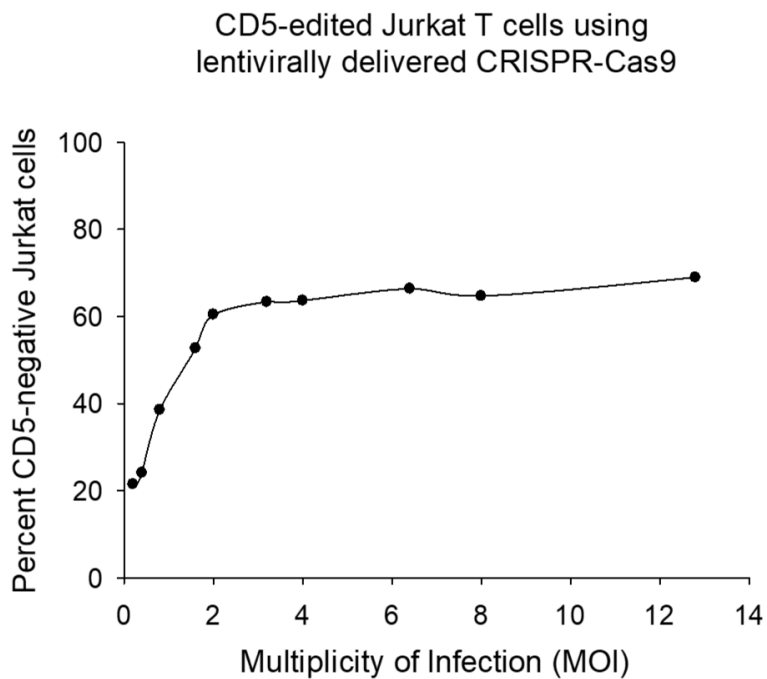


Figure 6: Lentiviral transduction of Jurkat T cells using MOIs ranging from 0.25 to 12.8. Flow cytometry was used to measure CD5-expression on Jurkat T cells on day 5 post transduction.

delivery (unpublished). As a result, we can introduce the CRISPR-Cas9 into the T cells using AAV, followed by lentiviral transduction to incorporate the CAR construct. This strategy is likely to produce a healthier cell product compared to strategies that include DNA electroporation, and we can therefore use these techniques to determine if there is an advantage to CD5-editing prior to CD5-CAR modification of T cells.

Our future focus is moving in the direction of utilizing $\gamma\delta$ T cells as an alternative to $\alpha\beta$ T cells. $\gamma\delta$ T cells represent a novel platform for CAR T-cell therapy and can be especially advantageous for the treatment of T-cell malignancies. While $\gamma\delta$ T cells may exhibit fratricide to the same degree as $\alpha\beta$ T cells, there is limited risk of T-cell aplasia as V γ 9V δ 2 expanded T cells are unlikely to form a memory response against the T-cell antigen. Additionally, because $\gamma\delta$ T cells are non-alloreactive, third-party donor cells can be utilized. They are short-lived and require multiple infusions for treatment, therefore T-cell exhaustion is not of primary concern. Utilizing $\gamma\delta$ T cells for CAR therapy can overcome some of the limitations to conventional CAR T-cell therapy, particularly in the setting of T-cell malignancies.

Chapter IV

$\gamma\delta$ T cells as an alternative effector cell type for CAR T-cell therapy

Abstract

Conventional CAR therapy equips $\alpha\beta$ T cells to attack malignant cells expressing a specific antigen, which can be strategically selected. However, there are limitations to utilizing $\alpha\beta$ T cells and many of these limitations can be addressed through the use of $\gamma\delta$ T cells. $\gamma\delta$ T cells bridge the innate and adaptive immune systems. Unlike $\alpha\beta$ T cells, $\gamma\delta$ T cells do not require priming, or MHC-presentation. They express endogenous mechanisms of cytotoxicity that provide inherent anti-tumor activity through recognition of stress antigens, heat shock proteins and chemokines. We have previously demonstrated $\gamma\delta$ T cells are consistently expanded up to 80-fold in serum-free conditions with IL-2 and zoledronic acid supplementation. However, as described herein, $\gamma\delta$ T cells are difficult to modify using two different transfection modalities. While recombinant HIV lentiviral vector modifies $\gamma\delta$ T cells to a greater degree than does transfection, we can only achieve moderate levels (<30% modified $\gamma\delta$ T cells). Using AAV serotype 6, we can achieve greater than 50% transduced $\gamma\delta$ T cells, which has not been achievable even with high MOIs of lentiviral vector. We demonstrate with AAV6, by day 6 post-transduction, the percentage of modified $\gamma\delta$ T cells is reduced by half. This is due to both dilution of the transgene as the cells divide as well as degradation of the transgene as a result of transient stability. Typically, CAR T-cell therapy is thought to require prolonged CAR T-cell expression in order to successfully eliminate the tumor, which would make AAV transduction a less optimal approach. However, $\gamma\delta$ T-cell therapy requires numerous infusions, as $\gamma\delta$ T cells do not persist for long *in vivo*. Therefore, episomal expression of the transgene is not a primary concern. We hypothesized a greater percentage of CAR-modified $\gamma\delta$ T cells will result in higher cytotoxic potential. Therefore, we predict we can achieve more rapid tumor control using AAV-modified cells compared to lentiviral vector-modified cells. Multiple infusions would be required to sustain the response until hematopoietic stem cell transplantation (HSCT).

Introduction

The majority of CAR therapies under investigation utilize $\alpha\beta$ T cells. T cells are approximately 60-70% of peripheral blood mononuclear cells (PBMCs) and can easily be expanded from healthy donors *ex vivo* (317; 318). However, expanding $\alpha\beta$ T cells from cancer patients can be difficult as they are often heavily pretreated with chemotherapeutics resulting in poorly expanding cells and/or deficits in cytotoxic potential (319). $\alpha\beta$ T cells cannot be isolated and expanded from a third-party donor for CAR T-cell therapy due to MHC-restrictions unless modifications are made to prevent GvHD reactions (319; 320). However, $\gamma\delta$ T cells, which make up 1-5% of PBMCs, are non-alloreactive and can therefore be used in an allogeneic setting (163; 318; 321). $V\gamma9V\delta2$ T cells, the most commonly studied subset for $\gamma\delta$ T-cell therapy, can be expanded *ex vivo* in serum-free conditions from healthy donors (163). These cells can be cryopreserved and stored until they are required in an allogeneic setting (173). Furthermore, while $\gamma\delta$ T cells do not require priming and can interact with antigen independently of MHC-recognition (321; 322), they can act as antigen-presenting cells to prime $\alpha\beta$ T cells (322; 323). Additionally, $\gamma\delta$ T cells trigger dendritic-cell maturation (318; 322; 324; 325), induce B cells to produce immunoglobulin (322), secrete proinflammatory cytokines (318; 326; 327), and recognize stress antigens (318; 321; 328; 329), heat shock proteins (330), phosphoantigens (321; 322; 329) and chemokines from tumor cells (181). Moreover, a 2015 Nature Medicine publication acknowledged $\gamma\delta$ T-cell infiltration into a variety of tumors was correlated with a more favorable prognosis (331).

The administration of $\gamma\delta$ T cells to cancer patients supplemented with zoledronic acid as well as administration of zoledronic acid to stimulate $\gamma\delta$ T cells *in vivo* have been assessed. However, while these clinical trials illustrate the natural anti-tumor activity of $\gamma\delta$ T cells, they have not been entirely successful, as the $\gamma\delta$ T cells did not exhibit tumor control (191; 332; 333). We hypothesize that expression of a CAR on $\gamma\delta$ T cells can enhance their cytotoxic activity against tumor cells. Our group focuses on the treatment of T-cell malignancies using CAR T-cell therapy. A major limitation to CAR T-cell therapy for the treatment of T-cell malignancies is T-cell aplasia resulting from memory-cell formation of CAR T cells targeting a T-cell antigen. Unfortunately, to date, very few tumor-specific antigens have been identified

that could address this problem (CD30, CD37 and TRBC1 as described in chapter 1) and those few antigens are only expressed on a small subset of cancers. To overcome this limitation, we propose utilizing V γ 9V δ 2 T cells. While V γ 9V δ 2 T cells express a similar antigen repertoire as T-cell malignancies, *ex vivo* expanded cells are predicted to persist for up to a few weeks *in vivo* and are unlikely to form memory cells targeting the T-cell antigen (321). Additionally, their reduced expansion *in vivo* can decrease the development of adverse reactions such as CRS, which is correlated with rapid proliferation of CAR T cells and tumor burden (40). Taken together, $\gamma\delta$ T cells are good candidates for effector cells for CAR T-cell therapies targeting T-cell malignancies. However, $\gamma\delta$ T cells are likely susceptible to fratricide, similar to $\alpha\beta$ T cells. As a result, only tumor-specific antigens can confer tumor-specificity (examples described in chapter 1) or rapid down-regulation of the antigen from the cell surface (results in only transient fratricide) (78). Alternatively, genome editing using CRISPR-Cas9 can be utilized to disrupt expression of the antigen on $\gamma\delta$ T cells to prevent fratricide. This chapter discusses our studies in $\gamma\delta$ T cells using CRISPR-Cas9 to edit the CD5 locus and using viral vector to express a CD5-CAR to generate a superior CAR product.

Unlike $\gamma\delta$ T cells, $\alpha\beta$ T cells have been well characterized in regards to CAR therapy and their transfection and transduction potential understood. Very few groups have recognized $\gamma\delta$ T cells for their potential in CAR therapy. As discussed in chapter 3, transfection techniques as opposed to viral transduction are commonly used to introduce Cas9 into primary cells to avoid long-term expression of the Cas9. Herein, we utilize both nucleoporation and electroporation, as previously described in chapter 3, to transfect $\gamma\delta$ T cells to disrupt CD5 gene expression using CRISPR-Cas9. Furthermore, as CD5 has previously been described to rapidly down-regulate from the T-cell surface (49; 78), genome editing may not be required for expansion of CD5-CAR-modified $\gamma\delta$ T cells. Therefore, in this chapter, we evaluate lentiviral and AAV transduction of $\gamma\delta$ T cells to determine if genome editing is required to produce an effective product. Our results demonstrate that while $\gamma\delta$ T cells are difficult to transfect with plasmid DNA using either nucleoporation or electroporation techniques, and the transduction efficiency of $\gamma\delta$ T cells is low using recombinant HIV lentiviral vector, we can achieve high levels of transduction (50% modified cells) using

AAV serotype 6. High levels of transduction are likely to result in high surface CD5-CAR expression despite anticipated down-regulation resulting from antigen/CAR interactions. Therefore, genome editing may not be a prerequisite for CD5-CAR T-cell therapy.

Methods and Materials

γδ T-cell expansion. γδ T cells were expanded from cryopreserved PBMCs purchased from AllCells (Alameda, California) or from fresh PBMCs isolated from 30-50 mL consented, healthy adult blood. PBMCs were isolated from blood using Ficoll-Paque density gradient and centrifugation according to the manufacturer's protocol. γδ T cells were expanded in serum-free conditions in OpTmizer media (Thermo Fisher Scientific, Waltham, MA) for two weeks supplemented with 5 μM zoledronic acid (Sigma Aldrich, ST Louis, MO) and 500-1000 IU/mL IL-2 (PeproTech, Rocky Hill, NJ). Cells are cultured with zoledronic acid until day 6 of expansion. γδ T cells are cultured at 1.5×10^6 cells/mL. Cell viability was measured by staining cells with a 1:1 dilution of 0.2% Trypan blue (Thermo Fisher Scientific, Waltham, MA) in PBS and using the Nexcelom Auto T4 Cellometer (Nexcelom, Lawrence, MA) to calculate the percent cell viability within a sample.

Nucleoporation of γδ T cells. PBMCs were nucleoporated on different days of expansion using the Lonza Nucleofector 2b Device and the Amaxa Human T-Cell Nucleofector kit (Lonza, Switzerland). γδ T cells were nucleoporated using programs T-020 and U-014 with 2.5 μg of CRISPR-Cas9 plasmid DNA. U-014 is programmed with milder parameters compared to those of T-020, however the specific parameters involved in program design are proprietary. Transfection efficiency was observed using eGFP. CD5-editing was determined using flow cytometry.

Electroporation of γδ T cells. γδ T cells were electroporated using the BTX ECM830 Square Wave Electroporator and BTXpress Solution (BTX, Holliston, MA) as described in chapter 3. γδ T cells were

electroporated using a variety of protocols that varied in parameters including buffer, cell number, day of expansion, voltage, pulse length, number of pulses, and interval between pulses. Cell viability was assessed on day 1 following transfection using Trypan blue as described above. Flow cytometry was used to measure CD5 expression.

Flow cytometry. Flow cytometry was performed using a BD LSRII Flow Cytometer (BD Biosciences, San Jose, CA). Data was analyzed using BD FACSDiva and FCS Express 6 software. Antibodies used included anti-CD5 PerCP/Cy5.5, anti-CD3 BV421 and anti- $\gamma\delta$ TCR (BD Biosciences, San Jose, CA). eFluor 780 fixable viability dye (Thermo Fisher Scientific, Waltham, MA) was used to quantify dead cells. CD5-Fc fusion protein (G&P Biosciences, Santa Clara, CA) was used to detect CD5-CAR with a secondary anti-IgG Fc antibody (Jackson ImmunoResearch Laboratories, West Grove, PA), as previously described (49). For the cytotoxicity assays, Violet Proliferation Dye 450 (VPD450) was used to label the target cells, and cell death was assessed using eFluor 780 (described below).

Lentiviral vector production. High-titer recombinant SIN lentiviral vector was produced and titered as previously described (49).

Lentiviral vector transduction of $\gamma\delta$ T cells. $\gamma\delta$ T cells were transduced with lentiviral vector between days 7 and 10 of expansion. Cells were incubated with viral vector at MOIs ranging from 12-72 at 50-100% vector. Culture medium was supplemented with 6 $\mu\text{g}/\text{mL}$ polybrene to facilitate transduction and was replaced with fresh medium after 18-24 hours. The transduced cells were cultured up to day 14 of expansion.

Culture of Jurkat T-cell line. Jurkat T cells were cultured in complete RPMI as previously described (49).

Cytotoxicity assay. Cytotoxicity assays were performed on day 12 of $\gamma\delta$ T-cell expansion. Jurkat target cells were labeled with VPD450 according to the manufacturer's protocol (BD Biosciences, San Jose, CA), 24-36 hours prior to flow cytometry. Effector (E) and target (T) cells were cultured for four hours in 12x75 mm FACS tubes at E:T ratios of 1:1, 3:1 and/or 5:1 in a total volume of 250 μ L at 37°C in 5% CO₂. The cells were subsequently stained with eFluor 780 (Thermo Fisher Scientific, Waltham, MA). eFluor 780 and VPD450 double-positive cells were quantified using flow cytometry.

AAV production. Plasmids encoding pAAV-GFP, pHelper, pAAV-Rep2Cap2, pAAV-Rep2Cap3, and pAAV-Rep2Cap6 were purchased from Cell Biolabs (San Diego, CA). The three different RepCap plasmids with different tissue tropism were purchased to confirm the serotype that provides the greatest transduction of T cells. A second pAAV-Rep2Cap3 was produced in our laboratory and included in our studies. The AAV-GFP control vector is expressed using the CMV promoter and contains ITR sequences from AAV serotype 2. The CD5-CAR construct was cloned into an AAV backbone and the UBC promoter was replaced by the MND promoter. The AAV-CD5-CAR plasmid also contains the ITRs from AAV2 and was made with pAAV-Rep2Cap6 and pHelper plasmids. 293T cells were transfected with pAAV-GFP or pAAV-CD5-CAR, pHelper and the appropriate RepCap plasmid. Cells were harvested on day 3 post-transfection and supernatants and cells were separated. Supernatants were incubated in a PEG solution at a final concentration of 8% PEG 8000-0.5 M NaCl overnight on ice. The following day, the supernatants were centrifuged for 30 minutes at 7,000g. Cell pellets were frozen in lysis buffer, and upon thawing, sodium deoxycholate was added at a final concentration of 0.5% and Pierce Universal Nuclease for Cell Lysis (Thermo Fisher Scientific, Waltham MA) at 0.1 μ L/mL. Cell lysates were incubated for 30 minutes at 37°C. MgCl₂ was added to cell lysates along with NaCl and salt active nuclease (SAN). Cell lysates were incubated for 30 minutes at 37°C. The pellet formed from centrifugation of supernatants incubated in PEG and NaCl was then resuspended in lysis buffer and combined with the crude lysate. Following a 15-minute incubation at 37°C, lysates were centrifuged for 15 minutes at 4°C at 3,000g and aliquoted into Type 70 Ti

centrifuge tubes (Beckman Coulter, Indianapolis, IN). The tubes were layered with 15% iodixanol buffered by 1M NaCl and 1X PBS-MK (PBS supplemented with MgCl₂ and KCl), followed by 25%, 40% and 54% iodixanol buffered by 1x PBS-MK. Tubes were centrifuged for 90 minutes at 58,500 RPM at 18°C. The 54%-40% interphase was isolated and diluted with an equal volume of 1x PBS-MK. The diluted iodixanol was loaded into a second centrifuge tube underlaid with 30% iodixanol followed by 40% and 54% iodixanol. A second centrifugation was performed for 90 minutes at 58,500 RPM at 10°C. The 54%-40% interphase was isolated and stored at 4°C. Buffer exchange and concentration was performed using 2x PBS-MK with 0.01% Puroic-F68. Vectors were stored at -80°C.

AAV6 functional titering. A functional titer was calculated to standardize AAV6 transductions using vector from different production lots. Jurkat T cells (100,000 cells) were transduced in culture medium as previously described with 5 or 10 μ L viral vector in duplicate. On day 3 post-transduction, flow cytometry was performed to quantify the percentage of GFP-expressing cells. Functional titer was calculated as (cell number) x (% GFP-modified cells) / (volume of viral vector (mL)).

AAV6 transduction of $\gamma\delta$ T cells. $\gamma\delta$ T cells were transduced between days 7-11 of expansion. Cells were incubated with 10-50% viral vector for 18-24 hours. Culture medium was subsequently replaced with fresh medium.

$\gamma\delta$ T-cell persistence in NOD.Cg-Prkdc^{scid} Il2rg^{tm1Wjl}/SzJ (NSG) mice. Mice were purchased from Jackson Laboratory (Bar Harbor, ME) and maintained in a pathogen-free environment. Mice were cared for according to the established principles of the Institutional Animal Care and Use Committee (IACUC), and all animal protocols were approved by the IACUC as previously described (49). $\gamma\delta$ T cells were expanded for twelve days *ex vivo* according to our expansion protocol and determined to be 70% pan- $\gamma\delta$ T cells by flow cytometry. NSG mice were randomized to four groups, with three mice per group. Mice were injected

with 5.0×10^6 , 1.0×10^7 or 1.5×10^7 cells. The fourth group did not receive $\gamma\delta$ T cells. Cells were re-suspended in 100 μ L phosphate buffered saline (PBS) for injection. Eight-week-old mice were intravenously injected via tail-vein with $\gamma\delta$ T cells. On days 1, 3, 6 and 8 post- $\gamma\delta$ T-cell injection, blood samples were collected from each mouse and analyzed by flow cytometry using BD LSRII Flow Cytometer (BD Biosciences, San Jose, CA). Antibodies used included anti-human CD45 FITC, anti-mouse CD45.1 APC and anti-human TCR γ/δ PE (BD Biosciences, San Jose, CA).

Statistics. Statistical significance was determined using one-way ANOVA. p -values were calculated with SigmaPlot, version 14.0 (Systat Software, Chicago, IL), and $p < 0.05$ is considered statistically significant.

Results

Expansion of $\gamma\delta$ T cells in serum-free conditions

We previously published a serum-free expansion protocol for $\gamma\delta$ T-cell expansion from PBMCs (163). PBMCs were either purchased as a cryopreserved product from AllCells (Alameda, California), or isolated from consented, healthy adult donor blood. While $\gamma\delta$ T cells exist as 1-5% of human PBMCs, we can expand them to, on average, 80% of the population within two weeks (**Figure 1A & 1B**). As exemplified in Figure 1, there is donor variability regarding $\gamma\delta$ T-cell expansion, and some donors will only expand to ~50% $\gamma\delta$ T cells. However, $\gamma\delta$ T-cell expansion does not differ between cells expanded from PBMCs purchased from AllCells and those from PBMCs isolated from fresh blood in our laboratory (**Figure 1A**). We previously published that total $\gamma\delta$ T-cell yield is correlated with the starting number of $\gamma\delta$ T cells and we can expand $\gamma\delta$ T cells 80-fold in fourteen days (163). Furthermore, we used flow cytometry to measure CD5 expression in $\gamma\delta$ T cells and observed a high percentage of CD5-expressing cells throughout expansion (**Figure 1C**).

Transfection of $\gamma\delta$ T cells using nucleoporation to introduce CRISPR-Cas9

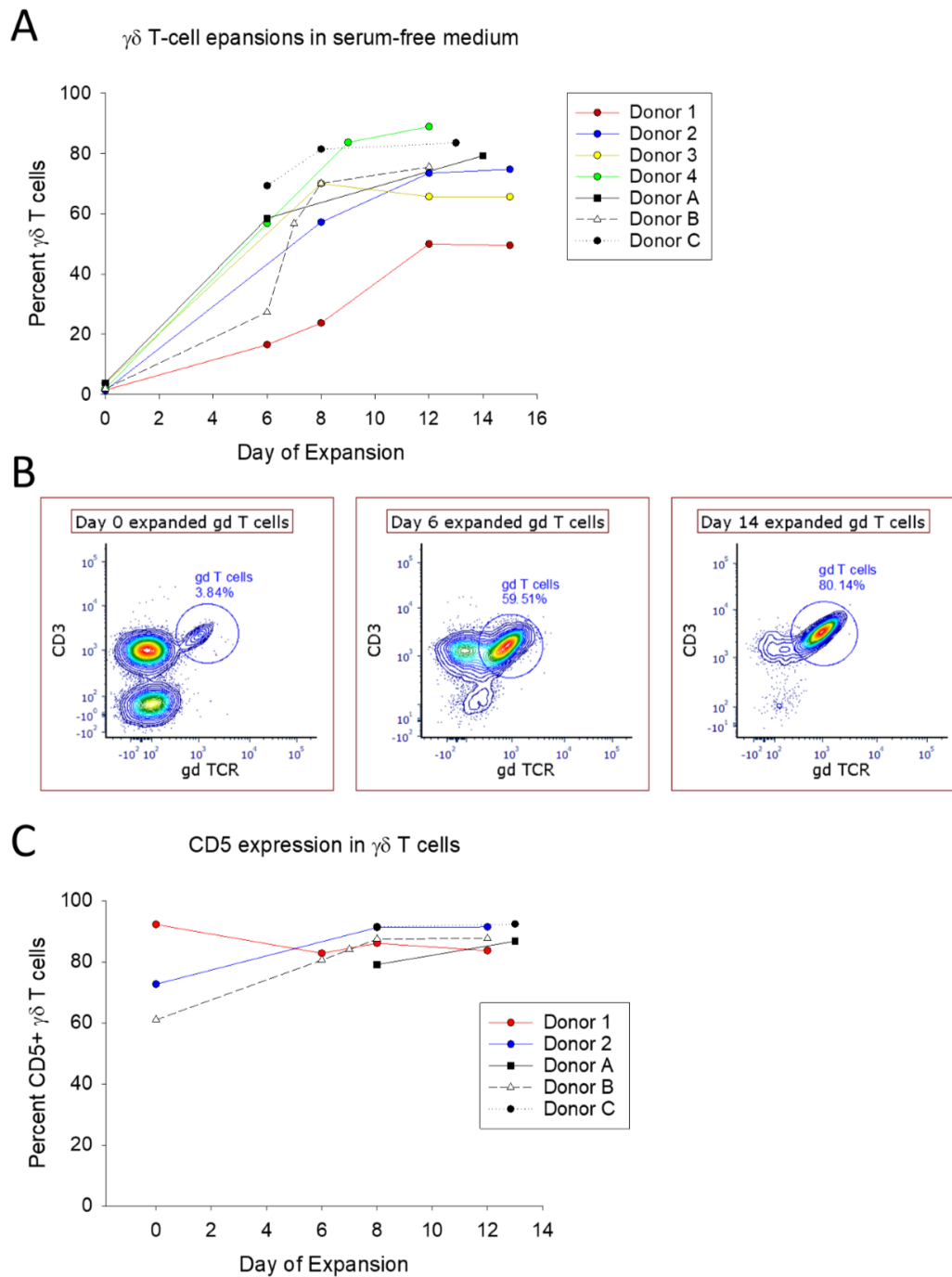
Figure IV-1: Expansion of $\gamma\delta$ T cells from PBMCs.

Figure 1: (A) $\gamma\delta$ T cells were expanded from PBMCs obtained from AllCells (Donors 1, 2, 3 and 4) or isolated from fresh blood (Donors A, B and C). (B) Representative flow cytometry plots illustrating the percentage of $\gamma\delta$ T cells on days 0, 6 and 14 of expansion. (C) CD5 expression in $\gamma\delta$ T cells at various time points within a two-week expansion.

$\gamma\delta$ T cells were expanded from PBMCs purchased from AllCells as described. On days 0, 6, 8 and 12 of $\gamma\delta$ T-cell expansion, cells were removed from culture and flow cytometry was performed to evaluate the CD5 expression on the cells. High expression of CD5 on $\gamma\delta$ T cells (>70% by day 6) (**Figure 1C**) can result in fratricide upon CD5-CAR-modification. To prevent fratricide, we used CRISPR-Cas9 targeting the CD5 locus to disrupt CD5 expression on $\gamma\delta$ T cells prior to CD5-CAR-modification.

On days 3, 6, 9 and 12 of $\gamma\delta$ T-cell expansion, the cells were nucleoporated to introduce CRISPR-Cas9 plasmid DNA as a means of disrupting the CD5 gene. DNA was not added to the mock nucleoporation cuvettes, however they were otherwise treated under identical conditions as those for the experimental samples. Cell viability was assessed the following day when the media was changed. On day five post-nucleoporation, CD5-expression was evaluated by flow cytometry and compared to its expression measured immediately prior to nucleoporation. The data suggests this program results in inefficient CD5-editing as there is no difference in CD5-expression in the cells after nucleoporation, compared to the expression measured before nucleoporation, regardless of the day of expansion on which the cells were nucleoporated (**Figure 2A**). We have demonstrated in both Jurkat T cells and primary $\alpha\beta$ T cells that our plasmid containing the gRNA and Cas9 are efficient at disrupting the CD5 gene (49). Therefore, we hypothesized the lack of editing was due to inefficient gene delivery, rather than poor functionality of the construct. Additionally, the cell viability was reduced to ~40% on average following nucleoporation. However, there was no difference in the viability between cells nucleoporated with or without DNA (with the exception of cells nucleoporated on day 12 of expansion) suggesting the nucleoporation conditions were too harsh for $\gamma\delta$ T cells (**Figure 2B**). Our data demonstrating poor editing efficiency and reduction in viability, was used to guide additional testing using an alternative method of transfection, as described below.

Transfection of $\gamma\delta$ T cells using electroporation techniques to introduce CRISPR-Cas9

As discussed in chapter 3, a wide variety of parameters can be regulated to optimize the transfection efficiency and cell viability of primary T cells. However, nucleoporation using the Amaxa prevents such

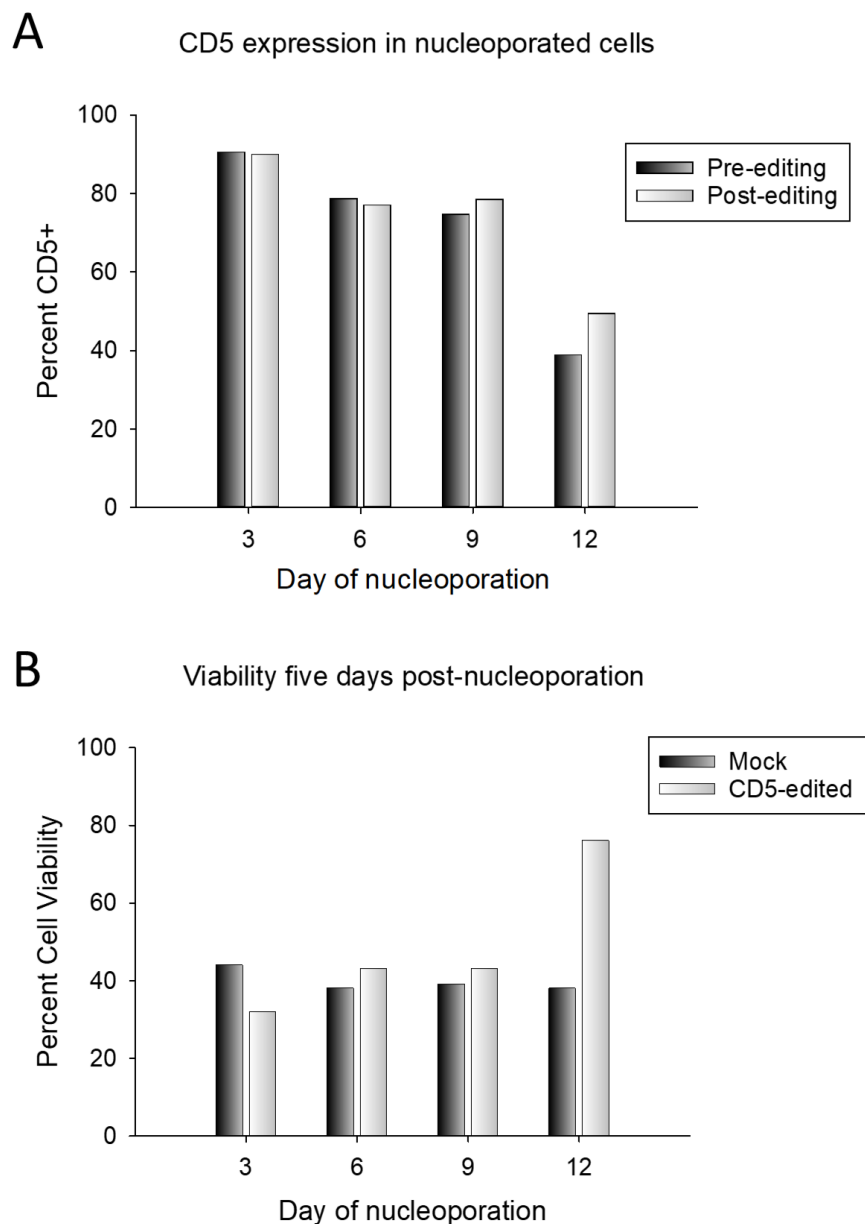
Figure IV-2: Nucleoporation of $\gamma\delta$ T cells

Figure 2: (A) CD5 expression on days 3, 6, 9 and 12 prior to nucleoporation (black) and five-days following nucleoporation (white). (B) Viability of cells was measured by Trypan blue on day 1 post-nucleoporation. Mock nucleoporated cells are depicted by black bars; cells nucleoporated with CD5 CRISPR-Cas9 are depicted by white bars.

optimization as the parameters are pre-programmed and specific, proprietary buffers are required. Our previous studies suggest primary cells may be more easily transfected using electroporation techniques as opposed to nucleoporation. Therefore, we assessed a variety of parameters to optimize electroporation of $\gamma\delta$ T cells similarly to our optimization of $\alpha\beta$ T-cell electroporation. Using two different donor $\gamma\delta$ T cells from AllCells, and one fresh blood donor expansion, we assessed electroporation parameters on days 7-9 of expansion. Before day 7, the percentage of $\gamma\delta$ T cells is too low to obtain efficient modification of $\gamma\delta$ T cells. Due to the *ex vivo* expansion of $\gamma\delta$ T cells (**Figure 1A & 1B**), our current protocol involves infusion of $\gamma\delta$ T cells on day 12. Therefore, all modifications must be completed prior to day 12. As a result, we focus on modification of $\gamma\delta$ T cells between days 7 and 9 of expansion using numerous protocols (**Table 1**).

We first tested a program on day 7 of expansion that is similar to the program used to electroporate $\alpha\beta$ T cells, albeit designed to be milder to preserve $\gamma\delta$ T-cell viability (2 pulses of 100V, each lasting 400 μ seconds, delivered with a 100 millisecond interval between pulses). However, while these parameters did not dramatically affect cell viability (65% cell viability), we did not observe any change in CD5 expression in the cells five days post-electroporation compared to expression detected in naïve $\gamma\delta$ T cells (**Figure 3A & 3B**). A harsher program on day 8 (300V delivered in 700 μ seconds) resulted in poor viability (19% cell viability), whereas a set of parameters on day 9 milder than the second attempt but harsher than the first did not have as large an effect on viability (3 pulses of 100V, each lasting 550 μ seconds delivered with 100 millisecond intervals; 48% cell viability), however none of these programs resulted in CD5-editing (**Figure 3C & 3D**). Using a second donor, we attempted to optimize electroporation of $\gamma\delta$ T cells using BTXpress Solution. However, all four of our protocols dramatically reduced the cellular viability ($\leq 30\%$) and no GFP expression was observed (used as a measure of CRISPR-Cas9 transgene expression) (**Figure 3E & Table 1**). Additional parameters were tested on $\gamma\delta$ T cells obtained from a third donor. These protocols were milder, with lower voltages and increased pulse number and length (day 7 protocols: 3 pulses of 70V or 50V, each lasting 1 or 2 milliseconds, respectively, delivered with 100 millisecond intervals; day 8

Figure IV- Table 1: Electroporation parameters for introducing CRISPR-Cas9 plasmid DNA into $\gamma\delta$ T cells.

Day of Expansion	Buffer	Temperature (°C)	DNA (μ g)	Number of cells	Voltage	Pulse Length	Number of pulses	Pulse interval	Day 1 Viability	Percent CD5-edited cells (subtracting CD5-negative cells in non-edited cells)
7	Pre-warmed OptiMEM	Room temp reaction	CRISPR-Cas9 100 μ g	5e5	100 V	400 μ seconds	2	100 milliseconds	65%	2.13%
8	Pre-warmed OptiMEM	Room temp reaction	CRISPR-Cas9 100 μ g	1e6	300 V	700 μ seconds	1		19%	-1.91%
9	Pre-warmed OptiMEM	Room temp reaction	CRISPR-Cas9 100 μ g	5e5	100 V	550 μ seconds	3	100 milliseconds	48%	-1.8%
8	Room temp BTXpress Solution	Room temp reaction	CRISPR-Cas9 100 μ g	1e6	100 V	2 milliseconds	5	100 milliseconds	22%	Not Viable
8	Room temp BTXpress Solution	Room temp reaction	CRISPR-Cas9 100 μ g	1e6	250 V	1 millisecond	3	100 milliseconds	16%	Not Viable
9	Room temp BTXpress Solution	Room temp reaction	CRISPR-Cas9 200 μ g	1e6	100 V	700 μ seconds	3	100 milliseconds	30%	No GFP observed
9	Room temp BTXpress Solution	Room temp reaction	CRISPR-Cas9 200 μ g	1e6	200 V	700 μ seconds	1		22%	No GFP observed
7	Room temp BTXpress Solution	Room temp reaction	CRISPR-Cas9 100 μ g	1e6	70 V	1 millisecond	3	100 milliseconds	75%	No GFP observed
7	Room temp BTXpress Solution	Room temp reaction	CRISPR-Cas9 100 μ g	1e6	50 V	2 milliseconds	3	100 milliseconds	79%	No GFP observed
8	Room temp BTXpress Solution	Room temp reaction	CRISPR-Cas9 100 μ g	1e6	80 V	2 milliseconds	5	100 milliseconds	57%	No GFP observed
8	Room temp BTXpress Solution	Room temp reaction	CRISPR-Cas9 200 μ g	1e6	80 V	2 milliseconds	5	100 milliseconds	50%	No GFP observed

Table 1: Trypan blue was used to measure viability on day 1 post-electroporation. Flow cytometry on day 12 of expansion was performed to assess CD5-expression on $\gamma\delta$ T cells, if GFP was observed by fluorescent microscopy.

Figure IV-3: CD5 expression and viability in $\gamma\delta$ T cells following CD5-editing by electroporation.

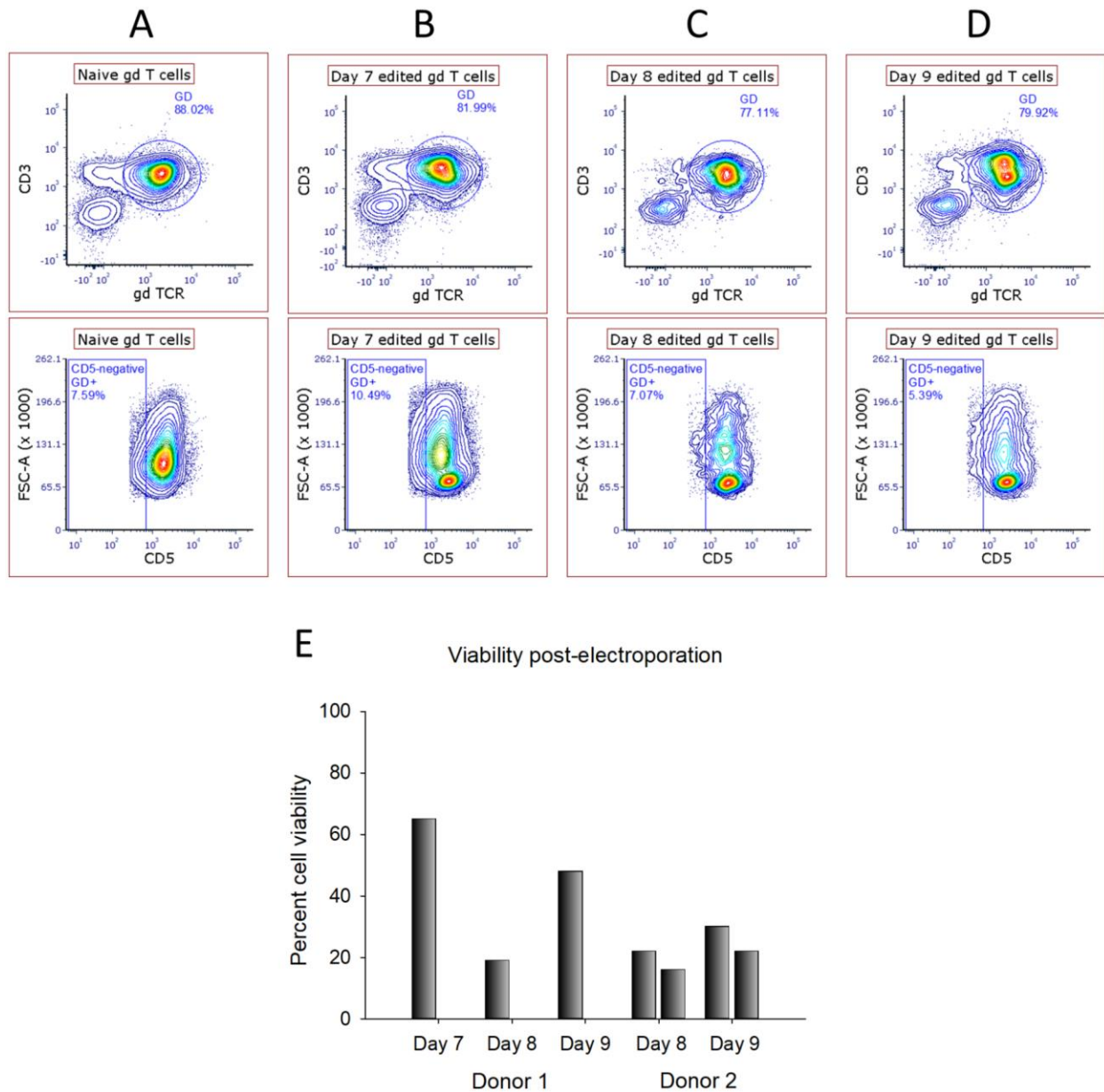


Figure 3: (A, B, C, D) Percentage of $\gamma\delta$ T cells (top) and CD5-expression (bottom) in each cell population. CD5 was evaluated by flow cytometry on day 12 of expansion. **(A)** Naïve $\gamma\delta$ T-cell population. **(B, C and D)** Cells edited on **(B)** day 7, **(C)** day 8 and **(D)** day 9. **(E)** Cell viability from two donors were measured on day 1 post-electroporation by Trypan blue staining.

protocols: 5 pulses of 80V, each lasting 2 milliseconds, delivered with 100 millisecond interval). While they preserved viability, no GFP was observed under any of these conditions (**Table 1**), despite usage of 200 μ g DNA in one of the protocols performed on day 8.

$\gamma\delta$ T cells have proven to be difficult to transfect using either nucleoporation or electroporation techniques. This greatly reduces the likelihood of achieving two modifications, i.e. CD5-editing followed by gene addition for CAR expression. However, it is unclear whether genome editing to disrupt expression of CD5 is required to achieve sufficient CD5-CAR expression and expansion of the modified $\gamma\delta$ T cells.

Lentiviral transduction of $\gamma\delta$ T cells to introduce a CD5-CAR

To determine if disruption of the CD5 locus is required to produce functional CD5-CAR-modified $\gamma\delta$ T cells, we transduced non-edited $\gamma\delta$ T cells with CD5-CAR lentiviral vector, with the hypothesis that CAR expression will sufficiently downregulate endogenous CD5 expression. Previous studies published by our laboratory demonstrate LDL-R expression peaks in $\gamma\delta$ T cells on day 6 of expansion, however, it remains high until day 9 (163). As LDL-R is the receptor by which VSVG-enveloped lentiviral vector infects a cell, we hypothesize high transduction efficiency can be achieved by transducing cells between days 6-9 of expansion. By day 7 or 8, the percentage of $\gamma\delta$ T cells in donor PBMC populations typically exceeds 60%, at which point $\gamma\delta$ T cells are transduced with lentiviral vector. We transduced $\gamma\delta$ T cells with CD5-CAR lentiviral vector at MOI 12-72, ranging from 50-100% vector. On days 12 or 13, trypan blue was used to assess cell viability and flow cytometry was performed to determine the transduction efficiency.

AllCells donors 1 and 2 were transduced with the CD5-CAR lentiviral vector at MOIs 12-17, with 50-75% vector ranging from single to triple transductions. Donor 1 was expanded two times and transduced either with MOI 14 on days 8 and 9, separately, or with MOI 12 on days 8, 9, and 10. Our data suggest at these low MOIs, a single transduction can yield as few as 3% GFP-modified cells. Multiple transductions on both days 8 and 9 or days 8, 9 and 10 resulted in 6% and 11% modified cells, respectively (**Figure 4A & 4B**). Donor 2 was transduced at MOI 17 and again at MOI 5 on days 8 and 10 of expansion. Cells were

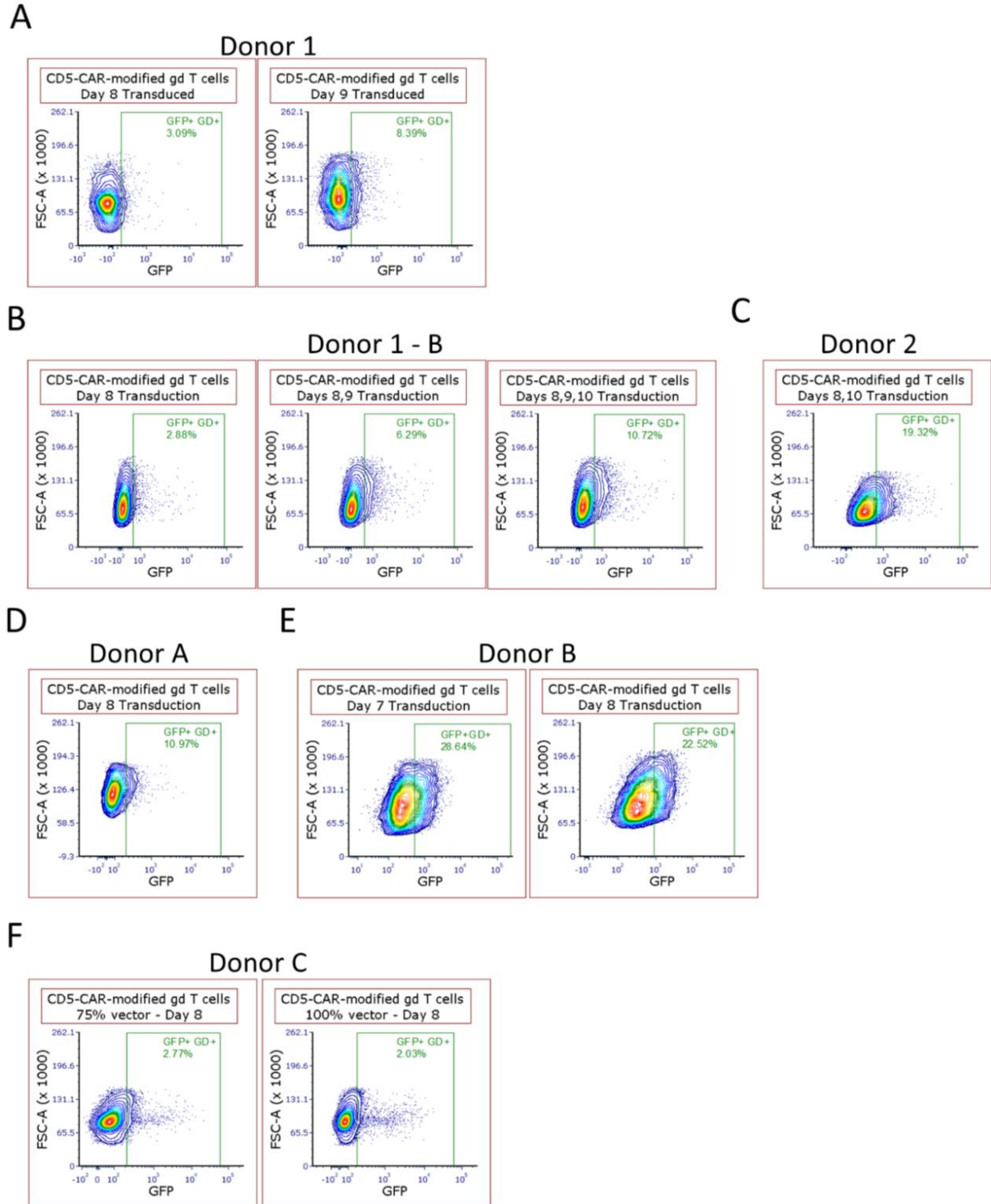
Figure IV-4: $\gamma\delta$ T cells transduced with CD5-CAR lentiviral vector.

Figure IV-4 continued: $\gamma\delta$ T cells transduced with CD5-CAR lentiviral vector.

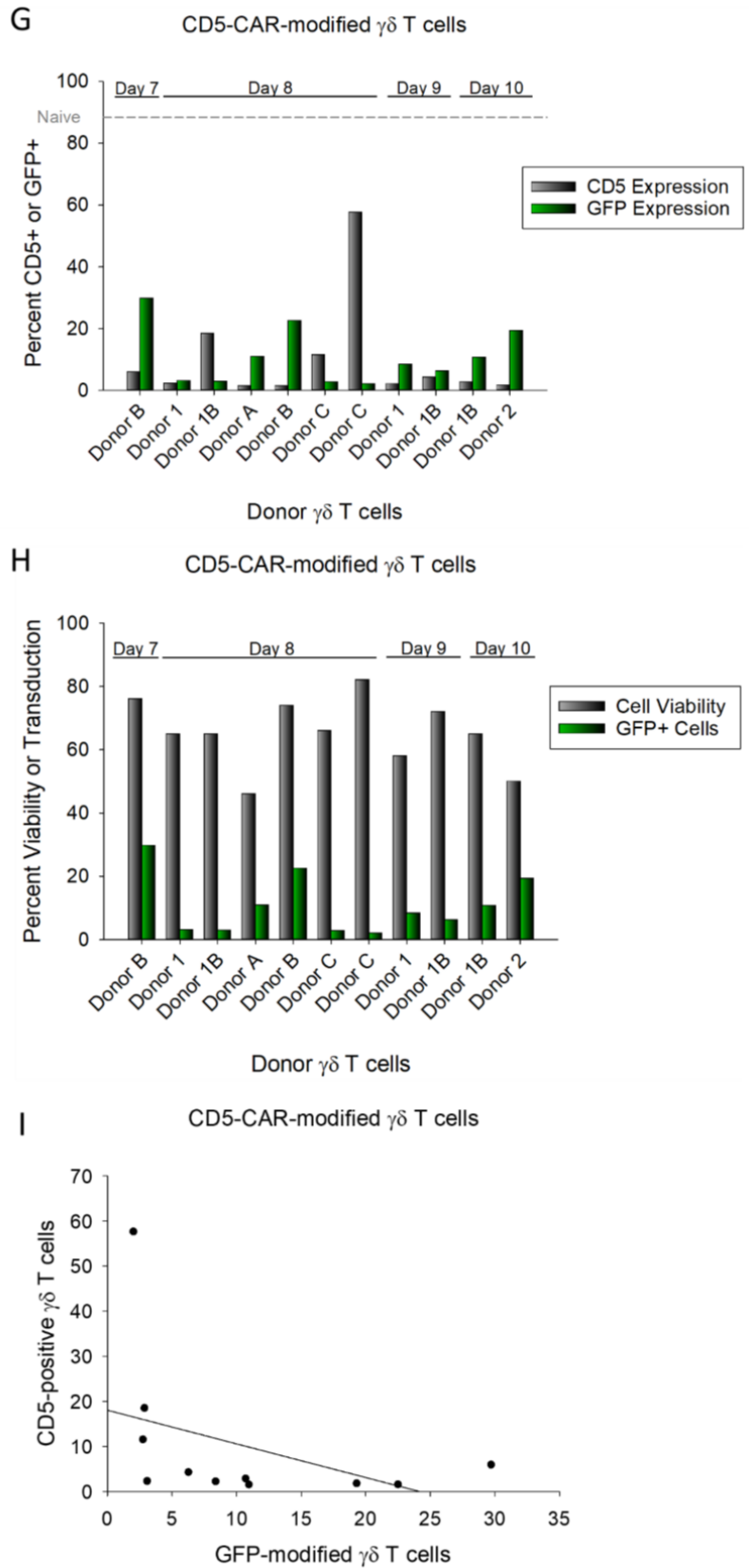


Figure 4: GFP and CD5 expression in $\gamma\delta$ T cells was assessed by flow cytometry as a measure of transduction. **(A)** AllCells donor 1 cells were transduced on day 8 (left) or day 9 (right) with CD5-CAR lentiviral vector at MOI 14. **(B)** AllCells donor 1 cells were transduced only on day 8 (left), double transduced on day 8 and 9 (middle) or triple transduced on days 8, 9 and 10 (right). Each transduction was at MOI 12. **(C)** AllCells donor 2 cells were transduced twice – on day 8 and again on day 10. The transduction on day 8 was at MOI 17, and MOI 5 on day 10. **(D)** $\gamma\delta$ T cells expanded from donor A fresh PBMCs were transduced twice on day 8 with CD5-CAR lentiviral vector at MOI 50 each time. **(E)** $\gamma\delta$ T cells expanded from donor B fresh PBMCs were transduced with CD5-CAR either on day 7 (left) or day 8 (right), each at MOI 72. **(F)** $\gamma\delta$ T cells expanded from donor C fresh PBMCs were transduced on day 8 of expansion with either 75% (left) or 100% (right) of lentiviral vector. 75% vector corresponds to MOI 43 and 100% vector corresponds to MOI 58. **(G)** Graphical representation of CD5 expression (black bars) in each donor $\gamma\delta$ T cells following CD5-CAR-modification and its relation to transduction as measured by GFP (green bars). **(H)** On day 12 or 13 of expansion, flow cytometry was performed and cell viability assessed. Cell viability of each donor was measured by Trypan blue staining (black bars). Flow cytometry was subsequently performed to assess GFP-expression as a measure of transduction (green bars), with the exception of donor B, in which flow cytometry was performed two days post-transduction. **(I)** Correlation between GFP expression as a measure of CD5-CAR transduction and CD5 antigen expression measured by flow cytometry.

transduced with 75% virus on day 8 for six hours, at which time additional media was added to dilute the vector. The following day, the media was replaced. On day 10, the cells were transduced again with 30% virus. Flow cytometry on day 12 of expansion revealed 19% GFP-positive cells (**Figure 4C**).

Donor cells derived from fresh blood were transduced as well with CD5-CAR lentiviral vector. Given the data we obtained using cells acquired from AllCells, we transduced Donor A cells on day 8 at MOI 50. Four hours later, supernatant was removed and replaced with additional media and fresh viral vector at MOI 50. Media was changed the following day. Despite the high MOI and double transduction, this protocol only resulted in 11% GFP-positive cells (**Figure 4D**). Donor B and C cells were transduced at higher MOIs, with donor B cells transduced on days 7 and 8 separately, while donor C cells were transduced on day 8. Donor B cells were transduced at MOI 72 resulting in about 30% and 22% GFP-positive cells on days 7 and 8, respectively, as measured by flow cytometry two days post-transduction (**Figure 4E**). Donor C cells were transduced at either MOI 43 or 58 on day 8, resulting in ~3% and 2% modified cells, respectively, as measured by flow cytometry on day 5 post-transduction (**Figure 4F**).

Despite low levels of CD5-CAR transduction, CD5-expression in $\gamma\delta$ T cells is down-regulated substantially (**Figure 4G**). Additionally, cell viability measured on day 12 or 13 of expansion is reduced following CD5-CAR-modification (**Figure 4H**), although overall the cells remain relatively healthy and the viability of the culture is restored over time (data not shown). The continued expansion of the cells and recovery following transduction suggests fratricide is not overwhelming in these cultures. This could potentially be due to low expression of the CD5-CAR due to poor transduction, or it could be due to the rapid down-regulation of the CD5 antigen, as previously evidenced (49; 78). We measured a weak negative correlation between transduction of $\gamma\delta$ T cells with CD5-CAR and CD5 antigen expression ($r^2=0.17$), with low levels of detectable CD5 at all ranges of gene modification. However, we predict a stronger correlation can be detected upon the addition of samples with a greater range of CD5-CAR expression (**Figure 4I**).

Cytotoxicity of CD5-CAR-modified $\gamma\delta$ T cells against a T-ALL cell line

Due to our observation of substantial CD5 down-regulation following CD5-CAR transduction of $\gamma\delta$ T cells, we hypothesize there might be sufficient interactions with CD5 antigen on target cells to result in enhanced cytotoxic activity. To test the cytotoxic potential of CD5-CAR-modified $\gamma\delta$ T cells, we cultured naïve or CD5-CAR-modified $\gamma\delta$ T cells with CD5-positive Jurkat T cells at various effector (E) to target (T) cell ratios for four hours at 37°C on day 12 of expansion. The cytotoxicity assay was performed using three donors and we observe donor variability in baseline cytotoxicity against Jurkat T cells by naïve $\gamma\delta$ T cells. Donor 1 CD5-CAR-modified $\gamma\delta$ T cells demonstrate enhanced cytotoxicity at a 5:1 E:T ratio (48.24% vs 74.9% dead Jurkat target cells) (**Figure 5A**), whereas Donor 2 and Donor B CD5-CAR-modified $\gamma\delta$ T cells do not. At the 5:1 E:T ratio, Donor 2 naïve and CD5-CAR-modified $\gamma\delta$ T cells killed 37.19% and 42.63% Jurkat T cells, respectively (**Figure 5B**). There were not enough cells to assess Donor B $\gamma\delta$ T-cell cytotoxicity at a 5:1 ratio, however, at a 3:1 ratio with Jurkat T cells, naïve and CD5-CAR-modified $\gamma\delta$ T cells resulted in 29.53% and 22.22% dead targets, respectively (**Figure 5C**). A graphical representation of the percent increase in cytotoxicity over baseline (naïve $\gamma\delta$ T-cell cytotoxicity against Jurkat T cells) suggests it remains undetermined whether transduction of <15% can yield a potential advantage to CD5-CAR-modification regarding cytotoxic activity against a T-ALL cell line (**Figure 5D**). However, if there is an advantage, it is unlikely to be clinically significant at this level of transduction. We hypothesize that greater CAR expression on $\gamma\delta$ T cells would result a significant advantage to CAR T-cell therapy using $\gamma\delta$ T cells against T-cell malignancies.

AAV6 results in greater transduction of $\gamma\delta$ T cells compared to that by lentiviral vector

We produced AAV vectors serotypes 2, 3 and 6, each encoding GFP. On day 11 of expansion, $\gamma\delta$ T cells expanded from fresh PBMCs were transduced with 25, 50 and 100 μ L of each vector and flow cytometry three days post-transduction was used to assess GFP expression. There is a correlation between the amount of viral vector used for the transduction and the amount of GFP measured in the cells. Furthermore, 100 μ L of AAV6 transduced $\gamma\delta$ T cells to a greater degree compared to the other serotypes.

Figure IV-5: Cytotoxicity of CD5-CAR-modified $\gamma\delta$ T cells against a T-ALL cell line.

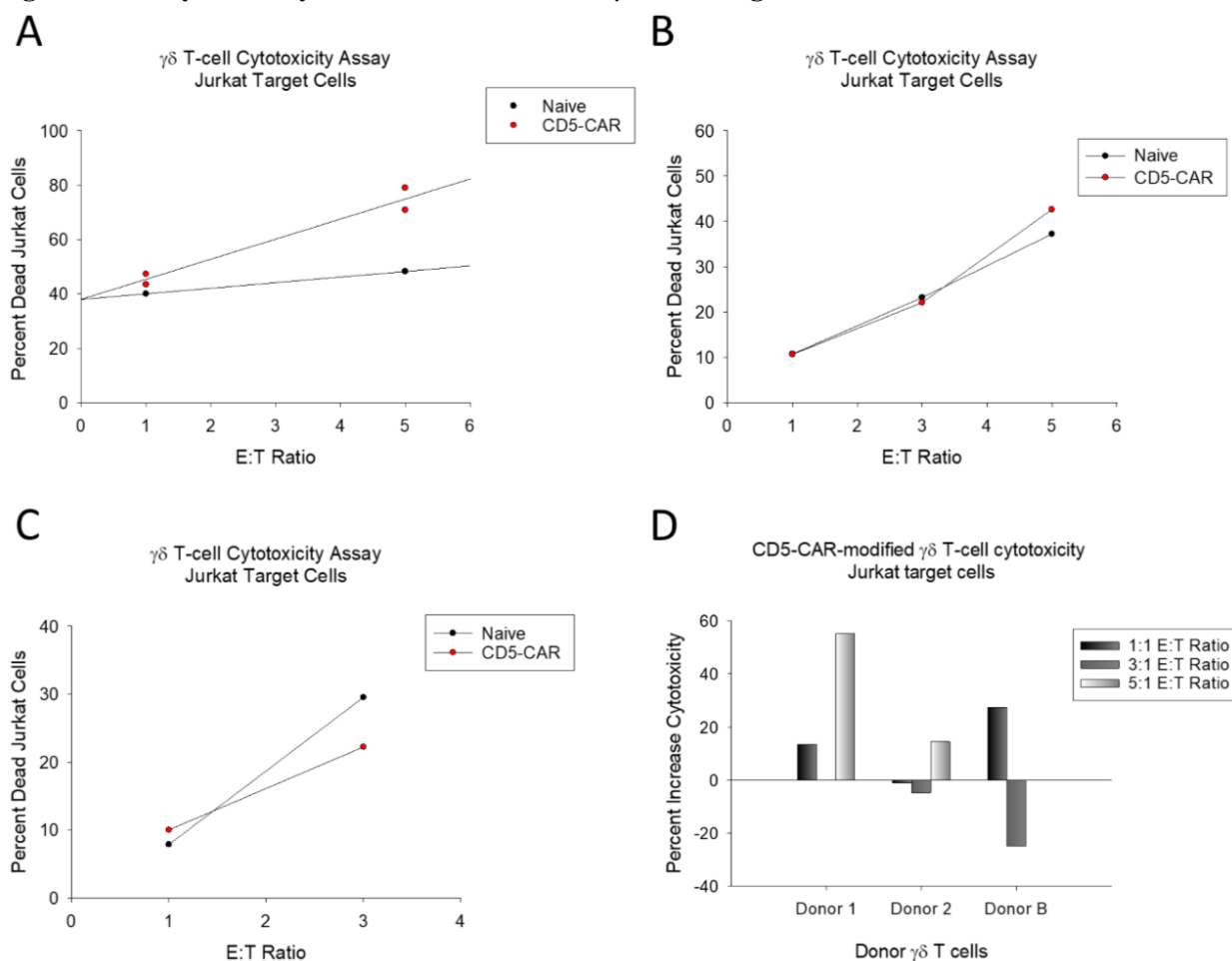


Figure 5: Cytotoxicity assays were performed on day 12 of expansion with Jurkat target cells for four hours. Black points represent naïve $\gamma\delta$ T-cell cytotoxicity and red points represent CD5-CAR-modified $\gamma\delta$ T-cell cytotoxicity. (A) Donor 1 naïve and CD5-CAR-modified $\gamma\delta$ T-cell cytotoxicity against Jurkat T cells at 1:1 and 5:1 E:T ratios. CD5-CAR-modified $\gamma\delta$ T-cell assays were performed in duplicate, as represented by two red points at each E:T ratio. Regression lines were drawn through the points. (B) Donor 2 naïve and CD5-CAR-modified $\gamma\delta$ T-cell cytotoxicity against Jurkat T cells at 1:1, 3:1 and 5:1 E:T ratios. (C) Donor B naïve and CD5-CAR-modified $\gamma\delta$ T-cell cytotoxicity against Jurkat T cells at 1:1 and 3:1 E:T ratios. (D) Percent increase in cytotoxicity by CD5-CAR-modified $\gamma\delta$ T cells over baseline. Baseline is measured as the percent cytotoxicity against Jurkat T cells by naïve $\gamma\delta$ T cells for each individual donor. CD5-CAR-modified $\gamma\delta$ T-cell cytotoxicity is compared to naïve $\gamma\delta$ T-cell cytotoxicity for each donor individually.

From 100 μL AAV6, $\gamma\delta$ T cells were 22% modified, compared to <2% modified by the other serotypes (**Figure 6A**). However, we cannot conclude from this data that AAV6 transduces $\gamma\delta$ T cells more efficiently as the titers for each vector are likely to vary and had not been calculated. On day 8 post-transduction (day 19 of expansion), $\gamma\delta$ T cells remained GFP-positive, however the percentage decreased to 9% as the transgene is diluted in a dividing population (data not shown). By the time the $\gamma\delta$ T cells were transduced, they had been in culture for almost two weeks, at which point $\gamma\delta$ T-cell proliferation is substantially slowed. Therefore, it will take longer for the transgene to become undetectable in the population. Nonetheless, our data showing high transduction of $\gamma\delta$ T cells by AAV6 supports previous findings that demonstrated AAV6 transduces hematopoietic stem and progenitor cells more effectively than can other serotypes (227; 228). As a result, we moved forward with AAV6 as a means of transducing $\gamma\delta$ T cells (**Figure 6B**).

To more accurately predict the effectiveness and reproducibility of AAV vector transduction, a functional titering method was developed. The functional titer of AAV6-GFP was measured by Jurkat T-cell transduction. Cells were transduced in duplicate with 5 or 10 μL vector and GFP was assessed on day 3 post-transduction. Using the cell number, volume of viral vector, and percent-modified $\gamma\delta$ T cells, we calculated a functional titer of 1.23×10^7 TU/mL (data not shown). We then transduced $\gamma\delta$ T cells on day 7 with different percentages viral vector to determine the amount of vector the cells can tolerate, as our preparation of AAV6 is in a high-salt PBS solution. Flow cytometry was performed on day 2 post-transduction. We observed similar viabilities following transduction at the variety of quantities tested with minimal reductions at the higher percentages (**Figure 6C**). Furthermore, we assessed the addition of 10% FBS to the culture in combination with viral vector. Our data suggests the addition of FBS protected the cellular viability in both naïve and transduced conditions (**Figure 6C**), however, this did not have a substantial impact on total number of live cells in the population (**Figure 6D**). The viability measurement is sensitive to noise and debris; therefore, the addition of replicates would more accurately report changes in viability. Unexpectedly, GFP expression is not influenced by the percentage of viral vector. Despite a higher MOI, $\gamma\delta$ T cells transduced with 40% viral vector display the same percentage of GFP-expressing

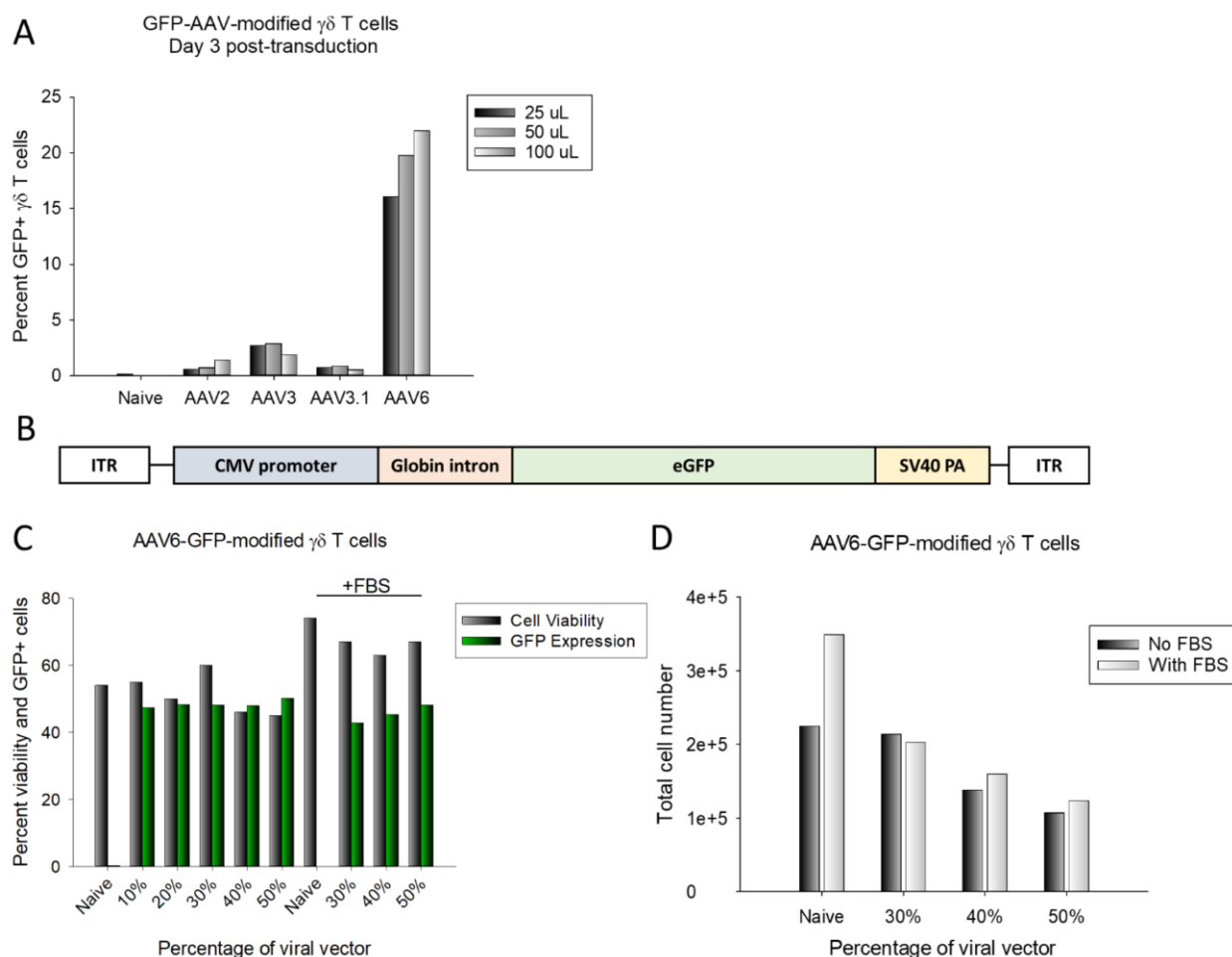
Figure IV-6: Transduction of $\gamma\delta$ T cells with AAV encoding GFP.

Figure 6: (A) GFP expression in $\gamma\delta$ T cells modified with AAV2, two different AAV3 vectors, or AAV6. All vectors encode GFP. Cells were transduced with 25 (black bar), 50 (gray bar) or 100 μ L (white bar) viral vector. (B) Schematic of the AAV6-GFP construct expressing eGFP under the control of the CMV promoter. This construct contains a globin intron and the ITRs are from AAV serotype 2. (C) Viability (measured by Trypan blue staining) and transduction efficiency (measured by GFP expression quantified by flow cytometry) of $\gamma\delta$ T cells at numerous viral vector doses. Some conditions were repeated to compare the addition of 10% FBS on cell viability and transduction efficiency. Flow cytometry was performed three days following transduction. (D) Total live cell number measured by Trypan blue staining and counting using the Nexalom Cellometer. AAV6-GFP transduction conditions with (white bars) and without FBS (black bars).

Figure IV-6 continued: Transduction of $\gamma\delta$ T cells with AAV encoding GFP.

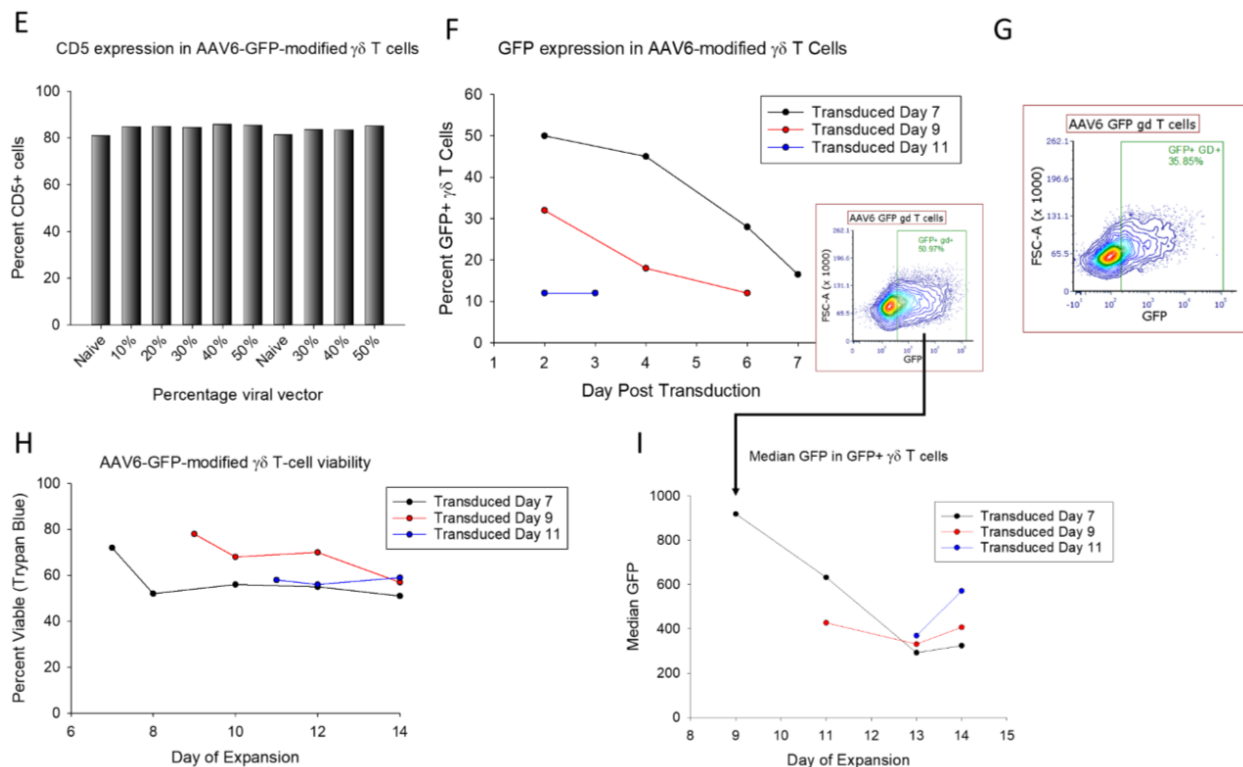


Figure 6 continued: (E) CD5 expression on $\gamma\delta$ T cells modified with AAV6-GFP. Flow cytometry was performed three days following transduction. (F, H and I) Cells were transduced with 22% viral vector on days 7 (black curve), 9 (red curve) or 11 (blue curve) of expansion. Flow cytometry was performed every two days. (F) GFP expression was measured in $\gamma\delta$ T cells transduced on different days with AAV6 encoding GFP (left). A representative flow cytometry plot of GFP expression day 2 post-transduction in $\gamma\delta$ T cells transduced on day 7 (right). (G) A second donor was transduced with 50% AAV6-GFP on both days 10 and 11 of expansion. Flow cytometry was performed on day 13 to assess GFP expression. (H) $\gamma\delta$ T-cell viability following transduction with AAV6. Viability was measured by Trypan blue staining. (I) Stability of GFP expression in AAV6-GFP-modified $\gamma\delta$ T cells over time. Median GFP was measured in GFP-positive $\gamma\delta$ T cells. The arrow from the flow cytometry plot in (F) indicates the gate utilized to measure median GFP over time.

cells compared to those transduced with only 20% vector (**Figure 6C**). However, there is a trend towards decreased total number of live cells as the dose of viral vector increases, suggesting a disadvantage towards using higher quantities of vector. This is expected due to the shift in osmolarity as the volume of vector increases, resulting in less optimal culture conditions (**Figure 6D**). Additionally, the percentage of CD5-expressing cells is not affected by GFP-modification of $\gamma\delta$ T cells (**Figure 6E**).

In order to determine if $\gamma\delta$ T-cell transduction is variable by day of transduction, we expanded $\gamma\delta$ T cells from fresh PBMCs and transduced them on days 7, 9 and 11. All transductions were identical, using 50 μ L vector at 22% of the final volume to transduce 3.5×10^5 cells. A new aliquot was used for each transduction. GFP expression was measured by flow cytometry every two days. By day 14 of expansion, $\gamma\delta$ T cells transduced on day 7 were 17% GFP-positive, compared to 50% modified cells on day 2 post-transduction, suggesting the transgene is diluted as the cells expand. Furthermore, we observed a difference in GFP-expression two days post-transduction in each population of $\gamma\delta$ T cells transduced at different time points. $\gamma\delta$ T cells transduced earlier in expansion revealed a greater degree of modification compared to cells transduced towards the end of expansion (day 7 transduction: 50% GFP; day 9 transduction: 32% GFP; day 11 transduction: 12% GFP). However, by day 14 of expansion, the gap in transgene expression had narrowed (**Figure 6F**). We transduced $\gamma\delta$ T cells expanded from a different donor twice with 50% AAV6-GFP on both days 10 and 11 and measured 36% GFP-positive cells on day 12 of expansion. Despite the larger dose of vector and second transduction, the percentage of GFP-modified cells matched that of $\gamma\delta$ T cells transduced on day 9 with 22% vector. However, the percent of GFP-positive cells was more than triple that observed when $\gamma\delta$ T cells were transduced on day 11 with 22% vector (**Figure 6G**). Cell viability did not differ between the $\gamma\delta$ T-cell populations transduced at different days of expansion. The cells had reduced viability immediately following transduction, however the viability plateaued and remained constant for the duration of the expansion. By day 14, the viability of $\gamma\delta$ T cells transduced on day 7, 9 or 11 was comparable, averaging 58% (**Figure 6H**). To determine the stability of the GFP transgene in $\gamma\delta$ T cells, we used flow cytometry to assess the median intensity of GFP expression within modified cells by

gating on GFP-positive $\gamma\delta$ T cells. Over time, there is a decrease in the median intensity of GFP within this population, suggesting the transgene is degraded or expression regulated within the cells. $\gamma\delta$ T cells transduced on day 11 demonstrate an increase in median intensity of GFP between days 2 and 3 post-transduction, which can likely be explained by peak transgene expression occurring between 48-72 hours post-transduction. Slight increases seen on day 14 regarding median intensity of GFP in $\gamma\delta$ T cells transduced on days 7 and 9 are likely due to experimental variation (**Figure 6I**).

AAV6 delivery of CD5-CAR to $\gamma\delta$ T cells is impeded by low viral titer

We demonstrated AAV6-GFP transduces $\gamma\delta$ T cells effectively, therefore, we engineered an AAV6 construct encoding the CD5-CAR (**Figure 7A**). This construct differs from the AAV6-GFP in that it contains the MND promoter instead of the CMV promoter, since the MND promoter is constitutively expressed in hematopoietic cells and is not susceptible to transcriptional silencing (334). The AAV6-CD5-CAR was titered on Jurkat T cells similar to the AAV6-GFP vector. The percentage of GFP-modified cells measured by flow cytometry was used to calculate the functional titer. The AAV6-CD5-CAR had a functional titer of 1.97×10^6 TU/mL, which was lower than that of the AAV6-GFP vector (**Figure 7B**). Nonetheless, we transduced two different donor $\gamma\delta$ T cells with AAV6-CD5-CAR. The first donor was transduced once on day 9 of expansion with 18% vector, which corresponded to MOI 0.23, calculated utilizing the functional titer. On day 12, flow cytometry revealed only 6% of the cells expressed GFP (**Figure 7C**). The second donor $\gamma\delta$ T cells were transduced twice with 20% vector, corresponding to MOI 0.25 on days 10 and 11. On day 13 of expansion, the cells were measured to be 6.5% GFP-modified (**Figure 7D**). Previous data using AAV6-GFP suggests we can add up to 50% vector to the $\gamma\delta$ T cells without significantly reducing viability. However, given the low transduction efficiency with 20% vector, we do not anticipate 50% vector will yield high transduction, particularly since previous data demonstrated no change in transduction efficiency when using 50% vector compared to 20%. In order to continue these studies, we need to produce higher titer AAV encoding the CD5-CAR to allow for greater CD5-CAR-

Figure IV-7: Transduction of $\gamma\delta$ T cells using an AAV6-CD5-CAR vector.

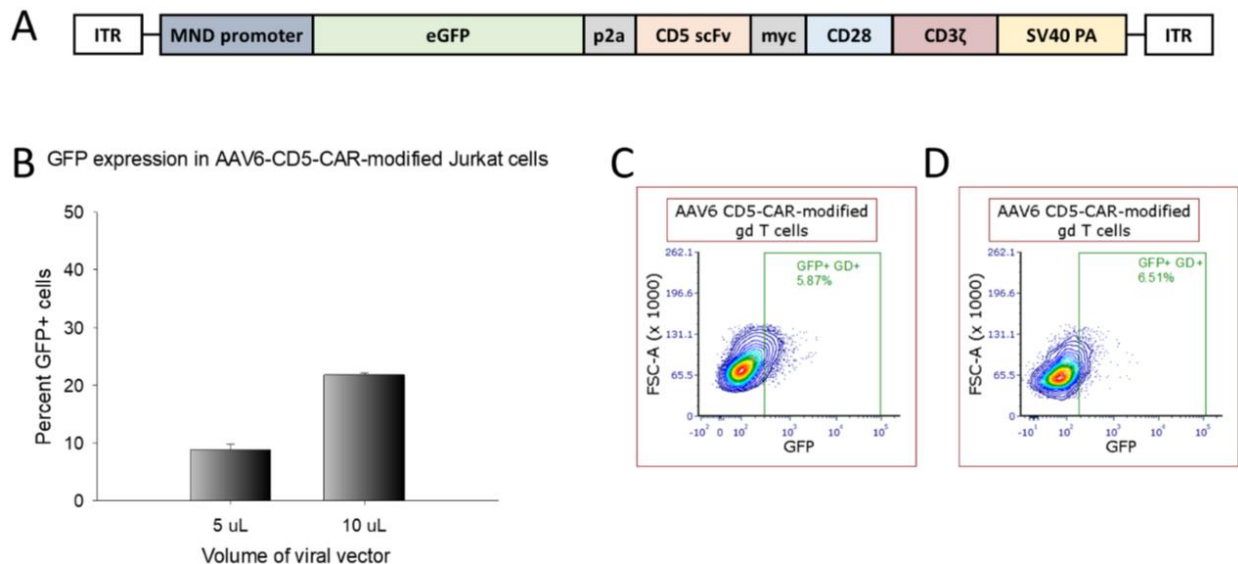


Figure 7: (A) Schematic of the AAV6-CD5-CAR bicistronic construct expressing eGFP and the transgene through a p2a sequence using the MND promoter. The ITRs are from AAV serotype 2. (B) Jurkat T cells were transduced with AAV6-CD5-CAR with 5 μ L or 10 μ L viral vector; n=2. Flow cytometry was performed on day 3 post-transduction to measure GFP expression. The functional titer of the vector was calculated from this experiment to be 5.02e5 TU/mL. (C & D) GFP expression in $\gamma\delta$ T cells transduced with AAV6-CD5-CAR as a measure of transduction. Two different donors are represented. Flow cytometry was performed on day 2 (B) or 3 (C) post-transduction.

modification of $\gamma\delta$ T cells.

Two advantages to using $\gamma\delta$ T cells for the treatment of T-cell malignancies is that they are predicted to have markedly reduced expansion compared to $\alpha\beta$ T cells and to persist for only a few weeks *in vivo* (321). As a result, there is reduced risk of cytokine release syndrome, minimal risk of T-cell aplasia, and in the event of adverse effects from the therapy, the cells will not expand and exacerbate the condition, nor will a safety mechanism be required to eliminate the cells.

Naïve $\gamma\delta$ T cells persist for 1-2 weeks in NOD *scid* IL2R γ -chain knockout (NSG) mice

To determine the persistence and confirm the lack of expansion of $\gamma\delta$ T cells in an *in vivo* mouse model, we injected NSG mice with one dose of naïve $\gamma\delta$ T cells. Four groups of mice consisting of three mice per group were followed. Each group received a different dose of $\gamma\delta$ T cells: 5×10^6 cells, 1×10^7 cells or 1.5×10^7 cells. One mouse from each group was sacrificed on days 1, 3 and 8.

Blood was collected on days 1, 3, 6 and 8 and analyzed by flow cytometry to determine the percentage of human T cells remaining. One mouse per group was sacrificed on days 1, 3 and 8, therefore peripheral blood was collected from all mice on day 1, two mice per group on day 3, and one mouse per group on days 6 and 8. There is a dose-dependent presence of $\gamma\delta$ T cells detected in mouse peripheral blood (data not shown). On day 1 post-injection, up to 3.4% $\gamma\delta$ T cells were detected in the peripheral blood. Each subsequent bleed is presented as a percentage of the cells detected on day 1. We observed a decrease in the percentage of $\gamma\delta$ T cells measured in the peripheral blood of mice over time, with fewer than 0.6% human cells detected by day 8 in the group that received the largest initial dose of cells (**Figure 8A**). Regardless of the treatment group, we demonstrated this decrease in $\gamma\delta$ T-cell detection over time with approximately half the cells remaining on day 6. By day 8 post-injection, there is a statistically significant decrease in $\gamma\delta$ T cells in the peripheral blood ($p=0.03$) (**Figure 8B**). Furthermore, on days 1, 3 and 8, one mouse from each group was sacrificed and cells isolated from the bone marrow and spleen. Flow cytometry was performed to analyze the human T-cell presence in each of these organs. While we measured human T cells

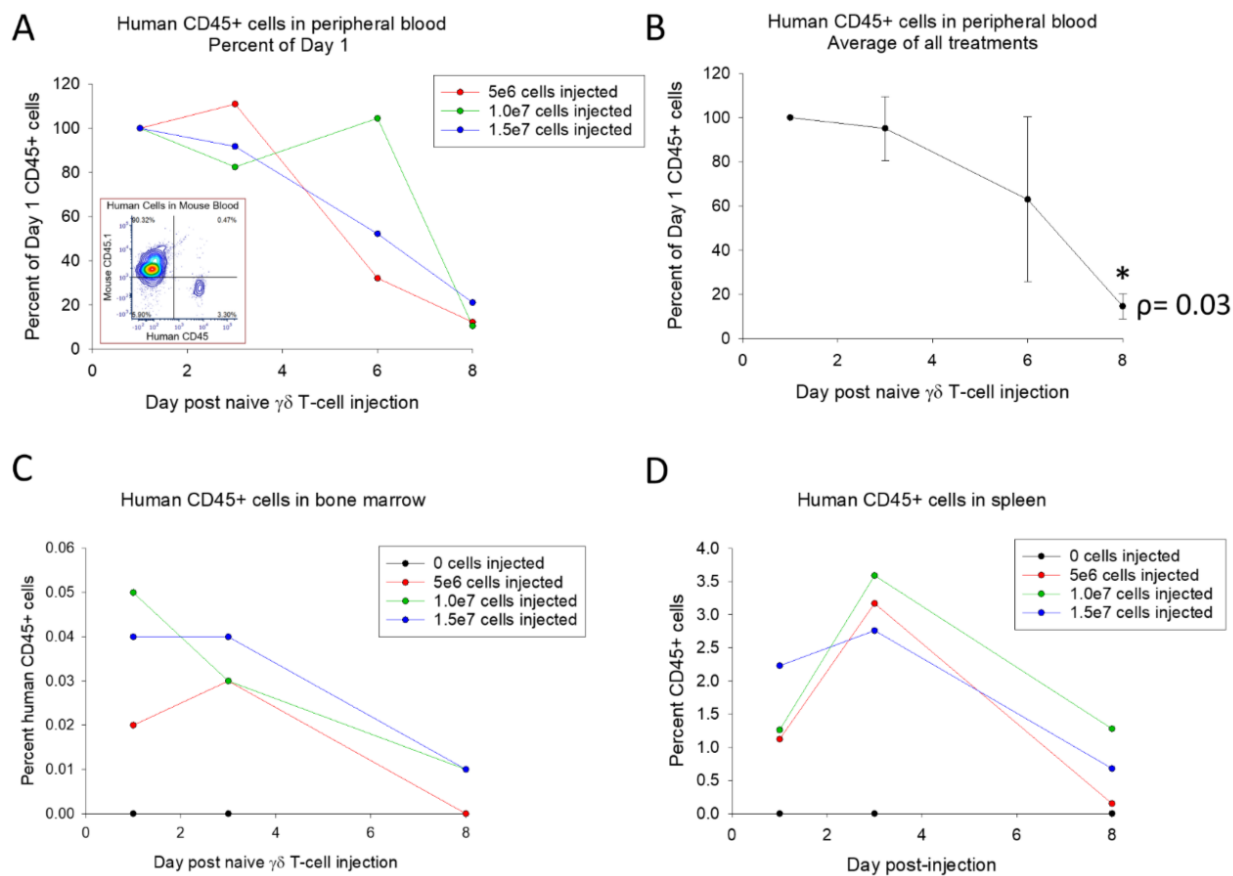
Figure IV-8: Persistence of naïve $\gamma\delta$ T cells in NSG mice.

Figure 8: $\gamma\delta$ T cells were injected into NSG mice. There were three mice per group: 5×10^6 cells (red curve), 1×10^7 cells (green curve), or 1.5×10^7 cells (blue curve). One mouse per group was sacrificed on days 1, 3 and 8. (A) The percentage of human T cells remaining in the peripheral blood as a percent of the cells detected on day 1. Mice were bled on days 1, 3, 6 and 8 post-injection. Day 3 data points represent averages from two mice. Inset is a representative flow cytometry plot illustrating detection of human T cells in mouse peripheral blood. (B) The T cells detected in the peripheral blood on each day as an average from all treatment groups. There is a statistically significant decline in peripheral blood human $\gamma\delta$ T cells by day 8 compared to day 1 post-injection ($\rho=0.03$). (C) The percentage of total human T cells detected in the bone marrow of NSG mice on days 1, 3 and 8 following $\gamma\delta$ T-cell injection. (D) The percentage of human T cells measured in the spleen of NSG mice after $\gamma\delta$ T-cell injection.

in the bone marrow on day 1 post injection, very few cells were detectable. The percentage of human cells in the bone marrow did not change considerably from day 1 to day 3, however, by day 8 post-injection, we were unable to detect human T cells in the bone marrow (**Figure 8C**). Similarly, a small percentage of human T cells were observed in the spleens (albeit more so than was found in the bone marrow). In each treatment group, however, the percentage of human cells had increased between days 1 and 3 (1.54% to 3.17%). By day 8, low levels of human cells remained in the spleens of mice from each group. Less than 1% human cells in mice treated with 5×10^6 or 1.5×10^7 cells remained by day 8, however in the mouse treated with 1×10^7 cells, ~1.3% of the cells were of human origin on day 8 post-injection (**Figure 8D**).

Discussion

$\gamma\delta$ T cells can be advantageous to $\alpha\beta$ T cells for CAR T-cell therapy under certain conditions. As described above, utilizing CAR therapy for the treatment of T-cell malignancies can be challenging due to poor expansion or cytotoxicity of patient cells, fratricide, T-cell aplasia, and product contamination. The use of allogeneic donors as opposed to autologous donors for CAR therapy can reduce cost of production and time to treatment as donor cells can be cryopreserved and stored until they are needed. This reduction in time to treatment is highly beneficial as many patients relapse or develop co-morbidities during the time it takes for their cells to be processed *ex vivo* (319).

However, one limitation to utilizing $\gamma\delta$ T cells for CAR T-cell therapy is difficulty modifying the cells. Furthermore, the antigen targeted by the CAR is likely to be expressed on the $\gamma\delta$ T cells as well, potentially requiring two modifications. In this chapter we demonstrate the complications of transfecting $\gamma\delta$ T cells using either nucleoporation or electroporation techniques. However, one limitation to our nucleoporation data is that only one donor was used to test nucleoporation of $\gamma\delta$ T cells. While this one donor was assessed on various days of expansion, it is possible there is high donor variability in transfectability. Alternatively, additional programs could be tested using the Amaxa. However, typically, milder programs that preserve cell viability are correlated with reduced gene transfer. The programs used

herein did not result in editing of the $\gamma\delta$ T cells and therefore it is likely milder programs would not enhance editing. However, this data is unsurprising as $\alpha\beta$ T cells were difficult to nucleoporate as well, as demonstrated in chapter 3. The majority of the cells had died, and of the surviving cells, ~40% were CD5-edited (49).

Unfortunately, electroporation techniques (assessed using three different donors on different days of expansion) were not effective at editing $\gamma\delta$ T cells either. As mentioned in chapter 3, we produced lentiviral vector encoding Cas9 and our gRNA sequence for editing CD5, under the control of two separate promoters. Jurkat T cells transduced with this CRISPR-Cas9 lentiviral vector demonstrated high efficiency of CD5-editing. However, as described herein, lentiviral vectors transduce $\gamma\delta$ T cells with very low efficiency. As a result, we predict we would not achieve sufficient CD5-editing in $\gamma\delta$ T cells using a lentiviral vector to deliver Cas9. Furthermore, use of a lentiviral vector to introduce Cas9 into the cell's genome is not a practical approach for a cellular product as constitutive expression of Cas9 is likely to result in off-target gene editing. Therefore, this approach represents a proof-of-principle strategy.

To date, fratricide has not been shown to occur in $\gamma\delta$ T cells, limiting the expansion and anti-tumor activity of the CAR-modified cells. Using $\alpha\beta$ T cells, a trial has been initiated based on data collected with CD5-CAR-modification that suggests CD5 internalization is rapid and complete, resulting in only limited and transient fratricide (MAGENTA trial, NCT03081910). The preclinical results suggest CRISPR-Cas9 genome editing of CD5 is not required to produce a functional CAR T-cell product. While we've previously demonstrated there are additional benefits to disrupting CD5 expression on the effector $\alpha\beta$ T cells, we may be able to produce a high-quality CD5-CAR T-cell product using $\gamma\delta$ T cells (49). The data in this chapter demonstrates internalization of CD5 occurs in $\gamma\delta$ T cells, similarly to that in $\alpha\beta$ T cells. As a result, we utilized lentiviral vector and AAV techniques to introduce the CD5-CAR into $\gamma\delta$ T cells in order to characterize the CAR-modified cells and to determine if CRISPR-Cas9 editing of the CD5 gene is required. Using a lentiviral vector we were unable to achieve sufficient transduction efficiency with a CD5-CAR in order to accurately assess this. To achieve higher levels of transduction, we adjusted the transduction

conditions as described, including the day of expansion, the MOI and the number of transductions. However, donor variability complicates determination of the most favorable conditions to achieve high efficiency. Using $\gamma\delta$ T cells derived from PBMCs from AllCells, we observed at MOI 12 on days 8 and 10 there were ~20% transduced cells, however at MOI 50 twice on day 8, with 4 hours lapse, we observed only 11% modified cells. As demonstrated, we cannot consistently achieve high transduction efficiency of $\gamma\delta$ T cells using lentiviral vector, despite high titer ($>5e7$ TU/mL).

Using AAV serotype 6 we have demonstrated consistent levels of 50% transduction when $\gamma\delta$ T cells are transduced on day 7 of expansion using high titer vector ($>1e7$ TU/mL). However, transduction of $\gamma\delta$ T cells earlier in expansion is not optimal as AAV delivered transgenes are expressed episomally and therefore are diluted as the cells expand. An AAV $\gamma\delta$ T-cell-based therapy optimally involves transduction followed by infusion into a patient on the subsequent day. Therefore, based on our established protocol, day 11 is the optimal day for transduction with AAV. As $\gamma\delta$ T cells do not expand substantially past day 11, the transduction observed on day 11 would persist until degradation or regulation of the transgene. Therefore, the lower efficiency observed from transducing $\gamma\delta$ T cells on day 11 may not be relevant because on day 14, they exhibit similar levels of transduction compared to cells transduced on day 7 (transduced on day 7 versus 11: 17% modified and 12% modified, respectively). Upon addition of further replicates, this gap in percent-modified cells on day 14 between cells transduced on day 7 and day 11 may narrow. This experiment was only performed once as we are changing the promoter from CMV to MND. The CMV promoter can be silenced in certain cell types and this silencing can skew our data (335-337), whereas the MND promoter is resistant to transcriptional silencing (338). Using the CMV promoter, it is unclear whether the transgene is being silenced or diluted and degraded. Therefore, these experiments will be repeated with vector that contains the MND promoter.

We have demonstrated high titer AAV6 transduces $\gamma\delta$ T cells, however, the functional titer achieved for the AAV6-CD5-CAR vector is much lower than that for the GFP vector ($5e5$ TU/mL). At the low titer, we were unable to achieve even moderate transduction of $\gamma\delta$ T cells. However, despite low levels

of transduction, we consistently observed substantial CD5-downregulation using a lentiviral vector. This is not the case with AAV6-CD5-CAR-modified $\gamma\delta$ T cells. We hypothesize the lack of CD5 downregulation results from low density CD5-CAR expression on the $\gamma\delta$ T cells when the transgene is delivered using AAV. This hypothesis is supported by a reduced shift in MFI of GFP upon transduction with AAV-CD5-CAR compared to the shift observed upon transduction with lentiviral vector (**Figure 9**). The data suggests there are fewer CAR molecules on the cell surface, and therefore there are fewer interactions between the CD5 antigen and CD5-CAR resulting in substantial down-regulation of CD5 only in cells transduced with lentiviral vector.

One question that remains is why can we produce high titer GFP vector but not high titer CD5-CAR vector? Some hypotheses include recombination of the ITRs and difficulty packaging a larger vector. Prior to vector production the ITRs are evaluated using restriction enzyme digests as well as Sanger sequencing (data not shown). Furthermore, the plasmid was evaluated by transfecting 293T cells, an easily transfectable cell line, to confirm the plasmid correctly encodes both eGFP and the CD5-CAR (data not shown). Therefore, we conclude the transgene and ITRs are correct and the question remains. This plasmid was previously utilized for viral production by Cincinnati Children's Hospital Medical Center and high titer was achieved. We demonstrated the ability to introduce the CD5-CAR into NK-92 cells using AAV6 acquired from Cincinnati (unpublished). We will remove eGFP from the construct to reduce the cargo size with the hypothesis that the reduced transgene size will improve packaging. CD5-Fc can be used as a marker of CD5-CAR expression and therefore eGFP is not required.

Once we achieve high transduction efficiency with the AAV6-CD5-CAR in $\gamma\delta$ T cells, we can assess cell surface expression of the CAR and fratricide to determine if genome editing would be advantageous. If genome editing is required for a functional product, we predict we can modify $\gamma\delta$ T cells with two AAV constructs. This will require optimization of the timing for delivery, with the Cas9 construct being delivered 2-3 days prior to the CAR. Given episomal expression of AAV-delivered transgene, delivery of the CAR later in expansion is optimal to allow for infusion on day 12 as per our current protocol.

Figure IV-9: GFP intensity correlates with CD5 expression in $\gamma\delta$ T cells transduced with CD5-CAR vectors.

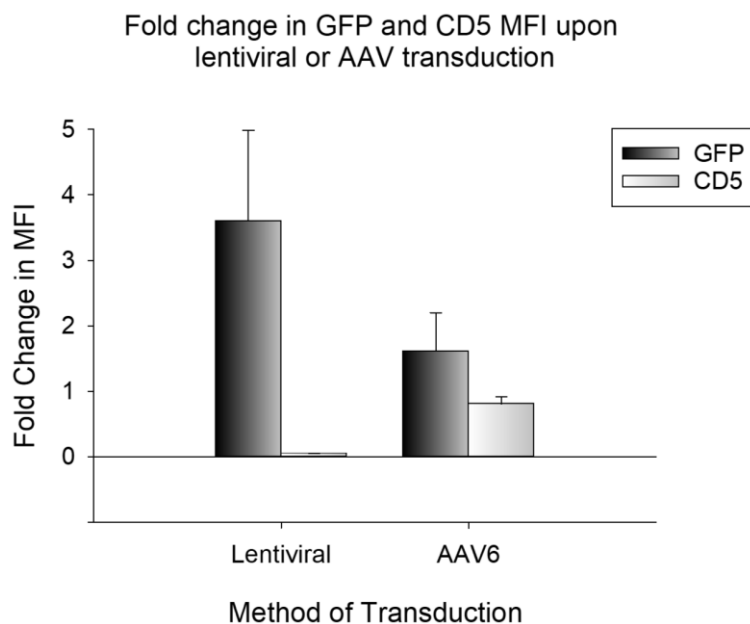


Figure 9: $\gamma\delta$ T cells modified with lentiviral vector or AAV6 encoding the CD5-CAR. Median intensity of GFP and CD5 expression were measured by flow cytometry. Lentiviral vector delivery and AAV6 delivery: n=2. Means and standard deviations are represented.

Once CD5 expression is disrupted, the $\gamma\delta$ T cells can be modified with a CD5-CAR with minimal fratricidal effects.

Upon substantial modification of $\gamma\delta$ T cells with the CD5-CAR, we will assess the CAR expression and CD5 downregulation on the $\gamma\delta$ T cells as well as their *in vitro* and *in vivo* cytotoxicity against T-ALL cell lines and primary tumor cells. Our *in vivo* data supports the limited lifespan of $\gamma\delta$ T cells and minimal *in vivo* expansion. As previously discussed, this is advantageous to reduce the secretion of cytokines upon antigen stimulation *in vivo* that is correlated to the massive expansion of CAR T cells resulting in life-threatening CRS. However, $\gamma\delta$ T-cell trafficking needs to be evaluated in a T-ALL mouse model as our studies demonstrate there is minimal $\gamma\delta$ T-cell trafficking to the bone marrow of healthy NSG mice. We hypothesize that chemokine secretion by the tumor cells will facilitate chemotaxis of $\gamma\delta$ T cells expressing the corresponding chemokine receptors, resulting in sufficient trafficking to the bone marrow. The *in vivo* data presented in this chapter will be used to design a strategic dosing regimen for CAR-modified $\gamma\delta$ T cells in a T-ALL mouse model.

Chapter V

Non-signaling chimeric antigen receptors (NSCARs) enhance antigen-directed killing by $\gamma\delta$ T cells in contrast to $\alpha\beta$ T cells

Lauren C. Fleischer^{1,2}, Scott A. Becker^{1,2}, Rebecca E. Ryan^{1,2}, Andrew Fedanov¹, Christopher B. Doering^{1,2}, H. Trent Spencer^{1,2}

¹Aflac Cancer and Blood Disorders Center, Department of Pediatrics, Emory University School of Medicine, Atlanta, Georgia; ²Program in Molecular and Systems Pharmacology, Graduate Division of Biological and Biomedical Sciences, Laney Graduate School, Emory University School of Medicine, Atlanta, Georgia

Abstract

Chimeric antigen receptor (CAR)-modified T cells have demonstrated efficacy against B-cell leukemias/lymphomas. However, redirecting CAR T cells to malignant T cells is more challenging due to product-specific cis- and trans-activation causing fratricide. Other challenges include the potential for product contamination and T-cell aplasia. We expressed non-signaling CARs (NSCARs) in $\gamma\delta$ T cells since donor-derived $\gamma\delta$ T cells can be used to prevent product contamination, and NSCARs lack signaling/activation domains, but retain antigen-specific tumor cell-targeting capability. As a result, NSCAR targeting requires an alternative cytotoxic mechanism, which can be achieved through utilization of $\gamma\delta$ T cells that possess MHC-independent cytotoxicity. We designed two distinct NSCARs and demonstrated that they do not enhance tumor-killing by $\alpha\beta$ T cells, as predicted. However, both CD5-NSCAR- and CD19-NSCAR-modified $\gamma\delta$ T cells enhanced cytotoxicity against T-ALL and B-ALL cell lines, respectively. CD5-NSCAR expression in $\gamma\delta$ T cells resulted in a 60% increase in cytotoxicity of CD5-expressing T-ALL cell lines. CD19-NSCAR-modified $\gamma\delta$ T cells exhibited a 350% increase in cytotoxicity against a CD19-expressing B-ALL cell line compared to the cytotoxicity of naïve cells. NSCARs may provide a mechanism to enhance antigen-directed anti-tumor cytotoxicity of $\gamma\delta$ T cells through the introduction of a high-affinity interaction while avoiding self-activation.

Introduction

Currently, the FDA has approved the use of two CAR T-cell therapies, Kymriah (339) and Yescarta (340). These therapies are approved to treat adult diffuse large B-cell lymphoma (341; 342) and Kymriah is also approved for pediatric B-cell acute lymphoblastic leukemia (B-ALL) (343). While these therapies have been successful in treating B-cell malignancies, there are additional challenges to translating CAR therapy for the treatment of T-cell malignancies. Many pre-clinical studies have developed strategies to treat T-cell malignancies, including CARs targeting antigens such as CD5 (45; 49; 55; 78; 80), CD7 (50; 53; 89), CD4 (58; 92) and CD3 (56; 112). However, shared expression of these antigens on the CAR T cells as well as cancer cells can result in fratricide, or CAR T cells killing other CAR T cells (49; 50; 52; 78;

112). Additionally, a recent report demonstrated evidence of product contamination resulting in clonal expansion of a single leukemic blast that had been modified with the CD19-CAR. The CD19-CAR masked the CD19 antigen from CAR T cells, causing resistance to the therapy (43). Furthermore, a memory response against T-cell antigens resulting in T-cell aplasia is lethal and is therefore not an option. While therapies targeting B-cell malignancies, such as Kymriah and Yescarta, result in potentially lifelong B-cell aplasia due to a memory response against the targeted antigen (40; 344), these patients can be treated with intravenous immunoglobulin (IVIG) to overcome this condition (345). However, due to increased demand for IVIG over recent years, the United States is currently experiencing a shortage of immunoglobulin.

Many groups have developed solutions to overcome these challenges to treating T-cell malignancies using CAR therapy. The simplest option is targeting an antigen that is absent or expressed at low levels on normal T cells such as CD30 (60; 102-104; 106), CD37 (61) or TRBC1 (109). Unfortunately, the majority of T-cell malignancies do not have high expression of these antigens, which limits their usefulness. An alternative strategy is to utilize donor-derived cells, which eliminates the risk of product contamination, as isolating normal T cells from malignant T cells is a significant obstacle. NK cells and $\gamma\delta$ T cells are non-alloreactive and can be used in an allogeneic setting without additional modifications. Additionally, the NK-derived lymphoma cell line, NK-92 cells, can be used as an alternative to T cells for CAR therapy (45; 49; 55; 56; 58; 80). However, the expansion of NK or NK-92 cells is time-consuming, genetic engineering can be challenging, and they are particularly sensitive to cryopreservation (153). Strategies to avoid T-cell aplasia have included incorporation of suicide genes and switches into CAR constructs to regulate their expression, provide control over robust responses and prevent memory cell formation (242; 245; 247; 248; 252-254), but they are not uniformly effective, and escape of a modified cancer clone could be problematic.

Few strategies that address all three challenges have been evaluated. Therefore, we generated non-signaling CARs (NSCARs) that, when introduced into $\gamma\delta$ T cells, enhance target cell killing while sparing the healthy, engineered cells. NSCARs lack the intracellular signaling domains typically present in a CAR (**Figure 1A**). As a result, NSCARs are non-activating. While expression of a non-signaling CAR is not

Figure V-1: Schematic of CD5-based and CD19-based NSCAR constructs.

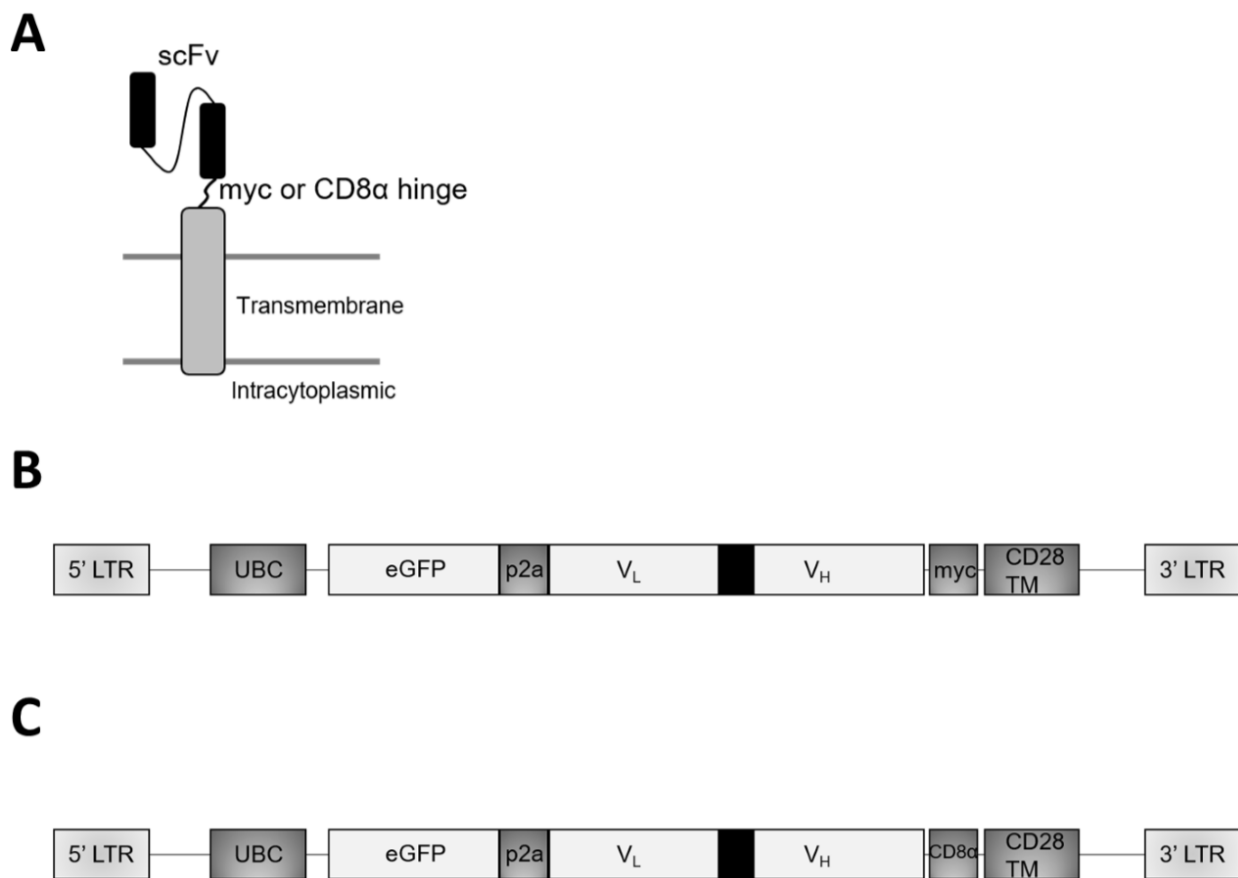


Figure 1. (A) NSCAR structure with CD28 transmembrane domain, truncated after two amino acids on the intracellular tail. **(B & C)** Bicistronic NSCAR transgenes in lentiviral vectors expressing enhanced green fluorescent protein (eGFP) and the NSCARs through the inclusion of a p2a sequence. Expression of both sequences are driven by the human ubiquitin C promoter (hUBC) with an interleukin-2 signal peptide. The CD5-NSCAR **(B)** includes a myc epitope tag, whereas the CD19-NSCAR **(C)** includes the CD8α hinge.

expected to affect $\alpha\beta$ T-cell cytotoxicity against tumor cells, we hypothesize NSCARs can enhance $\gamma\delta$ T-cell cytotoxicity because, in contrast to $\alpha\beta$ T cells, $\gamma\delta$ T cells possess alternative mechanisms of cytotoxicity and do not require stimulation through CD3 ζ in order to initiate target cell killing (160; 176-179). In addition, *ex vivo* expanded $\gamma\delta$ T cells are relatively short-lived with little expansion *in vivo*, which can help control cytokine release syndrome (CRS) and other adverse events resulting from CAR T-cell therapy. Furthermore, $\gamma\delta$ T cells are unlikely to cause GvHD as they interact with antigen independent of MHC-recognition, permitting use in an allogeneic setting (346; 347). We hypothesize NSCARs can act as anchors to tether the $\gamma\delta$ T cells to tumor cells expressing the targeted antigen. While the cells are in close proximity, the cytotoxic mechanisms endogenous to $\gamma\delta$ T cells can engage, ultimately resulting in tumor cell death.

Herein, we design two distinct NSCARs: CD5-NSCAR (**Figure 1B**) and CD19-NSCAR (**Figure 1C**). We compare $\gamma\delta$ T-cell expansion in naïve and NSCAR-modified populations and assess the cytotoxicity of NSCAR-modified $\gamma\delta$ T cells against T-ALL and B-ALL cell lines. Additionally, we evaluate the effect of CD5-NSCAR expression on the cytotoxicity of $\alpha\beta$ T cells. We further compared the CD19-NSCAR to the more traditional CD19-CAR. The results described herein demonstrate proof-of-concept that NSCAR expression in $\gamma\delta$ T cells enhances antigen-directed killing, and the mechanisms involved are fundamentally and biologically different in $\alpha\beta$ T cells.

Materials and Methods

Cell lines. The Jurkat cell line clone E6-1 was purchased from American Type Culture Collection (ATCC, Manassas, VA). As previously described, the Molt-4 and 697 cell lines were gifted by Dr. Douglas Graham (Emory University) (49). CD5-edited Jurkat T cells were generated as previously described (49). All cell lines were cultured in RPMI (Corning, Manassas, VA) supplemented with 10% fetal bovine serum (FBS) and 1% penicillin/streptomycin.

Engineering the NSCAR sequences. The CD5-CAR sequence, as previously described (49), was truncated to remove the CD3 ζ signaling domain as well as the intracellular portion of CD28. The entire transmembrane domain of CD28 as well as two intracellular amino acids remain. Additionally, we included a unique 21 base-pair sequence on the cytoplasmic end of the truncated CD28 for genetic determination of the proviral sequence. The vector is a bicistronic lentiviral construct, facilitating dual expression of enhanced green fluorescent protein (eGFP) and the NSCAR transgene using a p2a peptide sequence. The CD19-NSCAR was similarly generated by truncation of the CD19-CAR (unpublished) after the first two intracellular amino acids of CD28. Similar to the CD5-NSCAR, this vector is a bicistronic lentiviral construct, expressing eGFP and the NSCAR transgene using a p2a peptide sequence. However, the CD19-NSCAR has the CD8 α hinge where the CD5-NSCAR has the myc tag. The CD19-scFv sequence was generated from codon optimization of a published CD19-scFv sequence produced in a mouse hybridoma cell line (348).

Generation of CAR- and NSCAR-encoding lentiviral vectors. HIV-1-based recombinant lentiviral vectors for all CAR and NSCAR constructs were produced and titered, as previously described (49).

Lentiviral vector transduction of cell lines. Lentiviral vector transduction was carried out as previously described using 6 μ g/mL polybrene (EMD Millipore, Billerica, MA) (49). The transduced cells were cultured for at least five days prior to being used for downstream applications. Jurkat T cells were transduced at multiplicity of infection (MOI) of 0.5 or 1.

Expansion of $\gamma\delta$ T cells from healthy donor blood. Blood was obtained from consented, healthy adults with the assistance of the Emory Children's Clinical and Translational Discovery Core. PBMCs were isolated from 30-50 mL healthy donor blood using Ficoll-Paque density gradient and centrifugation following the manufacturer's protocol. PBMCs were expanded in serum-free conditions as previously described (163) for up to 13 days *in vitro*. On days 0 and 3, 5 μ g/mL zoledronic acid and 500 IU/mL IL-2

was added to the culture. Beginning on day 6, 1000 IU/mL IL-2 was added to the culture medium. Cells were cultured at 1.5×10^6 cells/mL.

Expansion of $\alpha\beta$ T cells from healthy donor blood. PBMCs were isolated from healthy donor blood as described above. A Pan T-cell isolation was performed using Miltenyi's Pan T-cell Isolation kit (Miltenyi Biotech, Germany) and the T cells were expanded in X-VIVO 15 media (Lonza, Switzerland) supplemented with 10% FBS, 1% penicillin/streptomycin, 50 ng/mL IL-2 and 5 ng/mL IL-7. Following T-cell isolation, cells were stimulated with CD3/CD28 Dynabeads at a 1:1 ratio for 24 hours (Thermo Fisher Scientific, Waltham, MA). Cells were cultured at 1×10^6 cells/mL.

Lentiviral vector transduction of $\gamma\delta$ T cells. Lentiviral vector transduction was carried out between days 7 and 9 of expansion. Cells were incubated with 60% vector in culture medium supplemented with 6 μ g/mL polybrene for 18-24 hours, at which point culture medium was replaced with fresh medium. The transduced cells were cultured for 3-5 days before being used for downstream applications.

Lentiviral vector transduction of $\alpha\beta$ T cells. Lentiviral vector transduction was carried out immediately upon removal of the CD3/CD28 Dynabeads. Cells were incubated with 60% vector in culture medium supplemented with 6 μ g/mL polybrene for 18-24 hours, at which point culture medium was replaced with fresh medium. The transduced cells were cultured for 6 days before being used for downstream applications.

Flow cytometry analysis. Analysis was performed using a BD LSRII Flow Cytometer (BD Biosciences, San Jose, CA). Data was analyzed using FCS Express 6 software. Antibodies used included anti-CD5 PerCP/Cy5.5, anti-CD3 BV421, anti- $\gamma\delta$ TCR PE and anti-CD69 APC-Cy7 (BD Biosciences, San Jose, CA). CD5-Fc fusion protein (G&P Biosciences, Santa Clara, CA) and CD19-Fc fusion protein (ACROBiosystems, Newark, DE) were used to detect anti-CD5 constructs and anti-CD19 constructs, respectively, with a secondary anti-IgG Fc antibody (Jackson ImmunoResearch Laboratories, West Grove,

PA), as previously described (49). Violet Proliferation Dye 450 (VPD450) was used to label the target cells in the cytotoxicity and co-culture studies, and cell death was assessed using eFluor 780 (described below). Degranulation of $\gamma\delta$ T cells was detected using anti-CD107a APC (BD Biosciences, San Jose, CA).

Western blotting. Jurkat T cells were lysed using RIPA buffer (Sigma-Aldrich, St. Louis, MO) and a protease inhibitor cocktail (Sigma-Aldrich, St. Louis, MO). Quantification of protein, separation by SDS-PAGE, and transfer to a nitrocellulose membrane were performed as previously described (49). The blocked membrane was incubated with an anti-CD5 mAb and HRP-labeled secondary antibody as previously described (49). Densitometry was performed using ImageJ.

Co-culture assay using NSCAR-modified Jurkat T cells and CD5-edited Jurkat T cells. Naïve and CD5-edited Jurkat T cells were transduced with the bicistronic lentiviral vector encoding CD5-NSCAR at MOI 1. After 18-24 hours, culture medium was replaced with fresh medium and on day 5, flow cytometry using BD LSRII Flow Cytometer (BD Biosciences, San Jose, CA) confirmed transduction by both eGFP and CD5-Fc binding. Transduced cells were cultured with naïve or CD5-edited Jurkat T cells previously labeled with VPD450 at modified to non-modified ratios of 1:1 and 1:3. Non-modified cells were labeled according to the manufacturer's protocol (BD Biosciences, San Jose, CA). The cells were cultured for 14 hours at final concentrations of 5×10^5 cells/mL. Changes in NSCAR expression on modified cells and CD5 expression on non-modified cells were assessed by flow cytometry.

Cytotoxicity assay. Cytotoxicity assays were performed on days 12 or 13 of $\gamma\delta$ T-cell expansion, or on day 6 post- $\alpha\beta$ T-cell transduction. Target cells were labeled with VPD450 using the manufacturer's protocol (BD Biosciences, San Jose, CA). Effector cells remained unstained. Effector (E) and target (T) cells were mixed in 12x75 mm FACS tubes at E:T ratios of 3:1 and 5:1 in a total volume of 250 μ L. $\gamma\delta$ T-cell cytotoxicity assays were incubated for 4 hours at 37°C in 5% CO₂ and $\alpha\beta$ T-cell cytotoxicity assays were incubated for 12 hours at 37°C in 5% CO₂. Following incubation, the cells were washed and stained with

eFluor 780 (Thermo Fisher Scientific, Waltham, MA). The double positive eFluor 780 and VPD450 cells were assessed using flow cytometry.

Protein shedding assay. On day 1 post-transduction, culture medium was changed on $\gamma\delta$ T cells and they were cultured for 48 hours under standard conditions as described above. After 48 hours, the supernatants were collected and filtered through a 0.22 micron, low-protein binding PVDF filter (MilliporeSigma, Burlington, MA). Jurkat T cells or 697 cells were then cultured for four hours in the filtered $\gamma\delta$ T-cell supernatants. Conditions involving incubation of Jurkat T cells and 697 cells in complete RPMI were included. Additional experiments were performed pre-incubating the $\gamma\delta$ T-cell supernatant with CD5-Fc or CD19-Fc for thirty minutes prior to using it to culture the cell lines. Following four hours, Jurkat T cells and 697 cells were washed to remove free proteins and stained with anti-CD5 or anti-CD19 antibodies, respectively, for flow cytometry.

Degranulation assay. CD19-CAR- and CD19-NSCAR-modified $\gamma\delta$ T cells were cultured with 697 cells in 12x75 mm FACS tubes at an E:T ratio of 5:1 in a total volume of 250 μ L and incubated for 12 hours at 37°C in 5% CO₂. 697 cells were labeled with VPD450 using the manufacturer's protocol prior to co-culture. Following the incubation, cells were stained for flow cytometry to analyze cell surface expression of CD107a using antibodies including anti-CD3 BV421, anti- $\gamma\delta$ TCR PE, anti-CD107a APC (BD Biosciences, San Jose, CA) and viability dye eFluor 780 (Thermo Fisher Scientific, Waltham, MA).

IFN γ ELISA. CD19-NSCAR-modified $\gamma\delta$ T cells were cultured with 697 cells as described above for the degranulation assay. Following the 12-hour incubation, cell culture supernatants were collected and stored at -80°C for 48 hours. IFN γ secretion was quantified by ELISA (Thermo Fisher Scientific, Waltham, MA) according to the manufacturer's protocol.

Statistical analysis. Statistical significance was determined using unpaired 2-tailed Student's *t* test and One-way ANOVA. All ρ -values were calculated with SigmaPlot, version 14.0 (Systat Software, Chicago, IL), and $\rho < 0.05$ was considered statistically significant.

Results

CD5 antigen and CD5-NSCAR are down-regulated in CD5-NSCAR-modified Jurkat T cells without altering activation

We and others have previously shown CD5-CAR expression on CD5-positive cells results in the down-regulation of the CD5 antigen from the cell surface (49; 78). To determine if CD5 down-regulation occurs upon CD5-NSCAR expression, Jurkat T cells were transduced with the CD5-NSCAR at MOIs 0.5 and 1 and CD5 expression was measured by flow cytometry. We detected a significant reduction in the percentage of CD5-positive Jurkat T cells, likely due to interactions with CD5-NSCAR on self and neighboring cells. As NSCARs do not contain a signaling cytoplasmic tail, we determined that these interactions causing CD5 down-regulation were not coupled with intracellular signaling. Even at low MOIs, detection of CD5 expression was reduced in transduced cells (MOI 0.5 and MOI 1: $\rho < 0.001$). At MOI 1, $< 5\%$ of the cells remained CD5-positive (**Figure 2A**).

We previously demonstrated CD5-CAR expression on CD5-positive Jurkat T cells results in increased activation, as measured by CD69, due to interactions between the CAR and the CD5 antigen (49). However, we hypothesized the CD5-NSCAR would not affect the activation levels of the cells since the NSCAR lacks the intracellular signaling domains typically found in a CAR construct. By flow cytometry, we determined there is no change in CD69 expression in CD5-NSCAR-modified Jurkat T cells compared to the levels of CD69 in naïve Jurkat T cells (**Figure 2B**).

We performed similar experiments with CD19-CAR- and CD19-NSCAR-modified Jurkat T cells. Jurkat T cells modified with the CD19-CAR or CD19-NSCAR did not demonstrate any change in detection of CD5 expression, with 95% of the cells expressing CD5, suggesting the down-regulation observed in

Figure V–2: CD5 expression and activation of NSCAR-modified Jurkat T cells.

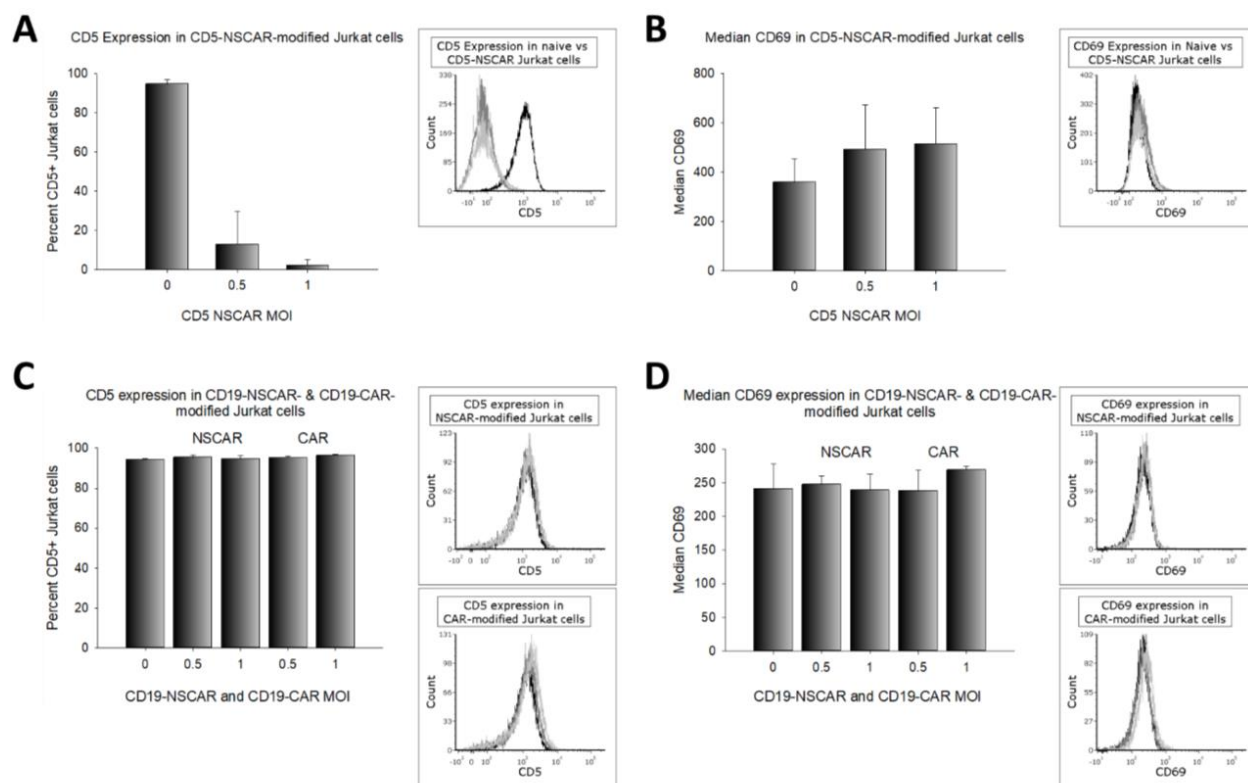


Figure 2: Flow cytometry was performed to measure CD5 and CD69 expression on Jurkat T cells five to six days post-transduction. In all figures, a representative flow cytometry overlay is illustrated on the right. Black curve: naïve; gray curve: MOI 0.5; light gray curve: MOI 1. **(A)** CD5 expression in naïve and CD5-NSCAR-modified Jurkat T cells. Naïve and MOI 1: n=4; MOI 0.5: n=3. **(B)** CD69 expression in naïve and CD5-NSCAR-modified Jurkat T cells. Naïve and MOI 1: n=5; MOI 0.5: n=3. **(C)** CD5 expression in naïve, CD19-CAR- and CD19-NSCAR-modified Jurkat T cells; n=3. **(D)** CD69 expression in naïve, CD19-CAR- and CD19-NSCAR-modified Jurkat T cells; n=3. Statistics were performed using a one-way ANOVA with Dunnett's method to compare to the naïve control group.

CD5-NSCAR-modified Jurkat T cells is due to interactions between the NSCAR and cognate antigen (**Figure 2C**). Jurkat T cells do not express CD19 and, as expected, there is no change in Jurkat T-cell activation, as measured by CD69 by flow cytometry, when modified with either a CD19-CAR or CD19-NSCAR (**Figure 2D**).

The CD5-NSCAR-modified Jurkat T cells and CD5-edited Jurkat T cells were analyzed for CD5-Fc surface expression using flow cytometry. CD5-edited Jurkat T cells were developed in our laboratory using CRISPR-Cas9 genome editing. The CD5-negative fraction of cells were isolated using FACS with >98% purity and expanded under standard Jurkat T-cell culture conditions, as described previously (49). Jurkat T cells transduced at an MOI 0.5 were, on average, 25% NSCAR-positive, whereas Jurkat T cells transduced at an MOI 1 were, on average, 70% NSCAR-positive. However, CD5-edited Jurkat T cells have a much higher percentage of NSCAR-expressing cells detected by flow cytometry when transduced with the CD5-NSCAR at the same MOIs. At MOIs 0.5 and 1, ~65% and ~90%, respectively, of CD5-edited Jurkat T cells were NSCAR-positive (**Figure 3A**). We see the emergence of a population of GFP-positive, CD5-NSCAR-negative Jurkat T cells following transduction of CD5-expressing cells, however, this population is substantially reduced in CD5-NSCAR-modified, CD5-edited Jurkat T cells (**Supplemental Figure 1A**). This suggests that CD5 expression on Jurkat T cells blocks or reduces expression of the CD5-NSCAR. These results are consistent with our previous findings using CD5-CAR-modified Jurkat T cells (49).

To determine if the expression of the CD5-NSCAR and CD5 antigen in Jurkat T cells vary over time, we measured NSCAR and CD5 expression on non-edited and CD5-edited Jurkat T cells by flow cytometry on days 5 and 15 post-transduction. On day 5, we observed approximately 20% NSCAR-positive cells at MOI 0.5 and approximately 50% NSCAR-positive cells at MOI 1, as previously noted. However, by day 15, the percentage of NSCAR-expressing Jurkat T cells was reduced to ~5% (MOI 0.5) and ~20% (MOI 1) (**Supplemental Figure 1B**). Nevertheless, the percentage of GFP-positive cells remained unchanged, suggesting the transduced cells were not dying or diluted in the culture (data not shown). Furthermore, while the CD5 expression levels on Jurkat T cells five days post-transduction were very low,

Figure V-3: CD5-NSCAR-modified Jurkat T cells cultured with non-modified Jurkat T cells.

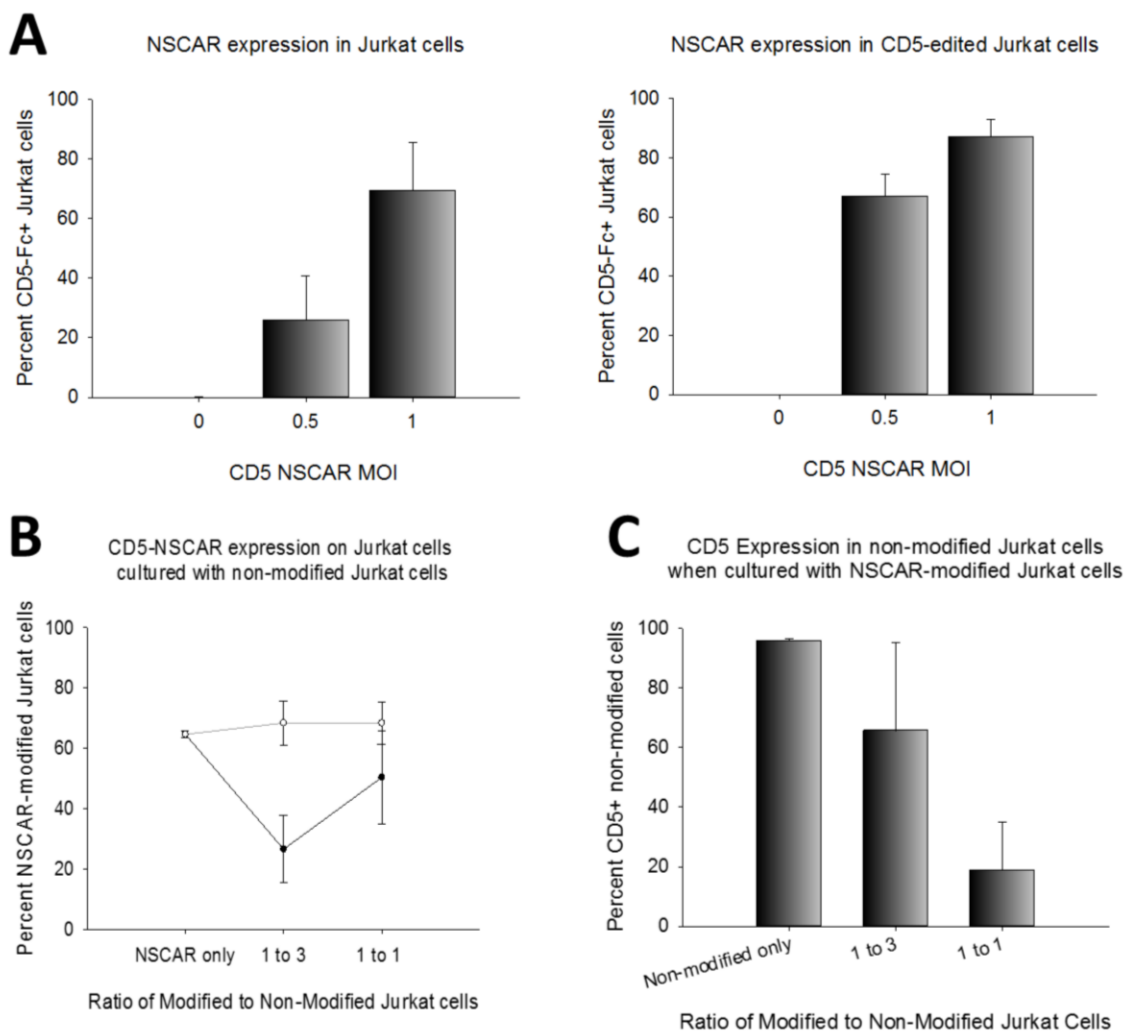


Figure 3: (A) CD5-NSCAR expression in non-edited (left) or CD5-edited (right) Jurkat T cells five days post-transduction. MOI 0.5: n=3; naïve and MOI 1: n=6 (non-edited Jurkat T cells), n=5 (CD5-edited Jurkat T cells). (B & C) CD5-NSCAR-modified Jurkat T cells were cultured with naïve (black curve) or CD5-edited (gray curve) Jurkat T cells at 1:1 or 1:3 modified to non-modified ratios. (B) CD5-NSCAR expression at each ratio. (C) CD5 expression in non-modified Jurkat T cells following co-culture with CD5-NSCAR-modified Jurkat T cells at each ratio. Flow cytometry was performed to measure CD5-Fc and CD5 antigen expression on Jurkat T cells. Statistics were performed using a 2-tailed Student's t test and one-way ANOVA with Dunnett's method to compare to the naïve group.

such a drastic down-regulation was not observed ten days later, suggesting the balance between CD5 expression and CD5-NSCAR expression shifts over time (**Supplemental Figure 1C**). The increase in CD5 antigen expression correlates with a decrease in CD5-NSCAR expression. In contrast, CD5-NSCAR expression on CD5-edited Jurkat T cells was much less variable between days 5 and 15, decreasing from 65% and 80% to 60% and 77%, at MOIs 0.5 and 1, respectively. To confirm the flow cytometry data, we performed Western blot analysis using an anti-CD5 antibody with whole cell lysates from Jurkat T cells or CD5-edited Jurkat T cells modified with the CD5-NSCAR. Whole cell lysates were collected on day 15 post-transduction. Western blot and densitometry revealed only slightly lower levels of CD5 protein in whole cell lysates of CD5-NSCAR-modified Jurkat T cells compared to CD5 protein levels in naïve Jurkat T cells (**Supplemental Figure 1D**). Non-modified and CD5-NSCAR-modified, CD5-edited Jurkat T cells displayed no signs of CD5 protein expression, as expected (data not shown).

Co-culture of CD5-NSCAR-modified Jurkat T cells with non-modified Jurkat T cells leads to CD5 antigen down-regulation in non-modified cells and CD5-NSCAR down-regulation in modified cells

We hypothesize that the CD5-NSCAR expressed on Jurkat T cells can interact with the CD5 antigen on self and neighboring cells, resulting in down-regulation of both proteins. To explore this further, we established a 14-hour co-culture to observe changes in CD5-NSCAR expression in Jurkat T cells when cultured with non-modified Jurkat T cells, as well as changes in CD5 antigen expression in the non-modified Jurkat T cells. We cultured CD5-NSCAR-modified and non-modified Jurkat T cells at 1:1 and 1:3 modified to non-modified ratios. After 14 hours, we observed a significant down-regulation in CD5-NSCAR expression when the cells were cultured at a low ratio of 1:3 with Jurkat T cells ($p < 0.001$). Despite a lack of statistical significance at the 1:1 ratio, the same trend was observed ($p = 0.078$). However, when CD5-NSCAR modified cells were cultured with non-modified, CD5-edited Jurkat T cells, there was no change in CD5-NSCAR expression at either ratio (**Figure 3B**). We conclude the CD5 antigens on non-modified Jurkat T cells can interact with the CD5-NSCAR on the modified Jurkat T cells, resulting in NSCAR-down-regulation. Therefore, there is a greater reduction in CD5-NSCAR expression in cultures

with a higher percentage of non-modified, CD5-expressing cells. Transduction of CD5-edited Jurkat T cells with the CD5-NSCAR produced similar results to those described above when cultured with non-edited Jurkat T cells or CD5-edited Jurkat T cells (At 1:3, $p < 0.001$; at 1:1, $p = 0.058$) (**Supplemental Figure 2A**).

Additionally, we measured the CD5 expression on the non-modified Jurkat T cells in the co-culture. The data demonstrated a significant decline in CD5 expression as the percentage of CD5-NSCAR-modified Jurkat T cells in the culture increased (at 1:3, $p = 0.097$; at 1:1, $p < 0.001$), with fewer than 20% of the cells expressing CD5 on the cell surface at the 1:1 ratio (**Figure 3C**). This suggests that when there are more CD5-NSCAR-expressing Jurkat T cells in the culture, there is an overall increase in the interactions between the CD5-NSCAR and CD5 antigen, resulting in greater down-regulation of the CD5 antigen on non-modified cells. Similar results were obtained when culturing CD5-edited, CD5-NSCAR-modified Jurkat T cells with non-modified Jurkat T cells. However, the CD5 on the non-modified Jurkat T cells down-regulated to a greater degree when they were cultured with CD5-edited, CD5-NSCAR-modified Jurkat T cells (95% reduction at the 1:1 ratio) compared to when they were in culture with non-edited, CD5-NSCAR-modified Jurkat T cells (80% reduction at the 1:1 ratio) (**Supplemental Figure 2B**).

NSCAR modification does not impede $\gamma\delta$ T-cell expansion and, contrary to CD19-NSCAR expression, CD5-NSCAR expression down-regulates CD5 antigen expression

$\gamma\delta$ T cells were expanded in serum-free conditions from healthy donor blood using IL-2 and zoledronate. On days 7-9 of expansion, flow cytometry was performed to determine the percentage of $\gamma\delta$ T cells and CD5 expression within the $\gamma\delta$ T-cell population. For each expansion, $\gamma\delta$ T cells were plated for lentiviral vector transduction and a non-transduced well was plated simultaneously. The expansion of naïve and NSCAR-modified $\gamma\delta$ T cells was monitored through day 12. The percentage of $\gamma\delta$ T cells in the population expanded consistently in both the naïve and CD5-NSCAR-modified cultures, with no significant differences in expansion ($p = 0.353$) (**Figure 4A & 4B**). Both populations of cells expanded ~ 2.5 -fold in the 4-5 days post-transduction suggesting expression of the CD5-NSCAR does not hinder $\gamma\delta$ T-cell expansion nor overall proliferation of the culture, despite the presence of CD5 antigen (**Figure 4C**). Similarly,

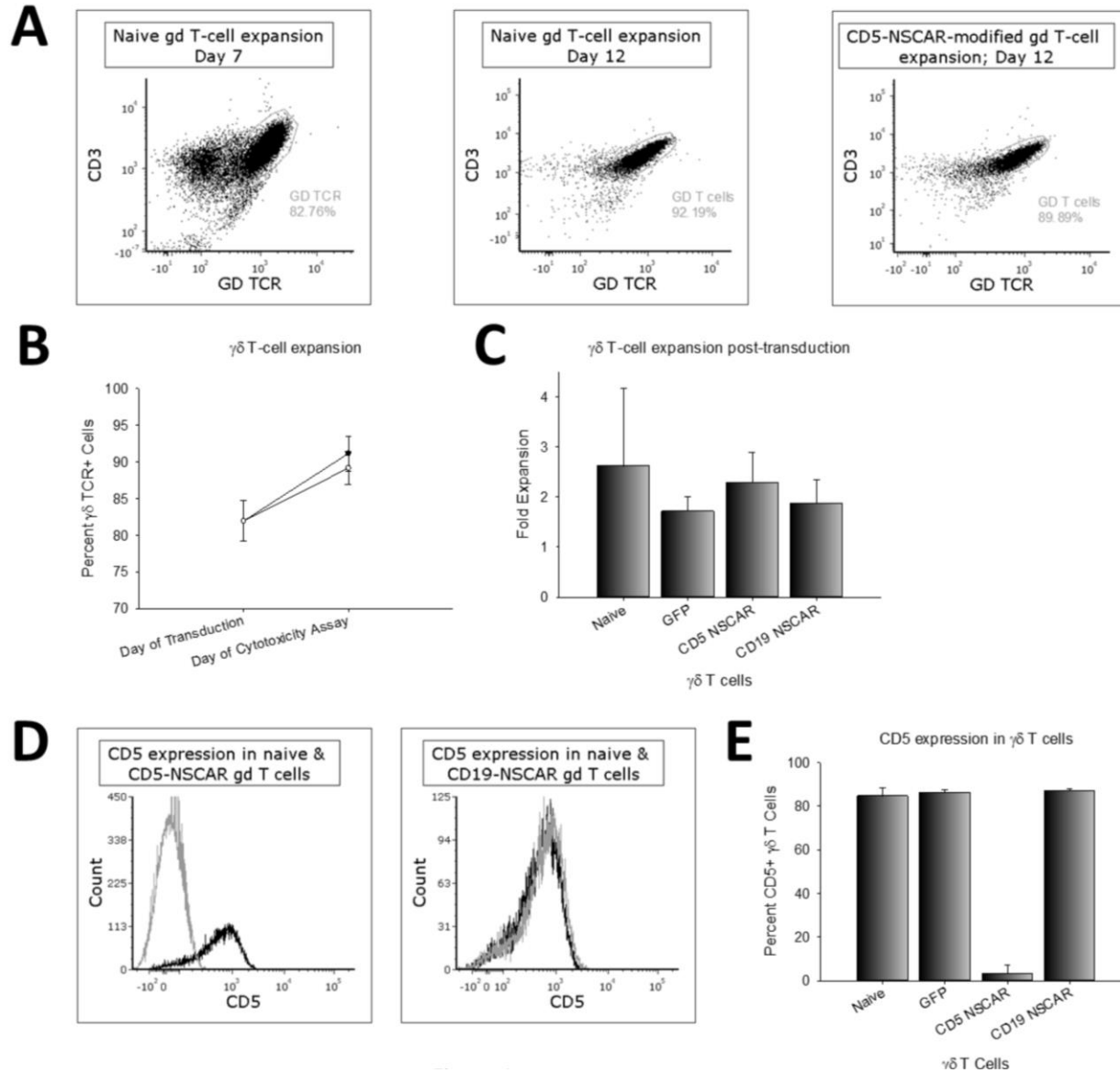
Figure V-4: NSCAR-modified $\gamma\delta$ T-cell expansion and CD5 down-regulation.

Figure 4: (A) Representative flow cytometry plots of $\gamma\delta$ T-cell expansion. The percentage of $\gamma\delta$ T cells on day 7 (left) is compared to the percentage of $\gamma\delta$ T cells on day 12 in naïve cells (middle) and CD5-NSCAR-modified $\gamma\delta$ T cells (right). (B) Percentage of $\gamma\delta$ T cells in a population of naïve (black curve) and CD5-NSCAR-modified $\gamma\delta$ T cells (gray curve) between day of transduction (7-9) and day of cytotoxicity assay (12-13); n=3. (C) Fold expansion of naïve, GFP-modified, CD5-NSCAR-modified and CD19-NSCAR-modified $\gamma\delta$ T cells. Naïve: n=5; GFP and CD5-NSCAR: n=3; CD19-NSCAR: n=2. (D) Representative

flow cytometry plots of CD5 expression in CD5-NSCAR-modified (left) and CD19-NSCAR-modified $\gamma\delta$ T cells (right). Black curve: naïve; gray curve: NSCAR-modified. (E) Graphical representation of CD5 expression in naïve and modified $\gamma\delta$ T cells. Naïve: n=8; GFP and CD19-NSCAR: n=2; CD5-NSCAR: n=5. Statistics were performed using 2-tailed Student's t test and one-way ANOVA with Dunnett's method to compare to the naïve control group. Each replicate represents an independent donor.

expansion of $\gamma\delta$ T cells modified with the CD19-NSCAR or GFP control lentiviral vectors on days 7-9 was evaluated for 4-5 days post-transduction. The control lentiviral vector encodes eGFP driven by the EF1 α promoter, as previously described (349). CD19-NSCAR- and GFP-modified $\gamma\delta$ T cells expanded comparable to naïve $\gamma\delta$ T cells (~2-fold) (**Figure 4C**). While $\gamma\delta$ T cells do not express CD19, these data provide evidence for the hypothesis that transduction alone does not affect $\gamma\delta$ T-cell expansion.

As the studies in Jurkat T cells indicate, interactions between CD5 antigen and CD5-NSCAR results in the apparent down-regulation of CD5. To determine if this occurs in $\gamma\delta$ T cells, CD5 expression on the cell surface of naïve and CD5-NSCAR-modified $\gamma\delta$ T cells was measured by flow cytometry. A significant decrease in the detection of CD5-expressing, CD5-NSCAR-modified $\gamma\delta$ T cells was observed compared to the detection of CD5-positive naïve $\gamma\delta$ T cells, with fewer than 10% of the cells expressing CD5 on the cell surface; $\rho < 0.001$. However, there was no significant down-regulation of CD5 expression in $\gamma\delta$ T cells modified with the CD19-NSCAR or GFP lentiviral vectors ($\rho > 0.05$) (**Figures 4D & 4E**).

NSCAR-modified $\gamma\delta$ T cells exhibit enhanced antigen-directed cytotoxicity

To determine if the CD5-NSCAR enhances the cytotoxicity of $\gamma\delta$ T cells, we prepared a cytotoxicity assay with Jurkat T cells and Molt-4 T cells, two CD5-positive/CD19-negative T-cell lines. Cytotoxicity assays were also performed using CD19-NSCAR-modified cells and 697 target cells, which is a CD19-positive/CD5-negative B-ALL cell line. Co-cultures were established at 3:1 or 5:1 effector to target (E:T) ratios and incubated for 4 hours at 37°C. The percent increase in cytotoxicity compared to non-modified $\gamma\delta$ T cells is shown in Figure 5. There was an increase in the cytotoxicity by CD5-NSCAR-modified $\gamma\delta$ T cells against both CD5-positive target cell lines compared to non-modified cells (**Figure 5A and 5B**). Additionally, we measured the cytotoxicity of GFP-modified $\gamma\delta$ T cells against Jurkat T cells. The data demonstrated donor variability, resulting in cells from half the donors exhibiting a decrease or no change in cytotoxicity upon GFP-modification, while the other half exhibited enhanced cytotoxicity. The greatest change in cytotoxicity was a 75% increase, however, the percentage of dead Jurkats only increased from 6% to 10.5% (data not shown). On average, at the 5:1 E:T ratio, the CD5-NSCAR-modified $\gamma\delta$ T cells

Figure V-5: NSCAR-modified $\gamma\delta$ T-cell cytotoxicity against T-ALL and B-ALL cell lines.

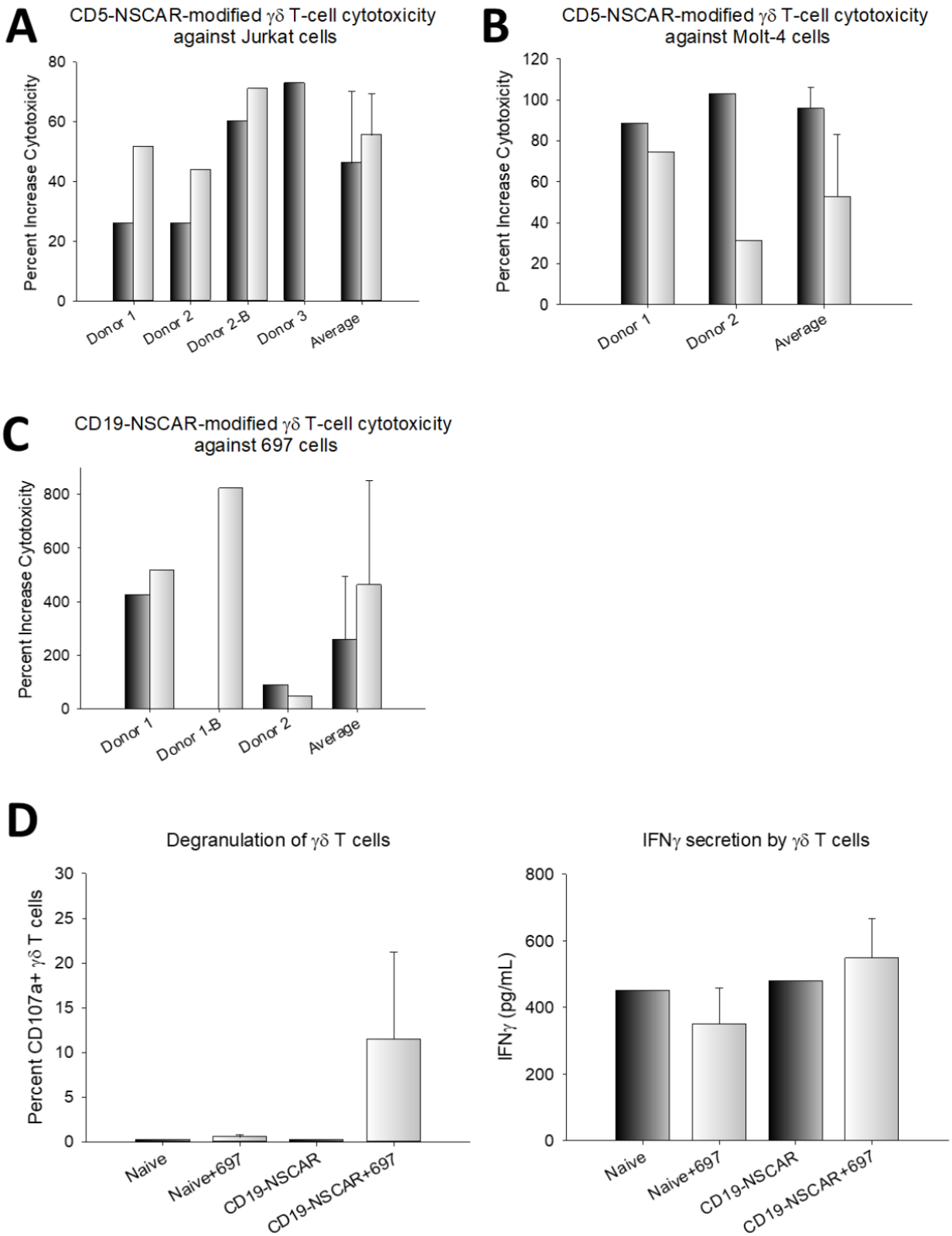


Figure 5: Effector cells and target cells were cultured at 3:1 (black bars) and 5:1 (white bars) effector to target (E:T) ratios for four hours. The percent increase in cytotoxicity by modified $\gamma\delta$ T cells compared to that of naïve $\gamma\delta$ T cells is graphed to account for donor variability in baseline cytotoxicity. The baseline is represented as the cytotoxicity of naïve $\gamma\delta$ T cells. Flow cytometry was used to measure eFluor780, VPD450 and GFP. **(A)** $\gamma\delta$ T-cell cytotoxicity against CD5-positive Jurkat cells. Three different donors modified with the CD5-NSCAR are shown separately, including the overall average cytotoxicity. One donor was repeated. **(B)** $\gamma\delta$ T-cell cytotoxicity against CD5-positive Molt-4 cells. Cells from two donors were modified with CD5-NSCAR lentiviral vector. **(C)** CD19-NSCAR-modified $\gamma\delta$ T-cell cytotoxicity against CD19-positive 697 cells. Cells from two donors were assessed. One donor was repeated. **(D)** 12-hour co-culture of CD19-NSCAR-modified $\gamma\delta$ T cells with 697 cells. CD107a expression was measured by flow cytometry six days post-transduction (left). ELISA was used to quantify IFN γ secretion by CD19-CAR- and CD19-NSCAR-modified $\gamma\delta$ T cells six days post-transduction (right). This experiment was performed in triplicate. Statistics were performed using a 2-tailed Student's t test to compare CD19-NSCAR degranulation or IFN γ secretion in co-culture with 697 cells compared to that of naïve cells cultured with 697 cells.

cultured with Jurkat T cells or Molt-4 cells resulted in 40% and 35% dead target cells, respectively, both of which correspond to a 50-60% increase in cytotoxicity compared to that of naïve $\gamma\delta$ T cells. Furthermore, the CD19-NSCAR enhanced cytotoxicity against 697 cells compared to that of naïve $\gamma\delta$ T cells, killing on average 32% of the target cells at the 5:1 E:T ratio, which was a 450% increase in killing compared to that of non-modified cells (**Figure 5C**). This data validates two NSCARs targeting different tumor-cell antigens demonstrating they can increase $\gamma\delta$ T-cell anti-tumor cytotoxicity *in vitro*. Moreover, the CD19-NSCAR expressed on $\gamma\delta$ T cells demonstrates similar cytotoxicity against 697 cells as compared to CD19-CAR-modified $\gamma\delta$ T cells ($\rho=0.905$ and $\rho=0.857$ at 3:1 and 5:1 E:T ratios, respectively) (**Supplemental Figure 3**). There was a high degree of donor variability in baseline cytotoxicity, consistent with previous findings (32; 350; 351), however an increase in cytotoxicity by NSCAR-modified $\gamma\delta$ T cells was routinely observed.

We hypothesized the NSCAR-modified $\gamma\delta$ T cells exhibit their cytotoxic activity through mechanisms endogenous to the $\gamma\delta$ T cell, specifically through the release of perforin and granzyme B as well as IFN γ . To evaluate this further, we cultured CD19-NSCAR-modified $\gamma\delta$ T cells with 697 target cells at a 5:1 E:T ratio and incubated the cells for 12 hours at 37°C. Following the incubation period, cells were evaluated for degranulation and supernatants were collected and analyzed for IFN γ secretion by ELISA. Upon co-culture with CD19-expressing target cells, there is significantly greater degranulation of CD19-NSCAR-modified $\gamma\delta$ T cells compared to degranulation of naïve $\gamma\delta$ T cells ($\rho=0.0182$). The IFN γ ELISA demonstrates a trend towards increased IFN γ secretion by CD19-NSCAR-modified $\gamma\delta$ T cells in co-culture with 697 cells compared to secretion by control cells, however, this data was not statistically significant ($\rho=0.101$) (**Figure 5D**).

NSCAR-modified $\alpha\beta$ T cells do not have enhanced anti-tumor cytotoxicity

To test our hypothesis that NSCAR expression requires MHC-independent mechanisms of cytotoxicity in order to affect cellular killing in an antigen-specific manner, we performed a cytotoxicity assay culturing CD5-NSCAR-modified $\alpha\beta$ T cells with Jurkat target cells at 3:1 and 5:1 E:T ratios. We predicted the CD5-NSCAR would not affect $\alpha\beta$ T-cell cytotoxicity. Others have previously published

studies using constructs similar to the NSCAR and demonstrated the truncated CAR does not increase T-cell activation as measured by CD25 (352), nor does it affect cellular proliferation or viability (50). Our data demonstrate there was no difference in naïve $\alpha\beta$ T-cell cytotoxicity against Jurkat T cells compared to the cytotoxicity of CD5-NSCAR-modified $\alpha\beta$ T cells against Jurkat T cells, with both resulting in 40-45% dead targets at each E:T ratio (3:1 E:T ratio: $\rho=0.618$; 5:1 E:T ratio: $\rho=0.639$) (**Figure 6**). Both donors were transduced equally by the CD5-NSCAR lentiviral vector and one donor was additionally modified with the CD5-CAR (**Supplemental Figure 4A**). CD5-CAR-modified $\alpha\beta$ T cells killed 80% of the Jurkat target cells (**Supplemental Figure 4B**), a 78% increase in cytotoxicity compared to that of naïve $\alpha\beta$ T cells.

NSCAR shed from the cell surface into the supernatant can interact with target cells

We hypothesized the apparent down-regulation of the NSCAR may be due, in part, to protein shedding from modified $\gamma\delta$ T cells resulting in lower NSCAR on the cell surface. To determine if shedding was occurring, $\gamma\delta$ T cells were cultured in fresh media on day 1 post-transduction. Non-modified cells were cultured under the same conditions and 48 hours later, the supernatants were collected and filtered. Jurkat T cells were cultured in the $\gamma\delta$ T-cell supernatant for four hours. Flow cytometry was performed to determine the CD5 expression levels on Jurkat T cells following culture in $\gamma\delta$ T-cell supernatant. Jurkat T cells cultured in their own media, or supernatant from naïve $\gamma\delta$ T cells, GFP-transduced $\gamma\delta$ T cells, or CD19-CAR-transduced $\gamma\delta$ T cells all expressed high levels of CD5 as measured by flow cytometry. However, Jurkat T cells cultured in the supernatant of CD5-CAR- or CD5-NSCAR-modified $\gamma\delta$ T cells demonstrated a significant reduction in CD5 antigen detection to ~25%. This suggests there was a factor in the supernatant of both CD5-CAR- and CD5-NSCAR-modified $\gamma\delta$ T cells that interacted with the Jurkat T cells, resulting in CD5 down-regulation or blocking of anti-CD5 antibody from binding CD5 on the T-cell surface (CAR and NSCAR: $\rho<0.001$) (**Figure 7A**). We hypothesized the extracellular portion of the CAR/NSCAR was cleaved from the cell surface and interacting with its cognate antigen. To test this, we pre-incubated the $\gamma\delta$ T-cell supernatant for thirty minutes with CD5-Fc, which is a soluble CD5 fused to the Fc portion of an IgG, prior to culturing the Jurkat T cells in the supernatants. Jurkat T cells cultured in the pre-incubated

Figure V-6: CD5-NSCAR-modified $\alpha\beta$ T-cell cytotoxicity.

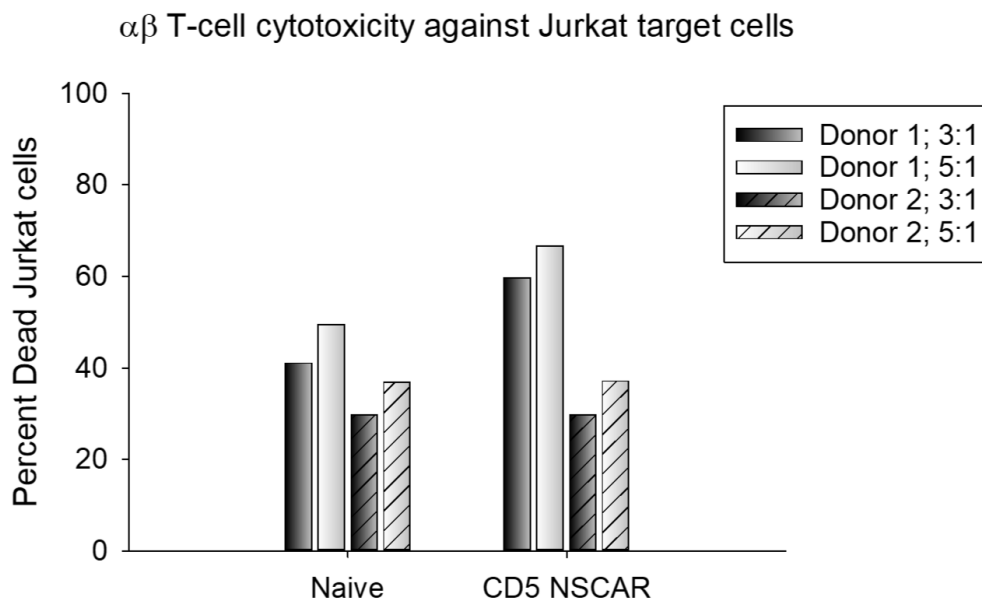


Figure 6: Effector cells and target cells were cultured at 3:1 (black bars) and 5:1 (white bars) effector to target (E:T) ratios for 12 hours. Cytotoxicity of naïve and CD5-NSCAR-modified $\alpha\beta$ T cells in culture with Jurkat T cells was determined by flow cytometry measuring eFluor780, VPD450 and GFP. Solid bars represent donor 1 and slashed bars represent donor 2. Statistics were performed using a 2-tailed Student's t test to compare cytotoxicity at each E:T ratio among donors.

Figure V-7: CD5 expression on Jurkat T cells when cultured in $\gamma\delta$ T-cell supernatant.

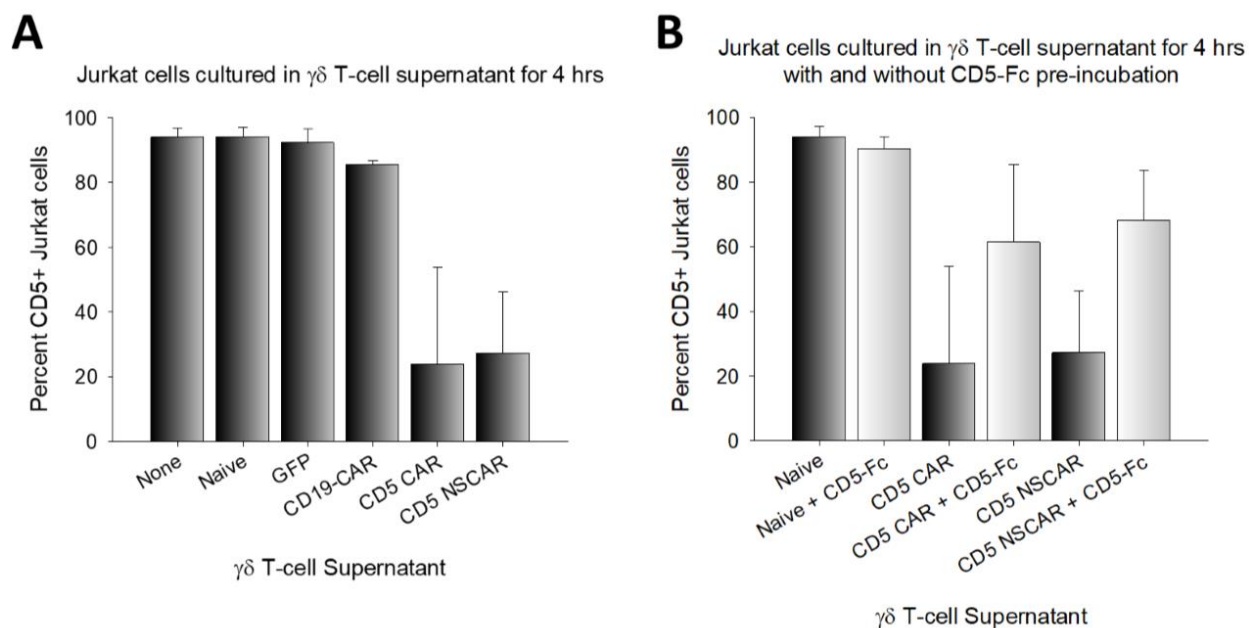


Figure 7: $\gamma\delta$ T cells were cultured for 48 hours prior to supernatant collection. Jurkat T cells were subsequently cultured in $\gamma\delta$ T-cell supernatant for four hours. **(A)** CD5 expression on Jurkat T cells cultured in $\gamma\delta$ T-cell supernatant. Sample size of groups: none and naïve: n=5; GFP and CD5-NSCAR: n=4; CD19-CAR and CD5-CAR: n=2. **(B)** CD5 expression on Jurkat T cells when $\gamma\delta$ T-cell supernatant was pre-incubated with CD5-Fc prior to Jurkat T-cell culture in the supernatant. This experiment was performed using cells from two donors. One-way ANOVA was performed using the Holm-Sidak method to compare to the naïve control group **(A)** or pairwise **(B)**. Each replicate represents an independent donor.

CD5-CAR- or CD5-NSCAR-modified $\gamma\delta$ T-cell supernatant no longer exhibited decreased detection of CD5 ($\rho=0.240$ and $\rho=0.402$, respectively). CD5 expression was measured at 60% and 70% of the population, respectively. Additionally, the pre-incubation did not affect the percentage of CD5-positive Jurkat T cells cultured in naïve $\gamma\delta$ T-cell supernatant ($\rho=0.956$). Furthermore, upon CD5-Fc pre-incubation, the percentage of CD5-expressing Jurkat T cells cultured in supernatants of CD5-CAR- or CD5-NSCAR-modified $\gamma\delta$ T cells did not significantly differ from that of cells cultured in pre-incubated naïve $\gamma\delta$ T-cell supernatants ($\rho=0.407$ and $\rho=0.584$, respectively) (**Figure 7B**).

Similar experiments were performed to determine if this effect was CD5-NSCAR-specific or if the CD19-NSCAR behaved similarly. $\gamma\delta$ T cells transduced with a CD19-NSCAR were cultured for 24-48 hours and the supernatants were then used to culture 697 cells for four hours as previously described. Following the four-hour incubation, CD19-positive 697 cells were measured by flow cytometry. 697 cells cultured in their own media or supernatant from naïve or GFP-modified $\gamma\delta$ T cells demonstrated no change in CD19 detection. However, there was a significant decrease in CD19 detection when 697 cells were cultured in supernatant from CD19-NSCAR-modified $\gamma\delta$ T cells ($\rho=0.048$), suggesting this effect is not specific to the CD5-NSCAR, nor to T-cell antigens (**Supplemental Figure 5A**). As described, reduction in CD19 detection could be due to down-regulation or blockade of antibody-binding due to CD19-NSCAR interactions with the CD19 antigen. CD19 expression had been reduced to 40% of 697 cells cultured in supernatant from CD19-NSCAR-modified $\gamma\delta$ T cells. Furthermore, pre-incubation of $\gamma\delta$ T-cell supernatant with soluble CD19-Fc under the conditions previously described prevented this reduction in CD19-expressing 697 cells. CD19 was detected in ~80% of the cells cultured in CD19-Fc pre-incubated supernatant from CD19-NSCAR-modified $\gamma\delta$ T cells. There is no difference between the percentage of CD19-expressing 697 cells cultured in the pre-incubated naïve $\gamma\delta$ T-cell supernatant compared to that of 697 cells cultured in the pre-incubated CD19-NSCAR-modified $\gamma\delta$ T-cell supernatant (**Supplemental Figure 5B**).

Discussion

$\gamma\delta$ T-cell therapy provides an alternative cellular vehicle for CAR therapy that may prove advantageous in particular settings, such as for the treatment of T-cell malignancies. We have developed a serum-free protocol for *ex vivo* expansion of V γ 9V δ 2 T cells (163; 173) and are testing the effectiveness of CAR-modified cells. During these studies, we found that CARs lacking a stimulating domain (i.e. NSCARs) retained their ability to enhance $\gamma\delta$ T-cell-directed killing, and that NSCARs can be valuable in a $\gamma\delta$ T-cell setting due to their non-stimulating properties. NSCARs prevent strong activation of $\gamma\delta$ T cells upon antigen stimulation and act as an anchor to tether the $\gamma\delta$ T cells to the tumor cells. We hypothesize this high-affinity interaction facilitates the engagement of natural, MHC-independent mechanisms of cytotoxicity. We demonstrated expression of a NSCAR targeting a T-cell antigen in $\gamma\delta$ T cells does not hinder their expansion, whereas a functional, signaling CAR targeting a T-cell antigen results in fratricide and hinders proliferation (50), with the exception being antigens that down-regulate rapidly (78). Additionally, we've shown CD5 antigen down-regulation in $\gamma\delta$ T cells modified with the CD5-NSCAR and that CD5 down-regulation is specific to expression of the CD5-NSCAR, as it is not observed in CD19-NSCAR-modified $\gamma\delta$ T cells. These results are similar to those we and others have shown using anti-CD5 CARs (49; 78).

We observed donor variability in both naïve $\alpha\beta$ and $\gamma\delta$ T-cell cytotoxicity against various cancer cell lines. However, despite the variability, NSCARs consistently enhanced $\gamma\delta$ T-cell cytotoxicity against cells expressing the targeted antigen. In contrast, NSCAR-modification of $\alpha\beta$ T cells did not affect antigen-directed cytotoxicity. We hypothesize this observed anti-cancer activity is due to the engagement of receptors on the $\gamma\delta$ T cells with their ligands on the leukemia cell lines. We predict the predominant mechanisms of action include NKG2D engagement. It was shown that the release of perforin and granzyme may facilitate NSCAR-mediated $\gamma\delta$ T-cell cytotoxicity and the release of these factors is likely downstream of NKG2D signaling. However, it is possible that additional $\gamma\delta$ T-cell mechanisms of cytotoxicity, such as Fas-FasL interactions, are involved. Future studies could clarify whether this mechanism is important to NSCAR-mediated $\gamma\delta$ T-cell cytotoxicity.

A primary advantage to $\gamma\delta$ T-cell therapy is the inherent anti-tumor cytotoxicity of $\gamma\delta$ T cells. We demonstrate NSCAR interactions with the cognate antigen enhance $\gamma\delta$ T-cell cytotoxicity. However, target antigen down-regulation is a known mechanism of tumor-cell escape from CAR-directed killing, and we show similar resistance mechanisms may occur with NSCARs. Unlike $\alpha\beta$ T cells, $\gamma\delta$ T cells have endogenous pathways leading to multiple potential mechanisms of cytotoxicity, which are independent of CAR expression. Therefore, in the event of antigen-down-regulation in subjects treated with NSCAR-modified $\gamma\delta$ T cells, these natural mechanisms of anti-tumor cytotoxicity can prevail, with continued killing of tumor cells. Many groups using CAR T-cell therapy for the treatment of B-cell malignancies have reported numerous cases of antigen-negative relapse (41). The tumor cells down-regulate the targeted antigen as a mechanism of escaping CAR T-cell killing. Naïve $\gamma\delta$ T-cell infusion into patients has demonstrated some anti-tumor activity (188-190) and therefore we hypothesize in the event of antigen down-regulation rendering NSCARs ineffective, $\gamma\delta$ T cells may still demonstrate anti-tumor activity. Furthermore, NSCAR transgenes are substantially shorter than CAR transgenes and multiple NSCARs can be expressed from a single vector, thereby reducing the possibility of antigen escape.

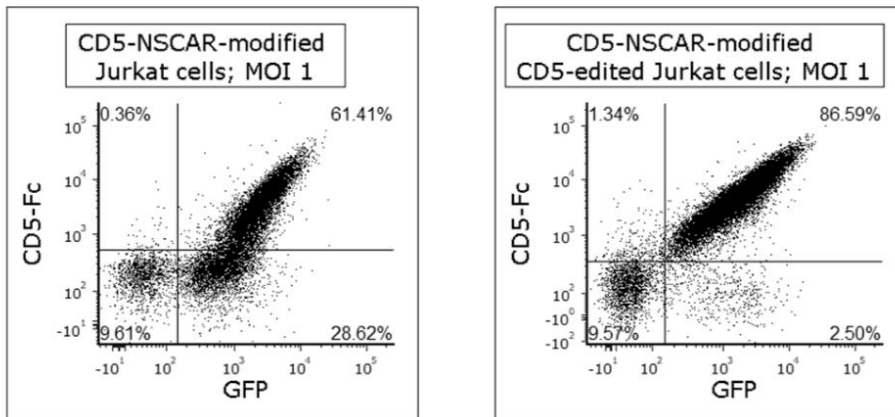
Additionally, we showed NSCARs were shed from the surface of $\gamma\delta$ T cells into the supernatant, and that shedding is not unique to NSCARs, as the results are consistent with those using a similar CD5-CAR sequence. Decreased expression of the NSCAR on the cell surface can result in decreased observed cytotoxicity. The mechanism of shedding is not well understood, but it is noteworthy that we engineered the CD5-NSCAR and CD19-NSCAR with different hinge regions. The CD5-NSCAR includes a myc tag while the CD19-NSCAR contains the CD8 α hinge, however, NSCAR-shedding is observed with both. Each NSCAR contains a 29 amino acid extracellular CD28 sequence, which may play a role in shedding, as CD28 shedding has been reported (353). There is an observed correlation between the CAR/NSCAR shedding and the transduction efficiency. Donors that yielded a greater percentage of cells expressing the transgene demonstrated a greater reduction in CD5 or CD19 detection on the target cells following culture in the $\gamma\delta$ T-cell supernatant. Studies to determine the mechanism of shedding and to characterize the protein in the supernatant are required to fully comprehend these observations. Identification of the mechanisms

involved can lead to the redesign of CARs and prevention of shedding, which can potentially result in greater antigen-directed cytotoxicity.

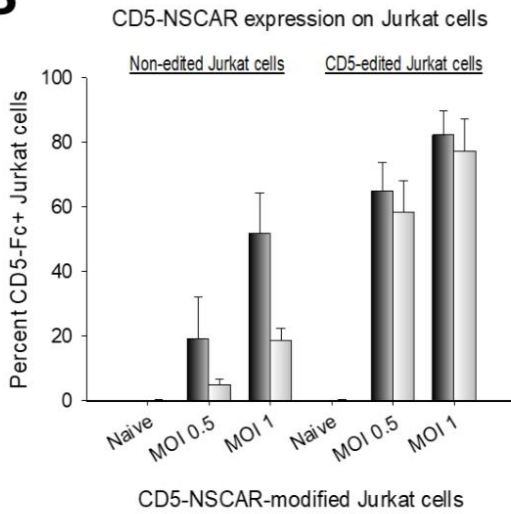
NSCARs have the potential to represent an alternative to CAR therapy, particularly in settings of T-cell malignancies using donor-derived cells, due to their ability to enhance $\gamma\delta$ T-cell cytotoxicity in an antigen-directed manner, without self-activating and hindering cellular proliferation. Understanding the mechanism of NSCAR shedding could result in a second generation of NSCARs that are resistant to shedding, a characteristic likely to enhance NSCAR-mediated cytotoxicity. Furthermore, studies assessing the role of NSCARs in additional aspects of $\gamma\delta$ T-cell tumor killing, such as trafficking to the tumor microenvironment, can influence the generation of another class of NSCARs that are superior to CARs in $\gamma\delta$ T cells. In the appropriate clinical setting, NSCARs have the potential to surpass CARs as a viable therapy, increasing anti-tumor efficacy and minimizing off-tumor cytotoxicity.

Supplemental Figure V-1: Variable expression of CD5-NSCAR and CD5 antigen expression in Jurkat T cells.

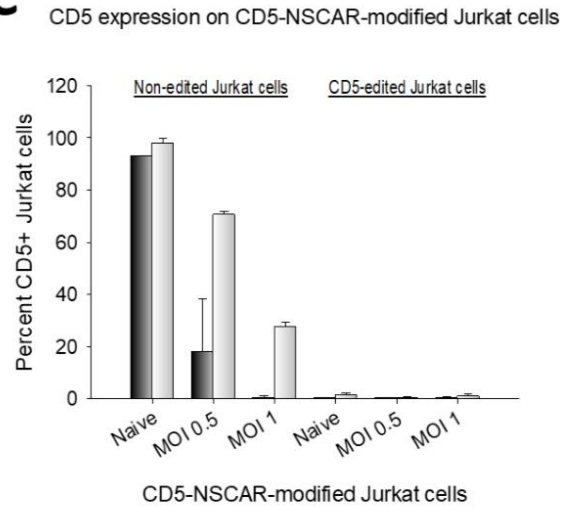
A



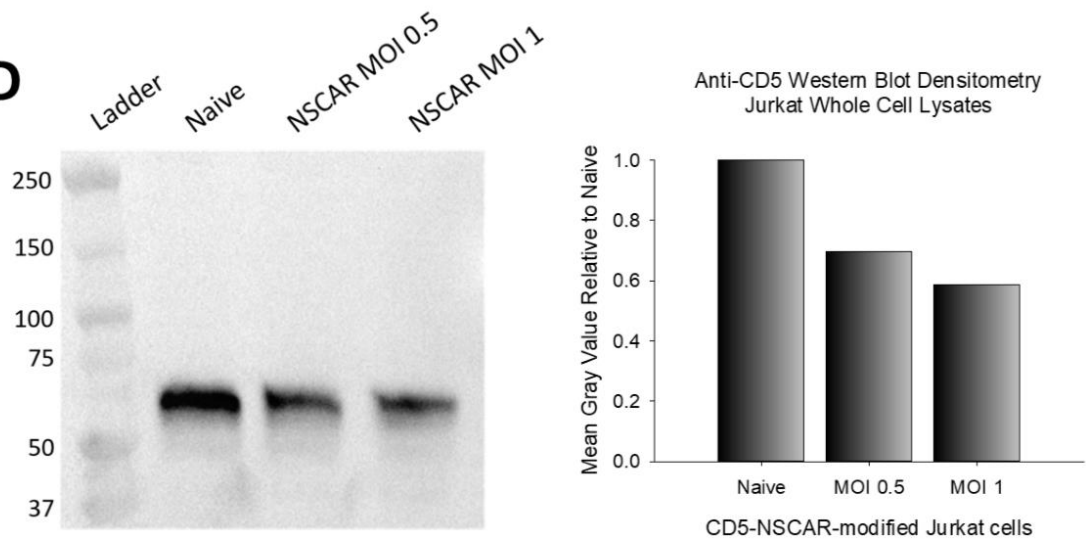
B



C

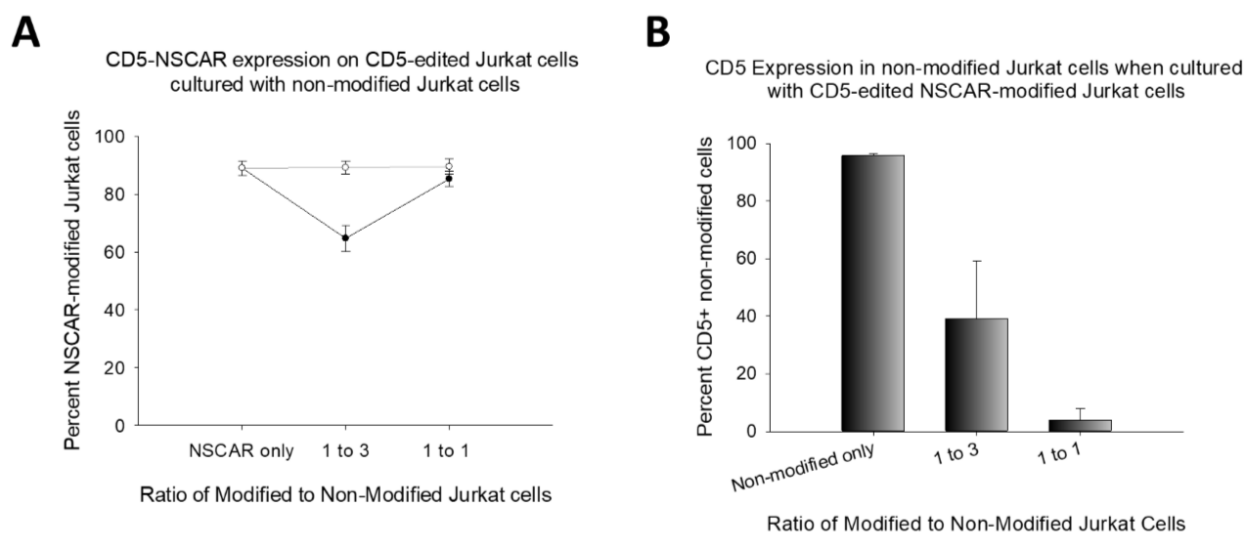


D



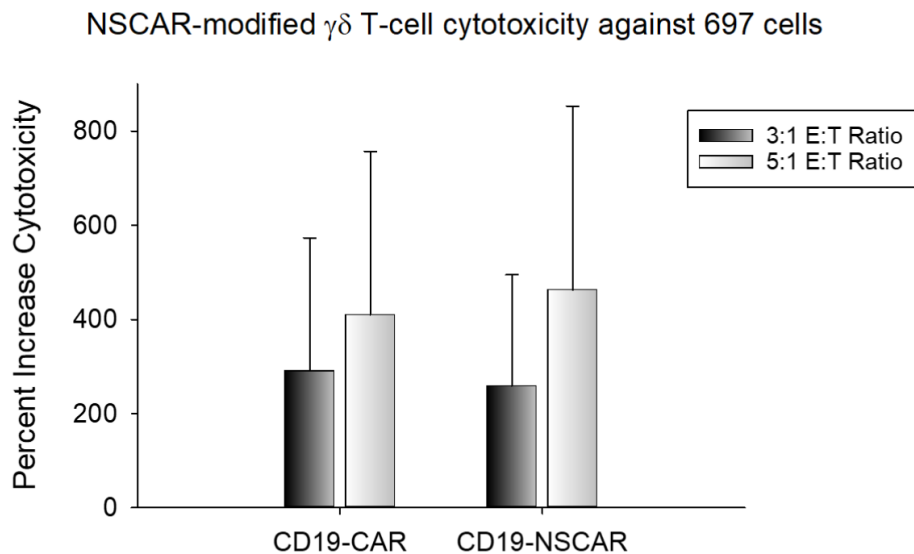
Supplemental Figure 1: Flow cytometry was performed on day 5 (black bars) and day 15 (white bars) to measure anti-CD5 and CD5-Fc binding. **(A)** Representative flow cytometry plots of CD5-NSCAR-modified Jurkat T cells (left) and CD5-edited Jurkat T cells (right). **(B)** The percentage of Jurkat T cells expressing the CD5-NSCAR on the cell surface on days 5 and 15 post-transduction. Experiments were performed in duplicate. Means and standard deviations are represented. **(C)** CD5 expression on Jurkat T cells on days 5 and 15 post- CD5-NSCAR transduction. Experiments were performed in duplicate. Means and standard deviations are represented. **(D)** Western blot analysis of naïve and CD5-NSCAR-modified Jurkat T-cell whole cell lysates on day 15 post-transduction. Membrane was blotted with anti-CD5 antibody. CD5 is detected at 54 kDa. Densitometry was performed using ImageJ.

Supplemental Figure V-2: CD5-NSCAR-modified CD5-edited Jurkat T cells cultured with non-modified Jurkat T cells.



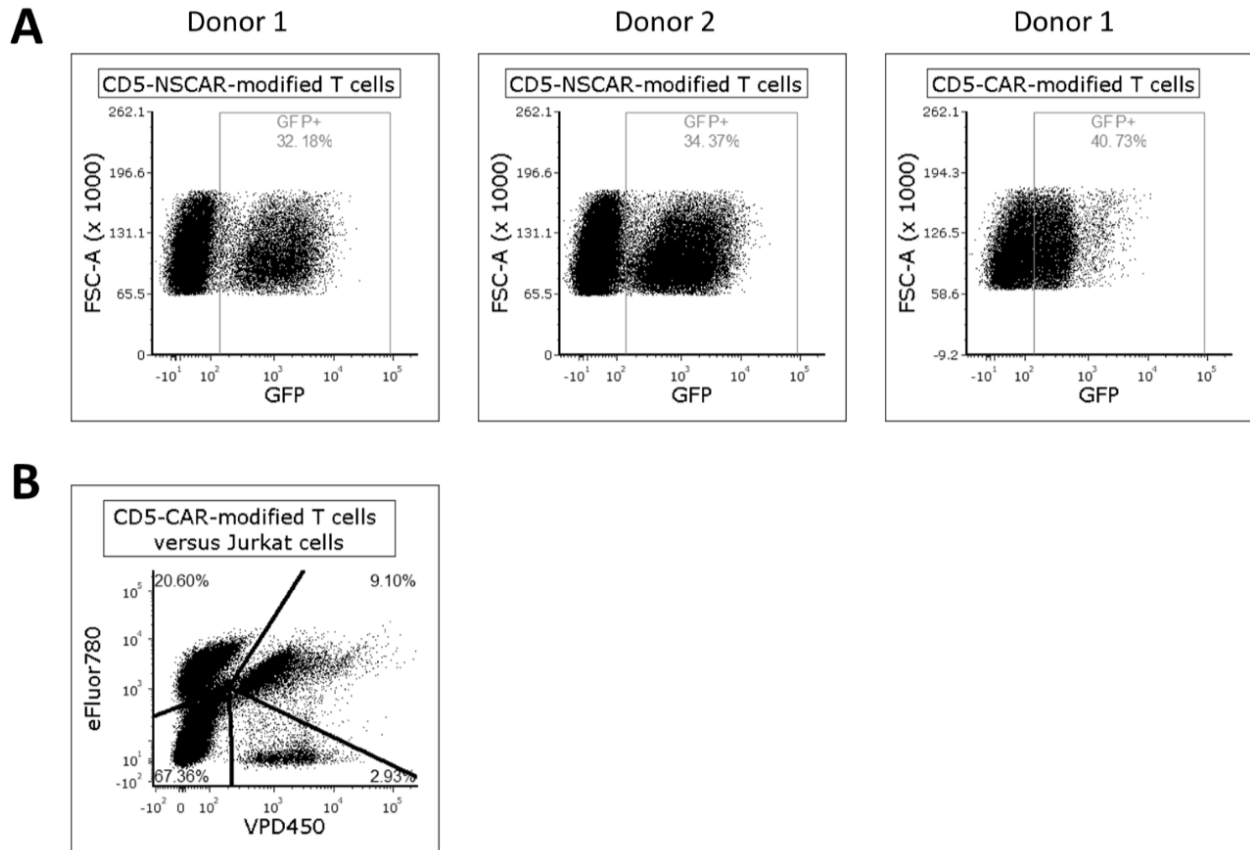
Supplemental Figure 2: Cells were cultured for 14 hours at 0:1, 1:3 and 1:1 ratios of modified to non-modified cells. Flow cytometry was used to detect CD5-NSCAR and CD5 antigen expression. **(A)** CD5-NSCAR expression on CD5-edited Jurkat T cells cultured with either naïve Jurkat T cells (black curve) or CD5-edited Jurkat T cells (gray curve). **(B)** CD5 expression on non-modified Jurkat T cells when cultured with CD5-NSCAR-modified, CD5-edited Jurkat T cells. Data represent means and standard deviations of four independent replicates.

Supplemental Figure V-3: CD19-NSCAR- and CD19-CAR-modified $\gamma\delta$ T-cell cytotoxicity against 697 cells.



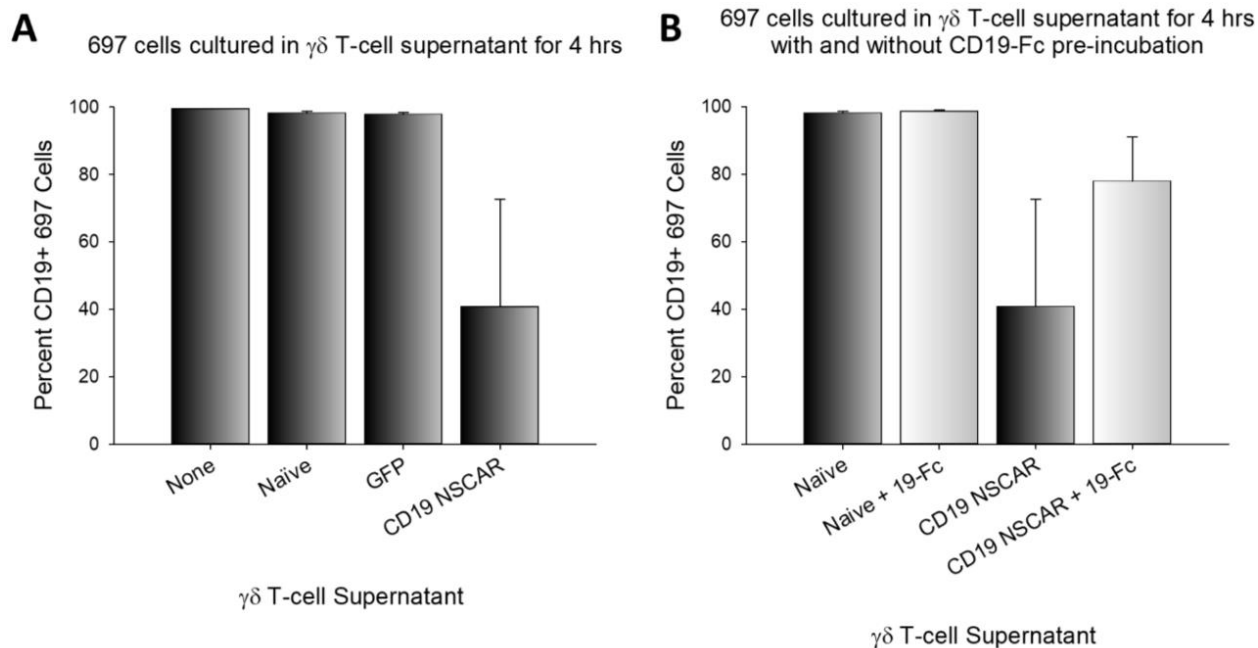
Supplemental Figure 3: Cells were cultured at 3:1 (black bars) and 5:1 (white bars) E:T ratios. Means and standard deviations are represented. N=3 for CAR-modified cells, however one donor was also assessed in duplicate at 5:1 ratio. N=2 for NSCAR-modified cells, however, at the 5:1 ratio, one donor was also assessed in duplicate. Statistics were performed using a 2-tailed Student's t test.

Supplemental Figure V-4: CD5-NSCAR- and CD5-CAR-modified $\alpha\beta$ T cells.



Supplemental Figure 4: (A) GFP expression in CD5-NSCAR-modified $\alpha\beta$ T cells from donor 1 (left) and donor 2 (middle) and in CD5-CAR-modified $\alpha\beta$ T cells from donor 1 (right) on day 6 post-transduction.

(B) CD5-CAR-modified $\alpha\beta$ T-cell cytotoxicity assay against Jurkat T cells at a 3:1 E:T ratio.

Supplemental Figure V-5: CD19 expression on 697 cells when cultured in $\gamma\delta$ T-cell supernatant.

Supplemental Figure 5: $\gamma\delta$ T cells were cultured for 48 hours prior to supernatant collection. 697 cells were subsequently cultured in $\gamma\delta$ T-cell supernatant for four hours. Flow cytometry was used to measure CD19 expression. **(A)** CD19 expression on 697 cells cultured in $\gamma\delta$ T-cell supernatant; n=2. **(B)** CD19 expression on 697 cells when $\gamma\delta$ T-cell supernatant was pre-incubated with CD19-Fc prior to 697 cell culture in the supernatant; n=2. One-way ANOVA with Dunnett's method was used to compare to the naïve control group. Each replicate represents an independent donor.

Chapter VI

Discussion, Implications and Future Directions

Discussion and Conclusions

CAR T-cell therapy for the treatment of T-cell malignancies is impeded by the difficulty of using a T cell to target and kill another T cell. The greatest challenges in this field include fratricide, T-cell aplasia and product contamination. As discussed, many solutions have been developed to address these challenges, including genome editing, PEBLs, Tet-OFF expression system, alternative effector cell types, transient CAR expression, and safety switches. Our laboratory specifically focuses on a few of these aspects, such as genome editing, alternative effector cell types, and transient CAR expression. We utilized CAR-modified NK-92 cells to avoid fratricide, T-cell aplasia, and reduce the risk of product contamination. Furthermore, we developed a CRISPR-Cas9 genome editing system to disrupt CD5 expression in T cells in order to limit fratricide and increase surface CAR expression. We explored the use of $\gamma\delta$ T cells as an alternative to $\alpha\beta$ T cells, which would result in T-cell aplasia, and NK-92 cells, which are difficult to expand *in vitro* and require irradiation prior to infusion into a patient. Our serum-free expansion protocol consistently expands $\gamma\delta$ T cells at least 80-fold to ~80% of the population (163). Furthermore, we developed a novel class of chimeric antigen receptors, referred to as NSCARs, that enhanced cytotoxic activity in $\gamma\delta$ T cells, however due to biological differences, do not have a cytotoxic effect in $\alpha\beta$ T cells.

The canonical CAR construct utilizes an scFv as the extracellular antigen recognition domain. Our goal was to identify a novel antigen recognition domain that could be utilized on a CAR scaffold to increase the repertoire of targetable antigens and epitopes. VLRs are great candidates for alternative antigen recognition domains. They represent the adaptive immune system of jawless vertebrates, such as lampreys and hagfish (354). VLRs are geometrically distinct from scFvs, a property that has potential to facilitate distinct interactions between each VLR and its antigen (355; 356). This difference in binding could allow the VLR to interact with epitopes that are not available to scFv-recognition. Furthermore, VLRs naturally exist as single-chain structures and do not require engineering to obtain a structure that can be used in a CAR construct (55; 357). On the contrary, scFvs are derived from immunoglobulin and necessitate further engineering into a single-chain fragment. It has been shown that VLRs can recognize as diverse an array of

antigens and epitopes with high specificity compared to that of immunoglobulins (267). Complete overlap between the repertoire of targetable antigens and epitopes by scFvs and VLRs is unlikely and therefore the ability to use VLRs in place of scFvs reveals a wider array of antigens that can be targeted. This can result in more opportunities to find a targetable tumor-specific antigen. The identification of tumor-specific antigens on T-cell malignancies would eliminate the risk of fratricide and T-cell aplasia without additional modifications to the construct or utilizing alternative effector cell types. The use of $\alpha\beta$ T cells would help to reduce the risk of relapse due to memory cells against the tumor target antigen.

However, utilizing VLRs in a CAR construct can result in immunogenicity in humans. As previously mentioned, VLRs consist of LRR cassettes. Similarly, toll-like receptors (TLRs), part of the human innate immune system, and VLRs have conserved LRR motifs (358; 359). Therefore, we hypothesize VLRs can be modified to mask the foreign protein from human immune recognition by altering VLR sequences to resemble those of human TLRs. This task requires a greater understanding of specific VLR sequences that are immunogenic so they can be strategically humanized.

While fratricide hinders the development of CAR T-cell therapeutics for the treatment of T-cell malignancies, the field has demonstrated that genome editing using TALENs or CRISPR-Cas9 can greatly reduce the effect of fratricide among CAR-modified T cells (49-51). Specifically, we utilized CRISPR-Cas9 to disrupt expression of CD5 in order to modify T cells with a CD5-CAR (49). Our laboratory has focused on targeting the CD5 antigen as it acts as a negative regulator for TCR signaling, and has previously been successful targeting CD5 using immunotoxin-conjugated monoclonal antibodies (68; 72; 76; 77; 258). As demonstrated herein, expression of the CD5 antigen is indirectly related to the expression of the CD5-CAR. Therefore, we propose that target antigen deletion from the CAR-modified cells has multiple benefits: limiting fratricide and increasing CAR surface expression. Our data was produced using nucleoporation of T cells with CRISPR-Cas9 plasmid DNA, however, this method resulted in poor viability of the T cells, rendering it a poor product despite cellular recovery (49). Through means of electroporation, we preserved cellular viability, however we were only able to achieve moderate levels of editing. Therefore, we used

FACS sorting to obtain a population consisting entirely of CD5-edited cells. However, this study did not demonstrate enhanced cytotoxicity by CD5-edited, CD5-CAR-modified T cells.

We hypothesized that electroporation followed by sorting and transduction diminished the health of the T cells, reducing cytotoxic activity. The percentage of cells expressing GFP as a measure of CD5-CAR expression is comparable, though reduced in the CD5-negative sorted fraction of cells. When modified with the CD5-CAR, cytotoxicity among naïve and the sorted fractions of CD5-positive and CD5-negative T cells are similar, however, as we've previously demonstrated, the CD5-edited cells express higher levels of CD5-CAR on the cell surface, therefore we would still expect to see higher levels of cytotoxic activity despite slightly lower transduction. An alternative hypothesis is that CD5-editing results in a hyperactive TCR as well as high CD5-CAR expression, which can in turn, increase exhaustion marker expression and result in activation-induced cell death (AICD). As a result, the transduced CD5-edited, CD5-CAR-modified T cells will preferentially undergo apoptosis. To test this hypothesis, we can measure the CD5-CAR-modified cells over time using the percent modified as well as total number of cells. If the cells expand and the percentage of CD5-CAR-modified cells decrease over time, we can determine the CD5-CAR-modified cells preferentially undergo apoptosis. Additionally, we can measure exhaustion markers on CD5-edited, CD5-CAR modified T cells to test the hypothesis that there are increased levels of exhaustion markers on these cells, resulting in apoptosis and decreased cytotoxic activity.

It has been shown that CD5 is down-regulated rapidly from the cell surface upon interaction with the CD5-CAR, therefore, only transient and limited fratricide is observed (78). Furthermore, a clinical trial has been initiated using CD5-CAR modified T cells that have not undergone additional modifications (MAGENTA trial, NCT03081910). However, this trial can only be successful if overexpression of the CD5-CAR is achieved, as only levels above endogenous CD5 antigen will result in surface expression of the CAR. While targeting CD5 may overcome the issue of fratricide, the concern regarding T-cell aplasia has not been addressed. Adjusting the effector cell type to NK-92 cells or $\gamma\delta$ T cells limits the risk of memory cell formation against a T-cell antigen. Our studies demonstrated NK-92 cells can be modified and sorted for CD5-CAR expression to exhibit anti-tumor cytotoxicity *in vitro* and in a T-ALL xenograft mouse model

(49). While NK-92 cells are an NK-derived lymphoma cell line, they have demonstrated safety in clinical trials. However, they require irradiation prior to infusion to prevent expansion of lymphoma cells in a patient (132; 133). As stated, no safety concerns have arisen from trials involving irradiated NK-92 cells, however, therapeutic effect of NK-92 CAR therapy has not been demonstrated (255). While NK-92 CAR therapy has potential that should continue to be investigated and optimized, particularly for the treatment of T-cell malignancies, we proposed evaluating the use of $\gamma\delta$ T cells as an alternative, less studied approach.

$\gamma\delta$ T cells are innate primary T cells that can be removed from a patient or donor upon leukapheresis and expanded *ex vivo* in serum-free conditions to clinically relevant numbers and as others have shown, can be used in an allogeneic setting as they are non-alloreactive (163; 321). We evaluated the ability to engineer the $\gamma\delta$ T cells with CRISPR-Cas9 in order to disrupt CD5 gene expression to prevent fratricide, a potential concern of $\gamma\delta$ T-cell CAR therapy targeting a T-cell antigen, although fratricide has not previously been considered in this population. Through transfection techniques including both nucleoporation and electroporation, we were unable to edit CD5 in $\gamma\delta$ T cells. However, our nucleoporation protocols were performed with cells from a single donor. Therefore, if we were to repeat these nucleoporation experiments in additional donors, we may obtain different results. Nonetheless, if there is high donor variability in transfectability using nucleoporation, it is not a good technique for modifying $\gamma\delta$ T cells as it would eliminate certain donors in a potentially unpredictable manner, thereby wasting resources in the expansion and nucleoporation processes. There are additional options for optimizing nucleoporation using the Amaxa that we hadn't assessed. We utilized two programs, one program that was recommended by Lonza for T-cell nucleoporation, and another program designed to preserve cell viability to a greater degree. While the parameters for each program cannot be adjusted, additional programs that are designed to preserve cell viability could be evaluated. Other options include using alternative buffers adjusting the salt concentrations as needed. Additionally, we could vary the cell number and quantity of DNA.

These parameters are among those that were varied in protocols assessing electroporation of $\gamma\delta$ T cells. Unfortunately, despite control over electroporation parameters, we did not reveal any advantages to

these techniques regarding CD5-editing in $\gamma\delta$ T cells using numerous protocols. One additional aspect of transfection that is likely to affect editing efficiency and viability is the quality of DNA transfected into the cells. We utilized a Qiagen Plasmid DNA Purification Maxi kit (Qiagen, Germany) to isolate high quality, endonuclease free DNA dissolved in Molecular Biology Grade DNase free, RNase free and endonuclease free water (Thomas Scientific, Swedesboro, NJ). The DNA was subsequently concentrated using a high-speed centrifuge in order to transfect cells with large quantities of DNA. DNA integrity was then confirmed by agarose gel electrophoresis (data not shown).

However, as previously discussed, rapid down-regulation of the CD5-antigen limits fratricide (78). If we can achieve high levels of CD5-CAR modification in $\gamma\delta$ T cells, we predict we will achieve sufficient surface expression of CD5-CAR to exhibit a strong anti-tumor response. Without CD5-editing of the $\gamma\delta$ T cells, a proportion of the CD5-CAR will be down-regulated, however, while this is likely to reduce the initial response against CD5-positive cells, it may also control exhaustion of the T cells, allowing for a greater degree of serial killing. Given the information that we and others in the field have collected, the benefits of CD5-CRISPR-Cas9 genome editing in T cells for the purpose of targeting CD5-positive T-cell malignancies using CAR T-cell therapy remains to be elucidated. Therefore, given the difficulty of transfecting $\gamma\delta$ T cells, we have focused our efforts on the transduction of these cells. Optimization using a lentiviral vector has resulted in 20-25% transduction of $\gamma\delta$ T cells when using a very high titer vector ($>3e8$ TU/mL). As mentioned in chapter 3, we have a lentiviral vector encoding Cas9 and a CD5-specific gRNA, however, at these levels of transduction, CD5-editing is unlikely to have an impact. Furthermore, only a small percentage of the CD5-edited cells will be transduced with the CD5-CAR, resulting in an even smaller effect on fratricide and CAR expression. Therefore, we propose CD5-editing in $\gamma\delta$ T cells is not a feasible approach using transfection or lentiviral transduction techniques.

To overcome these challenges to $\gamma\delta$ T-cell CAR therapy, we designed NSCARs. Due to the exclusion of the signaling domains, NSCARs will not result in fratricide. Therefore, $\gamma\delta$ T-cell NSCAR therapy has the potential to address all of the major challenges to current CAR therapy strategies: limited

fratricide due to lack of signaling, reduced risk of T-cell aplasia due to restricted persistence *in vivo*, and prevention of product contamination as $\gamma\delta$ T cells can be obtained from 3rd party donors. We demonstrate enhanced cytotoxicity exhibited by NSCAR-modified $\gamma\delta$ T cells *in vitro* against cancer cell lines expressing the targeted antigen. However, we demonstrate shedding of the NSCAR from the cell surface. The mechanism by which this occurs is currently under investigation in our laboratory, however, we hypothesize proteases are responsible for the NSCAR shedding. This decrease in NSCAR density on the cell surface is likely hindering the cytotoxic potential of NSCAR-modified $\gamma\delta$ T cells. We propose prevention of shedding can result in a further improvement in anti-tumor cytotoxicity. Furthermore, we observe shedding of our CD5-CAR as well, suggesting this mechanism or a similar mechanism occurs in CARs in addition to NSCARs. This phenomenon should be considered in current CAR constructs under investigation in clinical settings. Understanding this mechanism has the potential to dramatically affect the impact of CAR T-cell therapy.

Furthermore, transduction using a lentiviral vector results in only moderate transduction, which can be achieved only with a viral titer $>3e8$ TU/mL. Our preliminary data using AAV6 suggests we can greatly increase the transduction of $\gamma\delta$ T cells. Delivery of the NSCAR using AAV6 can therefore result in much higher expression of NSCAR on $\gamma\delta$ T cells. The higher NSCAR expression is likely to yield increased interactions between the NSCAR-modified $\gamma\delta$ T cells and tumor cells, facilitating tumor-cell death. As a result, we hypothesize the impact of $\gamma\delta$ T-cell NSCAR therapy will be enhanced upon optimization of transduction using AAV6 and prevention of NSCAR-shedding. We hypothesize that with sufficient levels of transduction, we can demonstrate there is a minimal effect on proliferation of our NSCAR-modified $\gamma\delta$ T cells compared to that of naïve $\gamma\delta$ T cells, suggesting there is only limited and transient fratricide. Furthermore, NSCARs are smaller than CARs, and therefore we can deliver two NSCARs targeting different antigens using a single AAV6 vector. This would help overcome an additional potential barrier of antigen-escape, commonly seen in patients treated with CD19-CAR T-cell therapy (19; 31; 38; 40).

Given the episomal expression of AAV-delivered transgene, we propose AAV6 can also be used to deliver the CD5 CRISPR-Cas9, if our studies suggest this therapy will be greatly enhanced by the addition of genome editing. $\gamma\delta$ T cells are modified more efficiently using our AAV6 transduction protocols compared to using our transfection protocols. Moreover, cell viability is much less affected when using AAV6, comparatively. Therefore, we hypothesize that we can modify $\gamma\delta$ T cells with two transgenes sequentially using AAV. Optimization regarding the quantity and MOI of AAV6 CRISPR-Cas9 is required to maximize CD5 disruption while avoiding off-target effects. This will require a greater understanding of the delay between AAV delivery and alteration of CD5 expression. Using this information, we can determine the optimal timing for both CRISPR-Cas9 and CAR delivery. However, Cas9 is a large protein, <4.0kb, therefore after removal of the eGFP reporter gene, the transgene will remain oversized for an AAV capsid (5.5 kb). Overstuffing an AAV capsid results in decreased packaging efficiency, which will in turn affect the transduction efficiency (360; 361).

The reduced persistence of $\gamma\delta$ T cells can be advantageous in conditions of severe side effects and toxicities to facilitate control over CAR expression. Additionally, as $\gamma\delta$ T cells are non-alloreactive, they can be used in an allogeneic setting, permitting greater control over dosing and ability to titrate the dose of cells, as well as permitting repeated dosing. As $\gamma\delta$ T cells do not persist for more than a couple of weeks *in vivo*, numerous injections will be required to fully combat the tumor. Allogeneic therapy is typically achieved at a substantially lower cost than autologous therapy as many doses can be produced and banked from each donor (362). However, the cost of additional viral vector required to transduce a greater number of cells for multiple infusions may offset the cost-effectiveness of allogeneic therapy. The *in vivo* data presented here will be used to design a strategic dosing regimen for CAR- or NSCAR-modified $\gamma\delta$ T cells in a T-ALL mouse model.

Future Directions and Implications

While we propose $\gamma\delta$ T cells are advantageous for using CAR therapy to treat T-cell malignancies, there are settings in which $\alpha\beta$ T cells are the favorable effector cells. The most studied malignancies for CAR T-cell therapy are B-ALL, CLL and DLBCL. CAR T-cell therapies targeting these diseases have utilized $\alpha\beta$ T cells, resulting in B-cell aplasia. However, thus far, B-cell aplasia in these patients has been managed through intravenous immunoglobulin (19; 363). Therefore, the consequence of B-cell aplasia is favorable to the higher risk of relapse that would exist if the patients did not have memory cells against a B-cell antigen. Additionally, when using a strategy targeting a tumor-specific antigen, $\alpha\beta$ T cells are valuable as effector cells. There would be minimal risk of off-tumor cytotoxicity and memory cells would help prevent antigen-positive relapse. However, few antigens have been identified with such tumor-specificity. Utilizing VLRs increases the potential of identifying a tumor-specific epitope that can be used for CAR therapy. For the treatment of T-cell malignancies, many adverse events are related to $\alpha\beta$ T-cell targeting of T-cell antigens, as described. Utilizing $\gamma\delta$ T cells as an alternative effector cell type for CAR therapy overcomes many of these negative side effects, resulting in a safer product that can be delivered to patients without delay.

As mentioned, numerous advantages for using $\gamma\delta$ T cells exist; however, there are a few limitations to $\gamma\delta$ T-cell CAR therapy as previously mentioned. Healthy donor blood samples can be processed for PBMC isolation and $\gamma\delta$ T cells expanded in serum-free conditions. We've demonstrated donor-dependent expansion, with some donors only expanding to ~50% $\gamma\delta$ T cells, with the remaining half consisting of $\alpha\beta$ T cells and NK cells. It is currently unknown what donor characteristics are optimal for achieving substantial expansion of $\gamma\delta$ T cells (>80% $\gamma\delta$ T cells). Preliminary data from our laboratory suggests donors who exercise at least three times a week are more likely to have greater $\gamma\delta$ T-cell expansions compared to those who exercise fewer than two times a week. However, as there are many confounding variables involved in this correlation, it remains to be elucidated i) whether the type of exercise is critical, ii) if the correlation is related to diet instead or overall lifestyle, or rather iii) if expansion is related to BMI and

percentage of body fat. If these variables can be narrowed, we can determine criteria for healthy donors to increase the likelihood of a successful expansion with each donor PBMCs.

However, donors that have been expanded to 95% $\gamma\delta$ T cells in culture still have 5% other cells remaining, likely a percentage of these are $\alpha\beta$ T cells. If a single $\alpha\beta$ T cell with a memory phenotype is modified with a CD5-CAR, it can expand *in vivo* upon antigen recognition and cause T-cell aplasia. The NK cells remaining in culture are not of concern, as they will not persist *in vivo*, are non-alloreactive and have inherent cytotoxicity mechanisms, similar to $\gamma\delta$ T cells. $\gamma\delta$ T-cell negative selection can be used during the expansion to remove $\alpha\beta$ T cells from the population, preventing the transduction of $\alpha\beta$ T cells with a CAR targeting a T-cell antigen. This both increases the overall percentage of $\gamma\delta$ T cells as well as removes the $\alpha\beta$ T cells, which are responsible for GvHD when used in an allogeneic setting and memory against the targeted antigen. Our laboratory has optimized the timing of the selection to investigate the superiority of a selected $\gamma\delta$ T-cell product. The data consistently demonstrated >95% $\gamma\delta$ T cells by day 12 of expansion. Moreover, the data suggests selection does not negatively impact cytotoxic potential of $\gamma\delta$ T cells. Selective depletion of $\alpha\beta$ T cells from our cell culture prior to modification will improve the impact of this therapy by reducing the risk of adverse events.

Further studies are required to determine the mechanism of cytotoxicity by NSCAR-modified $\gamma\delta$ T cells. We demonstrate enhanced anti-tumor cytotoxicity by NSCAR-modified $\gamma\delta$ T cells resulting from 4-hour co-cultures with target cells. However, it is possible that extending the cytotoxicity assay beyond 4 hours, will result in greater target cell death as a result of $\gamma\delta$ T-cell serial killing. One limitation to extending the cytotoxicity assay is that in a flow-based assay such as this, only intact cells can be detected and quantified. A longer co-culture can result in dead cells turning into debris and preventing their detection. Furthermore, future studies can include Annexin V staining for flow cytometry to measure the percentage of pre-apoptotic target cells to complement eFluor 780 staining, which measures the percentage of target cells that have already died.

Harnessing the potential of $\gamma\delta$ T cells for CAR or NSCAR therapy can have a vast impact on the field. The ability to utilize third party donors will greatly improve the consistency of the therapy, eliminate risk of product contamination, reduce variability from pre-treatment and decrease the time between determination of patient eligibility and treatment initiation. Utilizing AAV, $\gamma\delta$ T cells can potentially be modified with both CRISPR-Cas9 as well as a CAR to prevent fratricide. Alternatively, NSCAR-modified $\gamma\delta$ T cells can be used. We demonstrated the cytotoxicity against a B-ALL cell line is comparable between the CD19-NSCAR and CD19-CAR. However, in settings of T-cell targeting, the NSCAR is unlikely to result in fratricide due to the lack of signaling domains. As exemplified using $\alpha\beta$ T cells, NSCAR-mediated cytotoxicity has specific biological requirements to enhance T-cell cytotoxicity. Furthermore, two different NSCARs can be expressed in a single transgene, using a 2a sequence, further improving the therapy. $\gamma\delta$ T-cell CAR and NSCAR therapy have the potential to revolutionize this field by overcoming many of the challenges facing CAR therapy for the treatment of T-cell malignancies.

References

1. Belver L, Ferrando A. 2016. The genetics and mechanisms of T cell acute lymphoblastic leukaemia. *Nat Rev Cancer* 16:494-507
2. Hunger SP, Mullighan CG. 2015. Acute Lymphoblastic Leukemia in Children. *N Engl J Med* 373:1541-52
3. Phillips AA, Harewood JCK. 2018. Adult T Cell Leukemia-Lymphoma (ATL): State of the Art. *Curr Hematol Malig Rep* 13:300-7
4. Utsunomiya A, Choi I, Chihara D, Seto M. 2015. Recent advances in the treatment of adult T-cell leukemia-lymphomas. *Cancer Sci* 106:344-51
5. Matutes E. 2007. Adult T-cell leukaemia/lymphoma. *J Clin Pathol* 60:1373-7
6. Swerdlow SH, Campo E, Pileri SA, Harris NL, Stein H, et al. 2016. The 2016 revision of the World Health Organization classification of lymphoid neoplasms. *Blood* 127:2375-90
7. 1997. A clinical evaluation of the International Lymphoma Study Group classification of non-Hodgkin's lymphoma. The Non-Hodgkin's Lymphoma Classification Project. *Blood* 89:3909-18
8. Teras LR, DeSantis CE, Cerhan JR, Morton LM, Jemal A, Flowers CR. 2016. 2016 US lymphoid malignancy statistics by World Health Organization subtypes. *CA Cancer J Clin* 66:443-59
9. Laribi K, Alani M, Truong C, Baugier de Materre A. 2018. Recent Advances in the Treatment of Peripheral T-Cell Lymphoma. *Oncologist* 23:1039-53
10. Vose J, Armitage J, Weisenburger D, International TCLP. 2008. International peripheral T-cell and natural killer/T-cell lymphoma study: pathology findings and clinical outcomes. *J Clin Oncol* 26:4124-30
11. Einsiedel HG, von Stackelberg A, Hartmann R, Fengler R, Schrappe M, et al. 2005. Long-term outcome in children with relapsed ALL by risk-stratified salvage therapy: results of trial acute lymphoblastic leukemia-relapse study of the Berlin-Frankfurt-Munster Group 87. *J Clin Oncol* 23:7942-50
12. Reismuller B, Peters C, Dworzak MN, Potschger U, Urban C, et al. 2013. Outcome of children and adolescents with a second or third relapse of acute lymphoblastic leukemia (ALL): a population-based analysis of the Austrian ALL-BFM (Berlin-Frankfurt-Munster) study group. *J Pediatr Hematol Oncol* 35:e200-4
13. Winter SS, Dunsmore KP, Devidas M, Wood BL, Esiashvili N, et al. 2018. Improved Survival for Children and Young Adults With T-Lineage Acute Lymphoblastic Leukemia: Results From the Children's Oncology Group AALL0434 Methotrexate Randomization. *J Clin Oncol* 36:2926-34
14. Whittaker S, Hoppe R, Prince HM. 2016. How I treat mycosis fungoides and Sezary syndrome. *Blood* 127:3142-53
15. Arulogun SO, Prince HM, Ng J, Lade S, Ryan GF, et al. 2008. Long-term outcomes of patients with advanced-stage cutaneous T-cell lymphoma and large cell transformation. *Blood* 112:3082-7
16. Horwitz S, O'Connor OA, Pro B, Illidge T, Fanale M, et al. 2019. Brentuximab vedotin with chemotherapy for CD30-positive peripheral T-cell lymphoma (ECHELON-2): a global, double-blind, randomised, phase 3 trial. *Lancet* 393:229-40
17. Prince HM, Kim YH, Horwitz SM, Dummer R, Scarisbrick J, et al. 2017. Brentuximab vedotin or physician's choice in CD30-positive cutaneous T-cell lymphoma (ALCANZA): an international, open-label, randomised, phase 3, multicentre trial. *Lancet* 390:555-66
18. Kwong YL, Chan TSY, Tan D, Kim SJ, Poon LM, et al. 2017. PD1 blockade with pembrolizumab is highly effective in relapsed or refractory NK/T-cell lymphoma failing l-asparaginase. *Blood* 129:2437-42

19. Maude SL, Frey N, Shaw PA, Aplenc R, Barrett DM, et al. 2014. Chimeric antigen receptor T cells for sustained remissions in leukemia. *N Engl J Med* 371:1507-17
20. Davila ML, Riviere I, Wang X, Bartido S, Park J, et al. 2014. Efficacy and toxicity management of 19-28z CAR T cell therapy in B cell acute lymphoblastic leukemia. *Sci Transl Med* 6:224ra25
21. Lee DW, Kochenderfer JN, Stetler-Stevenson M, Cui YK, Delbrook C, et al. 2015. T cells expressing CD19 chimeric antigen receptors for acute lymphoblastic leukaemia in children and young adults: a phase 1 dose-escalation trial. *Lancet* 385:517-28
22. Schubert ML, Huckelhoven A, Hoffmann JM, Schmitt A, Wuchter P, et al. 2016. Chimeric Antigen Receptor T Cell Therapy Targeting CD19-Positive Leukemia and Lymphoma in the Context of Stem Cell Transplantation. *Hum Gene Ther*
23. Lim WA, June CH. 2017. The Principles of Engineering Immune Cells to Treat Cancer. *Cell* 168:724-40
24. Gross G, Waks T, Eshhar Z. 1989. Expression of immunoglobulin-T-cell receptor chimeric molecules as functional receptors with antibody-type specificity. *Proc Natl Acad Sci U S A* 86:10024-8
25. Finney HM, Lawson AD, Bebbington CR, Weir AN. 1998. Chimeric receptors providing both primary and costimulatory signaling in T cells from a single gene product. *J Immunol* 161:2791-7
26. Finney HM, Akbar AN, Lawson AD. 2004. Activation of resting human primary T cells with chimeric receptors: costimulation from CD28, inducible costimulator, CD134, and CD137 in series with signals from the TCR zeta chain. *J Immunol* 172:104-13
27. Wang J, Jensen M, Lin Y, Sui X, Chen E, et al. 2007. Optimizing adoptive polyclonal T cell immunotherapy of lymphomas, using a chimeric T cell receptor possessing CD28 and CD137 costimulatory domains. *Hum Gene Ther* 18:712-25
28. Gill S, June CH. 2015. Going viral: chimeric antigen receptor T-cell therapy for hematological malignancies. *Immunol Rev* 263:68-89
29. Kochenderfer JN, Dudley ME, Maric I, Feldman SA, Salit R, et al. 2011. Dramatic Regression of Chronic Lymphocytic Leukemia in the First Patient Treated With Donor-Derived Genetically-Engineered Anti-CD19-Chimeric-Antigen-Receptor-Expressing T Cells After Allogeneic Hematopoietic Stem Cell Transplantation. *Biology of Blood and Marrow Transplantation* 17
30. Grupp SA, Kalos M, Barrett D, Aplenc R, Porter DL, et al. 2013. Chimeric antigen receptor-modified T cells for acute lymphoid leukemia. *N Engl J Med* 368:1509-18
31. Lee DW, Kochenderfer JN, Stetler-Stevenson M, Cui YK, Delbrook C, et al. 2015. T cells expressing CD19 chimeric antigen receptors for acute lymphoblastic leukaemia in children and young adults: a phase 1 dose-escalation trial. *The Lancet* 385:517-28
32. Levine BL, Miskin J, Wonnacott K, Keir C. 2017. Global Manufacturing of CAR T Cell Therapy. *Mol Ther Methods Clin Dev* 4:92-101
33. Klebanoff CA, Khong HT, Antony PA, Palmer DC, Restifo NP. 2005. Sinks, suppressors and antigen presenters: how lymphodepletion enhances T cell-mediated tumor immunotherapy. *Trends Immunol* 26:111-7
34. Laport GG, Levine BL, Stadtmauer EA, Schuster SJ, Luger SM, et al. 2003. Adoptive transfer of costimulated T cells induces lymphocytosis in patients with relapsed/refractory non-Hodgkin lymphoma following CD34+-selected hematopoietic cell transplantation. *Blood* 102:2004-13
35. Dudley ME, Wunderlich JR, Yang JC, Sherry RM, Topalian SL, et al. 2005. Adoptive cell transfer therapy following non-myeloablative but lymphodepleting chemotherapy for the treatment of patients with refractory metastatic melanoma. *J Clin Oncol* 23:2346-57
36. Kalos M, Levine BL, Porter DL, Katz S, Grupp SA, et al. 2011. T cells with chimeric antigen receptors have potent antitumor effects and can establish memory in patients with advanced leukemia. *Sci Transl Med* 3:95ra73

37. Park JH, Geyer MB, Brentjens RJ. 2016. CD19-targeted CAR T-cell therapeutics for hematologic malignancies: interpreting clinical outcomes to date. *Blood* 127:3312-20
38. Grupp SA, Maude SL, Shaw PA, Aplenc R, Barrett DM, et al. 2015. Durable Remissions in Children with Relapsed/Refractory ALL Treated with T Cells Engineered with a CD19-Targeted Chimeric Antigen Receptor (CTL019). *Blood*
39. Topp MS, Gokbuget N, Zugmaier G, Klappers P, Stelljes M, et al. 2014. Phase II trial of the anti-CD19 bispecific T cell-engager blinatumomab shows hematologic and molecular remissions in patients with relapsed or refractory B-precursor acute lymphoblastic leukemia. *J Clin Oncol* 32:4134-40
40. Maude SL, Teachey DT, Porter DL, Grupp SA. 2015. CD19-targeted chimeric antigen receptor T-cell therapy for acute lymphoblastic leukemia. *Blood* 125:4017-23
41. Gardner R, Wu D, Cherian S, Fang M, Hanafi LA, et al. 2016. Acquisition of a CD19-negative myeloid phenotype allows immune escape of MLL-rearranged B-ALL from CD19 CAR-T-cell therapy. *Blood* 127:2406-10
42. Hamieh M, Dobrin A, Cabriolu A, van der Stegen SJC, Giavridis T, et al. 2019. CAR T cell trogocytosis and cooperative killing regulate tumour antigen escape. *Nature* 568:112-6
43. Ruella M, Xu J, Barrett DM, Fraietta JA, Reich TJ, et al. 2018. Induction of resistance to chimeric antigen receptor T cell therapy by transduction of a single leukemic B cell. *Nat Med* 24:1499-503
44. Le RQ, Li L, Yuan W, Shord SS, Nie L, et al. 2018. FDA Approval Summary: Tocilizumab for Treatment of Chimeric Antigen Receptor T Cell-Induced Severe or Life-Threatening Cytokine Release Syndrome. *Oncologist* 23:943-7
45. Gust J, Hay KA, Hanafi LA, Li D, Myerson D, et al. 2017. Endothelial Activation and Blood-Brain Barrier Disruption in Neurotoxicity after Adoptive Immunotherapy with CD19 CAR-T Cells. *Cancer Discov* 7:1404-19
46. Gust J, Taraseviciute A, Turtle CJ. 2018. Neurotoxicity Associated with CD19-Targeted CAR-T Cell Therapies. *CNS Drugs* 32:1091-101
47. Hunter BD, Jacobson CA. 2019. CAR T-cell associated neurotoxicity: Mechanisms, clinicopathologic correlates, and future directions. *J Natl Cancer Inst*
48. Karschnia P, Jordan JT, Forst DA, Arrillaga-Romany IC, Batchelor TT, et al. 2019. Clinical presentation, management, and biomarkers of neurotoxicity after adoptive immunotherapy with CAR T cells. *Blood* 133:2212-21
49. Raikar SS, Fleischer LC, Moot R, Fedanov A, Paik NY, et al. 2018. Development of chimeric antigen receptors targeting T-cell malignancies using two structurally different anti-CD5 antigen binding domains in NK and CRISPR-edited T cell lines. *Oncoimmunology* 7:e1407898
50. Gomes-Silva D, Srinivasan M, Sharma S, Lee CM, Wagner DL, et al. 2017. CD7-edited T cells expressing a CD7-specific CAR for the therapy of T-cell malignancies. *Blood* 130:285-96
51. Cooper ML, Choi J, Staser K, Ritchey JK, Devenport JM, et al. 2018. An "off-the-shelf" fratricide-resistant CAR-T for the treatment of T cell hematologic malignancies. *Leukemia* 32:1970-83
52. Mamonkin M, Mukherjee M, Srinivasan M, Sharma S, Gomes-Silva D, et al. 2018. Reversible Transgene Expression Reduces Fratricide and Permits 4-1BB Costimulation of CAR T Cells Directed to T-cell Malignancies. *Cancer Immunol Res* 6:47-58
53. Png YT, Vinanica N, Kamiya T, Shimasaki N, Coustan-Smith E, Campana D. 2017. Blockade of CD7 expression in T cells for effective chimeric antigen receptor targeting of T-cell malignancies. *Blood Adv* 1:2348-60
54. Kamiya T, Wong D, Png YT, Campana D. 2018. A novel method to generate T-cell receptor-deficient chimeric antigen receptor T cells. *Blood Adv* 2:517-28

55. Moot R, Raikar SS, Fleischer L, Querrey M, Tylawsky DE, et al. 2016. Genetic engineering of chimeric antigen receptors using lamprey derived variable lymphocyte receptors. *Mol Ther Oncolytics* 3:16026
56. Chen KH, Wada M, Firor AE, Pinz KG, Jares A, et al. 2016. Novel anti-CD3 chimeric antigen receptor targeting of aggressive T cell malignancies. *Oncotarget* 7:56219-32
57. Chen KH, Wada M, Pinz KG, Liu H, Lin KW, et al. 2017. Preclinical targeting of aggressive T-cell malignancies using anti-CD5 chimeric antigen receptor. *Leukemia* 31:2151-60
58. Pinz KG, Yakaboski E, Jares A, Liu H, Firor AE, et al. 2017. Targeting T-cell malignancies using anti-CD4 CAR NK-92 cells. *Oncotarget* 8:112783-96
59. Zheng J, Liu Y, Lau YL, Tu W. 2013. gammadelta-T cells: an unpolished sword in human anti-infection immunity. *Cell Mol Immunol* 10:50-7
60. Ramos CA, Ballard B, Zhang H, Dakhova O, Gee AP, et al. 2017. Clinical and immunological responses after CD30-specific chimeric antigen receptor-redirected lymphocytes. *J Clin Invest* 127:3462-71
61. Scarfo I, Ormhoj M, Frigault MJ, Castano AP, Lorrey S, et al. 2018. Anti-CD37 chimeric antigen receptor T cells are active against B- and T-cell lymphomas. *Blood* 132:1495-506
62. Antin JH, Emerson SG, Martin P, Gadol N, Ault KA. 1986. Leu-1+ (CD5+) B cells. A major lymphoid subpopulation in human fetal spleen: phenotypic and functional studies. *J Immunol* 136:505-10
63. Thomas Y, Glickman E, DeMartino J, Wang J, Goldstein G, Chess L. 1984. Biologic functions of the OKT1 T cell surface antigen. I. The T1 molecule is involved in helper function. *J Immunol* 133:724-8
64. Engleman EG, Warnke R, Fox RI, Dilley J, Benike CJ, Levy R. 1981. Studies of a human T lymphocyte antigen recognized by a monoclonal antibody. *Proc Natl Acad Sci U S A* 78:1791-5
65. Martin PJ, Hansen JA, Nowinski RC, Brown MA. 1980. A new human T-cell differentiation antigen: unexpected expression on chronic lymphocytic leukemia cells. *Immunogenetics* 11:429-39
66. Reinherz EL, Kung PC, Goldstein G, Schlossman SF. 1979. A Monoclonal Antibody with Selective Reactivity with Functionally Mature Human Thymocytes and All Peripheral Human T Cells. *J Immunol* 123:1312-7
67. Azzam HS, Grinberg A, Lui K, Shen H, Shores EW, Love PE. 1998. CD5 expression is developmentally regulated by T cell receptor (TCR) signals and TCR avidity. *J Exp Med* 188:2301-11
68. Dalloul A. 2009. CD5: a safeguard against autoimmunity and a shield for cancer cells. *Autoimmun Rev* 8:349-53
69. Pui CH, Behm FG, Crist WM. 1993. Clinical and biologic relevance of immunologic marker studies in childhood acute lymphoblastic leukemia. *Blood* 82:343-62
70. Patel JL, Smith LM, Anderson J, Abromowitch M, Campana D, et al. 2012. The immunophenotype of T-lymphoblastic lymphoma in children and adolescents: a Children's Oncology Group report. *Br J Haematol* 159:454-61
71. Campana D, van Dongen JJ, Mehta A, Coustan-Smith E, Wolvers-Tettero IL, et al. 1991. Stages of T-cell receptor protein expression in T-cell acute lymphoblastic leukemia. *Blood* 77:1546-54
72. Sigal LH. 2012. Basic science for the clinician 54: CD5. *J Clin Rheumatol* 18:83-8
73. Hillerdal V, Boura VF, Bjorkelund H, Andersson K, Essand M. 2016. Avidity characterization of genetically engineered T-cells with novel and established approaches. *BMC Immunol* 17:23
74. Liu X, Jiang S, Fang C, Yang S, Olalere D, et al. 2015. Affinity-Tuned ErbB2 or EGFR Chimeric Antigen Receptor T Cells Exhibit an Increased Therapeutic Index against Tumors in Mice. *Cancer Res* 75:3596-607

75. Dorothee G, Vergnon I, El Hage F, Le Maux Chansac B, Ferrand V, et al. 2005. In situ sensory adaptation of tumor-infiltrating T lymphocytes to peptide-MHC levels elicits strong antitumor reactivity. *J Immunol* 174:6888-97
76. Bertram JH, Gill PS, Levine AM, Boquiren D, Hoffman FM, et al. 1986. Monoclonal antibody T101 in T cell malignancies: a clinical, pharmacokinetic, and immunologic correlation. *Blood* 68:752-61
77. LeMaistre CF, Rosen S, Frankel A, Kornfeld S, Saria E, et al. 1991. Phase I trial of H65-RTA immunoconjugate in patients with cutaneous T-cell lymphoma. *Blood* 78:1173-82
78. Mamonkin M, Rouce RH, Tashiro H, Brenner MK. 2015. A T-cell-directed chimeric antigen receptor for the selective treatment of T-cell malignancies. *Blood* 126:983-92
79. Petersen CT, Hassan M, Morris AB, Jeffery J, Lee K, et al. 2018. Improving T-cell expansion and function for adoptive T-cell therapy using ex vivo treatment with PI3Kdelta inhibitors and VIP antagonists. *Blood Adv* 2:210-23
80. Xu Y, Liu Q, Zhong M, Wang Z, Chen Z, et al. 2019. 2B4 costimulatory domain enhancing cytotoxic ability of anti-CD5 chimeric antigen receptor engineered natural killer cells against T cell malignancies. *J Hematol Oncol* 12:49
81. Li Y, Hermanson DL, Moriarity BS, Kaufman DS. 2018. Human iPSC-Derived Natural Killer Cells Engineered with Chimeric Antigen Receptors Enhance Anti-tumor Activity. *Cell Stem Cell* 23:181-92 e5
82. Rabinowich H, Pricop L, Herberman RB, Whiteside TL. 1994. Expression and function of CD7 molecule on human natural killer cells. *The Journal of Immunology* 152:517-26
83. Coustan-Smith E, Mullighan CG, Onciu M, Behm FG, Raimondi SC, et al. 2009. Early T-cell precursor leukaemia: A subtype of very high-risk acute lymphoblastic leukaemia *The Lancet Oncology* 10:147-56
84. Campana D, van Dongen JJ, Mehta A, Coustan-Smith E, Wolvers-Tettero IL, et al. 1991. Stages of T-cell Receptor Protein Expression in T-cell Acute Lymphoblastic Leukemia *Blood* 77:1546-54
85. Zhang J, Ding L, Holmfeldt L, Wu G, Heatley SL, et al. 2012. The genetic basis of early T-cell precursor acute lymphoblastic leukaemia. *Nature* 481:157-63
86. Inukai T, Kiyokawa N, Campana D, Coustan-Smith E, Kikuchi A, et al. 2012. Clinical significance of early T-cell precursor acute lymphoblastic leukaemia: results of the Tokyo Children's Cancer Study Group Study L99-15. *Br J Haematol* 156:358-65
87. Bonilla FA, Kokron CM, Swinton P, Geha RS. 1997. Targeted gene disruption of murine CD7. *Int Immunol* 9:1875-83
88. Lee DM, Staats HF, Sundry JS, Patel DD, Sempowski GD, et al. 1998. Immunologic characterization of CD7-deficient mice. *J Immunol* 160:5749-56
89. You F, Wang Y, Jiang L, Zhu X, Chen D, et al. 2019. A novel CD7 chimeric antigen receptor-modified NK-92MI cell line targeting T-cell acute lymphoblastic leukemia. *Am J Cancer Res* 9:64-78
90. Tang J, Li J, Zhu X, Yu Y, Chen D, et al. 2016. Novel CD7-specific nanobody-based immunotoxins potently enhanced apoptosis of CD7-positive malignant cells. *Oncotarget* 7:34070-83
91. Yu Y, Li J, Zhu X, Tang X, Bao Y, et al. 2017. Humanized CD7 nanobody-based immunotoxins exhibit promising anti-T-cell acute lymphoblastic leukemia potential. *Int J Nanomedicine* 12:1969-83
92. Ma G, Shen J, Pinz K, Wada M, Park J, et al. 2019. Targeting T Cell Malignancies Using CD4CAR T-Cells and Implementing a Natural Safety Switch. *Stem Cell Rev* 15:443-7
93. Lapalombella R, Yeh YY, Wang L, Ramanunni A, Rafiq S, et al. 2012. Tetraspanin CD37 directly mediates transduction of survival and apoptotic signals. *Cancer Cell* 21:694-708
94. van Spruiel AB, Puls KL, Sofi M, Pouniotis D, Hochrein H, et al. 2004. A regulatory role for CD37 in T cell proliferation. *J Immunol* 172:2953-61

95. Barrena S, Almeida J, Yunta M, Lopez A, Fernandez-Mosteirin N, et al. 2005. Aberrant expression of tetraspanin molecules in B-cell chronic lymphoproliferative disorders and its correlation with normal B-cell maturation. *Leukemia* 19:1376-83
96. Pereira DS, Guevara CI, Jin L, Mbong N, Verlinsky A, et al. 2015. AGS67E, an Anti-CD37 Monomethyl Auristatin E Antibody-Drug Conjugate as a Potential Therapeutic for B/T-Cell Malignancies and AML: A New Role for CD37 in AML. *Mol Cancer Ther* 14:1650-60
97. Dürkop H, Latza U, Hummel M, Eitelbach F, Seed B, Stein H. 1992. Molecular cloning and expression of a new member of the nerve growth factor receptor family that is characteristic for Hodgkin's disease. *Cell* 68:421-7
98. Pierce JM, Mehta A. 2017. Diagnostic, prognostic and therapeutic role of CD30 in lymphoma. *Expert Rev Hematol* 10:29-37
99. Stein H, Mason DY, Gerdes J, O'Connor N, Wainscoat J, et al. 1985. The expression of the Hodgkin's disease associated antigen Ki-1 in reactive and neoplastic lymphoid tissue: evidence that Reed-Sternberg cells and histiocytic malignancies are derived from activated lymphoid cells. *Blood* 66:848-58
100. Ellis TM, Simms PE, Slivnick DJ, Jack HM, Fisher RI. 1993. CD30 is a signal-transducing molecule that defines a subset of human activated CD45RO+ T cells. *J Immunol* 151:2380-9
101. Zheng W, Medeiros LJ, Young KH, Goswami M, Powers L, et al. 2014. CD30 expression in acute lymphoblastic leukemia as assessed by flow cytometry analysis. *Leuk Lymphoma* 55:624-7
102. Hombach A, Heuser C, Sircar R, Tillmann T, Diehl V, et al. 1998. An anti-CD30 chimeric receptor that mediates CD3-zeta-independent T-cell activation against Hodgkin's lymphoma cells in the presence of soluble CD30. *Cancer Res* 58:1116-9
103. Hombach A, Heuser C, Sircar R, Tillmann T, Diehl V, et al. 1999. Characterization of a chimeric T-cell receptor with specificity for the Hodgkin's lymphoma-associated CD30 antigen. *J Immunother* 22:473-80
104. Park SI, Serody JS, Shea TC, Grover NS, Ivanova A, et al. 2017. A phase 1b/2 study of CD30-specific chimeric antigen receptor T-cell (CAR-T) therapy in combination with bendamustine in patients with CD30+ Hodgkin and non-Hodgkin lymphoma. *Journal of Clinical Oncology* 35:TPS3095-TPS
105. Ramos CA, Bilgi M, Gerken C, Dakhova O, Mei Z, et al. 2019. CD30-Chimeric Antigen Receptor (CAR) T Cells for Therapy of Hodgkin Lymphoma (HL). *Biology of Blood and Marrow Transplantation* 25:S63
106. Wang CM, Wu ZQ, Wang Y, Guo YL, Dai HR, et al. 2017. Autologous T Cells Expressing CD30 Chimeric Antigen Receptors for Relapsed or Refractory Hodgkin Lymphoma: An Open-Label Phase I Trial. *Clin Cancer Res* 23:1156-66
107. Sims JE, Tunnacliffe A, Smith WJ, Rabbitts TH. 1984. Complexity of human T-cell antigen receptor beta-chain constant- and variable-region genes. *Nature* 312:541-5
108. Tunnacliffe A, Kefford R, Milstein C, Forster A, Rabbitts TH. 1985. Sequence and evolution of the human T-cell antigen receptor beta-chain genes. *Proc Natl Acad Sci U S A* 82:5068-72
109. Maciocia PM, Wawrzyniecka PA, Philip B, Ricciardelli I, Akarca AU, et al. 2017. Targeting the T cell receptor beta-chain constant region for immunotherapy of T cell malignancies. *Nat Med* 23:1416-23
110. Went P, Agostinelli C, Gallamini A, Piccaluga PP, Ascani S, et al. 2006. Marker expression in peripheral T-cell lymphoma: a proposed clinical-pathologic prognostic score. *J Clin Oncol* 24:2472-9
111. Pui CH, Behm FG, Singh B, Schell MJ, Williams DL, et al. 1990. Heterogeneity of presenting features and their relation to treatment outcome in 120 children with T-cell acute lymphoblastic leukemia. *Blood* 75:174-9

112. Rasaiyaah J, Georgiadis C, Preece R, Mock U, Qasim W. 2018. TCRalpha/beta/CD3 disruption enables CD3-specific antileukemic T cell immunotherapy. *JCI Insight* 3
113. Das RK, Vernau L, Grupp SA, Barrett DM. 2019. Naive T-cell Deficits at Diagnosis and after Chemotherapy Impair Cell Therapy Potential in Pediatric Cancers. *Cancer Discov* 9:492-9
114. Rudolph ME, McArthur MA, Barnes RS, Magder LS, Chen WH, Sztein MB. 2018. Differences Between Pediatric and Adult T Cell Responses to In Vitro Staphylococcal Enterotoxin B Stimulation. *Front Immunol* 9:498
115. Thome JJ, Grinshpun B, Kumar BV, Kubota M, Ohmura Y, et al. 2016. Longterm maintenance of human naive T cells through in situ homeostasis in lymphoid tissue sites. *Sci Immunol* 1
116. Shearer WT, Rosenblatt HM, Gelman RS, Oyomopito R, Plaeger S, et al. 2003. Lymphocyte subsets in healthy children from birth through 18 years of age: the Pediatric AIDS Clinical Trials Group P1009 study. *J Allergy Clin Immunol* 112:973-80
117. Qasim W, Zhan H, Samarasinghe S, Adams S, Amrolia P, et al. 2017. Molecular remission of infant B-ALL after infusion of universal TALEN gene-edited CAR T cells. *Sci Transl Med* 9
118. McCreedy BJ, Senyukov VV, Nguyen KT. 2018. Off the shelf T cell therapies for hematologic malignancies. *Best Pract Res Clin Haematol* 31:166-75
119. Brehm C, Huenecke S, Quaiser A, Esser R, Bremm M, et al. 2011. IL-2 stimulated but not unstimulated NK cells induce selective disappearance of peripheral blood cells: concomitant results to a phase I/II study. *PLoS One* 6:e27351
120. Glienke W, Esser R, Priesner C, Suerth JD, Schambach A, et al. 2015. Advantages and applications of CAR-expressing natural killer cells. *Front Pharmacol* 6:21
121. Gong JH, Maki G, Klingemann HG. 1994. Characterization of a human cell line (NK-92) with phenotypical and functional characteristics of activated natural killer cells. *Leukemia* 8:652-8
122. Boissel L, Betancur M, Lu W, Wels WS, Marino T, et al. 2012. Comparison of mRNA and lentiviral based transfection of natural killer cells with chimeric antigen receptors recognizing lymphoid antigens. *Leuk Lymphoma* 53:958-65
123. Boissel L, Betancur M, Wels WS, Tuncer H, Klingemann H. 2009. Transfection with mRNA for CD19 specific chimeric antigen receptor restores NK cell mediated killing of CLL cells. *Leuk Res* 33:1255-9
124. Boissel L, Betancur-Boissel M, Lu W, Krause DS, Van Etten RA, et al. 2013. Retargeting NK-92 cells by means of CD19- and CD20-specific chimeric antigen receptors compares favorably with antibody-dependent cellular cytotoxicity. *Oncoimmunology* 2:e26527
125. Muller T, Uherek C, Maki G, Chow KU, Schimpf A, et al. 2008. Expression of a CD20-specific chimeric antigen receptor enhances cytotoxic activity of NK cells and overcomes NK-resistance of lymphoma and leukemia cells. *Cancer Immunol Immunother* 57:411-23
126. Chu J, Deng Y, Benson DM, He S, Hughes T, et al. 2014. CS1-specific chimeric antigen receptor (CAR)-engineered natural killer cells enhance in vitro and in vivo antitumor activity against human multiple myeloma. *Leukemia* 28:917-27
127. Rafiq S, Purdon TJ, Schultz L, Klingemann H, Brentjens RJ. 2015. NK-92 cells engineered with anti-CD33 chimeric antigen receptors (CAR) for the treatment of Acute Myeloid Leukemia (AML). *Cytotherapy* 17:S23
128. Sahm C, Schonfeld K, Wels WS. 2012. Expression of IL-15 in NK cells results in rapid enrichment and selective cytotoxicity of gene-modified effectors that carry a tumor-specific antigen receptor. *Cancer Immunol Immunother* 61:1451-61
129. Schonfeld K, Sahm C, Zhang C, Naundorf S, Brendel C, et al. 2015. Selective inhibition of tumor growth by clonal NK cells expressing an ErbB2/HER2-specific chimeric antigen receptor. *Mol Ther* 23:330-8

130. Seidel D, Shibina A, Siebert N, Wels WS, Reynolds CP, et al. 2015. Disialoganglioside-specific human natural killer cells are effective against drug-resistant neuroblastoma. *Cancer Immunol Immunother* 64:621-34
131. Han J, Chu J, Keung Chan W, Zhang J, Wang Y, et al. 2015. CAR-Engineered NK Cells Targeting Wild-Type EGFR and EGFRvIII Enhance Killing of Glioblastoma and Patient-Derived Glioblastoma Stem Cells. *Sci Rep* 5:11483
132. Arai S, Meagher R, Swearingen M, Myint H, Rich E, et al. 2008. Infusion of the allogeneic cell line NK-92 in patients with advanced renal cell cancer or melanoma: a phase I trial. *Cytotherapy* 10:625-32
133. Tonn T, Schwabe D, Klingemann HG, Becker S, Esser R, et al. 2013. Treatment of patients with advanced cancer with the natural killer cell line NK-92. *Cytotherapy* 15:1563-70
134. Suck G, Odendahl M, Nowakowska P, Seidl C, Wels WS, et al. 2016. NK-92: an 'off-the-shelf therapeutic' for adoptive natural killer cell-based cancer immunotherapy. *Cancer Immunol Immunother* 65:485-92
135. Farag SS, Fehniger TA, Ruggeri L, Velardi A, Caligiuri MA. 2002. Natural killer cell receptors: new biology and insights into the graft-versus-leukemia effect. *Blood* 100:1935-47
136. Farag SS, Caligiuri MA. 2006. Human natural killer cell development and biology. *Blood Rev* 20:123-37
137. Klingemann H, Boissel L, Toneguzzo F. 2016. Natural Killer Cells for Immunotherapy - Advantages of the NK-92 Cell Line over Blood NK Cells. *Front Immunol* 7:91
138. Maki G, Klingemann HG, Martinson JA, Tam YK. 2001. Factors regulating the cytotoxic activity of the human natural killer cell line, NK-92. *J Hematother Stem Cell Res* 10:369-83
139. Klingemann H. 2014. Are natural killer cells superior CAR drivers? *Oncoimmunology* 3:e28147
140. Voskoboinik I, Smyth MJ, Trapani JA. 2006. Perforin-mediated target-cell death and immune homeostasis. *Nat Rev Immunol* 6:940-52
141. Screpanti V, Wallin RP, Ljunggren HG, Grandien A. 2001. A central role for death receptor-mediated apoptosis in the rejection of tumors by NK cells. *J Immunol* 167:2068-73
142. Hank JA, Robinson RR, Surfus J, Mueller BM, Reisfeld RA, et al. 1990. Augmentation of antibody dependent cell mediated cytotoxicity following in vivo therapy with recombinant interleukin 2. *Cancer Res* 50:5234-9
143. Carson WE, Parihar R, Lindemann MJ, Personeni N, Dierksheide J, et al. 2001. Interleukin-2 enhances the natural killer cell response to Herceptin-coated Her2/neu-positive breast cancer cells. *Eur J Immunol* 31:3016-25
144. Parihar R, Dierksheide J, Hu Y, Carson WE. 2002. IL-12 enhances the natural killer cell cytokine response to Ab-coated tumor cells. *J Clin Invest* 110:983-92
145. Nguyen QH, Roberts RL, Ank BJ, Lin SJ, Lau CK, Stiehm ER. 1998. Enhancement of antibody-dependent cellular cytotoxicity of neonatal cells by interleukin-2 (IL-2) and IL-12. *Clin Diagn Lab Immunol* 5:98-104
146. Nguyen QH, Roberts RL, Ank BJ, Lin SJ, Thomas EK, Stiehm ER. 1998. Interleukin (IL)-15 enhances antibody-dependent cellular cytotoxicity and natural killer activity in neonatal cells. *Cell Immunol* 185:83-92
147. Friedberg JW, Neuberg D, Gribben JG, Fisher DC, Canning C, et al. 2002. Combination immunotherapy with rituximab and interleukin 2 in patients with relapsed or refractory follicular non-Hodgkin's lymphoma. *Br J Haematol* 117:828-34
148. Ernst D, Williams BA, Wang XH, Yoon N, Kim KP, et al. 2019. Humanized anti-CD123 antibody facilitates NK cell antibody-dependent cell-mediated cytotoxicity (ADCC) of Hodgkin lymphoma targets via ARF6/PLD-1. *Blood Cancer J* 9:6

149. Vivier E, Tomasello E, Baratin M, Walzer T, Ugolini S. 2008. Functions of natural killer cells. *Nat Immunol* 9:503-10
150. Vivier E, Raulet DH, Moretta A, Caligiuri MA, Zitvogel L, et al. 2011. Innate or adaptive immunity? The example of natural killer cells. *Science* 331:44-9
151. Bhat R, Watzl C. 2007. Serial killing of tumor cells by human natural killer cells--enhancement by therapeutic antibodies. *PLoS One* 2:e326
152. Zhang Y, Wallace DL, de Lara CM, Ghattas H, Asquith B, et al. 2007. In vivo kinetics of human natural killer cells: the effects of ageing and acute and chronic viral infection. *Immunology* 121:258-65
153. Klingemann H. 2015. Challenges of cancer therapy with natural killer cells. *Cytotherapy* 17:245-9
154. Iyengar R, Handgretinger R, Babarin-Dorner A, Leimig T, Otto M, et al. 2003. Purification of human natural killer cells using a clinical-scale immunomagnetic method. *Cytotherapy* 5:479-84
155. Koehl U, Brehm C, Huenecke S, Zimmermann SY, Kloess S, et al. 2013. Clinical grade purification and expansion of NK cell products for an optimized manufacturing protocol. *Front Oncol* 3:118
156. Sutlu T, Stellan B, Gilljam M, Quezada HC, Nahi H, et al. 2010. Clinical-grade, large-scale, feeder-free expansion of highly active human natural killer cells for adoptive immunotherapy using an automated bioreactor. *Cytotherapy* 12:1044-55
157. Angelo LS, Banerjee PP, Monaco-Shawver L, Rosen JB, Makedonas G, et al. 2015. Practical NK cell phenotyping and variability in healthy adults. *Immunol Res* 62:341-56
158. Kweon S, Phan MT, Chun S, Yu H, Kim J, et al. 2019. Expansion of Human NK Cells Using K562 Cells Expressing OX40 Ligand and Short Exposure to IL-21. *Front Immunol* 10:879
159. Pardoll DM, Fowlkes BJ, Bluestone JA, Kruisbeek A, Maloy WL, et al. 1987. Differential expression of two distinct T-cell receptors during thymocyte development. *Nature* 326:79-81
160. Born WK, Reardon CL, O'Brien RL. 2006. The function of gammadelta T cells in innate immunity. *Curr Opin Immunol* 18:31-8
161. Chien YH, Jores R, Crowley MP. 1996. Recognition by gamma/delta T cells. *Annu Rev Immunol* 14:511-32
162. Schild H, Mavaddat N, Litzenger C, Ehrich EW, Davis MM, et al. 1994. The nature of major histocompatibility complex recognition by $\gamma\delta$ T cells. *Cell* 76:29-37
163. Sutton KS, Dasgupta A, McCarty D, Doering CB, Spencer HT. 2016. Bioengineering and serum free expansion of blood-derived gammadelta T cells. *Cytotherapy* 18:881-92
164. Finkelshtein D, Werman A, Novick D, Barak S, Rubinstein M. 2013. LDL receptor and its family members serve as the cellular receptors for vesicular stomatitis virus. *Proc Natl Acad Sci U S A* 110:7306-11
165. Capsomidis A, Benthall G, Van Acker HH, Fisher J, Kramer AM, et al. 2018. Chimeric Antigen Receptor-Engineered Human Gamma Delta T Cells: Enhanced Cytotoxicity with Retention of Cross Presentation. *Mol Ther* 26:354-65
166. Rischer M, Pscherer S, Duwe S, Vormoor J, Jurgens H, Rossig C. 2004. Human gammadelta T cells as mediators of chimaeric-receptor redirected anti-tumour immunity. *Br J Haematol* 126:583-92
167. Harrer DC, Simon B, Fujii SI, Shimizu K, Uslu U, et al. 2017. RNA-transfection of gamma/delta T cells with a chimeric antigen receptor or an alpha/beta T-cell receptor: a safer alternative to genetically engineered alpha/beta T cells for the immunotherapy of melanoma. *BMC Cancer* 17:551
168. Deniger DC, Switzer K, Mi T, Maiti S, Hurton L, et al. 2013. Bispecific T-cells expressing polyclonal repertoire of endogenous gammadelta T-cell receptors and introduced CD19-specific chimeric antigen receptor. *Mol Ther* 21:638-47

169. Xiao L, Chen C, Li Z, Zhu S, Tay JC, et al. 2018. Large-scale expansion of Vgamma9Vdelta2 T cells with engineered K562 feeder cells in G-Rex vessels and their use as chimeric antigen receptor-modified effector cells. *Cytotherapy* 20:420-35
170. D'Asaro M, La Mendola C, Di Liberto D, Orlando V, Todaro M, et al. 2010. V gamma 9V delta 2 T lymphocytes efficiently recognize and kill zoledronate-sensitized, imatinib-sensitive, and imatinib-resistant chronic myelogenous leukemia cells. *J Immunol* 184:3260-8
171. Chargui J, Combaret V, Scaglione V, Iacono I, Peri V, et al. 2010. Bromohydrin pyrophosphate-stimulated Vgamma9delta2 T cells expanded ex vivo from patients with poor-prognosis neuroblastoma lyse autologous primary tumor cells. *J Immunother* 33:591-8
172. Todaro M, D'Asaro M, Caccamo N, Iovino F, Francipane MG, et al. 2009. Efficient killing of human colon cancer stem cells by gammadelta T lymphocytes. *J Immunol* 182:7287-96
173. Zoine JT, Knight KA, Fleischer LC, Sutton KS, Goldsmith KC, et al. 2019. Ex vivo expanded patient-derived $\gamma\delta$ T-cell immunotherapy enhances neuroblastoma tumor regression in a murine model. *Oncolmmunology* 8:1593804
174. Prinz I. 2011. Dynamics of the interaction of gammadelta T cells with their neighbors in vivo. *Cell Mol Life Sci* 68:2391-8
175. Meissner N, Radke J, Hedges JF, White M, Behnke M, et al. 2003. Serial analysis of gene expression in circulating gamma delta T cell subsets defines distinct immunoregulatory phenotypes and unexpected gene expression profiles. *J Immunol* 170:356-64
176. Urban EM, Chapoval AI, Pauza CD. 2010. Repertoire development and the control of cytotoxic/effector function in human gammadelta T cells. *Clin Dev Immunol* 2010:732893
177. Gallucci S, Matzinger P. 2001. Danger signals: SOS to the immune system. *Curr Opin Immunol* 13:114-9
178. Rincon-Orozco B, Kunzmann V, Wrobel P, Kabelitz D, Steinle A, Herrmann T. 2005. Activation of V gamma 9V delta 2 T cells by NKG2D. *J Immunol* 175:2144-51
179. Lanca T, Correia DV, Moita CF, Raquel H, Neves-Costa A, et al. 2010. The MHC class Ib protein ULBP1 is a nonredundant determinant of leukemia/lymphoma susceptibility to gammadelta T-cell cytotoxicity. *Blood* 115:2407-11
180. Nedellec S, Sabourin C, Bonneville M, Scotet E. 2010. NKG2D costimulates human V gamma 9V delta 2 T cell antitumor cytotoxicity through protein kinase C theta-dependent modulation of early TCR-induced calcium and transduction signals. *J Immunol* 185:55-63
181. Kabelitz D, Wesch D. 2003. Features and functions of gamma delta T lymphocytes: focus on chemokines and their receptors. *Crit Rev Immunol* 23:339-70
182. Li B, Bassiri H, Rossman MD, Kramer P, Eyuboglu AF, et al. 1998. Involvement of the Fas/Fas ligand pathway in activation-induced cell death of mycobacteria-reactive human gamma delta T cells: a mechanism for the loss of gamma delta T cells in patients with pulmonary tuberculosis. *J Immunol* 161:1558-67
183. Gogoi D, Chiplunkar SV. 2013. Targeting gamma delta T cells for cancer immunotherapy: bench to bedside. *Indian J Med Res* 138:755-61
184. Gober HJ, Kistowska M, Angman L, Jenö P, Mori L, De Libero G. 2003. Human T cell receptor gammadelta cells recognize endogenous mevalonate metabolites in tumor cells. *J Exp Med* 197:163-8
185. Uchida R, Ashihara E, Sato K, Kimura S, Kuroda J, et al. 2007. Gamma delta T cells kill myeloma cells by sensing mevalonate metabolites and ICAM-1 molecules on cell surface. *Biochem Biophys Res Commun* 354:613-8
186. Li J, Herold MJ, Kimmel B, Müller I, Rincon-Orozco B, et al. 2009. Reduced expression of the mevalonate pathway enzyme farnesyl pyrophosphate synthase unveils recognition of tumor cells by Vgamma9Vdelta2 T cells. *J Immunol* 182:8118-24

187. Zheng BJ, Chan KW, Im S, Chua D, Sham JS, et al. 2001. Anti-tumor effects of human peripheral gammadelta T cells in a mouse tumor model. *Int J Cancer* 92:421-5
188. Bennouna J, Bompas E, Neidhardt EM, Rolland F, Philip I, et al. 2008. Phase-I study of Innacell gammadelta, an autologous cell-therapy product highly enriched in gamma9delta2 T lymphocytes, in combination with IL-2, in patients with metastatic renal cell carcinoma. *Cancer Immunol Immunother* 57:1599-609
189. Nakajima J, Murakawa T, Fukami T, Goto S, Kaneko T, et al. 2010. A phase I study of adoptive immunotherapy for recurrent non-small-cell lung cancer patients with autologous gammadelta T cells. *Eur J Cardiothorac Surg* 37:1191-7
190. Meraviglia S, Eberl M, Vermijlen D, Todaro M, Buccheri S, et al. 2010. In vivo manipulation of Vgamma9Vdelta2 T cells with zoledronate and low-dose interleukin-2 for immunotherapy of advanced breast cancer patients. *Clin Exp Immunol* 161:290-7
191. Nicol AJ, Tokuyama H, Mattarollo SR, Hagi T, Suzuki K, et al. 2011. Clinical evaluation of autologous gamma delta T cell-based immunotherapy for metastatic solid tumours. *Br J Cancer* 105:778-86
192. Cavazzana-Calvo M, Payen E, Negre O, Wang G, Hehir K, et al. 2010. Transfusion independence and HMGA2 activation after gene therapy of human beta-thalassaemia. *Nature* 467:318-22
193. Hacein-Bey-Abina S, Von Kalle C, Schmidt M, McCormack MP, Wulffraat N, et al. 2003. LMO2-associated clonal T cell proliferation in two patients after gene therapy for SCID-X1. *Science* 302:415-9
194. Merten OW, Hebben M, Bovolenta C. 2016. Production of lentiviral vectors. *Mol Ther Methods Clin Dev* 3:16017
195. Kumar M, Keller B, Makalou N, Sutton RE. 2001. Systematic determination of the packaging limit of lentiviral vectors. *Hum Gene Ther* 12:1893-905
196. al Yacoub N, Romanowska M, Haritonova N, Foerster J. 2007. Optimized production and concentration of lentiviral vectors containing large inserts. *J Gene Med* 9:579-84
197. Hacein-Bey-Abina S, Garrigue A, Wang GP, Soulier J, Lim A, et al. 2008. Insertional oncogenesis in 4 patients after retrovirus-mediated gene therapy of SCID-X1. *J Clin Invest* 118:3132-42
198. Braun CJ, Boztug K, Paruzynski A, Witzel M, Schwarzer A, et al. 2014. Gene therapy for Wiskott-Aldrich syndrome--long-term efficacy and genotoxicity. *Sci Transl Med* 6:227ra33
199. Barrett DM, Zhao Y, Liu X, Jiang S, Carpenito C, et al. 2011. Treatment of advanced leukemia in mice with mRNA engineered T cells. *Hum Gene Ther* 22:1575-86
200. Yoon SH, Lee JM, Cho HI, Kim EK, Kim HS, et al. 2009. Adoptive immunotherapy using human peripheral blood lymphocytes transferred with RNA encoding Her-2/neu-specific chimeric immune receptor in ovarian cancer xenograft model. *Cancer Gene Ther* 16:489-97
201. Beatty GL, Haas AR, Maus MV, Torigian DA, Soulen MC, et al. 2014. Mesothelin-specific chimeric antigen receptor mRNA-engineered T cells induce anti-tumor activity in solid malignancies. *Cancer Immunol Res* 2:112-20
202. Svoboda J, Rheingold SR, Gill SI, Grupp SA, Lacey SF, et al. 2018. Nonviral RNA chimeric antigen receptor-modified T cells in patients with Hodgkin lymphoma. *Blood* 132:1022-6
203. Deniger DC, Yu J, Huls MH, Figliola MJ, Mi T, et al. 2015. Sleeping Beauty Transposition of Chimeric Antigen Receptors Targeting Receptor Tyrosine Kinase-Like Orphan Receptor-1 (ROR1) into Diverse Memory T-Cell Populations. *PLoS One* 10:e0128151
204. Thokala R, Olivares S, Mi T, Maiti S, Deniger D, et al. 2016. Redirecting Specificity of T cells Using the Sleeping Beauty System to Express Chimeric Antigen Receptors by Mix-and-Matching of VL and VH Domains Targeting CD123+ Tumors. *PLoS One* 11:e0159477

205. Morita D, Nishio N, Saito S, Tanaka M, Kawashima N, et al. 2018. Enhanced Expression of Anti-CD19 Chimeric Antigen Receptor in piggyBac Transposon-Engineered T Cells. *Mol Ther Methods Clin Dev* 8:131-40
206. Bishop DC, Xu N, Tse B, O'Brien TA, Gottlieb DJ, et al. 2018. PiggyBac-Engineered T Cells Expressing CD19-Specific CARs that Lack IgG1 Fc Spacers Have Potent Activity against B-ALL Xenografts. *Mol Ther* 26:1883-95
207. Wang J, Lupo KB, Chambers AM, Matosevic S. 2018. Purinergic targeting enhances immunotherapy of CD73(+) solid tumors with piggyBac-engineered chimeric antigen receptor natural killer cells. *J Immunother Cancer* 6:136
208. Tsukahara T, Iwase N, Kawakami K, Iwasaki M, Yamamoto C, et al. 2015. The Tol2 transposon system mediates the genetic engineering of T-cells with CD19-specific chimeric antigen receptors for B-cell malignancies. *Gene Ther* 22:209-15
209. Tipanee J, Chai YC, VandenDriessche T, Chuah MK. 2017. Preclinical and clinical advances in transposon-based gene therapy. *Biosci Rep* 37
210. Cooney AL, Singh BK, Sinn PL. 2015. Hybrid nonviral/viral vector systems for improved piggyBac DNA transposon in vivo delivery. *Mol Ther* 23:667-74
211. Singh H, Manuri PR, Olivares S, Dara N, Dawson MJ, et al. 2008. Redirecting specificity of T-cell populations for CD19 using the Sleeping Beauty system. *Cancer Res* 68:2961-71
212. Huang X, Guo H, Kang J, Choi S, Zhou TC, et al. 2008. Sleeping Beauty transposon-mediated engineering of human primary T cells for therapy of CD19+ lymphoid malignancies. *Mol Ther* 16:580-9
213. Nakazawa Y, Matsuda K, Kurata T, Sueki A, Tanaka M, et al. 2016. Anti-proliferative effects of T cells expressing a ligand-based chimeric antigen receptor against CD116 on CD34(+) cells of juvenile myelomonocytic leukemia. *J Hematol Oncol* 9:27
214. Nakazawa Y, Huye LE, Salsman VS, Leen AM, Ahmed N, et al. 2011. PiggyBac-mediated cancer immunotherapy using EBV-specific cytotoxic T-cells expressing HER2-specific chimeric antigen receptor. *Mol Ther* 19:2133-43
215. Xu JY, Ye ZL, Jiang DQ, He JC, Ding YM, et al. 2017. Mesothelin-targeting chimeric antigen receptor-modified T cells by piggyBac transposon system suppress the growth of bile duct carcinoma. *Tumour Biol* 39:1010428317695949
216. Huang X, Park H, Greene J, Pao J, Mulvey E, et al. 2015. IGF1R- and ROR1-Specific CAR T Cells as a Potential Therapy for High Risk Sarcomas. *PLoS One* 10:e0133152
217. Huang G, Yu L, Cooper LJ, Hollomon M, Huls H, Kleinerman ES. 2012. Genetically modified T cells targeting interleukin-11 receptor alpha-chain kill human osteosarcoma cells and induce the regression of established osteosarcoma lung metastases. *Cancer Res* 72:271-81
218. Kebriaei P, Singh H, Huls MH, Figliola MJ, Bassett R, et al. 2016. Phase I trials using Sleeping Beauty to generate CD19-specific CAR T cells. *J Clin Invest* 126:3363-76
219. Naso MF, Tomkowicz B, Perry WL, 3rd, Strohl WR. 2017. Adeno-Associated Virus (AAV) as a Vector for Gene Therapy. *BioDrugs* 31:317-34
220. Penaud-Budloo M, Le Guiner C, Nowrouzi A, Toromanoff A, Chereil Y, et al. 2008. Adeno-associated virus vector genomes persist as episomal chromatin in primate muscle. *J Virol* 82:7875-85
221. Duan D, Sharma P, Yang J, Yue Y, Dudas L, et al. 1999. Circular Intermediates of Recombinant Adeno-Associated Virus Have Defined Structural Characteristics Responsible for Long-Term Episomal Persistence in Muscle Tissue. *J Virol* 72:8568-77
222. Wu P, Phillips MI, Bui J, Terwilliger EF. 1998. Adeno-Associated Virus Vector-Mediated Transgene Integration into Neurons and Other Nondividing Cell Targets. *J Virol* 72:5919-26
223. Smith RH. 2008. Adeno-associated virus integration: virus versus vector. *Gene Ther* 15:817-22

224. Li H, Malani N, Hamilton SR, Schlachterman A, Bussadori G, et al. 2011. Assessing the potential for AAV vector genotoxicity in a murine model. *Blood* 117:3311-9
225. Mietzsch M, Broecker F, Reinhardt A, Seeberger PH, Heilbronn R. 2014. Differential adeno-associated virus serotype-specific interaction patterns with synthetic heparins and other glycans. *J Virol* 88:2991-3003
226. Agbandje-McKenna M, Kleinschmidt J. 2011. AAV capsid structure and cell interactions. *Methods Mol Biol* 807:47-92
227. Song L, Li X, Jayandharan GR, Wang Y, Aslanidi GV, et al. 2013. High-efficiency transduction of primary human hematopoietic stem cells and erythroid lineage-restricted expression by optimized AAV6 serotype vectors in vitro and in a murine xenograft model in vivo. *PLoS One* 8:e58757
228. Song L, Kauss MA, Kopin E, Chandra M, Ul-Hasan T, et al. 2013. Optimizing the transduction efficiency of capsid-modified AAV6 serotype vectors in primary human hematopoietic stem cells in vitro and in a xenograft mouse model in vivo. *Cytotherapy* 15:986-98
229. Zincarelli C, Soltys S, Rengo G, Rabinowitz JE. 2008. Analysis of AAV serotypes 1-9 mediated gene expression and tropism in mice after systemic injection. *Mol Ther* 16:1073-80
230. Ciceri F, Bonini C, Markt S, Zappone E, Servida P, et al. 2007. Antitumor effects of HSV-TK-engineered donor lymphocytes after allogeneic stem-cell transplantation. *Blood* 109:4698-707
231. Tiberghien P, Ferrand C, Lioure B, Milpied N, Angonin R, et al. 2001. Administration of herpes simplex-thymidine kinase-expressing donor T cells with a T-cell-depleted allogeneic marrow graft. *Blood* 97:63-72
232. Bonini C, Ferrari G, Verzeletti S, Servida P, Zappone E, et al. 1997. HSV-TK gene transfer into donor lymphocytes for control of allogeneic graft-versus-leukemia. *Science* 276:1719-24
233. Ciceri F, Bonini C, Stanghellini MTL, Bondanza A, Traversari C, et al. 2009. Infusion of suicide-gene-engineered donor lymphocytes after family haploidentical haemopoietic stem-cell transplantation for leukaemia (the TK007 trial): a non-randomised phase I-II study. *The Lancet Oncology* 10:489-500
234. Di Stasi A, Tey SK, Dotti G, Fujita Y, Kennedy-Nasser A, et al. 2011. Inducible apoptosis as a safety switch for adoptive cell therapy. *N Engl J Med* 365:1673-83
235. Zhou X, Di Stasi A, Tey SK, Krance RA, Martinez C, et al. 2014. Long-term outcome after haploidentical stem cell transplant and infusion of T cells expressing the inducible caspase 9 safety transgene. *Blood* 123:3895-905
236. Griffioen M, van Egmond EH, Kester MG, Willemze R, Falkenburg JH, Heemskerk MH. 2009. Retroviral transfer of human CD20 as a suicide gene for adoptive T-cell therapy. *Haematologica* 94:1316-20
237. Introna M, Barbui AM, Bambiacioni F, Casati C, Gaipa G, et al. 2000. Genetic modification of human T cells with CD20: a strategy to purify and lyse transduced cells with anti-CD20 antibodies. *Hum Gene Ther* 11:611-20
238. Saif MA, Borrill R, Bigger BW, Lee H, Logan A, et al. 2015. In vivo T-cell depletion using alemtuzumab in family and unrelated donor transplantation for pediatric non-malignant disease achieves engraftment with low incidence of graft vs. host disease. *Pediatr Transplant* 19:211-8
239. Greco R, Oliveira G, Stanghellini MT, Vago L, Bondanza A, et al. 2015. Improving the safety of cell therapy with the TK-suicide gene. *Front Pharmacol* 6:95
240. Tasian SK, Kenderian SS, Shen F, Ruella M, Shestova O, et al. 2017. Optimized depletion of chimeric antigen receptor T cells in murine xenograft models of human acute myeloid leukemia. *Blood* 129:2395-407
241. Petrov JC, Wada M, Pinz KG, Yan LE, Chen KH, et al. 2018. Compound CAR T-cells as a double-pronged approach for treating acute myeloid leukemia. *Leukemia* 32:1317-26

242. Philip B, Kokalaki E, Mekkaoui L, Thomas S, Straathof K, et al. 2014. A highly compact epitope-based marker/suicide gene for easier and safer T-cell therapy. *Blood* 124:1277-87
243. Diaconu I, Ballard B, Zhang M, Chen Y, West J, et al. 2017. Inducible Caspase-9 Selectively Modulates the Toxicities of CD19-Specific Chimeric Antigen Receptor-Modified T Cells. *Mol Ther* 25:580-92
244. Tey SK, Dotti G, Rooney CM, Heslop HE, Brenner MK. 2007. Inducible caspase 9 suicide gene to improve the safety of allodepleted T cells after haploidentical stem cell transplantation. *Biol Blood Marrow Transplant* 13:913-24
245. Hoyos V, Savoldo B, Quintarelli C, Mahendravada A, Zhang M, et al. 2010. Engineering CD19-specific T lymphocytes with interleukin-15 and a suicide gene to enhance their anti-lymphoma/leukemia effects and safety. *Leukemia* 24:1160-70
246. Narayanan P, Lapteva N, Seethammagari M, Levitt JM, Slawin KM, Spencer DM. 2011. A composite MyD88/CD40 switch synergistically activates mouse and human dendritic cells for enhanced antitumor efficacy. *J Clin Invest* 121:1524-34
247. Duong MT, Collinson-Pautz MR, Morschl E, Lu A, Szymanski SP, et al. 2019. Two-Dimensional Regulation of CAR-T Cell Therapy with Orthogonal Switches. *Mol Ther Oncolytics* 12:124-37
248. Budde LE, Berger C, Lin Y, Wang J, Lin X, et al. 2013. Combining a CD20 chimeric antigen receptor and an inducible caspase 9 suicide switch to improve the efficacy and safety of T cell adoptive immunotherapy for lymphoma. *PLoS One* 8:e82742
249. Serafini M, Manganini M, Borleri G, Bonamino M, Imberti L, et al. 2004. Characterization of CD20-transduced T lymphocytes as an alternative suicide gene therapy approach for the treatment of graft-versus-host disease. *Hum Gene Ther* 15:63-76
250. Di Gaetano N, Cittera E, Nota R, Vecchi A, Grieco V, et al. 2003. Complement activation determines the therapeutic activity of rituximab in vivo. *J Immunol* 171:1581-7
251. Marin V, Cribioli E, Philip B, Tettamanti S, Pizzitola I, et al. 2012. Comparison of different suicide-gene strategies for the safety improvement of genetically manipulated T cells. *Hum Gene Ther Methods* 23:376-86
252. Wang X, Chang WC, Wong CW, Colcher D, Sherman M, et al. 2011. A transgene-encoded cell surface polypeptide for selection, in vivo tracking, and ablation of engineered cells. *Blood* 118:1255-63
253. Koneru M, O'Cearbhaill R, Pendharkar S, Spriggs DR, Brentjens RJ. 2015. A phase I clinical trial of adoptive T cell therapy using IL-12 secreting MUC-16(ecto) directed chimeric antigen receptors for recurrent ovarian cancer. *J Transl Med* 13:102
254. Wu CY, Roybal KT, Puchner EM, Onuffer J, Lim WA. 2015. Remote control of therapeutic T cells through a small molecule-gated chimeric receptor. *Science* 350:aab4077
255. Tang X, Yang L, Li Z, Nalin AP, Dai H, et al. 2018. First-in-man clinical trial of CAR NK-92 cells: safety test of CD33-CAR NK-92 cells in patients with relapsed and refractory acute myeloid leukemia. *Am J Cancer Res* 8:1083-9
256. Osman N, Ley SC, Crumpton MJ. 1992. Evidence for an association between the T cell receptor/CD3 antigen complex and the CD5 antigen in human T lymphocytes. *Eur J Immunol* 22:2995-3000
257. Berland R, Wortis HH. 2002. Origins and functions of B-1 cells with notes on the role of CD5. *Annu Rev Immunol* 20:253-300
258. Bikah G, Carey J, Ciallella JR, Tarakhovskiy A, Bondada S. 1996. CD5-mediated negative regulation of antigen receptor-induced growth signals in B-1 B cells. *Science* 274:1906-9
259. Wiedenheft B, Sternberg SH, Doudna JA. 2012. RNA-guided genetic silencing systems in bacteria and archaea. *Nature* 482:331-8

260. Jinek M, Chylinski K, Fonfara I, Hauer M, Doudna JA, Charpentier E. 2012. A programmable dual-RNA-guided DNA endonuclease in adaptive bacterial immunity. *Science* 337:816-21
261. Mojica FJ, Diez-Villasenor C, Garcia-Martinez J, Almendros C. 2009. Short motif sequences determine the targets of the prokaryotic CRISPR defence system. *Microbiology* 155:733-40
262. Barrangou R, Fremaux C, Deveau H, Richards M, Boyaval P, et al. 2007. CRISPR provides acquired resistance against viruses in prokaryotes. *Science* 315:1709-12
263. Doench JG, Hartenian E, Graham DB, Tothova Z, Hegde M, et al. 2014. Rational design of highly active sgRNAs for CRISPR-Cas9-mediated gene inactivation. *Nat Biotechnol* 32:1262-7
264. Cong L, Zhang F. 2015. Genome engineering using CRISPR-Cas9 system. *Methods Mol Biol* 1239:197-217
265. Kaya H, Mikami M, Endo A, Endo M, Toki S. 2016. Highly specific targeted mutagenesis in plants using *Staphylococcus aureus* Cas9. *Sci Rep* 6:26871
266. Herrin BR, Cooper MD. 2010. Alternative adaptive immunity in jawless vertebrates. *J Immunol* 185:1367-74
267. Mariuzza RA, Velikovsky CA, Deng L, Xu G, Pancer Z. 2010. Structural insights into the evolution of the adaptive immune system: the variable lymphocyte receptors of jawless vertebrates. *Biol Chem* 391:753-60
268. Boehm T, McCurley N, Sutoh Y, Schorpp M, Kasahara M, Cooper MD. 2012. VLR-based adaptive immunity. *Annu Rev Immunol* 30:203-20
269. Kasahara M, Sutoh Y. 2014. Two forms of adaptive immunity in vertebrates: similarities and differences. *Adv Immunol* 122:59-90
270. Yu C, Ali S, St-Germain J, Liu Y, Yu X, et al. 2012. Purification and identification of cell surface antigens using lamprey monoclonal antibodies. *J Immunol Methods* 386:43-9
271. Kirchdoerfer RN, Herrin BR, Han BW, Turnbough CL, Jr., Cooper MD, Wilson IA. 2012. Variable lymphocyte receptor recognition of the immunodominant glycoprotein of *Bacillus anthracis* spores. *Structure* 20:479-86
272. Studnicka GM, Soares S, Better M, Williams RE, Nadell R, Horwitz AH. 1994. Human-engineered monoclonal antibodies retain full specific binding activity by preserving non-CDR complementarity-modulating residues. *Protein Eng* 7:805-14
273. Huston JS, McCartney J, Tai MS, Mottola-Hartshorn C, Jin D, et al. 1993. Medical applications of single-chain antibodies. *Int Rev Immunol* 10:195-217
274. Lee-MacAry AE, Ross EL, Davies D, Laylor R, Honeychurch J, et al. 2001. Development of a novel flow cytometric cell-mediated cytotoxicity assay using the fluorophores PKH-26 and TO-PRO-3 iodide. *J Immunol Methods* 252:83-92
275. Renaudineau Y, Hillion S, Saraux A, Mageed RA, Youinou P. 2005. An alternative exon 1 of the CD5 gene regulates CD5 expression in human B lymphocytes. *Blood* 106:2781-9
276. Cradick TJ, Qiu P, Lee CM, Fine EJ, Bao G. 2014. COSMID: A Web-based Tool for Identifying and Validating CRISPR/Cas Off-target Sites. *Mol Ther Nucleic Acids* 3:e214
277. Brinkman EK, Chen T, Amendola M, van Steensel B. 2014. Easy quantitative assessment of genome editing by sequence trace decomposition. *Nucleic Acids Res* 42:e168
278. Henze G, Fengler R, Hartmann R, Kornhuber B, Janka-Schaub G, et al. 1991. Six-year experience with a comprehensive approach to the treatment of recurrent childhood acute lymphoblastic leukemia (ALL-REZ BFM 85). A relapse study of the BFM group. *Blood* 78:1166-72
279. Burke MJ, Verneris MR, Le Rademacher J, He W, Abdel-Aziz H, et al. 2015. Transplant Outcomes for Children with T Cell Acute Lymphoblastic Leukemia in Second Remission: A Report from the Center for International Blood and Marrow Transplant Research. *Biol Blood Marrow Transplant* 21:2154-9

280. Bakr M, Rasheed W, Mohamed SY, Al-Mohareb F, Chaudhri N, et al. 2012. Allogeneic hematopoietic stem cell transplantation in adolescent and adult patients with high-risk T cell acute lymphoblastic leukemia. *Biol Blood Marrow Transplant* 18:1897-904
281. Raetz EA, Borowitz MJ, Devidas M, Linda SB, Hunger SP, et al. 2008. Reinduction platform for children with first marrow relapse of acute lymphoblastic Leukemia: A Children's Oncology Group Study[corrected]. *J Clin Oncol* 26:3971-8
282. Laurent G, Pris J, Farcet JP, Carayon P, Blythman H, et al. 1986. Effects of therapy with T101 ricin A-chain immunotoxin in two leukemia patients. *Blood* 67:1680-7
283. Koehler M, Hurwitz CA, Krance RA, Coustan-Smith E, Williams LL, et al. 1994. XomaZyme-CD5 immunotoxin in conjunction with partial T cell depletion for prevention of graft rejection and graft-versus-host disease after bone marrow transplantation from matched unrelated donors. *Bone Marrow Transplant* 13:571-5
284. Byers VS, Henslee PJ, Kernan NA, Blazar BR, Gingrich R, et al. 1990. Use of an anti-pan T-lymphocyte ricin a chain immunotoxin in steroid-resistant acute graft-versus-host disease. *Blood* 75:1426-32
285. Tarakhovskiy A, Kanner S, Hombach J, Ledbetter J, Muller W, et al. 1995. A role for CD5 in TCR-mediated signal transduction and thymocyte selection. *Science* 269:535-7
286. Krammer PH, Arnold R, Lavrik IN. 2007. Life and death in peripheral T cells. *Nat Rev Immunol* 7:532-42
287. Hermanson DL, Kaufman DS. 2015. Utilizing chimeric antigen receptors to direct natural killer cell activity. *Front Immunol* 6:195
288. Suck G, Odendahl M, Nowakowska P, Seidl C, Wels WS, et al. 2015. NK-92: an 'off-the-shelf therapeutic' for adoptive natural killer cell-based cancer immunotherapy. *Cancer Immunol Immunother*
289. Romanski A, Uherek C, Bug G, Seifried E, Klingemann H, et al. 2016. CD19-CAR engineered NK-92 cells are sufficient to overcome NK cell resistance in B-cell malignancies. *J Cell Mol Med* 20:1287-94
290. Oelsner S, Friede ME, Zhang C, Wagner J, Badura S, et al. 2017. Continuously expanding CAR NK-92 cells display selective cytotoxicity against B-cell leukemia and lymphoma. *Cytotherapy* 19:235-49
291. Chu Y, Hochberg J, Yahr A, Ayello J, van de Ven C, et al. 2015. Targeting CD20+ Aggressive B-cell Non-Hodgkin Lymphoma by Anti-CD20 CAR mRNA-Modified Expanded Natural Killer Cells In Vitro and in NSG Mice. *Cancer Immunol Res* 3:333-44
292. Esser R, Muller T, Stefes D, Kloess S, Seidel D, et al. 2012. NK cells engineered to express a GD2-specific antigen receptor display built-in ADCC-like activity against tumour cells of neuroectodermal origin. *J Cell Mol Med* 16:569-81
293. Jiang H, Zhang W, Shang P, Zhang H, Fu W, et al. 2014. Transfection of chimeric anti-CD138 gene enhances natural killer cell activation and killing of multiple myeloma cells. *Mol Oncol* 8:297-310
294. Shimasaki N, Coustan-Smith E, Kamiya T, Campana D. 2016. Expanded and armed natural killer cells for cancer treatment. *Cytotherapy* 18:1422-34
295. Li L, Allen C, Shivakumar R, Peshwa MV. 2013. Large volume flow electroporation of mRNA: clinical scale process. *Methods Mol Biol* 969:127-38
296. Chu Y, Flower A, Cairo MS. 2016. Modification of Expanded NK Cells with Chimeric Antigen Receptor mRNA for Adoptive Cellular Therapy. *Methods Mol Biol* 1441:215-30
297. Brouns SJ, Jore MM, Lundgren M, Westra ER, Slijkhuis RJ, et al. 2008. Small CRISPR RNAs guide antiviral defense in prokaryotes. *Science* 321:960-4
298. Ran FA, Hsu PD, Wright J, Agarwala V, Scott DA, Zhang F. 2013. Genome engineering using the CRISPR-Cas9 system. *Nat Protoc* 8:2281-308

299. Anders C, Niewoehner O, Duerst A, Jinek M. 2014. Structural basis of PAM-dependent target DNA recognition by the Cas9 endonuclease. *Nature* 513:569-73
300. Cyranoski D. 2016. First trial of CRISPR in people. *Nature* 535:476-7
301. Chmielewski M, Hombach A, Heuser C, Adams GP, Abken H. 2004. T cell activation by antibody-like immunoreceptors: increase in affinity of the single-chain fragment domain above threshold does not increase T cell activation against antigen-positive target cells but decreases selectivity. *J Immunol* 173:7647-53
302. Chmielewski M, Hombach AA, Abken H. 2011. CD28 cosignalling does not affect the activation threshold in a chimeric antigen receptor-redirected T-cell attack. *Gene Ther* 18:62-72
303. Wherry EJ. 2011. T cell exhaustion. *Nature Immunology* 12:492-9
304. Hoseini SS, Dobrenkov K, Pankov D, Xu XL, Cheung NK. 2017. Bispecific antibody does not induce T-cell death mediated by chimeric antigen receptor against disialoganglioside GD2. *Oncoimmunology* 6:e1320625
305. Guo X, Jiang H, Shi B, Zhou M, Zhang H, et al. 2018. Disruption of PD-1 Enhanced the Anti-tumor Activity of Chimeric Antigen Receptor T Cells Against Hepatocellular Carcinoma. *Front Pharmacol* 9:1118
306. Sengupta S, Katz SC, Sengupta S, Sampath P. 2018. Glycogen synthase kinase 3 inhibition lowers PD-1 expression, promotes long-term survival and memory generation in antigen-specific CAR-T cells. *Cancer Lett* 433:131-9
307. Chong EA, Melenhorst JJ, Lacey SF, Ambrose DE, Gonzalez V, et al. 2017. PD-1 blockade modulates chimeric antigen receptor (CAR)-modified T cells: refueling the CAR. *Blood* 129:1039-41
308. Ren J, Liu X, Fang C, Jiang S, June CH, Zhao Y. 2017. Multiplex Genome Editing to Generate Universal CAR T Cells Resistant to PD1 Inhibition. *Clin Cancer Res* 23:2255-66
309. Van Tendeloo VF, Ponsaerts P, Lardon F, Nijs G, Lenjou M, et al. 2001. Highly efficient gene delivery by mRNA electroporation in human hematopoietic cells: superiority to lipofection and passive pulsing of mRNA and to electroporation of plasmid cDNA for tumor antigen loading of dendritic cells. *Blood* 98:49-56
310. Van De Parre TJ, Martinet W, Schrijvers DM, Herman AG, De Meyer GR. 2005. mRNA but not plasmid DNA is efficiently transfected in murine J774A.1 macrophages. *Biochem Biophys Res Commun* 327:356-60
311. Stacey KJ, Ross IL, Hume DA. 1993. Electroporation and DNA-dependent cell death in murine macrophages. *Immunol Cell Biol* 71 (Pt 2):75-85
312. Quintarelli C, Orlando D, Boffa I, Guercio M, Polito VA, et al. 2018. Choice of costimulatory domains and of cytokines determines CAR T-cell activity in neuroblastoma. *Oncoimmunology* 7:e1433518
313. Ramos CA, Rouse R, Robertson CS, Reyna A, Narala N, et al. 2018. In Vivo Fate and Activity of Second- versus Third-Generation CD19-Specific CAR-T Cells in B Cell Non-Hodgkin's Lymphomas. *Mol Ther* 26:2727-37
314. Lau CH, Suh Y. 2017. In vivo genome editing in animals using AAV-CRISPR system: applications to translational research of human disease. *F1000Res* 6:2153
315. Mingozi F, High KA. 2011. Therapeutic in vivo gene transfer for genetic disease using AAV: progress and challenges. *Nat Rev Genet* 12:341-55
316. Duan D, Sharma P, Yang J, Yue Y, Dudus L, et al. 1998. Circular intermediates of recombinant adeno-associated virus have defined structural characteristics responsible for long-term episomal persistence in muscle tissue. *J Virol* 72:8568-77
317. Autissier P, Soulas C, Burdo TH, Williams KC. 2010. Evaluation of a 12-color flow cytometry panel to study lymphocyte, monocyte, and dendritic cell subsets in humans. *Cytometry A* 77:410-9

318. Zhao Y, Niu C, Cui J. 2018. Gamma-delta (gammadelta) T cells: friend or foe in cancer development? *J Transl Med* 16:3
319. Ruella M, Kenderian SS. 2017. Next-Generation Chimeric Antigen Receptor T-Cell Therapy: Going off the Shelf. *BioDrugs* 31:473-81
320. Reddy P. 2003. Pathophysiology of acute graft-versus-host disease. *Hematol Oncol* 21:149-61
321. Handgretinger R, Schilbach K. 2018. The potential role of gammadelta T cells after allogeneic HCT for leukemia. *Blood* 131:1063-72
322. Vantourout P, Hayday A. 2013. Six-of-the-best: unique contributions of gammadelta T cells to immunology. *Nat Rev Immunol* 13:88-100
323. Brandes M, Willimann K, Moser B. 2005. Professional antigen-presentation function by human gammadelta T Cells. *Science* 309:264-8
324. Devilder MC, Maillat S, Bouyge-Moreau I, Donnadiou E, Bonneville M, Scotet E. 2006. Potentiation of antigen-stimulated V gamma 9V delta 2 T cell cytokine production by immature dendritic cells (DC) and reciprocal effect on DC maturation. *J Immunol* 176:1386-93
325. Eberl M, Roberts GW, Meuter S, Williams JD, Topley N, Moser B. 2009. A rapid crosstalk of human gammadelta T cells and monocytes drives the acute inflammation in bacterial infections. *PLoS Pathog* 5:e1000308
326. Chomarat P, Kjeldsen-Kragh J, Quayle AJ, Natvig JB, Miossec P. 1994. Different cytokine production profiles of gamma delta T cell clones: relation to inflammatory arthritis. *Eur J Immunol* 24:2087-91
327. Battistini L, Borsellino G, Sawicki G, Poccia F, Salvetti M, et al. 1997. Phenotypic and cytokine analysis of human peripheral blood gamma delta T cells expressing NK cell receptors. *J Immunol* 159:3723-30
328. Raulet DH, Guerra N. 2009. Oncogenic stress sensed by the immune system: role of natural killer cell receptors. *Nat Rev Immunol* 9:568-80
329. Bonneville M, O'Brien RL, Born WK. 2010. Gammadelta T cell effector functions: a blend of innate programming and acquired plasticity. *Nat Rev Immunol* 10:467-78
330. O'Brien RL, Born W. 1991. Heat shock proteins as antigens for gamma delta T cells. *Semin Immunol* 3:81-7
331. Gentles AJ, Newman AM, Liu CL, Bratman SV, Feng W, et al. 2015. The prognostic landscape of genes and infiltrating immune cells across human cancers. *Nat Med* 21:938-45
332. Coleman RE, Winter MC, Cameron D, Bell R, Dodwell D, et al. 2010. The effects of adding zoledronic acid to neoadjuvant chemotherapy on tumour response: exploratory evidence for direct anti-tumour activity in breast cancer. *Br J Cancer* 102:1099-105
333. Naoe M, Ogawa Y, Takeshita K, Morita J, Shichijo T, et al. 2010. Zoledronate stimulates gamma delta T cells in prostate cancer patients. *Oncol Res* 18:493-501
334. Halene S, Wang L, Cooper RM, Bockstoce DC, Robbins PB, Kohn DB. 1999. Improved expression in hematopoietic and lymphoid cells in mice after transplantation of bone marrow transduced with a modified retroviral vector. *Blood* 94:3349-57
335. Brooks AR, Harkins RN, Wang P, Qian HS, Liu P, Rubanyi GM. 2004. Transcriptional silencing is associated with extensive methylation of the CMV promoter following adenoviral gene delivery to muscle. *J Gene Med* 6:395-404
336. Qin JY, Zhang L, Clift KL, Hular I, Xiang AP, et al. 2010. Systematic comparison of constitutive promoters and the doxycycline-inducible promoter. *PLoS One* 5:e10611
337. Yu X, Geng W, Zhao H, Wang G, Zhao Y, et al. 2017. Using a Commonly Down-Regulated Cytomegalovirus (CMV) Promoter for High-Level Expression of Ectopic Gene in a Human B Lymphoma Cell Line. *Med Sci Monit* 23:5943-50

338. Challita PM, Skelton D, el-Khoueiry A, Yu XJ, Weinberg K, Kohn DB. 1995. Multiple modifications in cis elements of the long terminal repeat of retroviral vectors lead to increased expression and decreased DNA methylation in embryonic carcinoma cells. *J Virol* 69:748-55
339. Sheridan C. 2017. First approval in sight for Novartis' CAR-T therapy after panel vote. *Nat Biotechnol* 35:691-3
340. Mullard A. 2017. Second anticancer CAR T therapy receives FDA approval. *Nat Rev Drug Discov* 16:818
341. Bouchkouj N, Kasamon YL, de Claro RA, George B, Lin X, et al. 2019. FDA Approval Summary: Axicabtagene Ciloleucel for Relapsed or Refractory Large B-cell Lymphoma. *Clin Cancer Res* 25:1702-8
342. Schuster SJ, Bishop MR, Tam CS, Waller EK, Borchmann P, et al. 2019. Tisagenlecleucel in Adult Relapsed or Refractory Diffuse Large B-Cell Lymphoma. *N Engl J Med* 380:45-56
343. Bach PB, Giralt SA, Saltz LB. 2017. FDA Approval of Tisagenlecleucel: Promise and Complexities of a \$475000 Cancer Drug. *JAMA* 318:1861-2
344. Park JH, Riviere I, Gonen M, Wang X, Senechal B, et al. 2018. Long-Term Follow-up of CD19 CAR Therapy in Acute Lymphoblastic Leukemia. *N Engl J Med* 378:449-59
345. Callahan C, Barry A, Fooks-Parker S, Smith L, Baniewicz D, Hobbie W. 2019. Pediatric Survivorship: Considerations Following CAR T-Cell Therapy. *Clin J Oncol Nurs* 23:35-41
346. Deniger DC, Moyes JS, Cooper LJ. 2014. Clinical applications of gamma delta T cells with multivalent immunity. *Front Immunol* 5:636
347. Morita CT, Beckman EM, Bukowski JF, Tanaka Y, Band H, et al. 1995. Direct presentation of nonpeptide prenyl pyrophosphate antigens to human $\gamma\delta$ T cells. *Immunity* 3:495-507
348. Nicholson IC, Lenton KA, Little DJ, Decorso T, Lee FT, et al. 1997. Construction and characterisation of a functional CD19 specific single chain Fv fragment for immunotherapy of B lineage leukaemia and lymphoma. *Molecular Immunology* 34:1157-65
349. Doering CB, Denning G, Shields JE, Fine EJ, Parker ET, et al. 2018. Preclinical Development of a Hematopoietic Stem and Progenitor Cell Bioengineered Factor VIII Lentiviral Vector Gene Therapy for Hemophilia A. *Hum Gene Ther* 29:1183-201
350. Salmikangas P, Kinsella N, Chamberlain P. 2018. Chimeric Antigen Receptor T-Cells (CAR T-Cells) for Cancer Immunotherapy - Moving Target for Industry? *Pharm Res* 35:152
351. Aleksandrova K, Leise J, Priesner C, Melk A, Kubaink F, et al. 2019. Functionality and Cell Senescence of CD4/ CD8-Selected CD20 CAR T Cells Manufactured Using the Automated CliniMACS Prodigy(R) Platform. *Transfus Med Hemother* 46:47-54
352. Watanabe N, Bajgain P, Sukumaran S, Ansari S, Heslop HE, et al. 2016. Fine-tuning the CAR spacer improves T-cell potency. *Oncoimmunology* 5:e1253656
353. Hebbar M, Jeannin P, Magistrelli G, Hatron PY, Hachulla E, et al. 2004. Detection of circulating soluble CD28 in patients with systemic lupus erythematosus, primary Sjogren's syndrome and systemic sclerosis. *Clin Exp Immunol* 136:388-92
354. Guo P, Hirano M, Herrin BR, Li J, Yu C, et al. 2009. Dual nature of the adaptive immune system in lampreys. *Nature* 459:796-801
355. Han BW, Herrin BR, Cooper MD, Wilson IA. 2008. Antigen recognition by variable lymphocyte receptors. *Science* 321:1834-7
356. Velikovskiy CA, Deng L, Tasumi S, Iyer LM, Kerzic MC, et al. 2009. Structure of a lamprey variable lymphocyte receptor in complex with a protein antigen. *Nat Struct Mol Biol* 16:725-30
357. Herrin BR, Alder MN, Roux KH, Sina C, Ehrhardt GR, et al. 2008. Structure and specificity of lamprey monoclonal antibodies. *Proc Natl Acad Sci U S A* 105:2040-5
358. Jin MS, Kim SE, Heo JY, Lee ME, Kim HM, et al. 2007. Crystal structure of the TLR1-TLR2 heterodimer induced by binding of a tri-acylated lipopeptide. *Cell* 130:1071-82

359. Kang JY, Nan X, Jin MS, Youn SJ, Ryu YH, et al. 2009. Recognition of lipopeptide patterns by Toll-like receptor 2-Toll-like receptor 6 heterodimer. *Immunity* 31:873-84
360. Dong JY, Fan PD, Frizzell RA. 1996. Quantitative analysis of the packaging capacity of recombinant adeno-associated virus. *Hum Gene Ther* 7:2101-12
361. Chamberlain K, Riyad JM, Weber T. 2016. Expressing Transgenes That Exceed the Packaging Capacity of Adeno-Associated Virus Capsids. *Hum Gene Ther Methods* 27:1-12
362. Harrison RP, Zylberberg E, Ellison S, Levine BL. 2019. Chimeric antigen receptor-T cell therapy manufacturing: modelling the effect of offshore production on aggregate cost of goods. *Cytotherapy* 21:224-33
363. Porter DL, Hwang WT, Frey NV, Lacey SF, Shaw PA, et al. 2015. Chimeric antigen receptor T cells persist and induce sustained remissions in relapsed refractory chronic lymphocytic leukemia. *Sci Transl Med* 7:303ra139